Population Genomics and Quantitative Genetics of Polar Bears (*Ursus maritimus*)

by

René Michael Malenfant

A thesis submitted in partial fulfillment of the requirements for the degree of

Doctor of Philosophy

in

Systematics and Evolution

Department of Biological Sciences
University of Alberta

Abstract

Polar bears (*Ursus maritimus*) were among the first large mammals to be assessed for genetic variation in the wild, and they remain a common subject of genetics studies. Although recent advances in genotyping technology have allowed for more accurate determination of population structure and the detection of adaptive variation, most modern research has focused on historical divergence between polar bears and brown bears—a topic with little relevance to current management. The goal of this dissertation is to develop and use large datasets to better describe contemporary genetic variation in polar bears. To this end, I first describe a reanalysis of global polar bear population structure using nuclear microsatellites and mitochondrial DNA. This reanalysis was necessitated by the publication of a study suffering from flaws in design and analysis, most notably non-convergence of BAYESASS, a program used to estimate migration rates. In this reanalysis, I have rectified these errors, and—in contrast to the original study—I show that there is no evidence of strong directional movement in response to recent climate-change-induced loss of sea ice. Second, I describe the development of a custom 9K Illumina Infinium BeadChip for polar bears from restriction-site associated DNA (RAD) and transcriptome sequencing. I show the utility of this chip for sex determination of samples from harvested individuals, and that it gives realistic estimates of population structure and linkage disequilibrium (LD) decay. Third, I perform a more comprehensive Canada-wide population genetic analysis using genotypes from this BeadChip, which provides higher resolution than microsatellites. I confirm the presence of four moderately differentiated genetic clusters of polar bears across the Canadian Arctic, including the Beaufort Sea, the Canadian Arctic Archipelago, Norwegian Bay, and the Hudson Bay Complex. I also confirm the presence of east–west substructure within the Canadian Arctic Archipelago and north–south substructure within the Hudson Bay Complex. Evidence for adaptive differentiation

between these clusters is limited. For the two remaining data chapters, I narrow my focus to the Western Hudson Bay management unit, where Environment and Climate Change Canada researchers have conducted mark–recapture studies and collected phenotypic data since 1966. First, I describe the construction of a 4449-individual multigenerational pedigree for Western Hudson Bay bears—among the most extensive pedigrees for any large mammal in the world. I show that inbreeding is rare in this subpopulation, and I document the first known pair of identical twin bears and six new cases of cub adoption. These results are discussed in the context of inclusive fitness theory. Finally, I use this pedigree to estimate the heritability of four routinely measured adult traits: head length, zygomatic breadth, body length, and axillary girth (a measure that is partially dependent on fatness). I then use the BeadChip to perform association studies of these traits. I find moderate heritability (h^2 = 0.34–0.48) for strictly skeletal traits and lower heritability (h^2 = 0.17) for axillary girth, and I show that variability in these traits is not convincingly affected by any genes of large effect in LD with markers on the BeadChip. Implications for future adaptation are discussed. Collectively, this dissertation represents the most comprehensive assessment of contemporary polar bear genetic variation that has ever been conducted, not only within Western Hudson Bay, but also at the Canadian and circumpolar levels.

Preface

All research conducted for this thesis forms part of a research collaboration between the University of Alberta (led by Dr. Corey Davis) and Environment and Climate Change Canada (led by Dr. Evan Richardson). Other major contributors to this collaboration include Nick Lunn (Environment and Climate Change Canada), Markus Dyck (Nunavut Department of Environment), Martyn Obbard (Ontario Ministry of Natural Resources), and Jodie Pongracz (Northwest Territories Department of Environment and Natural Resources). All analyses conducted herein using these shared datasets are my own original work.

Appendix 1 of this thesis has been published as Genomic Resources Development Consortium, D.W. Coltman, C.S. Davis, N.J. Lunn, R.M. Malenfant, and E.S. Richardson (2014), "Genomic Resources Notes accepted 1 August 2013–30 September 2013", *Molecular Ecology Resources* **14**, 219. I conducted all analyses and drafted the manuscript. CSD conceived of the study and its design, and prepared all samples for sequencing and genotyping. CSD, RMM, and DWC collaborated in finalizing experimental design and the nature of the analyses. NJL and ESR provided samples. All authors commented on and approved the final manuscript.

Chapter 2 and Appendix 2 of this thesis have been published as R.M. Malenfant, C.S. Davis, C.I. Cullingham, and D.W. Coltman (2016), "Circumpolar genetic structure and recent gene flow of polar bears: a reanalysis", *PLoS ONE* 11, e0148967. All authors conceived of the study. I determined the nature of all analyses, conducted all analyses, and drafted the manuscript. All authors commented on and approved the final manuscript.

Chapter 3 and Appendix 3 of this thesis have been published as R.M. Malenfant, D.W. Coltman, and C.S. Davis (2015), "Design of a 9K Illumina BeadChip for polar bears (*Ursus maritimus*) from RAD and transcriptome sequencing", *Molecular Ecology Resources* **15**, 587–600. I conducted all analyses and drafted the manuscript. CSD conceived of the study and its design, and prepared all samples for sequencing and genotyping. CSD, RMM, and DWC collaborated in finalizing experimental design and the nature of the analyses. All authors commented on and approved the final manuscript.

Chapter 4 and Appendix 4 of this thesis are the result of collaborative work between R.M. Malenfant, D.W. Coltman, E.S. Richardson, M.G. Dyck, N.J. Lunn, M. Obbard, J. Pongracz, S.N. Atkinson, K.L. Laidre, E.W. Born, and C.S. Davis. CSD conceived of the study. ESR, MGD, NJL, MO, JP, SNA, KLL, and EWB provided samples and data. I determined the nature of all analyses together with DWC and CSD, conducted all analyses, and drafted the manuscript. Not all coauthors have seen or approved this chapter.

Chapter 5 and Appendix 5 of this thesis were accepted for publication in *Polar Biology* on Dec. 15, 2015 as R.M. Malenfant, D.W. Coltman, E.S. Richardson, N.J. Lunn, I. Stirling, E. Adamowicz, and C.S. Davis, "Evidence of adoption, monozygotic twinning, and low inbreeding rates in a large genetic pedigree of polar bears", doi:10.1007/s00300-015-1871-0. CSD, IS, and ESR conceived of the study. IS, NL, and ESR conducted fieldwork and provided samples; CSD and EA conducted lab work. I determined the nature of all analyses, conducted all analyses, and drafted the manuscript together with CSD and DWC. All authors commented on and approved the final manuscript.

Chapter 6 and Appendix 6 of this thesis are the result of collaborative work between R.M. Malenfant, D.W. Coltman, E.S. Richardson, N.J. Lunn, and C.S. Davis. CSD conceived of the study. ESR and NJL provided samples and data. I determined the nature of all analyses together with DWC and CSD, conducted all analyses, and drafted the manuscript. Not all coauthors have seen or approved this chapter.

Acknowledgments

I would like to thank my supervisors, Corey Davis and David Coltman for their ongoing support and mentorship. I would also like to thank supervisory committee member Paul Stothard, and my candidacy examiners Andy Derocher and Felix Sperling for their advice and encouragement. I would also like to thank my other collaborators, especially Evan Richardson for his continuing support of this project, as well as Nick Lunn, Markus Dyck, Martyn Obbard, Ian Stirling, Jodie Pongracz, Stephen Atkinson, and Beth Adamowicz. I would also like to thank members of the Coltman lab for helpful discussions and advice, particularly Josh Miller, Jamie Gorrell, Cathy Cullingham, Jocelyn Poissant, Aaron Shafer, and Sascha Jeffers, as well as Michelle Viengkone of the Davis lab. Maura, Andrew, and Alex listened to me grumble. My parents, Sandra and Mike, have always supported me in everything that I do.

In addition, I would like to thank: Dennis Andriashek and Wendy Calvert for performing sample collection and maintenance in Western Hudson Bay; Janice Cooke for use of her computing facilities; Marsha Branigan for permission to use samples collected in the Northwest Territories; John Woods, Ian Hatter, Sarah Boyle, Parks Canada, and the West Slopes Bear Research Project for permission to use a grizzly sample in our population genetics study; Mike Harte for providing information about Nunavut harvest samples; Mitch Taylor for discussions regarding Norwegian Bay; Jon Aars, Stanislav Belikov, Todd Atwood for permission to use non-Canadian samples in SNP chip development; and Colin Coros of Delta Genomics (Edmonton, AB, Canada) who provided low-cost SNP-chip genotyping. In addition, our population genetics study would have been impossible without the samples contributed by numerous Inuit harvesters.

This project was funded by grants to CSD from Environment Canada (grant ID 1009997) and the World Wildlife Fund (contract number G-1213-015-00-D) and by an NSERC Discovery Grant to DWC (grant ID 312207-2011). I have been funded by scholarships from Alberta Innovates-Technology Futures, the University of Alberta, and the Province of Alberta. Financial and logistical support of the long-term study of polar bears in Western Hudson Bay have been provided by Care for the Wild International, the Churchill Northern Studies Centre, Environment and Climate Change Canada, the Isdell Family Foundation, Manitoba Conservation, Natural Sciences and Engineering Research Council, Nunavut Wildlife Research Trust Fund, Parks Canada Agency, the Strategic Technology Applications of Genomics in the Environment

(STAGE) funding program, Wildlife Media Inc., World Wildlife Fund (Canada), and World Wildlife Fund Arctic Programme.

Table of Contents

List of Tables

List of Figures

Chapter 1: Introduction

1.1 General introduction

Polar bears (*Ursus maritimus*) are Holarctic marine mammals that depend on sea ice as a platform for mating and locomotion, and for hunting their preferred prey, pagophilic seals, such as ringed seals (*Pusa hispida*) and bearded seals (*Erignathus barbatus*). Once threatened by unsustainable harvesting, more recently, polar bears have become the iconic species of global warming, as Arctic sea ice is increasingly lost to climate change. Loss of sea ice causes decreased access to prey, resulting in greater movement and longer fasting periods (Derocher *et al.* 2004). This has been predicted to have a number of effects on polar bear populations, including changes in population sizes and boundaries, as well as declines in body condition and growth rates (Derocher *et al.* 2004). Studies suggest that altered gene flow (Peacock *et al.* 2015b) and a reduction in the estimated body masses of solitary female polar bears (Stirling & Parkinson 2006) of the southerly Western Hudson Bay management unit may have already begun.

The Agreement on the Conservation of Polar Bears was signed by the five Polar Bear Range States—Canada, United States, Greenland (Denmark), Norway, and Russia—in 1973 and came into force in 1976. It commits each of the Range States to conducting a national research program and managing polar bears based on the best available scientific data. Because of these commitments—and because of public interest and support for polar bear conservation—polar bears were among the first large mammals to be assessed for genetic variation in the wild (Allendorf *et al.* 1979). Early studies using allozymes showed low variation both within and among populations, suggesting either high rates of gene flow or high selective pressure among polar bears at the loci used (Allendorf *et al.* 1979; Larsen *et al.* 1983). Thus, genetic studies tended to support the notion that polar bears harbour little adaptive genetic variation and form a single global population (cf. Pedersen 1945), despite conflicting evidence from movement data (e.g., Stirling *et al.* 1975) and skull morphology (e.g., Wilson 1976).

Advances in genotyping technology have allowed for improved estimates of polar bear population structure, including population studies using nuclear microsatellites (Campagna *et al.* 2013; Crompton *et al.* 2008; Crompton *et al.* 2014; Cronin *et al.* 2006; Kutschera *et al.* 2016; Paetkau *et al.* 1999; Paetkau *et al.* 1995; Peacock *et al.* 2015b) and mitochondrial DNA haplotypes

(Campagna *et al.* 2013; Cronin *et al.* 2006; Kutschera *et al.* 2016; Peacock *et al.* 2015b). While these studies confirm that polar bears comprise multiple discrete populations, no study has yet used high-resolution marker sets to determine population structure, nor assessed whether these populations might differ at adaptive loci. Further, these studies have provided conflicting results on the population structure of polar bears, particularly regarding the presence of a unique genetic cluster of polar bears in an isolated management unit called Norwegian Bay near the northernmost reaches of the Canadian Arctic Archipelago (Paetkau *et al.* 1999; Peacock *et al.* 2015b).

The sequencing of a complete mitochondrial genome (Delisle & Strobeck 2002) and the construction of a draft nuclear genome (Liu *et al.* 2014) have permitted increasingly complex genetic analyses; however, to date, most research using these resources has focused on dating the divergence between polar bears and brown bears (*U. arctos*) or describing subsequent hybridization between these species (Bidon *et al.* 2014; Bidon *et al.* 2015; Cahill *et al.* 2013; Cahill *et al.* 2015; Cronin *et al.* 2014; Edwards *et al.* 2011; Hailer *et al.* 2012; Kutschera *et al.* 2014; Lan *et al.* 2016; Lindqvist *et al.* 2010; Miller *et al.* 2012b). The most comprehensive analyses based on the nuclear (Liu *et al.* 2014) and mitochondrial (Welch *et al.* 2014) genomes suggest that the two species diverged approximately 400,000 years ago, and in the time since their divergence, polar bears have experienced strong selection in genes related to heart function and metabolism, leading to the fixation of beneficial alleles. However, few studies have harnessed the genome to focus specifically on standing adaptive genetic variation. In one targeted study, polar bears were found to have low diversity at some major histocompatibility (MHC) loci (Weber *et al.* 2013). Because the MHC region is expected to be hypervariable, this—together with previous reports of low allozyme variation—may suggest that little adaptive variation remains in polar bears, perhaps owing to strong past selection or bottlenecking during climatic fluctuations. However, studies of expression levels using quantitative PCR (Bowen *et al.* 2015b) and high-throughput sequencing (Bowen *et al.* 2015a) have uncovered pathways connected to alopecia in polar bears, indicating that the search for standing variation may benefit from next-generation technologies such as transcriptomics.

Reduced representation libraries, including restriction-site associated DNA (RAD) (Andrews *et al.* 2016; Baird *et al.* 2008) and transcriptomes (Alvarez *et al.* 2015) provide viable alternatives to complete genome resequencing for discovering and genotyping single-nucleotide

polymorphisms (SNPs). However, next-generation sequencing is expensive, and it generates huge amounts of data that are bioinformatically cumbersome (Pop & Salzberg 2008), and which have comparatively high genotyping error rates that necessitate caution when performing association analyses (Wall *et al.* 2014). For these reasons, SNP arrays retain currency in studies of population structure and genetic architecture in humans and domestic species (e.g., Bermingham *et al.* 2014; Kijas *et al.* 2012; Wang *et al.* 2012). These factors have motivated the cross-species application of SNP arrays to wild species (e.g., Johnston *et al.* 2011; Miller *et al.* 2012a) and the development of new, taxon-specific arrays (e.g., Kawakami *et al.* 2014a; van Bers *et al.* 2012). Wildlife populations to which SNP arrays have been applied have typically been pedigreed, since pedigrees facilitate the construction of linkage maps (e.g., Kawakami *et al.* 2014b; van Oers *et al.* 2014) and the calculation of breeding values, which can be used as response variables for genome-wide association studies (e.g., Johnston *et al.* 2011; Miller 2015).

In this dissertation, I describe the development and application of a custom Illumina BeadChip for polar bears. This SNP array was used to genotype bears from across the Canadian portion of their range. At a multi-population level, I use SNP genotypes from this chip—along with microsatellite genotypes and mitochondrial haplotypes—to resolve reported discrepancies in the population structure and gene flow of polar bears and to test for adaptive differences between populations. At a within-population level, I use the SNP array to seek genetic variants that may be associated with body size differences in Western Hudson Bay. Western Hudson Bay is the best-studied management unit of polar bears in the world, where mark–recapture sessions have been conducted annually since the 1960s, and for which thousands of individuals have been measured by Environment and Climate Change Canada and microsatellite-genotyped at the University of Alberta. I use these data to generate a pedigree and apply the SNP array for association studies.

1.2 Thesis objectives and data chapters

This thesis is divided into five data chapters, first documenting in Chapter 2 a reanalysis of circumpolar population structure using microsatellites and mitochondrial DNA. In Chapter 3, I describe the process by which I used next-generation sequencing to develop a medium-density SNP array for polar bears. In Chapter 4, I use this SNP chip to conduct a higher-resolution study of population structure of Canadian polar bears. Chapter 5 describes the process by which I developed a large pedigree for the polar bears of Western Hudson Bay for use in the quantitative

genetics research that follows. Finally, in Chapter 6, I combine data from the SNP chip and the Western Hudson Bay pedigree to calculate the heritability of body size in polar bears and test for association of genetic markers with body size.

In **Chapter 2**, I reanalyse the circumpolar population structure of polar bears based on nuclear microsatellites and mitochondrial DNA. This reanalysis was necessitated by the publication of a problematic study in PLOS ONE (Peacock *et al.* 2015a; Peacock *et al.* 2015b), which I perceived to have a number of serious methodological flaws, resulting in conclusions that were inconsistent with previously published studies and with my own preliminary population genetics work described in Chapters 3 and 4. Specifically, in this chapter, I redress issues in the original publication such as unbalanced sample sizes, systematically missing data, incorrect calculation of F_{ST} and of significance levels, and misleading estimates of recent gene flow resulting from non-convergence of the program BAYESASS.

In **Chapter 3**, I describe the design and initial application of a medium-density SNP array for polar bears, which I use in later chapters to re-examine their population structure within Canada and to determine the genetic contribution to body size in the Western Hudson Bay management unit. The array was created using SNPs detected in restriction-site associated DNA (RAD) sequencing of polar bears from across their circumpolar range and in the blood/fat transcriptome sequencing of individuals from Western Hudson Bay.

In **Chapter 4,** I present a higher-resolution analysis of population structure of Canadian polar bears, using the SNP array. We perform Bayesian clustering analyses, test for sex-biased dispersal, calculate effective population sizes, show patterns of allelic diversity, check for F_{ST} outliers that may indicate adaptive differentiation among clusters, and describe a possible path by which polar bears may have migrated into Canada after it once again became habitable for polar bears after the end of the last ice age. The study includes comparisons between SNPs and microsatellites genotyped for the same individuals.

In **Chapter 5**, I develop a multigenerational pedigree of polar bears, which comprises 4449 individuals from the Western Hudson Bay management unit. Relationships were inferred from field data and multi-locus microsatellite genotypes from samples collected between 1966 and 2011. I document the first-ever detected pair of identical polar bear twins, and six new putative

cases of cub adoption. I place these cases of adoption in an ecological and evolutionary context with specific reference to the concept of inclusive fitness.

In **Chapter 6**, I use the Western Hudson Bay pedigree to generate the first-ever estimates of heritability of the adult body size of polar bears, using phenotypic data collected in this management unit between 1966 and 2011 during capture–mark–recapture handling. To do this, I apply the animal model—a linear mixed model that includes a random effect for genetic variance—to obtain the breeding value of each individual using best linear unbiased prediction (BLUP). I then perform an association study on these breeding values using the SNP array in an effort to identify loci that may contribute to variation in body size. Results are compared with a more recent method that estimates heritabilities and marker effects directly from genetic data without the use of a pedigree.

Chapter 2: Circumpolar genetic structure and recent gene flow of polar bears: a reanalysis

2.1 Abstract

Recently, an extensive study of 2,748 polar bears (*Ursus maritimus*) from across their circumpolar range was published in PLOS ONE, which used microsatellites and mitochondrial haplotypes to apparently show altered population structure and a dramatic change in directional gene flow towards the Canadian Archipelago—an area believed to be a future refugium for polar bears as their southernmost habitats decline under climate change. Although this study represents a major international collaborative effort and promised to be a baseline for future genetics work, methodological shortcomings and errors of interpretation undermine some of the study's main conclusions. Here, we present a reanalysis of this data in which we address some of these issues, including: (1) highly unbalanced sample sizes and large amounts of systematically missing data; (2) incorrect calculation of F_{ST} and of significance levels; (3) misleading estimates of recent gene flow resulting from non-convergence of the program BAYESASS. In contrast to the original findings, in our reanalysis we find six genetic clusters of polar bears worldwide: the Hudson Bay Complex, the Western and Eastern Canadian Arctic Archipelago, the Western and Eastern Polar Basin, and—importantly—we reconfirm the presence of a unique and possibly endangered cluster of bears in Norwegian Bay near Canada's expected last sea-ice refugium. Although polar bears' abundance, distribution, and population structure will certainly be negatively affected by ongoing—and increasingly rapid—loss of Arctic sea ice, these genetic data provide no evidence of strong directional gene flow in response to recent climate change.

2.2 Introduction

Polar bears (*Ursus maritimus*) are Holarctic marine mammals that are dependent on sea ice as a platform for mating, reproduction, and locomotion. The southern boundary of their distribution is limited by the extent of the sea ice, which forms the habitat for their primary prey, pagophilic seals such as ringed seals (*Pusa hispida*) and bearded seals (*Erignathus barbatus*). Though long-distance swimming (Pagano *et al.* 2012) and overland migration (Sahanatien & Derocher 2010) are possible, open water, land, and multiyear ice—which is too thick for seals to create breathing holes—generally form barriers to movement and gene flow (Paetkau *et al.* 1999; Taylor *et al.* 2001). Although polar bears have large home ranges (Ferguson *et al.* 1999) and are capable of travelling vast distances (Durner & Amstrup 1995), gene flow among subpopulations appears to be limited (Paetkau *et al.* 1995). Currently, 19 management units (MUs) of polar bears are recognized globally, including the Arctic Basin, which is believed to be poor-quality habitat that hinders movement of bears across the area of the North Pole (Obbard *et al.* 2009). MUs have been delineated based on radio-telemetry data (primarily of females), hunter tag returns (primarily of males), and genetic data (Amstrup *et al.* 2010; Obbard & Middel 2012; Obbard *et al.* 2009; Paetkau *et al.* 1999; Taylor & Lee 1995; Taylor *et al.* 2001).

The genetic structure of polar bears has been well characterized in a number of previous studies. The most important of these studies used 16 microsatellites and assignment tests to detect four moderately differentiated genetic clusters across the Arctic, corresponding to the Hudson Bay Complex, the Canadian Arctic Archipelago, the Polar Basin, and Norwegian Bay (Paetkau *et al.* 1999). Each of these clusters is represented in Canada, and all were recently re-detected in a population genetics study of Canadian polar bears using newly collected samples and thousands of single-nucleotide polymorphisms (SNPs) (Malenfant *et al.* 2015a). Of particular interest is the small, isolated Norwegian Bay MU of the Canadian High Arctic, which is separated from surrounding MUs by thick ice, land, and polynyas (Taylor *et al.* 2001; Taylor *et al.* 2009), and which has been reported as genetically divergent (Malenfant *et al.* 2015a; Paetkau *et al.* 1999) and perhaps phenotypically distinct (Taylor *et al.* 2001). Other key population genetics findings include differentiation of Akimiski Island from the rest of Hudson Bay (Crompton *et al.* 2008; Crompton *et al.* 2014; Viengkone 2015), east–west differentiation in the Polar Basin (Miller *et al.* 2012b), and differentiation in the Canadian Archipelago in the area of the Gulf of Boothia and M'Clintock Channel MUs (Campagna *et al.* 2013).

In a recent study published in PLOS ONE, Peacock *et al.*, 2015 (Peacock *et al.* 2015b) (henceforth referred to as PC2015) present an analysis based on an impressive dataset of up to 21 nuclear microsatellites and the mitochondrial control region (plus $tRNA^{Pro}$, $tRNA^{Thr}$, and partial cytb) obtained from 2748 and 411 polar bears respectively. Individuals were included from 18 of 19 global MUs (omitting the largely uninhabitable Arctic Basin). Key findings from this study include: (1) a revision of global population genetic structure for polar bears, with three–four major genetic clusters differing somewhat from those that have previously been reported (i.e., Malenfant *et al.* 2015a; Paetkau *et al.* 1999): the Canadian Arctic Archipelago, Southern Canada, and the Polar Basin (further subdivided into eastern and western sub-clusters); (2) highly directional recent gene flow into the Canadian Arctic Archipelago from Southern Canada and the Eastern Polar Basin, perhaps due to altered sea-ice conditions caused by climate change, (3) male-biased gene flow, (4) a possible role for the Canadian Arctic Archipelago (and other scattered areas such as the Barents Sea) as interglacial refugia. Most striking among their results, however, is the disappearance of the Norwegian Bay genetic cluster—an important change that is never discussed in PC2015.

Upon examination of the article's methods and supplementary material, we discovered a number of serious errors that call into question the population grouping used in the paper and other conclusions. These include the following (all references to tables and figures are those from PC2015):

- Large amounts of systematically missing data (i.e., genotypes for 5/21 microsatellite loci are missing in at least 6/18 MUs) and differences in sample sizes among MUs that are of two orders of magnitude (Supplementary Table S1).

- Miscalculation of F_{ST} and other measures of genetic differentiation because of the retention of loci with missing data, such that average pairwise F_{ST} between all MUs globally is actually negative for microsatellites (–0.03), with values ranging as low as –0.26 (Supplementary Table S5; Supplementary Figure S4).

- Bonferroni correction of significance thresholds that incorrectly account for the number of loci rather than the number of tests (Supplementary Tables S4, S5, S6, S7).

- Probable non-convergence of the program BAYESASS (Supplementary Table S8; see below for explanation).

- Retention of the M'Clintock Channel, Norwegian Bay, and Viscount Melville MUs in population-level analyses of mitochondrial DNA (mtDNA) despite small sample sizes (i.e., $N \leq 3$) that are inadequate for estimating haplotype frequencies, and treatment of the Laptev Sea MU as a single subpopulation despite huge geographical discontinuity in sampling and significant deviation from Hardy–Weinberg equilibrium (Supplementary Table S1).

2.2.1 Non-convergence of BAYESASS

The most important conclusion in PC2015 is that there has been a recent influx of polar bears into the Canadian Arctic Archipelago from Southern Canada (and the Eastern Polar Basin) in response to recent climate change. They also report a surprising 29-fold difference in directional gene flow from the Eastern Polar Basin to the Western Polar Basin. However, the results given in the Supplementary Material (Supplementary Table S8 of PC2015) strongly suggest that their BAYESASS analysis of recent gene flow failed to converge. Non-convergence is a common problem for BAYESASS (Faubet *et al.* 2007; Meirmans 2014), and non-converged runs often show a bimodal distribution of proportions of non-migrants ($Prop_{non\text{-}mig}$) with some populations having $Prop_{non\text{-}mig} < 0.73$ and the remainder having $Prop_{non\text{-}mig} > 0.9$ (Meirmans 2014). Non-convergence is particularly likely when F_{ST} values are low, and immigration rates may be particularly untrustworthy if they have narrow confidence intervals near one of the prior bounds (i.e., 0 or 1/3) (Faubet *et al.* 2007). This is because BAYESASS bounds $Prop_{non\text{-}mig}$ between 0.667 and 1 (Faubet *et al.* 2007; Wilson & Rannala 2005). In Supplementary Table S8 of PC2015, $Prop_{non\text{-}mig}$ (and 95% CIs) are reported for the four genetic clusters as: Eastern Polar Basin = 0.941 (0.888–0.993), Western Polar Basin = 0.678 (0.657–0.699), Canadian Archipelago = 0.699 (0.621–0.777), and Southern Canada = 0.952 (0.912–0.991). These results follow the bimodal distribution described above, and all 95% CIs either overlap the lower bound or are <0.01 from the upper bound. Although it is stated in PC2015 that 3–4 runs resulted in similar estimates, this does not indicate that runs converged or that results are accurate, because multiple runs often get trapped near the program's bounds (Meirmans 2014).

To address some of these issues, we reanalysed the original dataset. Because the analyses in PC2015 were numerous and wide-ranging, we focused primarily on estimates of contemporary

population structure, noting that the generation of contemporary genetic clusters was an important first step for some additional downstream analyses in the original paper, since they formed the groupings between which to test migration, etc. Therefore, this reanalysis may also have implications for some other findings in PC2015. In our opinion, it represents our best estimate to date of the contemporary worldwide population structure of polar bears.

2.3 Materials and Methods

2.3.1 Nuclear microsatellite data

We downloaded the microsatellite genotypes used in PC2015 from datadryad.org (doi: 10.5061/dryad.v2j1r). Individual-specific information, such as lat–long coordinates, year of sampling, population of sampling, sex, age, etc. are available in Table S11 of PC2015. Methods of DNA extraction, microsatellite genotyping, and genotype quality control are provided in Supporting Information S1 of PC2015. Microsatellite genotypes were heavily biased towards the Davis Strait (N = 1050) and the Barents Sea (N = 454), Chukchi Sea (N = 266), and Southern Beaufort Sea (N = 233) MUs. Genetic data were compiled from disparate sources (each having been genotyped at different sets of loci), and therefore there are systematic patterns of missing data (Figure 2.1). Notably, missing data exceeds 80% for marker MU26 and 30% in the Barents Sea MU. Because various programs treat missing data differently (e.g., STRUCTURE ignores missing genotypes, GENODIVE assigns missing genotypes random values based on allele frequencies, and BAYESASS imputes missing genotypes), we reduced the dataset to include only the 14 loci reliably genotyped in all 18 MUs (Figure 2.1). After an initial analysis, we noticed that Gulf of Boothia was unexpectedly quite divergent from other MUs when using the stepwise-mutation model. We then discovered that the PC2015 genotypes for the locus CXX20 were duplicated from the locus CXX110 for many Gulf of Boothia individuals. We replaced these errant CXX20 genotypes with the original genotypes from Paetkau *et al.* (1999).

In PC2015, first-degree relatives were excluded based on field data; however, their microsatellite dataset for Davis Strait includes 1050 individuals sampled mostly between 2005 and 2007 (out of an estimated population size of 2158 individuals (Peacock *et al.* 2013)), and therefore likely still includes many unknown first- and second-degree relatives, the presence of which can cause inaccurate STRUCTURE results (Anderson & Dunham 2008; Rodriguez-Ramilo & Wang 2012). STRUCTURE also struggles with unbalanced sample sizes (Kalinowski 2011) and typical

pairwise F_{ST} calculations can be biased by unequal sample sizes as well (Bhatia *et al.* 2013). Therefore, for MUs having more than 30 microsatellite-genotyped individuals, we used the *sample()* function in R 3.2.0 (R Core Team 2015) to randomly select 30 fully genotyped individuals for inclusion in the reduced dataset used in this paper. We used 30 individuals as a cutoff because this was the number used in the last global analysis of population structure (Paetkau *et al.* 1999), and because this number has been shown to be adequate for estimating allele frequencies and F_{ST} from microsatellite data (Hale *et al.* 2012). One individual from the Laptev Sea had missing data at all loci and was discarded. Our final dataset contained 495 individuals (Table A2.1). After filtering all loci and individuals, we checked for Hardy–Weinberg equilibrium in each subpopulation in GENODIVE 2.0b27 (Meirmans & Van Tienderen 2004) using Nei's G_{IS} statistic (Nei 1987) (1000 permutations) and for linkage disequilibrium (LD) between loci using Fisher's method across MUs in GENEPOP 4.3 (default settings; Rousset 2008). Unless otherwise indicated, a significance level of $\alpha = 0.05$ was used for all tests, with a Holm correction (Holm 1979) in the *p.adjust()* function of R to account for multiple tests where appropriate.

2.3.2 Mitochondrial sequence data

We obtained haplotypes from GenBank according to accession numbers and haplotype counts specified in Supplementary Table S2 of PC2015. The haplotypes UMACR17 and UMACR87 were identical, so we combined these haplotype counts in our dataset. We aligned sequences using MAFFT 7.221 (1PAM/κ=2 scoring matrix and default settings for auto-strategy; Katoh *et al.* 2002) and after trimming extraneous bases from the ends of the alignment, we found that UMACR88 and UMACR3 were also identical, so we merged these counts as well. We estimated the optimal substitution model under the corrected Akaike information criterion (AICc; Hurvich & Tsai 1989) using JMODELTEST 2.1.7 (default settings; Darriba *et al.* 2012; Guindon & Gascuel 2003) and calculated summary statistics for mtDNA using ARLEQUIN 3.5.2.2 (Excoffier & Lischer 2010).

2.3.3 Genetic differentiation, principal component analysis, and AMOVAs

To determine if microsatellites were likely to underestimate population differentiation because of high mutation rates or marker diversity, we tested for a correlation between G_{ST} and H_S using CODIDI 1.0 (100,000 permutations; Wang 2015). We calculated pairwise F_{ST} values (Excoffier *et al.* 1992; Michalakis & Excoffier 1996) between MUs, as well as AMOVAs

(Michalakis & Excoffier 1996) using GENODIVE. We also calculated pairwise R_{ST} (Michalakis & Excoffier 1996; Slatkin 1995) using SPAGEDI 1.4b (Hardy & Vekemans 2002); however, these results are not presented because an allele-size permutation test (10,000 permutations; Hardy *et al.* 2003) suggested that microsatellite allele sizes were uninformative. To explore the data, we performed a principal component analysis (PCA) of individual genetic variation using ADEGENET 1.4-2 (centred and scaled, missing data set to mean; (Jombart 2008; Jombart & Ahmed 2011)). To examine the robustness of our primary conclusion (i.e., the divergence of Norwegian Bay) to the 30-individual sampling process we used to generate our reduced dataset, we also plotted PCAs for 100 additional randomly generated subsamples of the full dataset. We generated a population tree using the recommendations for the infinite-allele model in Takezaki and Nei (1996): we estimated the topology of the tree with unweighted pair-group method with arithmetic mean (UPGMA) in POPTREEW (Takezaki *et al.* 2014) using Nei's D_A (Nei *et al.* 1983), then we unrooted the tree and estimated branch lengths using Nei's standard distance (D_S) (Nei 1978) using non-negative least squares in PHANGORN 1.99-13 (Schliep 2011).

For mtDNA, we calculated pairwise F_{ST} and Φ_{ST} values (and their corresponding AMOVAs (Excoffier *et al.* 1992)) using ARLEQUIN. For Φ_{ST} calculations, distances between haplotypes were calculated using the Tamura & Nei substitution model (Tamura & Nei 1993) with gamma-distributed rate heterogeneity ($\alpha = 0.021$), which was determined as the optimal model of evolution under the AICc. Significance of all pairwise measures was assessed using 10,000 permutations. We also conducted exact tests of population differentiation in GENEPOP for microsatellites and in ARLEQUIN for mtDNA (default settings). Significance of AMOVAs was not tested because of circularity in the logic of doing so for pre-clustered groups (Meirmans 2015). Pairwise F_{ST} values for microsatellites and pairwise Φ_{ST} values for mtDNA were compared with the expectation of $F_{ST}(nu) = 1 - e^{0.25 \times \ln[1 - F_{ST}(mt)]}$ (Zink & Barrowclough 2008), as was used in PC2015, to determine whether polar bears exhibit male-biased gene flow.

2.3.4 Clustering methods and isolation by distance

The settings used for STRUCTURE analysis (e.g., number of repetitions, length of burn-in, priors) were not given in PC2015. We followed the recommendations of Gilbert *et al.*, 2012 (Gilbert *et al.* 2012): 20 independent runs of 200,000 iterations (incl. 100,000 burn-in iterations) using the correlated allele frequencies model with no location prior using STRUCTURE 2.3.4 (Falush

et al. 2003; Pritchard *et al.* 2000). Runs were clustered and averaged using CLUMPAK 1.1 (default settings; (Kopelman *et al.* 2015)), and support for *K*-values was generated in CLUMPAK's "Best *K*" feature using the Evanno method (Evanno *et al.* 2005) and the Pritchard method (Pritchard *et al.* 2010). As has been recommended in the case of low genetic differentiation (Latch *et al.* 2006), we compared the output from STRUCTURE with output from BAPS 6.0 using its non-spatial admixture mode (K_{max} = 20; N_{min} = 5; N_{it} = 100; N_{ref_ind} = 200; N_{ref_it} = 10; (Corander & Marttinen 2006; Corander *et al.* 2008a)). To infer genetic clusters for individuals used in the original study but not included in our reduced dataset, we used trained clustering in BAPS (Cheng *et al.* 2011; Corander *et al.* 2006; Corander *et al.* 2008a), using non-admixed individuals from each genetic cluster as the training set. We also grouped MUs using AMOVA-based *K*-means clustering in GENODIVE for *K*=6, which was found to be the optimal *K*-value in Structure analyses. Finally, to confirm the hierarchical structure (i.e., east–west differentiation) that we detected within the Canadian Arctic Archipelago and the Polar Basin, we ran Structure on the full set of samples collected within each of these MUs using LOCPRIOR=1 to improve the power to detect weak differentiation (Hubisz *et al.* 2009).

Isolation by distance (IBD) can confound clustering analyses (Meirmans 2012b). Because the optimal Structure results for *K*=6 showed an east–west cline in *Q*-values across the Polar Basin, and because there was a large sampling discontinuity in the middle of this cline (i.e., in the Laptev Sea MU), we suspected that one of these two clusters may have been spuriously generated by IBD. To test for IBD across this region, we performed a Mantel test between genetic distances (Rousset 2000) and geographical distances (calculated in SPAGEDI) for all individuals that were highly assigned (i.e., CLUMPAK-averaged $Q \geq 0.7$) to either the Eastern or Western Basin clusters (N = 62). To determine if IBD alone might be responsible for observed east–west genetic clustering in the Basin, we performed a partial Mantel test of association between a matrix of genetic distances and a model matrix denoting whether each pair of individuals belonged to the same genetic cluster (=0) or not (=1), while conditioning on geographical distances (cf. Drummond & Hamilton 2007). Both tests were conducted in VEGAN 2.2-1 (Oksanen *et al.* 2015), using 10,000 permutations to test for significance.

2.3.5. Migration rates

Using BAYESASS 3.0.3 (Wilson & Rannala 2003), we attempted to re-estimate rates of gene flow between five of our six regions (Eastern & Western Polar Basin, Eastern & Western Archipelago, Hudson Complex) and—for comparison—between three of the four major regions identified as optimal by Paetkau *et al.* (1999) and in our K=4 STRUCTURE results (i.e., Polar Basin, Archipelago, Hudson Complex). We omitted Norwegian Bay from both of these runs because its small sample size might result in non-converged estimates (Meirmans 2014), and before running BAYESASS, we used assignment tests in GENODIVE to remove any significant (default settings, 1000 permutations) immigrants from Norwegian Bay found in other MUs. Because our dataset of ~30 samples per MU does not accurately reflect differences in MU population size that would affect gene-flow estimates when MUs were merged into regions, we generated balanced subsets using the sampling regimes shown in Table A2.4. Individuals were selected for inclusion in these subsets blindly (i.e., without viewing their genetic cluster membership) while attempting to obtain geographical balance and high sample sizes of 100–150 individuals per region, which have been shown to be correlated with the probability of convergence (Meirmans 2014). For direct comparison with PC2015, we also generated a balanced subset corresponding to their four regions (Eastern & Western Polar Basin, Archipelago, Hudson Complex). For all BAYESASS runs, we followed the recommendations of Faubet *et al.*, 2007 (i.e., ten runs with different random seeds, N_{it} = 21,000,000, $N_{burn\text{-}in}$ = 2,000,000, sampling interval = 2,000), and we used the Bayesian deviance (as calculated in the *calculateDeviance.R* script from Meirmans, 2014) to select the best run. Convergence of parameter estimates in these best runs was also assessed by manual examination of trace files, and by using the Heidelberger-and-Welch diagnostics (Heidelberger & Welch 1983) in BOA 1.1.8-1 (Smith 2007). Significant differences in proportions of immigrant ancestry were assessed using non-overlapping 95% CIs. To ensure that we were not unintentionally broadening CIs by using only 14 loci, we also performed runs for all datasets including all 21 loci. Finally, to test whether the placement of the Laptev Sea MU (which straddles the apparent boundary between the Western and Eastern Polar Basin clusters) affected our results, we also considered a run that excluded this MU entirely.

2.4 Results

2.4.1 Nuclear microsatellite and mitochondrial DNA statistics

We found that one MU, the Laptev Sea, exhibits significant heterozygote deficiency (G_{IS} = 0.15, $P < 0.001$; Table 2.1), likely because of a Wahlund effect (Wahlund 1928) caused by discontinuous sampling in this MU: there is a >1,400 km gap between western and eastern Laptev Sea samples. Because subpopulation deviation from Hardy–Weinberg equilibrium affects *F*-statistics, we followed Paetkau *et al.* (1999) in excluding the Laptev Sea from all MU-based analyses such as LD and pairwise F_{ST}. For AMOVAs and BAYESASS analyses of gene flow among major genetic clusters, we apportioned the Laptev Sea MU's eastern and western samples into the eastern and western Polar Basin clusters, respectively.

No locus deviated significantly from Hardy–Weinberg equilibrium. Two pairs of loci were in significant LD (G10B–G10J, G10B–G10X); however, both had $P = 0$ in one MU, which causes problems for Fisher's method (Waples 2015), and neither pair is located on the same genomic scaffold (Malenfant *et al.* 2015a). Even if the scaffolds were contiguous within a chromosome, these markers would be separated by >5 Mb, and at these distances, LD is negligible in polar bears (Malenfant *et al.* 2015a). Therefore, we assumed these were false positives, and we elected to keep all 14 microsatellite markers for subsequent analysis. H_S and G_{ST} were not significantly negatively correlated ($r = –0.008$, $P = 0.467$), indicating that microsatellites were unlikely to underestimate population differentiation because of high mutation rates or marker diversity. Three MUs had inadequate sampling (i.e., $N \leq 3$, $k = 1$) to accurately determine mitochondrial haplotype frequencies: namely, M'Clintock Channel, Norwegian Bay, and Viscount Melville Sound. Therefore, we excluded these MUs in pairwise population comparisons and AMOVAs of mtDNA.

2.4.2 Clustering of individuals and management units

CLUMPAK-averaged admixture plots for K=2–7 are shown in Figure 2.2. Progressively, they show the addition of clusters that largely correspond to the following, with some apparent admixture and migration: K=2: the Polar Basin, K=3: the Canadian Arctic Archipelago, K=4: Norwegian Bay, K=5: west–east differentiation in the Polar Basin, K=6: west–east differentiation in the Canadian Arctic Archipelago, K=7: apparent noise. Although the Evanno ΔK method selected K=2 (Figure 2.3b), likelihood was maximized at K=6 (Figure 2.3a)—this was the number

of clusters preferred using the Pritchard method (Figure 2.3c), and there was also a small peak in ΔK at this value.

The six genetic clusters we detected correspond roughly to: the Hudson Complex (incl. Labrador), the Eastern Archipelago, the Western Archipelago, Norwegian Bay, the Eastern Polar Basin, and the Western Polar Basin. Because these results were geographically defensible and corresponded roughly with previously discovered genetic structure in the Archipelago (Paetkau *et al.* 1999) and across the Polar Basin (Miller *et al.* 2012b), we accepted K=6 for our STRUCTURE analysis. Regional STRUCTURE analyses using the full dataset and LOCPRIOR=1 also detected east–west differentiation within the Archipelago and within the Basin, with possible additional clusters present in the Gulf of Boothia and in the Chukchi Sea (Figure A2.2). GENODIVE clustering of MUs for K=6 reached similar conclusions as STRUCTURE (cf. shaded areas in Table 2.2), splitting the Archipelago into Eastern (KB, BB, northern DS) and Western (VM, GB, MC, LS) clusters and splitting the Polar Basin into Eastern (EG, KS, BS, eastern LP) and Western (SB, NB, CS, western LP) clusters.

There is significant IBD across the Polar Basin (Mantel test: $r = 0.2354$, $P < 0.0001$), though genetic clustering remained marginally significant after accounting for IBD (partial Mantel test: $r = 0.141$, $P < 0.0001$). Therefore, we decided to retain both the Eastern and the Western Basin clusters, though we note that traversable distances between individuals in this region will be underestimated by SPAGEDI if it calculates distances over the poor-quality Arctic Basin MU. Results are mapped in Figure 2.4.

Mixture analysis in BAPS found K=6 as being optimal; however, one of these clusters contained only a single individual with missing data at four loci, perhaps indicative of the unexpected effects that missing data can have upon such methods. This single-individual cluster was discarded prior to admixture analysis. The remaining clusters were: the Hudson Complex, the Eastern and Western Canadian Arctic Archipelago, the Polar Basin, and Norwegian Bay. Results of the BAPS admixture analysis based on these five clusters is found in Figure A2.3; they differ from the optimal Structure results for K=6 in that there is less admixture and no distinction of the Eastern/Western Polar Basin. Trained clustering in BAPS using K=5 gave sensible estimates of genetic-cluster membership for all individuals not included in our main study (Figure A2.4).

2.4.2 Population differentiation

Our PCA and population tree reveal four broad groupings of MUs that correspond to the clusters identified by our Structure results for K=4 and by Paetkau *et al.* (1999) (Figure 2.5): the Polar Basin (CS, SB, BS, NB, EG, KS), the Archipelago (MC, VM, LS, BB, KB, GB), Norwegian Bay (NW), and the Hudson Complex (DS, FB, WH, SH). These four groupings were also seen in most of our other 100 randomly resampled subsets of individuals (Figures A2.5, A2.6). The six genetic clusters selected by GENODIVE explain ~3.9% of the nuclear genetic variation and ~9.4% of genetic variation in mtDNA. MU designations within clusters explain 0.8% and 6.0% for microsatellites and mtDNA respectively (Tables 2.3, 2.4). Overall, MUs were slightly to moderately differentiated (average pairwise microsatellite F_{ST} = 0.04). Tests of pairwise population differentiation revealed many significant differences between major genetic clusters, but few significant differences within clusters. In total, 121/136 (≈89%) of population pairs were significantly differentiated after a Holm correction based on nuclear F_{ST}, genic, or genotypic differentiation (compared to only 20% in PC2015, who also included tests for R_{ST}). Importantly, all tests of genetic differentiation show that Norwegian Bay is significantly differentiated from all other MUs (Tables 2.2, A2.2). Though Gulf of Boothia differed significantly from most nearby MUs in tests of genotypic and genic differentiation of nuclear markers (Table A2.2), it was not as well differentiated from other members of the Western Archipelago using pairwise F_{ST} or Φ_{ST} (Table 2.2) or tests of haplotypic differentiation for mtDNA (Table A2.3).

2.4.3 Recent gene flow and sex-biased dispersal

All "best" BAYESASS runs for each population grouping (selected based on the deviance) were at stationarity after burn-in, according to Heidelberger-and-Welch diagnostics. Estimates were surprisingly robust to large amounts of systematically missing data, as results for 14 loci and 21 loci were nearly identical in terms of means and confidence intervals (Figure 2.6); however, because runs for 14 loci had larger effective sample sizes, we discuss these results below. All runs gave highly similar estimates of gene flow among the Polar Basin, the Hudson Complex (incl. Labrador), and the Canadian Arctic Archipelago. In no case was there a significant difference in the proportion of migrants into any of these populations. Within these major clusters, BAYESASS suggested highly directional gene flow from the Western Polar Basin into the Eastern Polar Basin, and from the Western Archipelago into the Eastern Archipelago; however, these highly directional estimates are likely untrustworthy, as discussed below. Immigration rates and proportions of non-

migrant ancestry are given in Tables A2.5–A2.7. Exclusion of the Laptev Sea MU did not change the estimates of migration (Table A2.8).

To test for sex-biased dispersal across MU boundaries, we plotted pairwise F_{ST} for microsatellites against pairwise Φ_{ST} for mtDNA, as in PC2015 (Figure 2.7b). In contrast to estimates from PC2015, more points lie on or above the line of expectation (i.e., the line at which microsatellites differentiate populations as well as mitochondrial haplotypes), and the extreme values most supportive of strong male-biased dispersal, such as zero-estimates for microsatellites F_{ST} and one-estimates for mtDNA Φ_{ST} are absent. Inferences of sex-biased dispersal can also be made from the *R*-ratios of mitochondrial and nuclear *F*-statistics from AMOVAs, where $R \ll 1$ suggests female-biased dispersal and $R \gg 4$ suggests male-biased dispersal (Karl *et al.* 2012). In our AMOVAs, *R*-ratios were $\Phi_{SC}:F_{SC} = 8.3:1$ for genetic variance among MUs within clusters and $\Phi_{CT}:F_{CT} = 2.4:1$ for genetic variance among clusters.

2.5 Discussion

2.5.1 Worldwide population structure of polar bears

In contrast to PC2015, but similarly to Paetkau *et al.*, 1999 , we detected four major genetic clusters of polar bears worldwide, additionally finding east–west sub-clusters in the Polar Basin and in the Canadian Archipelago. These findings corroborate previous studies of polar bear genetic structure (Campagna *et al.* 2013; Malenfant *et al.* 2015a; Miller *et al.* 2012b; Paetkau *et al.* 1999). We note that we failed to detect a unique genetic cluster of bears on Akimiski Island in James Bay of the Southern Hudson Bay MU (Crompton *et al.* 2014; Obbard & Middel 2012; Peacock *et al.* 2015b), which were not considered separately in this range-wide analysis because of low sample size. Our pairwise F_{ST} values between MUs were very similar to those calculated by Paetkau *et al.* (1999), and differ tremendously from those in PC2015, which appear to have been incorrectly calculated: most values in PC2015 are negative, and they range as low as –0.26. Although negative values from the Weir-and-Cockerham estimator of F_{ST} (Weir & Cockerham 1984) are possible (especially when sample sizes and sample variance in allele frequencies are low), they are typically not this extreme. We were unable to reproduce PC2015's F_{ST} values using GENODIVE, FSTAT, or GENEPOP on the full dataset; in all cases, the calculated values were similar to our own and those of Paetkau *et al.* 1999. Only when ARLEQUIN was used under certain conditions were we able to reproduce these values. Specifically, the errant values in PC2015 are an artefact caused by large

amounts of missing data; they result only when one fails to enforce *any* missing-data cutoff in ARLEQUIN (Table A2.9). When a reasonable missing data cutoff (e.g., 5%) is used, then sensible F_{ST} values consistent with our own and those of Paetkau *et al.*, 1999 are produced (Table A2.9).

Under our grouping of MUs, the variance explained by genetic clusters (~4% for nuclear, ~9% for mitochondrial) was maximized through *K*-means clustering, and suggests moderate divergence among clusters. The four major genetic clusters are mostly separated by landmasses and multiyear ice that form barriers to gene flow for polar bears. The Hudson Complex and the Canadian Archipelago are separated by Baffin Island, Labrador, and the Melville Peninsula (Peacock *et al.* 2010; Taylor *et al.* 2001); the Archipelago and the Polar Basin are separated by Greenland in the east and by Banks and Victoria Islands in the west (Bethke *et al.* 1996; Taylor *et al.* 2001); and Norwegian Bay and the Archipelago are separated by thick multiyear ice, islands, and polynyas (Taylor *et al.* 2001). Genetic structure within the four major clusters is likely driven by broad-scale site fidelity to breeding and denning areas (Cherry *et al.* 2013; Lone *et al.* 2013; Taylor *et al.* 2001) and annual reuse of geographically predictable hunting grounds, such as tide cracks and lead systems (Mauritzen *et al.* 2001; Taylor *et al.* 2001).

Based on our reanalysis of the original data from PC2015, we have re-established Norwegian Bay as a distinct genetic cluster of polar bears near the northernmost reaches of Canada. Norwegian Bay is currently estimated to comprise 203 individuals (95% CI: 115–291; (IUCN/SSC Polar Bear Specialist Group 2015)), and—together with the neighbouring Queen Elizabeth Islands—it has previously been proposed as a separate designatable unit of polar bears based on ecological and genetic factors (Thiemann *et al.* 2008a). The status of this cluster is particularly relevant for polar bear conservation, as it is expected to coincide with Canada's last sea-ice refugium (Hamilton *et al.* 2014). This subpopulation has anecdotally been reported to be phenotypically unique (Taylor *et al.* 2001), and we are currently conducting additional genetic analyses on this cluster, including genome scans on more recently collected samples. The Norwegian Bay cluster was likely not revealed in the analyses of PC2015 because of highly unequal sample sizes, and perhaps also by the presence of many related individuals in Davis Strait, which can confound Structure analyses (Anderson & Dunham 2008; Kalinowski 2011; Rodriguez-Ramilo & Wang 2012). In addition, genetic clusters in PC2015 were selected partially based on comparison of AMOVAs, and the existence of Norwegian Bay as a separate genetic cluster was

not among the hypotheses tested (Supplementary Table S7 of PC2015). In addition, all AMOVAs for microsatellites in PC2015 have negative Θ_{SC} values or purportedly explain negative percentages of variance. We were unable to reproduce these unusual AMOVA results using ARLEQUIN on the full dataset (e.g., Table A2.10).

Although an analysis of sex-biased dispersal was presented in PC2015, it gave erroneous results because of incorrectly calculated F_{ST} values and the inclusion of populations with inadequate mtDNA sampling (Figure 2.7a). After correcting for these issues, we find there is little evidence that gene flow is strongly male-biased using the method in PC2015. In contrast, in AMOVAs, mitochondrial Φ_{SC} values were 8.3× nuclear F_{SC} values (whereas Φ_{CT} is only 2.4× F_{CT}), which may suggest male-biased dispersal within—but not among—genetic clusters (however, cf. Figure 2.7b). Unfortunately, this comparison is hindered by different sampling regimes for mtDNA vs. nuclear DNA, including low within-cluster sampling of mtDNA (Table 2.2). In addition, any direct comparison of differentiation between uniparentally and diparentally inherited markers must be interpreted with caution, as such methods generally assume an effective-population-size ratio of 4:1, which is often untrue (Chesser & Baker 1996). Though it would be better to perform sex-specific comparisons using nuclear markers, these methods may be underpowered unless bias in gene flow is extreme (i.e., 80:20), and they may also suffer from pseudoreplication (Goudet *et al.* 2002; Prugnolle & de Meeus 2002). Therefore, the true extent of sex-biased dispersal in polar bears remains undetermined. Previous genetic studies have also reported conflicting findings of male-biased dispersal (Campagna *et al.* 2013; Zeyl *et al.* 2009b), as have radio-telemetry studies of home-range size (Amstrup *et al.* 2001; Laidre *et al.* 2013). Based on distances between recaptures, male polar bears appear to have only slightly larger home ranges than females, and this is perhaps because females move less when accompanied by cubs (Taylor *et al.* 2001).

2.5.2 Are polar bears migrating en masse into the Canadian Archipelago?

Polar bears rely on sea ice as a platform for locomotion (Mauritzen *et al.* 2003), hunting (Rode *et al.* 2015), mating (Ramsay & Stirling 1986b), and—in some areas—denning (Amstrup & Gardner 1994). If climate change continues to reduce the extent and duration of Arctic sea ice, polar bears are likely to respond with altered movement patterns, resulting in increased mixing and gene flow between adjacent subpopulations (Derocher *et al.* 2004). To determine if changes in movement were already occurring, PC2015 compared recent gene flow (i.e., over the past two

generations) calculated using BAYESASS with historical gene flow (i.e., time since the most recent common ancestor) calculated using MIGRATE (Beerli 2009). They found an apparent reversal of gene flow over time, suggesting a recent influx of polar bears into the Canadian Archipelago from Southern Canada. However, the sampling regime for their BAYESASS analysis was not described in the manuscript, and their results show known signs of non-convergence (Faubet *et al.* 2007; Meirmans 2014). A correction to the Supplementary Material of PC2015 (Peacock *et al.* 2015a) published while our manuscript was in review states that individuals were randomly sampled from within the four populations used, with sample sizes of 26, 34, 60, and 60, for the Western Basin, Eastern Basin, Canadian Archipelago and Southern Canada, respectively. Unfortunately, BayesAss typically works best when sample sizes are much larger than this (Meirmans 2014), and we were unable to reproduce these results using our own geographically balanced sampling regime with >100 samples per region.

In fact, within the Polar Basin, our BAYESASS results detected exactly the opposite pattern of PC2015: namely, ~60-fold directional gene flow into the Eastern Polar Basin from the Western Polar Basin. This pattern held true in all 40 runs that included an Eastern–Western Polar Basin split. Similarly, our BAYESASS results showed ~30-fold directional gene flow from the Western Archipelago into the Eastern Archipelago, though this pattern only held true in 8/20 runs; the remaining 12/20 runs suggested ~30-fold directional gene flow from the Eastern Archipelago into the Western Archipelago. Estimates of these immigration rates were close to the upper bound of 1/3 and—taken together—this suggests that *all estimates of gene flow within the Archipelago and the Polar Basin in both this paper and in PC2015 are untrustworthy*, probably because of low genetic differentiation ($F_{ST} \approx 0.01$) between these regions (Faubet *et al.* 2007; Meirmans 2014; Wilson & Rannala 2005). We similarly failed to confirm directional gene flow from the (Eastern) Polar Basin into the Canadian Archipelago; in all of our reanalyses, migration rates between these regions are not significantly directional. Although not significantly different, we did find that immigration into the Canadian Archipelago from Southern Canada (~4.9%) was slightly higher than in the reverse direction (~2.1%). The robustness of this finding across our different sampling regimes and the sampling regime of PC2015 suggests that there may be slight northward gene flow into the Archipelago. Finally, we note that even our preferred BAYESASS run (i.e., the 3-cluster run in Figure 2.6) may be interpreted as having not reached convergence, since proportions of non-migration have been estimated with small variance near the upper bound (Table A2.5). However,

we believe that these estimates of low gene flow are realistic because the regions are largely separated by land and multiyear ice.

Among the first analyses conducted in PC2015 were decadal comparisons of population structure to determine if it was safe to pool samples collected between the 1980s and the 2010s (Supplementary Table S3 of PC2015). Their results showed that population composition had not changed significantly over this period in any of the regions examined. If polar bears had experienced substantial directional gene flow in response to recent climate change, it seems unlikely that this would not have resulted in detectable changes to population structure over this period, especially since PC2015's high immigration rates of ~15% from both the Eastern Polar Basin and Southern Canada suggest that the Canadian Archipelago would likely not be demographically independent (Waples & Gaggiotti 2006). Although Arctic sea ice has been declining in thickness and extent in some regions since at least the 1950s (Kwok & Rothrock 2009; Polyak *et al.* 2010), the rapid loss of sea ice since the mid-1990s has been unprecedented over the last 1,450 years (Kinnard *et al.* 2011). Therefore, we would expect to see changes in composition from the 1980s to the contemporary samples; however, no such changes were observed. Though our Structure plots suggest a substantial amount of migration and admixture among clusters, there is no clear pattern of directional gene flow. Further, these results might overestimate the amount of mating between genetic clusters, since Structure may be sensitive but not specific with respect to admixture (Bohling *et al.* 2013), and cluster membership is estimated with extremely broad credible intervals when using a small number of markers (Putman & Carbone 2014; Viengkone 2015). Therefore, we find the suggestion of mass gene flow into the Archipelago from Southern Canada and the Polar Basin uncompelling, and we strongly caution against managing Arctic Archipelago MUs as if they were being replenished by immigration.

2.6 Conclusions

The three–four major genetic clusters selected in PC2015 were selected based on faulty analyses, including miscalculated F_{ST} values, AMOVAs, and significance levels. The study was also compromised by highly unbalanced sample sizes and possibly by the inclusion of first- and second-degree relatives, as well as retention of large amounts of systematically missing data. One consequence of these data and analysis issues was the failure to detect a distinct subpopulation of polar bears in Norwegian Bay near Canada's expected last sea-ice refugium. BayesAss results

suggesting a recent influx of bears into the Archipelago and the Western Polar Basin showed known signs of non-convergence, and they were not supported in our own runs of the program. We therefore find the suggestion of strong recent directional gene flow into the Archipelago uncompelling. Many of these problems became obvious only upon examining the paper's supplementary material; the original authors of PC2015 should be commended for the well-documented results they made available, which allowed us to detect the issues in their study. Recently, supplementary material has been accused of being poorly peer-reviewed, thereby threatening the integrity of the scientific literature (Pop & Salzberg 2015). We hope that this example will serve as a reminder to both authors and reviewers to scrutinize this supplementary material more closely in the future. In the interest of even greater openness, we have deposited inputs, outputs, and scripts used to perform our analyses at Open Science Framework (http://osf.io/kqcr4). We encourage both reviewers and readers to further explore this invaluable dataset.

Table 2.1. Genetic diversity statistics for 18 management units of polar bears. For microsatellite data, a maximum of 30 individuals have been retained from each management unit from the original dataset of 2,748 individuals, and only the 14 loci indicated in Figure 2.1 have been used. Molecular diversity indices for mitochondrial DNA were calculated in ARLEQUIN using pairwise differences with no gamma correction.

	Nuclear microsatellites							Mitochondrial DNA				
Management unit (abbr.)	**N**	**YoC**	***K***	$\%_{Miss}$	H_O	H_E	G_{IS}	**N**	**YoC**	***K***	***h***	π
Baffin Bay (BB)	30	2003	6.43	0	0.74	0.73	–0.01	30	2007	11	0.88	0.0059
Barents Sea (BS)	30	2000	6.36	0	0.66	0.66	0.00	30	1998	13	0.90	0.0057
Chukchi Sea (CS)	30	1997	7.00	0	0.68	0.70	0.02	35	2000	17	0.93	0.0061
Davis Strait (DS)	30	2006	6.71	0	0.67	0.69	0.02	121	2006	21	0.87	0.0039
East Greenland (EG)	30	1990	6.50	0	0.66	0.67	0.02	–		–	–	–
Foxe Basin (FB)	30	2002	6.29	0	0.71	0.69	–0.03	26	2008	6	0.71	0.0028
Gulf of Boothia (GB)	30	2001	6.29	0	0.70	0.72	0.02	16	2008	6	0.68	0.0034
Kane Basin (KB)	30	1994	6.43	0	0.73	0.72	–0.01	–		–	–	–
Kara Sea (KS)	17	1994	5.36	0	0.62	0.64	0.04	17	1994	7	0.84	0.0044
Laptev Sea (LP)	14	2000	5.79	2.6	0.59	0.70	**0.15**	14	2000	11	0.97	0.0061
Lancaster Sound (LS)	30	2002	6.57	0	0.74	0.71	–0.03	34	2007	11	0.86	0.0066
M'Clintock Channel (MC)	14	1996	5.50	0	0.71	0.69	–0.03	2	2008	1	0	0
Northern Beaufort Sea (NB)	30	1989	6.79	0	0.68	0.69	0.00	–		–	–	–
Norwegian Bay (NW)	30	1995	6.21	0	0.68	0.69	0.01	3	2008	1	0	0
Southern Beaufort Sea (SB)	30	2001	6.79	0	0.65	0.68	0.04	30	1997	15	0.94	0.0073
Southern Hudson Bay (SH)	30	2008	5.86	0	0.66	0.66	0.00	23	2008	8	0.58	0.0019
Viscount Melville Sound (VM)	30	1991	6.29	0	0.64	0.66	0.03	3	2008	1	0	0
Western Hudson Bay (WH)	30	1998	6.14	0	0.65	0.67	0.02	27	2007	9	0.86	0.0047

N, number of individuals genotyped; YoC, mean year of sample collection; *K*, number of alleles; $\%_{Miss}$, percentage of genotypes missing; H_O, observed heterozygosity; H_E, expected heterozygosity; G_{IS}, heterozygosity-based estimator of individual-level inbreeding within a subpopulation; *h*, haplotype diversity; π, nucleotide diversity. In the G_{IS} column, boldface denotes significant deviation from Hardy–Weinberg equilibrium.

Table 2.2. Pairwise F_{ST} values for nuclear microsatellites (below diagonal) and pairwise Φ_{ST} values for mitochondrial DNA (above diagonal); significant values are bolded. MU abbreviations are as in Table 2.1. Lines demarcate the four major clusters discovered by Paetkau *et al.* (1999), which correspond to our STRUCTURE results for K=4. From left to right, these are: the Hudson Complex, the Canadian Arctic Archipelago, Norwegian Bay, and the Polar Basin. Shading denotes the west–east clusters within the Basin and the Archipelago detected by K-means clustering in GENODIVE. These six clusters include additional east–west substructure within the Archipelago and within the Polar Basin. DS is an admixture zone showing affinity for both Hudson Complex and the Archipelago, with southern samples tending to belong to the Hudson Complex cluster and northern samples tending to belong to the Eastern Archipelago cluster. LP has been excluded from all comparisons because it deviates significantly from Hardy–Weinberg equilibrium. For mitochondrial DNA, MC, VM, and NW were omitted because sample sizes were too small (i.e., $N \leq 3$, $k = 1$) to accurately estimate haplotype frequencies.

	SH	**WH**	**FB**	**DS**	**BB**	**KB**	**LS**	**GB**	**MC**	**VM**	**NW**	**NB**	**SB**	**CS**	**LP**	**KS**	**BS**	**EG**
SH	–	0.11	0.04	0.11	0.06		0.15	0.00					0.16	0.05		**0.44**	0.12	
WH	0.01	–	0.05	**0.14**	**0.19**		**0.30**	0.13					**0.31**	**0.23**		**0.47**	**0.25**	
FB	0.01	0.01	–	0.06	0.06		0.19	0.05					**0.23**	0.13		**0.47**	0.14	
DS	**0.03**	**0.03**	0.01	–	**0.15**		**0.33**	0.13					**0.34**	**0.17**		**0.47**	**0.23**	
BB	**0.05**	**0.05**	**0.03**	**0.01**	–		0.02	0.02					0.10	0.06		0.20	0.03	
KB	**0.05**	**0.05**	**0.04**	**0.02**	0.00	–												
LS	**0.05**	**0.05**	**0.04**	**0.02**	0.01	0.01	–	0.09					0.02	0.09		0.13	0.10	
GB	**0.05**	**0.04**	**0.03**	**0.02**	0.01	**0.02**	0.00	–					0.10	0.03		**0.37**	0.10	
MC	**0.06**	**0.05**	**0.04**	**0.03**	0.02	0.01	0.00	0.01	–									
VM	**0.07**	**0.05**	**0.05**	**0.04**	**0.03**	**0.02**	0.00	**0.02**	0.01	–								
NW	**0.07**	**0.06**	**0.05**	**0.04**	**0.03**	**0.03**	**0.02**	**0.04**	**0.04**	**0.03**	–							
NB	**0.09**	**0.08**	**0.06**	**0.05**	**0.04**	**0.04**	**0.02**	**0.04**	**0.03**	**0.03**	**0.05**	–						
SB	**0.10**	**0.08**	**0.07**	**0.06**	**0.04**	**0.05**	**0.03**	**0.04**	**0.03**	**0.04**	**0.07**	0.01	–	0.07		0.15	0.11	
CS	**0.10**	**0.09**	**0.07**	**0.07**	**0.04**	**0.05**	**0.04**	**0.05**	**0.03**	**0.04**	**0.06**	0.00	0.00	–		**0.18**	0.08	
LP															–			
KS	**0.09**	**0.07**	**0.06**	**0.05**	**0.04**	**0.04**	**0.03**	**0.05**	0.02	**0.03**	**0.06**	0.01	0.01	0.01		–	0.07	
BS	**0.10**	**0.08**	**0.07**	**0.05**	**0.04**	**0.04**	**0.04**	**0.05**	**0.03**	**0.05**	**0.07**	**0.02**	**0.02**	**0.02**		0.01	–	
EG	**0.09**	**0.08**	**0.06**	**0.05**	**0.03**	**0.03**	**0.03**	**0.05**	**0.03**	**0.04**	**0.05**	**0.02**	**0.02**	**0.02**		0.01	0.00	–

Table 2.3. Hierarchical analysis of molecular variance (AMOVA) for nuclear microsatellites among management units within the six genetic clusters identified in this paper and shown in Table 2.2. For this analysis, we followed PC2015 by including northern Davis Strait in the Eastern Archipelago cluster and southern Davis Strait in the Hudson cluster. Western Laptev was included in the Western Basin cluster and Eastern Laptev was included in the Eastern Basin cluster. However, results did not differ significantly when the Laptev Sea and Davis Strait MUs were excluded entirely.

Source of variation	**% variance**	***F*-statistic**	***F*-value**
Within individuals	94.32%	F_{IT}	0.057
Among individuals in MUs	1.07%	F_{IS}	0.011
Among MUs in clusters	0.79%	F_{SC}	0.008
Among clusters	3.87%	F_{CT}	0.039

Table 2.4. Hierarchical analysis of molecular variance (AMOVA) for mitochondrial DNA among management units within the six genetic clusters identified in this paper and shown in Table 2.2. Note that many management units (incl. the entire Norwegian Bay cluster) were excluded entirely from this AMOVA because of inadequate sampling. Because we lacked sample location information for downloaded haplotypes, we were unable to split Davis Strait or the Laptev Sea into northern/southern or eastern/western samples; therefore, these MUs were removed for this calculation in addition to the MUs that were removed for low sample sizes in Table 2.2.

Source of variation	**% variance**	***Φ*-statistic**	***Φ*-value**
Among individuals in MUs	84.54%	Φ_{ST}	0.155
Among MUs in clusters	6.04%	Φ_{SC}	0.067
Among clusters	9.43%	Φ_{CT}	0.094

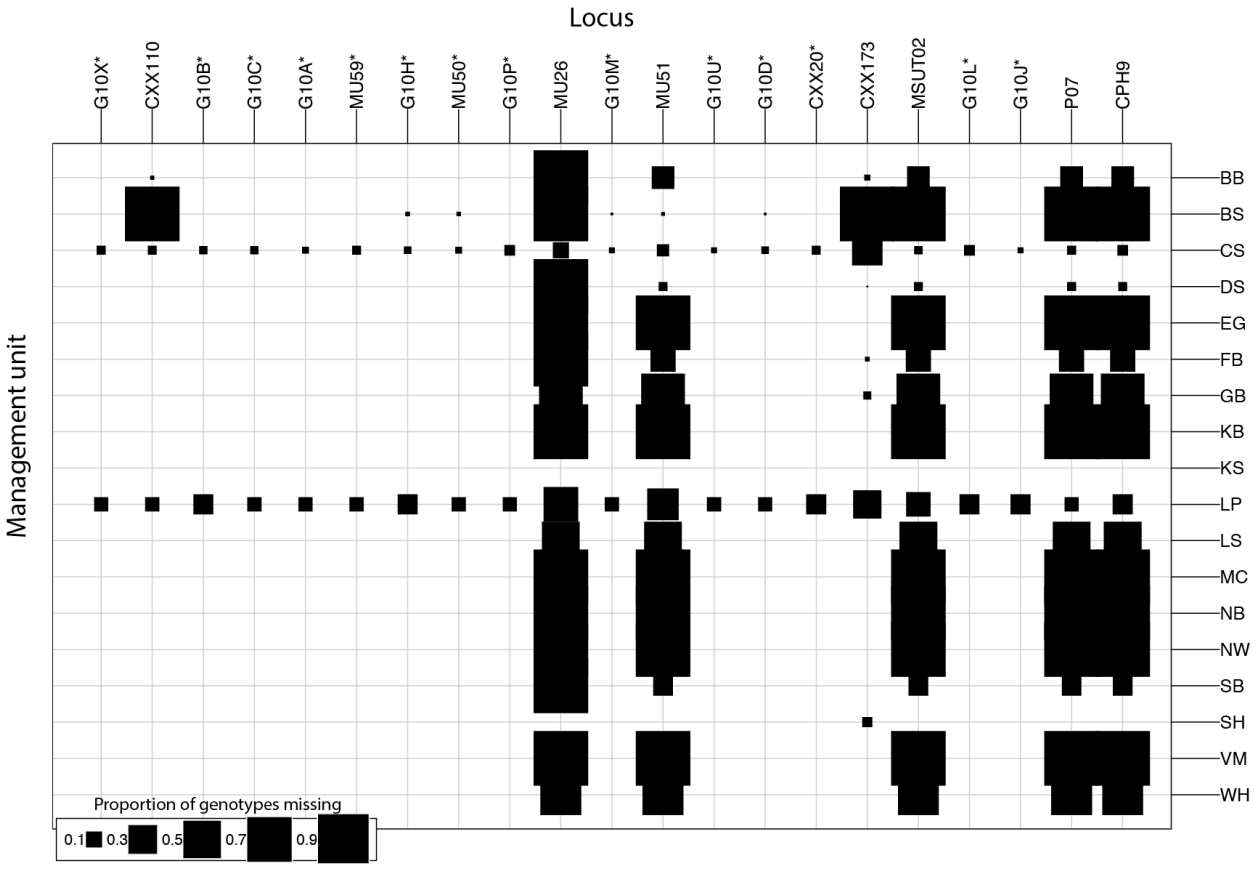

Figure 2.1. Missing data in Peacock et al. (2015b). The size of the square at each management unit–locus intersection is proportional to the amount of missing data at that locus in that management unit. Management unit abbreviations are as in Table 2.1. Asterisks denote loci that were retained for the reanalysis presented in this paper.

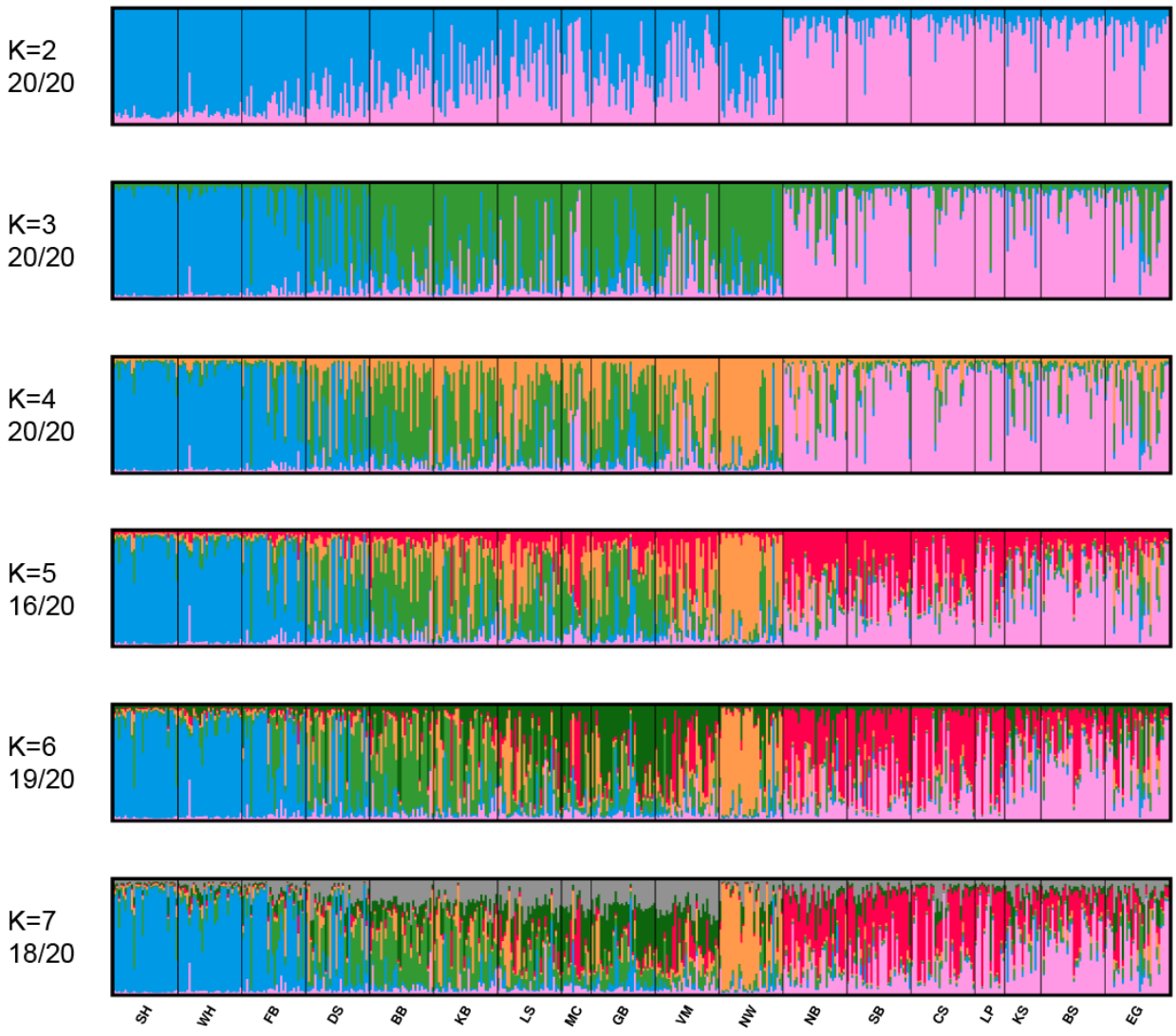

Figure 2.2. CLUMPAK-averaged STRUCTURE outputs for 20 independent runs of *K*=2–7, which were clustered and averaged using CLUMPAK. Numbers under each K-value indicate the proportion of runs that converged to the solution presented. Minority modes supported by at least two runs are provided in Figure A2.10. Management unit abbreviations are as in Table 2.1.

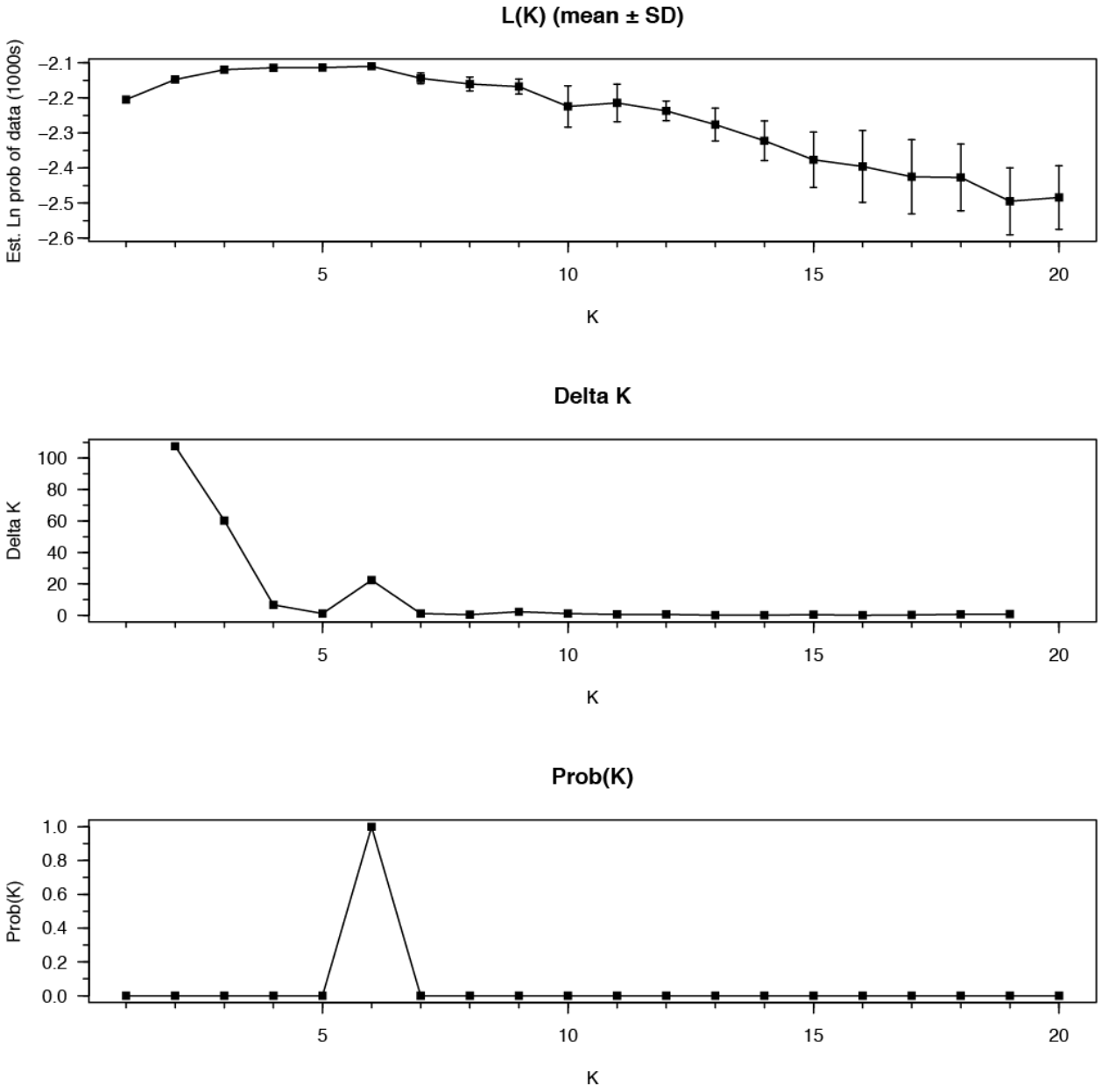

Figure 2.3. (a) STRUCTURE output of mean likelihood ± SD calculated from 20 independent runs for each value of *K* from 1 to 20. (b) *ΔK* calculated using the Evanno method in CLUMPAK. (c) Probability of K calculated using the Pritchard method in CLUMPAK.

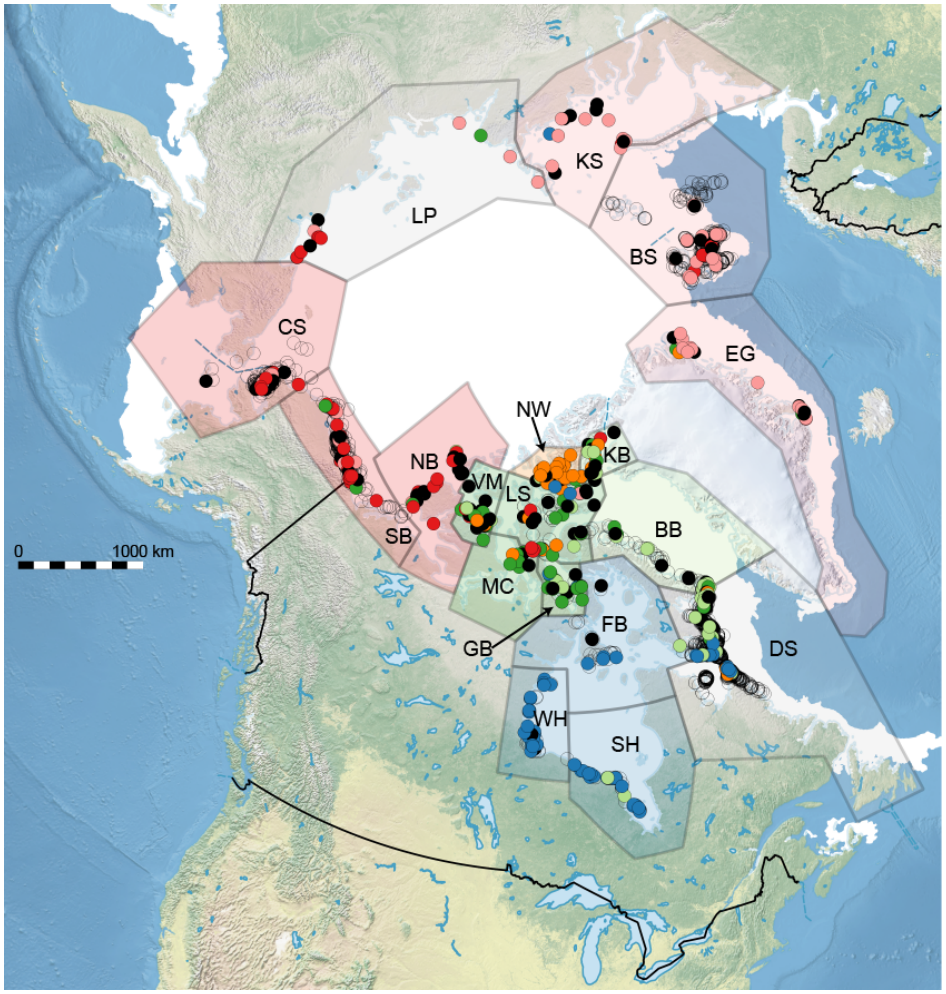

Figure 2.4. Sampling locations for 476 of the 495 polar bears used in this analysis; the remainder did not have lat–long coordinates. Individuals are colour-coded by genetic cluster similarly to the colour scheme for K=6 in Figure 2.2. Black samples are unassigned (i.e., $Q_{max} < 0.5$). Uncoloured individuals are those that were used in the original study but were not included in our random subset of 30 individuals per management unit; their predicted cluster memberships based on BAPS trained clustering are shown in Figure A2.3. Management unit abbreviations are as in Table 2.1. Approximate sea ice extent during the breeding season is shown using measurements for April 15, 2008 (Fetterer *et al.* 2010, updated daily), though there is great spatial heterogeneity in sea ice thickness and concentration, as well as great intra-seasonal and inter-annual variability. Note that this map (and the data) does not reflect a 2014 boundary change between NB and SB made by the territorial governments and the co-management boards with management authority for these two subpopulations, because it has not yet been evaluated by the IUCN Polar Bear Specialist Group.

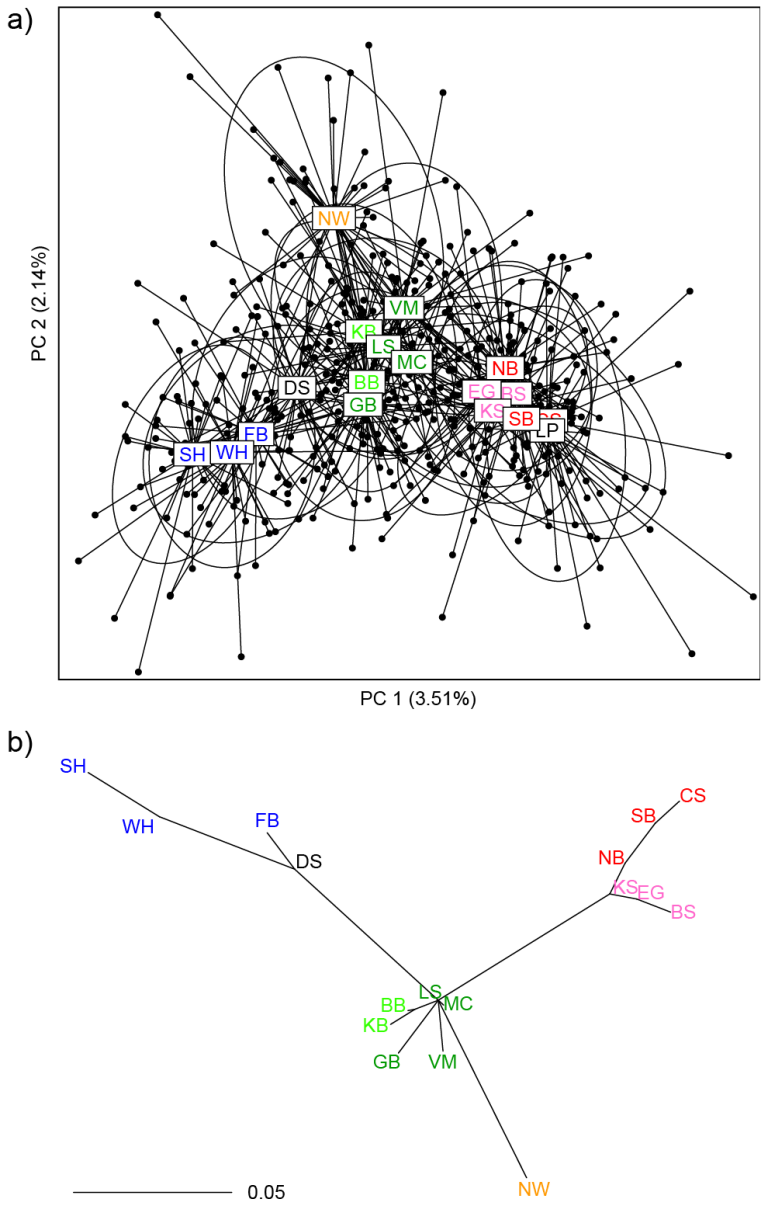

Figure 2.5. (a) Principal component analysis of genetic variation. Each point represents an individual; each individual is connected to a label indicating the centroid of the management unit in which it was sampled. The inertia ellipse for each management unit contains approximately two-thirds of all individuals sampled there. (b) Population tree. The scale bar indicates Nei's standard distance; branch lengths were estimated using non-negative least squares, and the tree has an R^2 (Kalinowski 2009) of 0.903. Samples from the Laptev Sea (LP) have been excluded in (b) because a large spatial discontinuity in sampling in this management unit resulted in it being significantly out of Hardy–Weinberg equilibrium. Management unit abbreviations are as in Table 2.1 and are coloured as in Figure 2.4.

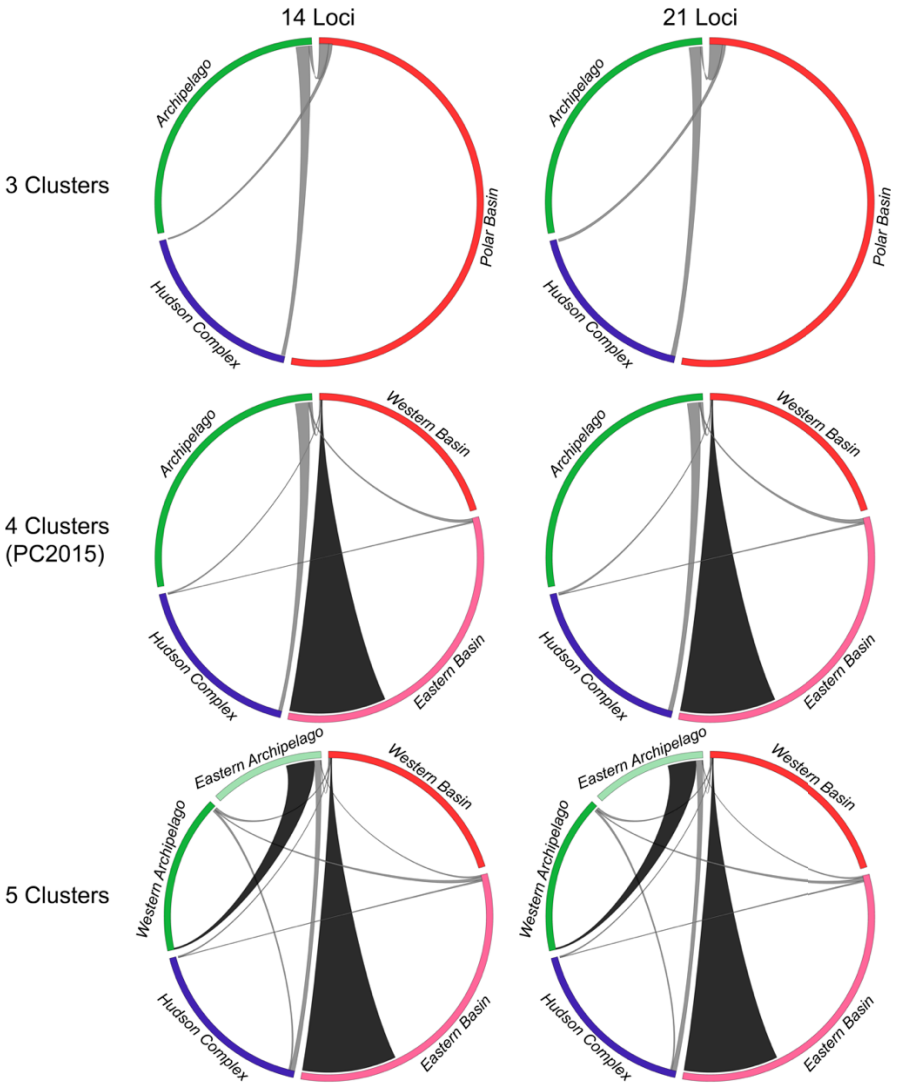

Figure 2.6. CIRCOS plots of gene flow using 14 or 21 loci among: three clusters corresponding to our STRUCTURE results for *K*=4 (excl. Norwegian Bay samples), four clusters identified in PC2015 (excl. Norwegian Bay samples), and five clusters corresponding to our STRUCTURE results for *K*=6 (excl. Norwegian Bay samples). Segment colours are as in Figure 2.4 and are sized proportionally to the population size estimates in S4 Table, though polar bear population sizes are estimated with very broad confidence intervals, particularly in the Polar Basin, where reliable estimates are not available for most MUs. The width of each ribbon where it meets a segment on the circumference indicates the proportion of migrants into (but not out of) each region. Black ribbons are significantly directional based on non-overlapping 95% CIs of immigration rates; grey ribbons are not significantly directional.

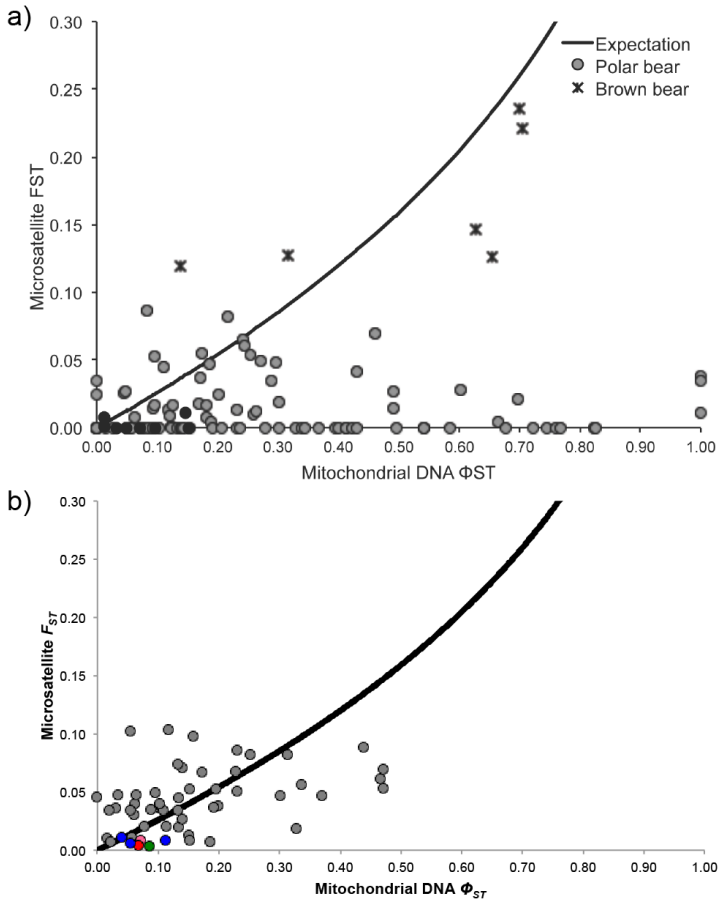

Figure 2.7. Comparisons of pairwise F_{ST} values for nuclear microsatellites with Φ_{ST} values from mitochondrial DNA; the line indicates the expectation of $F_{ST}(nu) = 1 - e^{0.25 \times \ln[1-F_{ST}(mt)]}$ under isolation as given in (Zink & Barrowclough 2008). (a) Supplementary Figure S4 from Peacock *et al.* (2015b), reproduced here under the terms of its Creative Commons CC0 license. (b) A recreated version of this graph, generated using our recalculated F_{ST} and Φ_{ST} values. In (b), M'Clintock Channel, Norwegian Bay, and Viscount Melville Sound were excluded because of inadequate sample sizes for mitochondrial DNA ($N \leq 3$) and the Laptev Sea was excluded because this MU was significantly out of Hardy–Weinberg equilibrium. Points for brown bears were not recalculated and are not shown. Coloured points indicate intra-cluster MU pairs (coloured as in Figure 2.4); grey points indicate inter-cluster MU pairs.

Chapter 3: Design of a 9K Illumina BeadChip for polar bears (*Ursus maritimus*) from RAD and transcriptome sequencing

3.1 Abstract

Single-nucleotide polymorphisms (SNPs) offer numerous advantages over anonymous markers such as microsatellites, including improved estimation of population parameters, finer-scale resolution of population structure, and more precise genomic dissection of quantitative traits. However, many SNPs are needed to equal the resolution of a single microsatellite, and reliable large-scale genotyping of SNPs remains a challenge in non-model species. Here, we document the creation of a 9K Illumina Infinium BeadChip for polar bears (*Ursus maritimus*), which will be used to investigate: 1) the fine-scale population structure among Canadian polar bears, and 2) the genomic architecture of phenotypic traits in the Western Hudson Bay subpopulation. To this end, we used restriction-site associated DNA (RAD) sequencing from 38 bears across their circumpolar range, as well as blood/fat transcriptome sequencing of 10 individuals from Western Hudson Bay. 6000 RAD SNPs and 3000 transcriptomic SNPs were selected for the chip, based primarily on genomic spacing and gene function respectively. Of the 9000 SNPs ordered from Illumina, 8042 were successfully printed, and—after genotyping 1450 polar bears—5441 of these SNPs were found to be well clustered and polymorphic. Using this array, we show rapid linkage disequilibrium decay among polar bears, we demonstrate that in a subsample of 78 individuals, our SNPs detect known genetic structure more clearly than 24 microsatellites genotyped for the same individuals, and that these results are not driven by the SNP ascertainment scheme. Here we present one of the first large-scale genotyping resources designed for a threatened species.

3.2 Introduction

Single-nucleotide polymorphisms (SNPs) are the most common type of sequence variation in the genome (Brumfield *et al.* 2003) and have many advantages over other markers, including better-understood mutational processes, lower rates of homoplasy, more even genomic distribution, and lower genotyping error rates (Ball *et al.* 2010; Morin *et al.* 2004). However, due to their biallelic nature and lower heterozygosity, each individual SNP is inherently less informative than a highly polymorphic genetic marker such as a microsatellite, and—depending on species and application—up to 20 times as many SNPs as microsatellites may be needed to achieve similar resolution (Guichoux *et al.* 2011). Because they are easier to genotype in large numbers, SNPs can provide more accurate parentage assignments (Hauser *et al.* 2011) and linkage maps (Ball *et al.* 2010), better estimates of population genetic parameters (Coates *et al.* 2009) and genome-wide heterozygosity (Miller *et al.* 2013), better inference of population structure (Liu *et al.* 2005), and finer-scale trait localization in genome-wide association studies (GWAS; Jorgenson & Witte 2007).

SNP genotyping is easily automated and is cost-effective at large scales, and SNPs are now the most commonly used genetic marker for studies of humans and livestock, with millions of SNPs discovered in many domestic species (e.g., Frazer *et al.* 2007; Gibbs *et al.* 2009; Lindblad-Toh *et al.* 2005). With the advent of next-generation sequencing and customizable SNP genotyping arrays, SNPs are gradually gaining predominance for many applications in molecular ecology as well (Ekblom & Galindo 2011). However, because SNP polymorphism decays exponentially with species divergence time (Miller *et al.* 2012a), the cross-species transferability of SNPs is limited and they generally must be developed anew for each species. Smaller-scale SNP assays (e.g., Sequenom iPLEX, Illumina GoldenGate) have been created for a number of natural populations, such as Antarctic fur seals (*Arctocephalus gazella*; Hoffman *et al.* 2012) and jack/lodgepole pine (*Pinus* spp.; Cullingham *et al.* 2013). Because of cost, larger-scale SNP genotyping assays, such as Illumina's Infinium BeadChip, have seen limited use outside of agro-economically or biomedically valuable species, though they have previously been developed for great tits (*Parus major*; van Bers *et al.* 2012), house sparrows (*Passer domesticus*; Hagen *et al.* 2013), and flycatchers (*Ficedula* spp.; Kawakami *et al.* 2014a).

In this paper, we document our development of a 9K Illumina Infinium BeadChip array for polar bears (*Ursus maritimus*), a Holarctic species of pagophilic marine mammal that is currently threatened because of anticipated climate-change-induced habitat loss (Wiig *et al.* 2015). Population boundaries are expected to change in response to habitat change, which may cause population overlap and genetic mixing (Derocher *et al.* 2004), and genetic monitoring of such changes would benefit from the development of high-resolution genetic tools. Our SNP array was developed with the primary goal of reassessing the population structure of Canadian polar bears (Paetkau *et al.* 1999) with a focus on the fine-scaled population structure of the southerly Hudson Complex and Labrador ecoregions (*sensu* Spalding *et al.* 2007). SNPs have already proved useful for detecting population substructure in polar bears: using only 100 SNPs, Miller *et al.* (2012b) detected significant genetic clusters corresponding to the eastern and western polar basin, which were previously thought to comprise a single cluster and are only slightly genetically differentiated using microsatellites (Paetkau *et al.* 1999). Together with a recently created pedigree of 4106 polar bears from Western Hudson Bay (Malenfant *et al.*, forthcoming), this array will also be used for quantitative genetic analysis of phenotypic data collected by Environment and Climate Change Canada since the 1960s that show an ongoing decline in body size and condition due to loss of sea ice (Stirling & Derocher 2012).

To some extent, the dual purposes of our chip—population genomics and quantitative genetics—are at odds with one another: in a GWAS, loci with higher minor allele frequency (MAF) have greater power to detect an association (Spencer *et al.* 2009), whereas retention of rare alleles is important in population genetics to reduce bias in estimates of population parameters (Lachance & Tishkoff 2013). Therefore, we selected restriction-site associated DNA (RAD; Baird *et al.* 2008) SNPs without a strict MAF cutoff for use in population genomics and transcriptomic SNPs in potential genes of interest with an apparent MAF cutoff of 0.2 for use in Western Hudson Bay quantitative genetics. Although SNPs have recently been used to characterize the divergence of polar bears and brown bears (*U. arctos*) and the species' subsequent hybridization and adaptation (Cahill *et al.* 2013; Cronin *et al.* 2014; Liu *et al.* 2014; Miller *et al.* 2012b), this paper marks the first major step in application of SNPs to the large-scale population genomics and quantitative genetics of contemporary polar bear populations.

3.3 Materials and methods

3.3.1 Transcriptome sequencing, assembly, annotation, and SNP detection

Our transcriptome assembly and SNP detection process is fully described in Genomic Resources Development Consortium *et al.* (2014). In brief, we used a candidate-gene approach, in which our goal was to select SNPs within putative genes of interest having moderate or high minor allele frequency based on read counts in Western Hudson Bay. We obtained blood and fat samples from 10 sedated wild polar bears (five lactating females and five unrelated dependent cubs) in Western Hudson Bay, which were immediately preserved in RNA*later*. After creating four pooled libraries (i.e., adult blood, adult fat, cub blood, cub fat) of duplex-specific thermostable nuclease normalized cDNA, we performed paired-end sequencing (2×100-nt reads) in four lanes of a flow cell on an Illumina HiSeq 2000 (i.e., one lane per pooled library).

We assembled the four pooled transcriptomes separately by aligning chastity-filtered Illumina reads to the draft polar bear genome (Li *et al.* 2011) using BOWTIE, TOPHAT, and CUFFLINKS (Langmead *et al.* 2009; Trapnell *et al.* 2009; Trapnell *et al.* 2010). Putative transcript identities were assigned using BLAST (blastx; Altschul *et al.* 1997) against a complete mammalian RefSeq protein database. "Full-length" transcripts (i.e., those covering ≥90% of their best BLAST hit) were further annotated with Gene Ontology (Ashburner *et al.* 2000) information using BLAST2GO (Conesa *et al.* 2005). After removal of read duplicates, SNPs were detected from a SAMTOOLS-generated pileup (Durbin *et al.* 2009) using a custom Perl script (parameters: coverage ≥ 10, frequency of minor allele ≥ 0.2, read support for minor allele ≥ 3, number of alleles = 2) developed to better handle REFSKIPs in our spliced alignment, and were screened for systematic Illumina errors using SYSCALL (posterior probability ≥ 0.95; Meacham *et al.* 2011). Flanking regions for probe design were extracted directly from genomic sequence, obviating the need to check if probes overlapped an exon–exon boundary in the transcriptome.

3.3.2 RAD sequencing and SNP detection

Currently, 20,000–25,000 polar bears exist in 19 global subpopulations (Obbard *et al.* 2009), and approximately two-thirds of all bears are estimated to live in the 13 subpopulations that are partially or wholly under Canadian jurisdiction. These subpopulations fall into four major genetic clusters (Paetkau *et al.* 1999; i.e., the Beaufort Sea, the Arctic Archipelago, Norwegian Bay, and Hudson/Labrador; cf. Figure 3.1) which correspond roughly to differences in sea ice

condition (Amstrup *et al.* 2007) and diet (Thiemann *et al.* 2008b). Because we initially planned to do a range-wide population genetics study (but were unable to obtain non-Canadian samples after SNP chip development), we performed RAD sequencing on a collection of 38 bears from across their global range (Table A3.1), primarily using DNA extracted from skin or blood samples collected from 1986–1996 and stored at –40°C at the University of Alberta since the last global assessment of population structure (Paetkau *et al.* 1999). When available, more recent samples were used, which were provided by hunters from Canada's legal harvest or collected during scientific sampling conducted under the auspices of local governmental authorities. Handling procedures were approved by federal, provincial, or territorial Animal Care Committees.

Total genomic DNA for 32 Canadian samples, a pool of three Russian samples, a pool of two American samples, and a single Svalbard sample (Table A3.1) were submitted to Biota Sciences (Portland, OR, USA), who generated the RAD library and performed sequencing using their proprietary LongRead® protocol. In brief, each individual sample (or pool of samples) was digested with Sbf1, barcode-linker adapted (incl. 6-nt barcodes), sheared, reverse-adapted, size-selected, and pooled prior to sequencing. Samples were sequenced by Illumina FastTrack Genotyping Services (San Diego, CA, USA) as five lanes of paired-end (2×100 nt) reads on an Illumina HiSeq2000. All quality control, assembly, alignment, and SNP calling were performed by Biota Sciences using proprietary pipelines of open-source software. The polar bear genome had not yet been released at the time that RAD sequencing was performed, therefore a *de novo* assembly was created with VELVET (Zerbino & Birney 2008) for the individual with the highest median coverage (149,046 RAD clusters having 5×–500× coverage; median coverage = 102). This assembly was used as a reference sequence against which to align reads from other individuals using BOWTIE (Langmead *et al.* 2009), and SNPs were called using SAMTOOLS. Only SNPs that were suitable for probe design (i.e., ≥50 flanking bases on each side of the SNP are known, with no other SNPs within 25 bases of the desired SNP) were retained, and each SNP must have been unambiguously located on the reference and been genotyped in ≥75% of the RAD-sequenced individuals.

3.3.3 SNP chip development

Illumina's Infinium iSelect HD BeadChip is a hybrid platform allowing the simultaneous examination of two different SNP assays known as "Infinium I" and "Infinium II", which use

allele-specific primer extension (ASPE) and single-base extension (SBE) respectively for SNP allele determination (Gunderson 2009). The SBE Infinium-II assay can only interrogate [A/C], [A/G], [C/T], and [G/T] SNPs, however, each SNP can be genotyped using a single probe; whereas the ASPE Infinium-I assay can genotype all SNP classes but each requires two probes. Because BeadChips are priced based on the number of probes rather than the number of SNPs interrogated, it is more economical to use Infinium-II assays whenever possible. Therefore, we followed other studies that have prioritized Infinium-II SNPs or used them exclusively (e.g., Hagen *et al.* 2013; Ramos *et al.* 2009; Tosser-Klopp *et al.* 2014; van Bers *et al.* 2012), and our first step was to exclude triallelic and Infinium-I SNPs from both our transcriptomic and our RAD data.

We filtered our remaining transcriptomic SNPs by mapping each gene's ontology category onto a customized GO Slim created using OBO-EDIT 2.1 (Day-Richter *et al.* 2007) for the 63 categories of biological interest in Table A3.2. The polar bear genome became available in 2011 in the interim between RAD sequencing and SNP chip development (as 72,214 unannotated scaffolds; N50 = 16 Mb, longest = 67 Mb), therefore we filtered RAD contigs by BLASTing (blastn, e-value = 10^{-5}; Altschul *et al.* 1997) the 121-nt SNP-flanking sequences within each RAD contig to the polar bear genome, retaining only those that mapped unambiguously. We submitted all remaining SNPs to Illumina for probe design and scoring, retaining all SNPs with design score ≥ 0.8. We then BLASTed (blastn-short: e-value = 100, word size = 7) all 50-nt probes to the polar bear genome, retaining only those SNPs whose probes mapped unambiguously.

We manually selected 6000 RAD SNPs from across the genome, attempting to obtain a number relative to the length of each scaffold while maintaining high probe-design scores. Because the extent of linkage disequilibrium (LD) was previously unknown in polar bears, we intentionally selected RAD SNPs with a variety of spacings (min. = 10 kb). To reduce the effects of ascertainment, RAD SNPs were selected without any consideration of origin or frequency in the ascertainment sample. 2988 transcriptomic SNPs were also selected manually based on design score and gene product. 12 additional genic SNPs (in ACSL1, ADRB2, APOB, CYPTA1, GCG, GYS2, IGF1, IGF1R, IGSF1, MAP2K, PPARD, and SST) previously discovered in our lab through Sanger sequencing were also included. (These 12 SNPs are included in the "transcriptomic SNPs" for all analyses in this paper.) All 9000 probe designs were then submitted to Illumina for printing.

3.3.4 SNP chip and microsatellite genotyping

We genotyped 1464 polar bear samples on the chip, including 1450 individuals and 14 duplicate samples for estimation of genotyping error rates. Samples were collected between 1985 and 2012, and DNA was extracted using DNeasy Blood & Tissue Kits (Qiagen, Hilden, Germany) and quantified using a NanoDrop™ spectrophotometer. 250 ng (50 ng/ml) of genomic DNA was used for whole-genome amplification, BeadChip hybridization, primer extension, and staining. These procedures were conducted according to Illumina's recommended protocols at the University of Alberta and at Delta Genomics. SNPs were genotyped using GENOMESTUDIO 2011.1 (Genotyping Module 1.9; Illumina) using its automated clustering feature (default settings) after the removal of low-quality samples (i.e., genotyping success rate < 0.9). Clustering patterns for all SNPs were manually examined, and SNPs were removed if they were monomorphic, had low call rates, or had unusual clustering patterns suggestive of problematic loci (cf. Hoffman *et al.* 2012). SNPs were flagged (but not removed) if they displayed clustering patterns suggesting sex-linked inheritance (Figure A3.1). Of the 1450 individuals typed, 865 were from Western Hudson Bay, 299 were from other subpopulations in the Hudson and Labrador ecoregions, 282 were from all remaining Canadian subpopulations, and four were from the Arctic Basin.

To compare population structure determined using SNP and microsatellite markers (see below for "Preliminary population genetics study"), we also genotyped 78 individuals at 24 microsatellite loci. Alleles were resolved on an Applied Biosystems 3730 DNA Analyzer and sized relative to GENESCAN size standards. Genotyping was performed using the program GENEMAPPER (Applied Biosystems, Foster City, CA, USA). Genomic locations of microsatellite loci were obtained using e-PCR (Schuler 1997), summary statistics for each microsatellite locus were calculated using GENALEX 6.501 (Peakall & Smouse 2012), and tests of LD between each pair of loci were conducted using GENEPOP ON THE WEB 4.2 (Rousset 2008).

3.3.5 Linkage disequilibrium decay and sex determination

We modified the open-source program PLINK 1.07 (Purcell *et al.* 2007) to allow it to handle all 72,214 scaffolds of the polar bear genome. We then used PLINK to calculate pairwise LD (measured as the correlation coefficient r^2) between all pairs of SNPs having MAF≥0.01 and located within 1 Mb of each other on the same scaffold, for individuals sampled in each of the four major genetic clusters of polar bears previously identified by Paetkau *et al.* (1999) and for the

complete dataset. Because our extensive sampling in Western Hudson Bay includes many family groups, we used pedigree information from this subpopulation (Malenfant *et al.*, forthcoming) to exclude 547 non-founders before calculating allele frequencies and r^2. We binned all r^2 values into 5-kb units and calculated per-bin averages.

In total, 950 females and 500 males were typed, including ≳15 males and ≳15 females from each Canadian subpopulation; 939 female samples and 488 male samples passed quality control. Our array contained 107 X-chromosome SNPs, so we wished to determine if it was capable of sexing individuals based on X-chromosome heterozygosity. We used PLINK 1.9's check-sex feature on 91 MAF-filtered and LD-pruned X-chromosome SNPs (call rate ≥ 0.9, MAF = 0.01, --indep-pairphase 107 1 0.5). Cutoffs for male and female sex calls were made by examining the empirical distribution of inbreeding values for each sex.

3.3.6 Preliminary population genetics study

To assess the suitability of this SNP chip for population genomics, we performed a preliminary study using three males and three females selected randomly from each Canadian subpopulation (78 individuals in total), which we grouped into genetic clusters: the Beaufort Sea (*N*=12), the Arctic Archipelago (*N*=36), Norwegian Bay (*N*=6), and the Hudson Complex (incl. Labrador; *N*=24). We first removed all SNPs having minor allele frequency <0.01, then, because STRUCTURE is sensitive to LD caused by physical linkage between loci (Pritchard *et al.* 2000), we used PLINK's pairwise LD pruning to remove one locus from each pair of loci with r^2>0.5 within a sliding window of 10 SNPs. To test if our RAD ascertainment scheme affected our findings of population structure, we similarly generated a dataset for transcriptomic SNPs.

For both pruned SNP datasets and microsatellites, principal component analyses (PCAs) were performed in ADEGENET 1.4-1 (Jombart & Ahmed 2011) for R 3.1.0, and F_{ST} values were calculated in SPAGEDI 1.4b (Hardy & Vekemans 2002; Weir & Cockerham 1984). For all three datasets, we conducted 20 independent STRUCTURE 2.3.4 runs for *k*=1–7 using the admixture model with correlated allele frequencies (Falush *et al.* 2003). SNPs were run for 200,000 iterations (incl. 100,000 burn-in iterations); microsatellites were run for 600,000 iterations (incl. 100,000 burn-in iterations). The optimal number of genetic clusters was assessed using the output from STRUCTURE HARVESTER 0.6.93 (Earl & Vonholdt 2012), and assignment plots were created using CLUMPP 1.1.2 (Jakobsson & Rosenberg 2007) and DISTRUCT 1.1 (Rosenberg 2004).

3.4 Results

3.4.1 High-throughput sequencing, SNP detection, and chip development

Full results of the SNP discovery and winnowing process are given in Table 3.1. For the transcriptomic data, we generated a total of 371,258 transcripts, of which 36,755 were deemed to be "full length", and we identified 63,020 putative SNPs (Genomic Resources Development Consortium *et al.* 2014). RAD sequencing resulted in 4.6–34.2 million reads per individual (mean ± SD = $14.2\times10^6 \pm 7.7\times10^6$), and alignment to the assembly gave 42,001 SNP-containing RAD contigs in total, 22,978 of which were suitable for printing on a SNP chip (mean per-individual coverage ± SD = 49.7 ± 26.2). 8042 of the 9000 SNPs submitted to Illumina were successfully printed on the chip (≈89.4%). The average (±SD) design score of SNPs submitted to Illumina for printing was 0.97±0.05, and variation in design score over this range was independent of whether SNPs were successfully printed (P=0.521; Table A3.4; Figure A3.2).

Of the 5386 successfully printed RAD SNPs and 2656 successfully printed transcriptomic SNPs, 3411 SNPs and 2030 SNPs respectively were found to be well-clustered, polymorphic, and to have high call rates in GENOMESTUDIO (Table 3.1). The high-quality RAD SNPs were located on 269 scaffolds representing ~2.25 Gb of sequence, or approximately 97.4% of the polar bear draft genome, with average spacing of ~734.6 kb. The number of polymorphic RAD SNPs per scaffold was highly correlated with scaffold length (r^2 = 0.94; Figure 3.2a), and appeared relatively evenly spaced when viewed as a heat map with 1-Mb bins (Figure 3.2b). Transcriptomic SNPs were located on 227 scaffolds, including 21 scaffolds (totalling 22,579,814 bp) not covered by RAD SNPs. Putative gene identities for all transcriptomic SNPs are given in the Online Supplementary Material (doi: 10.13140/RG.2.1.3344.2326). Allele frequency spectra differed considerably for RAD and transcriptomic SNPs (Figure 3.3). The average MAF across all samples was 0.186 ± 0.150 (RAD = 0.141 ± 0.139; transcriptome = 0.262 ± 0.136).

VCF quality score was negatively correlated with the probability that a RAD SNP was polymorphic on the chip (P<0.001; Table A3.4, Figure A3.2), and of the 1934 RAD SNPs that were monomorphic among all individuals genotyped on the chip, 1892 (≈97.8%) had minor alleles that were observed in only one RAD-sequenced sample. 138 RAD SNPs had minor alleles observed in the original sequence data only among the Russia, Chukchi, or Svalbard samples that were not re-genotyped on the chip. Both RAD sequencing depth and the number of sequenced

individuals containing the minor allele were significant positive predictors of RAD SNPs being polymorphic on the chip (P<0.001; Table A3.4; Figure A3.2). Likewise, MAF and sequencing depth were significant positive predictors of transcriptomic SNPs being polymorphic on the chip (P<0.001; Table A3.4; Figure A3.2).

24 individuals were excluded because of low sample quality (i.e., call score < 0.9), leaving 1427 individuals for all downstream analysis. No genotyping inconsistencies were detected among any of the 14 duplicate samples. Because RAD SNPs and transcriptomic SNPs were selected independently during chip design, six transcriptomic SNPs on the chip were inadvertent duplicates of RAD SNPs. These duplicates consistently gave identical genotypes, and whenever relevant, the transcriptomic SNP of each pair was excluded in downstream analysis, such as in calculation of LD decay.

No clustering suggestive of Y-linked inheritance was detected, and SNPs were not located on any of the five scaffolds identified as the polar bear Y chromosome by Bidon *et al.* (2014). 107 SNPs had clustering patterns suggestive of X-linked inheritance, which were located unambiguously on 30 genomic scaffolds (Online Supplementary Material, Table A3.5), including all 12 scaffolds previously identified as part of the X chromosome by Cahill *et al.* (2013). In total, these 30 scaffolds represent 99,830,649 bp of sequence, or approximately 80.6% of the polar bear X chromosome as estimated from the size of the ~123.9 Mb dog X chromosome. Scaffold 141 contained SNPs suggesting both X-linked and autosomal inheritance. Distributions of X-chromosome F-values for males and females are given in Figure 3.4. Cutoffs for genetic sexing were empirically estimated as F≤0.7 for females and F≥0.9 for males, according to which, the sexes of six genetically male samples and four genetically female samples had been incorrectly supplied to us. Four male samples were dropped because of low call rate on the X-chromosome and three females were of genetically indeterminate sex using this method. Sexes of harvested samples were significantly more likely to have been incorrectly supplied than scientifically collected samples (7/238 vs. 3/1185; G-test of independence with Williams' correction: G=12.75, d.f.=1, P<0.001). Six X-linked SNPs were heterozygous among 44,254 total male genotypes, suggesting an error rate of 0.014%. All X-linked SNPs were excluded from subsequent LD and population genetics analyses.

3.4.2 Linkage disequilibrium decay

We found that LD decays rapidly, though the rate of LD decay in Norwegian Bay was substantially lower than in any other genetic cluster (Figure 3.5). In all groups of polar bears except for Norwegian Bay, binned r^2 values never exceed 0.4, suggesting that strong LD ($r^2 \geq 0.5$) generally decays within 5000 bp. Likewise, moderate LD ($r^2 \geq 0.2$) does not extend beyond 30,000 bp in any group of polar bears except for Norwegian Bay, in which it is observed at distances of up to 120,000 bp. LD appears to asymptote to the background at ~600 kb.

3.4.3 Preliminary population genetics study

Complete 24-locus microsatellite genotypes were obtained for all 78 individuals. Summary statistics for each locus are given in Table A3.3. Though two pairs of microsatellite loci were linked on the same scaffold, no pair displayed significant LD after a strict Bonferroni correction. The results of the RAD and transcriptomic principal component analyses are highly similar (i.e., near-perfect mirror images) and provide clear separation between genetic clusters in contrast to microsatellites, in which the inertia ellipses containing ~2/3 of data points overlap substantially (Figure 3.6).

Average pairwise F_{ST} was calculated as 0.054 and 0.049 using RAD and transcriptomic SNPs respectively—and 0.064 for microsatellites—suggesting moderate differentiation among regions (Table 3.2). Pairwise F_{ST} values were highly similar for both SNP ascertainment schemes: though transcriptomic F_{ST} values were equal to or less than those calculated from RAD SNPs, they generally differed by less than 0.01, and 95% confidence intervals for the two SNP types overlap. Though F_{ST} values from both SNP types were consistently lower than those calculated from microsatellites, this difference was not significant, because of broad confidence intervals for microsatellites.

For microsatellites, k=3 was selected using both the Evanno "ΔK" and Pritchard "$\Pr(K|X)$" methods. For both RAD and transcriptomic SNPs, k=2 was suggested as optimal using the Evanno method, while the Pritchard method selected k=4. Because the Evanno method often returns only the top level of stratification in a hierarchical population structure (Evanno *et al.* 2005), and because the Pritchard method seems to outperform the Evanno method in cases of slight or moderate genetic differentiation (Waples & Gaggiotti 2006), we chose to accept k=4 for both SNP datasets. Admixture plots from STRUCTURE analyses are shown in Figure 7; plots of ΔK and

Pr($K|X$) are given in Figure S3 (Supplementary Material). STRUCTURE results for SNPs for k=4 correspond strongly with the four previously known genetic clusters, however at these sample sizes, microsatellites cannot distinguish between the Beaufort Sea and the Canadian Archipelago. A number of samples belonging to the Archipelago cluster are apparent in Hudson–Labrador: these represent samples from Davis Strait—an area that is actually intermediate between clusters (Paetkau *et al.* 1999).

3.5 Discussion

3.5.1 SNP chip design

SNP chip design was successful: approximately 89.4% of submitted SNPs were printed on the array, which is comparable to the ~90% success rate in many other BeadChip design studies (e.g., Kawakami *et al.* 2014a; McCue *et al.* 2012; Tosser-Klopp *et al.* 2014; van Bers *et al.* 2012). Illumina design score was not a significant determinant of design success over the range of values used, suggesting that in the design of a medium-density SNP chip—as long as a suitable minimum such as 0.8 is enforced—design score may be treated as a secondary consideration to factors such as evenness of spacing between SNPs or to factors that predict true polymorphism, such as sequencing depth and minor allele frequency. This suggested design score cutoff of 0.8 corresponds to the most stringent tier of SNPs used in designing the BovineSNP50 (Matukumalli *et al.* 2009) and PorcineSNP60 (Ramos *et al.* 2009) arrays, which achieved design successes in excess of 95%.

Approximately one-third of printed SNPs were found to be monomorphic among all individuals typed on the chip, even though all Canadian samples used for SNP ascertainment were re-genotyped on the chip. This is lower than the 75–95% polymorphism rate often achieved in other SNP chip studies (e.g., Hagen *et al.* 2013; van Bers *et al.* 2012; Xu *et al.* 2014). Because our RAD ascertainment panel also contained non-Canadian bears that were not chip-genotyped, a small number (≤138) of these apparently monomorphic SNPs may represent alleles private to non-Canadian subpopulations; however, most are likely a side effect of our RAD SNP selection scheme, in which—unlike most previous studies—we actively avoided selecting SNPs based on MAF to minimize the effects of ascertainment (although there is necessarily an intrinsic bias caused by ascertainment in only a few individuals). Although we were successful in retaining a large number of rare alleles in our RAD data (Figure 3.3), this came at a cost: ~98% of

monomorphic RAD SNPs were discovered in a single sample. When loss of rare alleles is not a concern, we strongly recommend selecting SNPs called in at least two sequenced individuals. In contrast to our RAD data, transcriptomic data showed more obvious signs of ascertainment, having a dearth of rare alleles. This is due to our enforcement of an apparent MAF cutoff of 20% in the transcriptomic data, as well as the source of ascertainment: transcriptomic SNPs were ascertained in Western Hudson Bay and ~80% of individuals in the total sample were from that subpopulation or neighbouring subpopulations.

Similarly to van Bers *et al.* (2012), we found that VCF quality score was negatively associated with the probability that a RAD SNP was found to be polymorphic on the chip. This may indicate susceptibility in SAMTOOLS' SNP-calling algorithm to systematic or sequence-specific Illumina error (Meacham *et al.* 2011; Nakamura *et al.* 2011). Though methods exist to calculate the probability of systematic error (SYSCALL; Meacham *et al.* 2011) and recalibrate qualities based on confirmed SNPs (GATK-VQSR; DePristo *et al.* 2011), these were not used as part of Biota's SNP-calling protocol. In the absence of such procedures, it seems that VCF quality score may sometimes poorly predict true polymorphism, and MAF and read depth may be better criteria when selecting SNPs for chip design. Though we used SYSCALL on our transcriptomic data prior to SNP selection, ~22% of printed transcriptomic SNPs were still found to be monomorphic on the chip. Though RNA editing is rare, RNA normalization may result in a relative amplification of rare edited variants leading to false SNP calls in high-throughput sequencing data (van Bers *et al.* 2012). Therefore, when designing a genomic SNP assay from transcriptomic data, it may be beneficial to screen for RNA editing prior to SNP selection (e.g., using REDITOOLS: Picardi & Pesole 2013). Another likely source of error is the rudimentary SNP-calling script we created, which is based strictly on frequency of read counts for each allele. In contrast to more advanced Bayesian approaches (e.g., Li *et al.* 2008) that use base quality to determine the probability of error for each genotype, our SNP-calling script did not use these qualities, instead relying on SAMTOOLS for the removal of all low-quality bases from the pileup prior to SNP calling. This may suggest that the default cutoff for SAMTOOLS (Phred score $\geq$ 13) is too low for external frequentist methods of SNP calling using pooled, non-barcoded samples.

3.5.2 Implications for future studies

We found no evidence suggesting that SNP ascertainment scheme affected estimates of population structure, though this may be because of homogenization of allele frequencies due to removal of loci with low MAF in this small sample. All analyses using RAD and transcriptomic SNPs gave highly similar results, and—consistent with the assertion that STRUCTURE is robust to ascertainment (Lachance & Tishkoff 2013)—both SNP datasets yielded virtually identical STRUCTURE results displaying substantially less admixture than microsatellites. Using these modest sample sizes, SNPs are able to recover all four major genetic clusters originally identified with population assignment tests using 16 microsatellites and hundreds of individuals (Paetkau *et al.* 1999). In contrast, our 24 microsatellites were unable to distinguish the Arctic Archipelago and the Beaufort Sea in this study, despite their pairwise F_{ST} of ~0.039 for this marker type. SNP results were concordant with each other with respect to the population of origin of all individuals, but not with those of microsatellites, which suggested that some individuals sampled in the Archipelago had strong ancestry from the Hudson–Labrador cluster. Because our goal is to characterize fine-scale genetic structure, particularly around Hudson Bay, the ability to identify genetically differentiated groups from a small sample size is an asset.

Differences between microsatellites and SNPs were most pronounced in the PCAs, in which microsatellites again failed to clearly separate the Archipelago and Hudson Bay. Though PCAs are easily influenced by ascertainment scheme (Albrechtsen *et al.* 2010), we obtained near-identical results from both SNP datasets, suggesting that these results accurately reflect the large-scale population structure of polar bears in Canada. Pairwise F_{ST} did not differ significantly irrespective of marker type, though this was partially attributable to broad confidence intervals for microsatellites. F_{ST} values obtained from SNPs are more precise and are more likely to be accurate: as few as 4 individuals per population can give accurate F_{ST} estimates for >1000 SNPs (Willing *et al.* 2012), whereas 25–30 individuals may be needed for microsatellites (Hale *et al.* 2012).

In total, SNP genotyping yielded 5441 well-clustered polymorphic SNPs (incl. 6 transcriptomic duplicates) representing 290 scaffolds that comprise ~98% of the genome. Further, we used sex-specific clustering patterns to identify >20% of the polar bear X chromosome that was previously unknown. Expanding the known X chromosome from <60% to ~80% will improve accuracy in assessments of its contribution to sexual dimorphism (cf. Robinson *et al.* 2013) and

may allow for improved estimates of sex-biased admixture (Cahill *et al.* 2013). One scaffold (141) contained SNPs suggesting both X-linked and autosomal inheritance, which may represent errors in BLAST results for probe sequences, a chimeric genome assembly, or the scaffold may overlap the boundary of a pseudoautosomal region. Patterns of heterozygosity among X-linked SNPs were extremely reliable predictors of sex: of 1423 individuals tested, only 3 (=0.21%) could not be sexed unambiguously. Two of these three samples were from Norwegian Bay, an area that likely suffers from low genome-wide heterozygosity because of its small effective population size. Ten (=0.70%) supplied sexes were determined to have been incorrect, and sexes of harvested samples were more likely to have been incorrectly supplied, perhaps indicating misreporting by hunters (to match sex-specific harvesting quotas) or better curation of scientifically collected samples. This heterozygosity method precludes the need to sex samples using existing PCR-multiplex and gel electrophoretic methods (Bidon *et al.* 2013), and demonstrates the applicability of BeadChips for forensics.

LD decays rapidly in most polar bear subpopulations. Slower LD decay in Norwegian Bay reflects its insular nature. In contrast to other subpopulations comprising many hundreds or thousands of bears, Norwegian Bay is a small high Arctic subpopulation of $N \approx 203$ individuals (Taylor *et al.* 2009), and an effective population size of $N_e \approx 36.9$ (based on the N_e/N ratio for polar bears from Cronin *et al.* 2009), which has likely resulted in loss of genetic diversity through inbreeding and drift (Frankham *et al.* 2014). Our LD estimates may generally be deflated by our combination of ascertainment schemes or otherwise affected by the methods with which SNPs were selected, as LD calculations are sensitive to ascertainment (Nielsen & Signorovitch 2003). In particular, because we enforced a minimum distance of 10kb between RAD SNPs and selected only one SNP per gene in the transcriptome, most r^2 calculations in the leftmost two bins of Figure 5 are between transcriptomic and RAD SNPs, whose allele frequency spectra differ considerably. In addition, r^2 is sensitive to MAF, and is likely to increase with higher MAF cutoffs, especially at shorter distances (Yan *et al.* 2009). Nevertheless, the extent of LD among most polar bear subpopulations—including the Hudson Complex, which contains our quantitative genetics study area—is much shorter than in domestic species (e.g., Gray *et al.* 2009), more closely resembling outbred populations of dogs (Gray *et al.* 2009) and humans (Dawson *et al.* 2002). Power in an association study depends on LD between marker and causal locus, and with human-like patterns of LD decay, 300,000–1,000,000 SNPs may be needed to completely represent the genome (Tsui

et al. 2003). Although we will be unable to conduct a true "genome-wide association study" with this SNP chip, we hope that our inclusion of transcriptomic markers and use of methods such as chromosome partitioning (Robinson *et al.* 2013) will allow us to describe the genomic architecture of phenotypic traits in polar bears.

In this paper, we have described the development of a new genotyping array for polar bears and its application to 1450 individuals sampled throughout the Canadian Arctic. In contrast to the sequencing data used to develop the chip—which led to high levels of monomorphism on the chip despite an average sequencing depth of ~50× per individual per locus—chip genotypes were highly reliable, with an estimated error rate of <0.014% based on duplicate samples, loci and male heterozygosity on the X chromosome. By allowing for simultaneous genotyping and sexing of samples, the array also has clear application for forensics. This project represents the broadest-scale genotyping effort ever undertaken for polar bears and one of the largest-scale genetic resources yet produced for a threatened species.

3.6 Data accessibility

SNPs developed from RAD sequencing are available on Dryad (.vcf), as is our customized version of PLINK, and inputs/outputs for the various population genetics analyses in this paper (doi: 10.5061/dryad.b35td). Transcriptome development and SNP discovery have been previously described in Molecular Ecology Resources (doi: 10.1111/1755-0998.12190), and the .vcf and annotation files are archived in Dryad (doi: 10.5061/dryad.606j6).

Table 3.1. Results of SNP winnowing during the SNP chip design and typing phases. "Chip-suitable" = "≥50 flanking bases on each side of the SNP are known, with no other SNPs within 25 bases of the desired SNP". "Uniquely BLASTing" = "SNP-flanking contigs and the 50-bp Illumina probe sequence align uniquely to the polar bear genome." Polymorphism, clustering behaviour and call rate were based on examination of genotypes in GENOMESTUDIO in a sample of 1450 individuals, including all individuals from Canadian subpopulations used for RAD library and transcriptome construction.

		RAD	Transcriptome
SNP chip design	Total SNPs discovered	42,001	63,032
	Chip-suitable	22,978	49,849
	Infinium II	20,428	42,758
	Uniquely BLASTing	18,222	36,947
	Submitted for printing	6000	3000
	Successfully printed	5386	2656
SNP chip typing	Polymorphic	3452	2084
	Good clustering	3418	2047
	Call rate ≥ 0.9	3411	2030

Table 3.2. Pairwise F_{ST} values calculated between the four major genetic clusters of polar bears from Paetkau et al. (1999): the Arctic Archipelago (N=36), the Beauforts (N=12), Hudson Complex (incl. Labrador; N=24), and Norwegian Bay (N=6), using 3046 LD-pruned RAD SNPs, 1778 LD-pruned transcriptomic SNPs, and 24 microsatellites. 95% confidence intervals for average pairwise F_{ST} were calculated from standard errors obtained from jackknifing over loci in SPAGEDI.

	RAD	Transcriptome	Microsatellites
Archipelago–Beaufort	0.028	0.028	0.039
Archipelago–Hudson	0.027	0.025	0.027
Archipelago–Norwegian Bay	0.046	0.040	0.053
Beaufort–Hudson	0.055	0.052	0.065
Beaufort–Norwegian Bay	0.089	0.075	0.097
Hudson–Norwegian Bay	0.079	0.072	0.100
Average (95% CI)	0.054 (0.051–0.057)	0.049 (0.044–0.053)	0.064 (0.040–0.088)

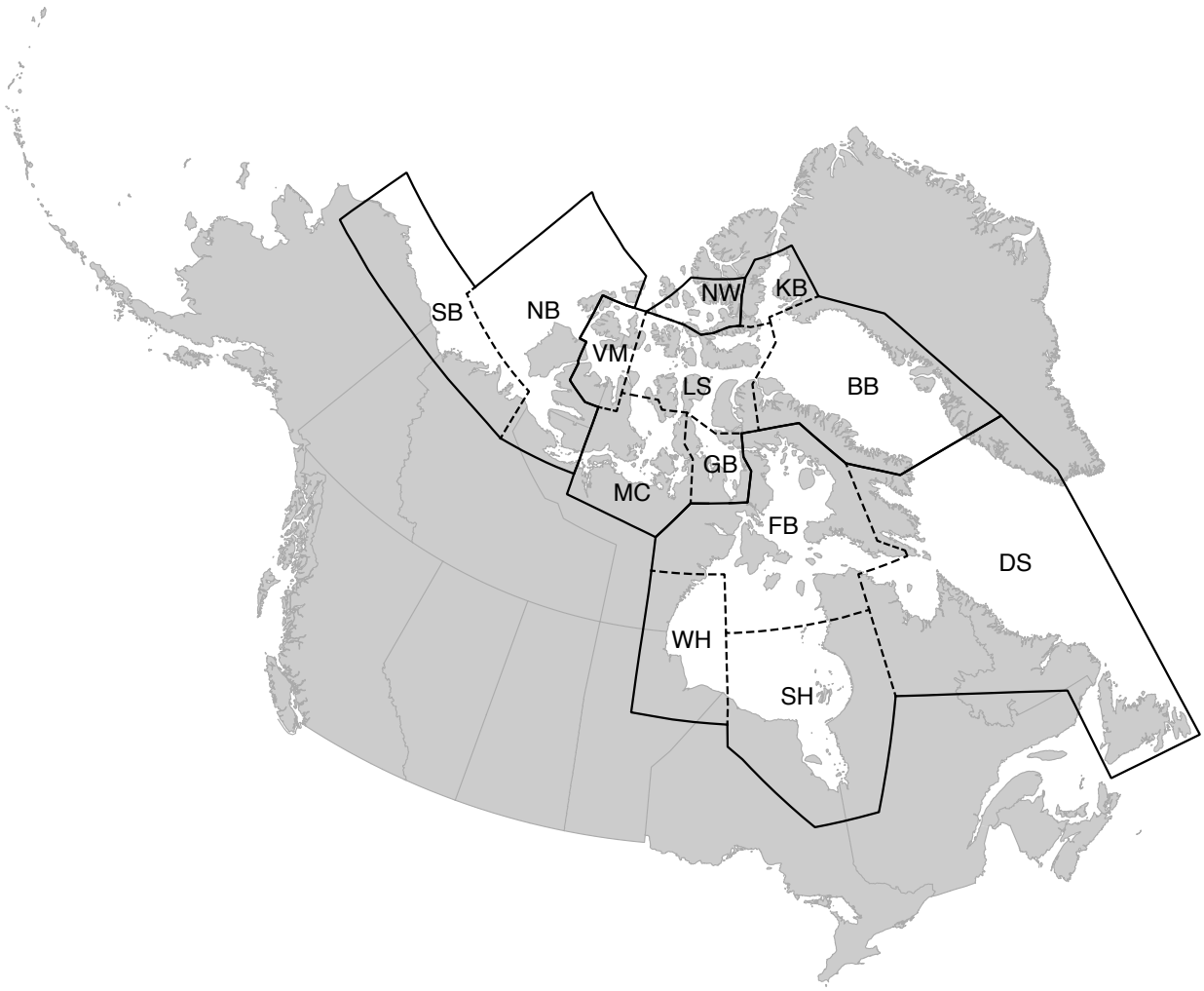

Figure 3.1. Canadian polar bear subpopulations and genetic clusters from Paetkau et al. (1999). Genetic clusters are separated by solid lines; subpopulations within clusters are separated by dashed lines. As used in the present paper, genetic clusters are: the Arctic Archipelago, comprising Baffin Bay (BB), the Gulf of Boothia (GB), Kane Basin (KB), Lancaster Sound (LS), M'Clintock Channel (MC), and Viscount Melville Sound (VM); the Beauforts, comprising the Northern Beaufort Sea (NB) and the Southern Beaufort Sea (SB); the Hudson Complex (incl. Labrador), comprising Davis Strait (DS), Foxe Basin (FB), Southern Hudson Bay (SH), and Western Hudson Bay (WH); and Norwegian Bay (NW), which comprises only a single subpopulation.

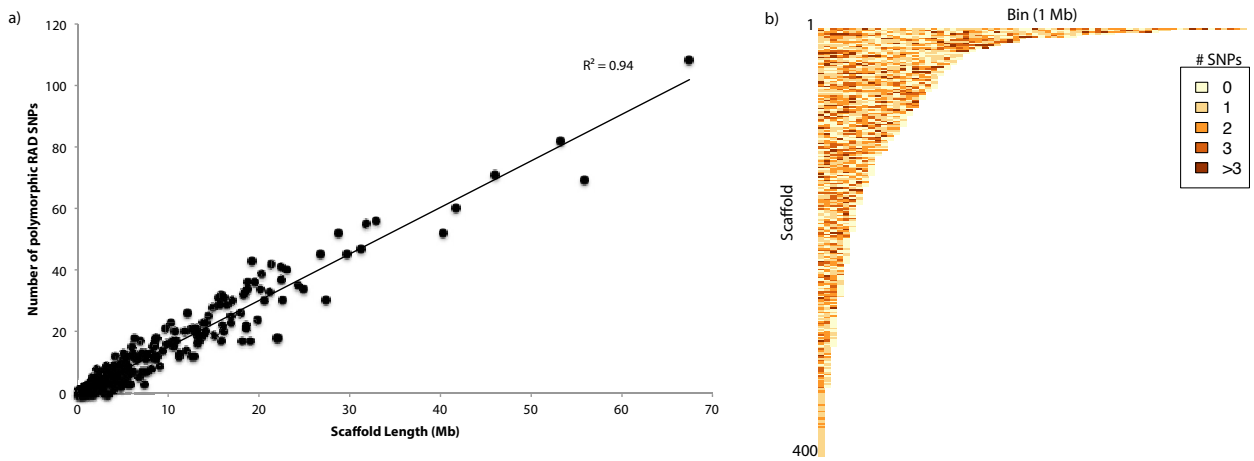

Figure 3.2. a) Least-squares regression of the number of polymorphic RAD SNPs printed on the chip per scaffold as a function of scaffold length. b) Heat map showing distribution of the 3411 polymorphic RAD SNPs across 270 scaffolds of the polar bear genome, with each scaffold divided into 1-Mb bins. Scaffolds are arranged in order of decreasing size, from scaffold1 (67,462,175 bp) to scaffold400 (64,680 bp). Scaffolds in this range that do not contain any SNPs are not displayed.

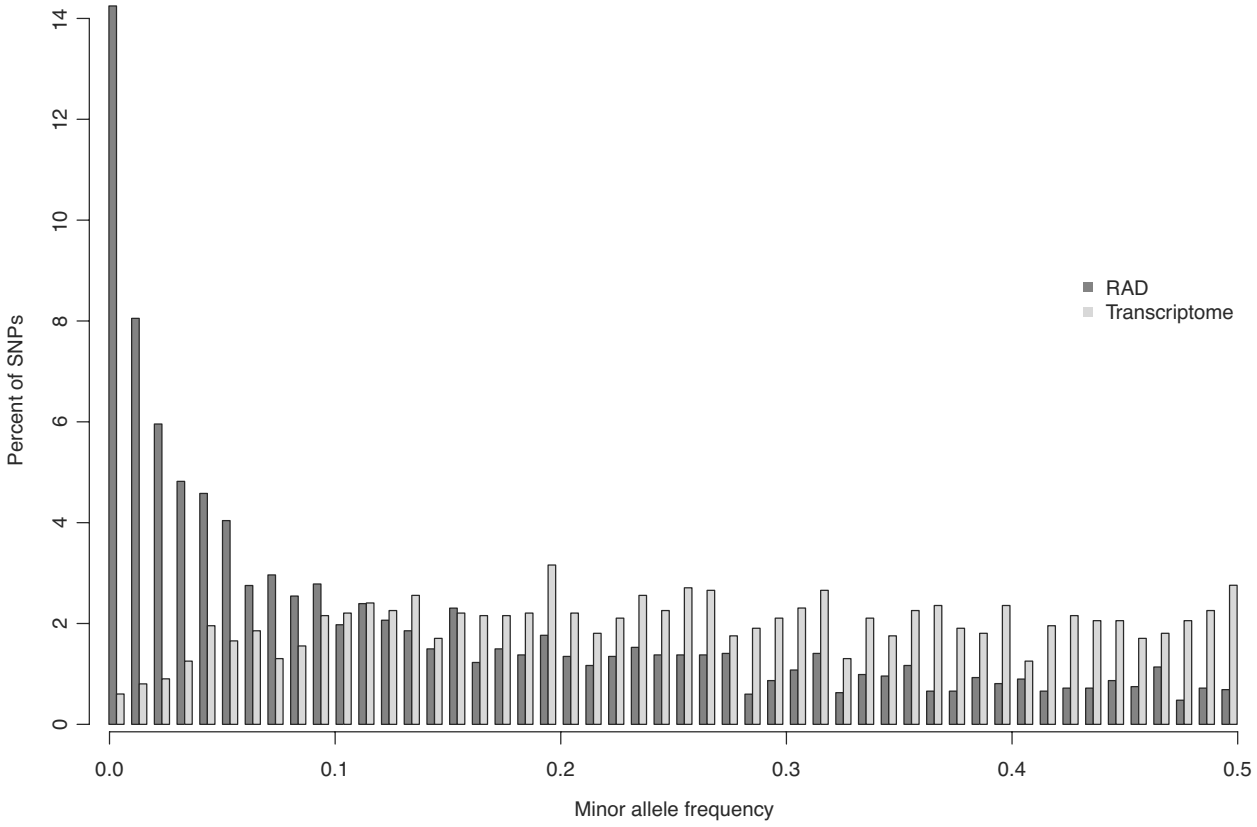

Figure 3.3. Allele frequency spectra for RAD and transcriptomic SNPs among all founder bears sampled (N=880).

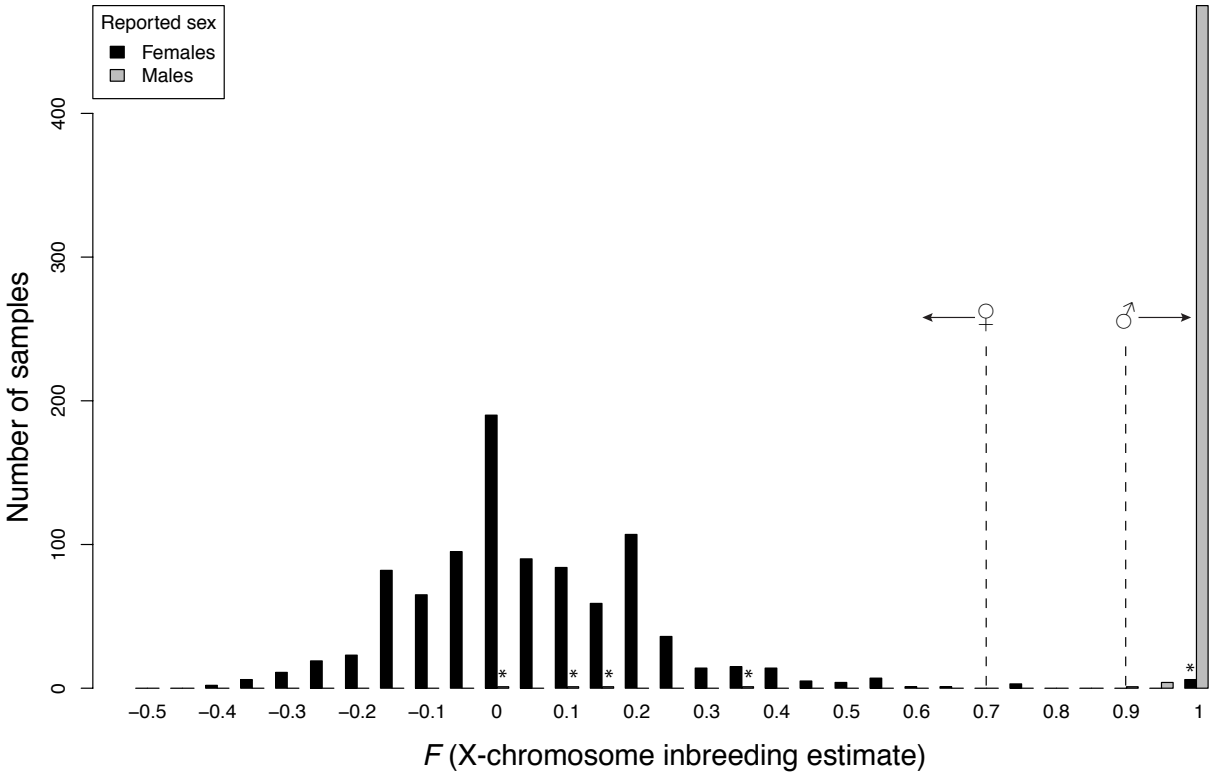

Figure 3.4. Histogram of X-chromosome inbreeding estimates for 1423 individuals (X-chromosome call rate ≥ 0.9), 939 of which were reported as female and 484 of which were reported as male. Dashed lines indicate empirically estimated cut-offs for genetically female samples (♀: ≤0.7) and genetically male samples (♂: ≥0.9); individuals between these boundaries are of indeterminate sex. Asterisks denote samples whose sex was likely misreported.

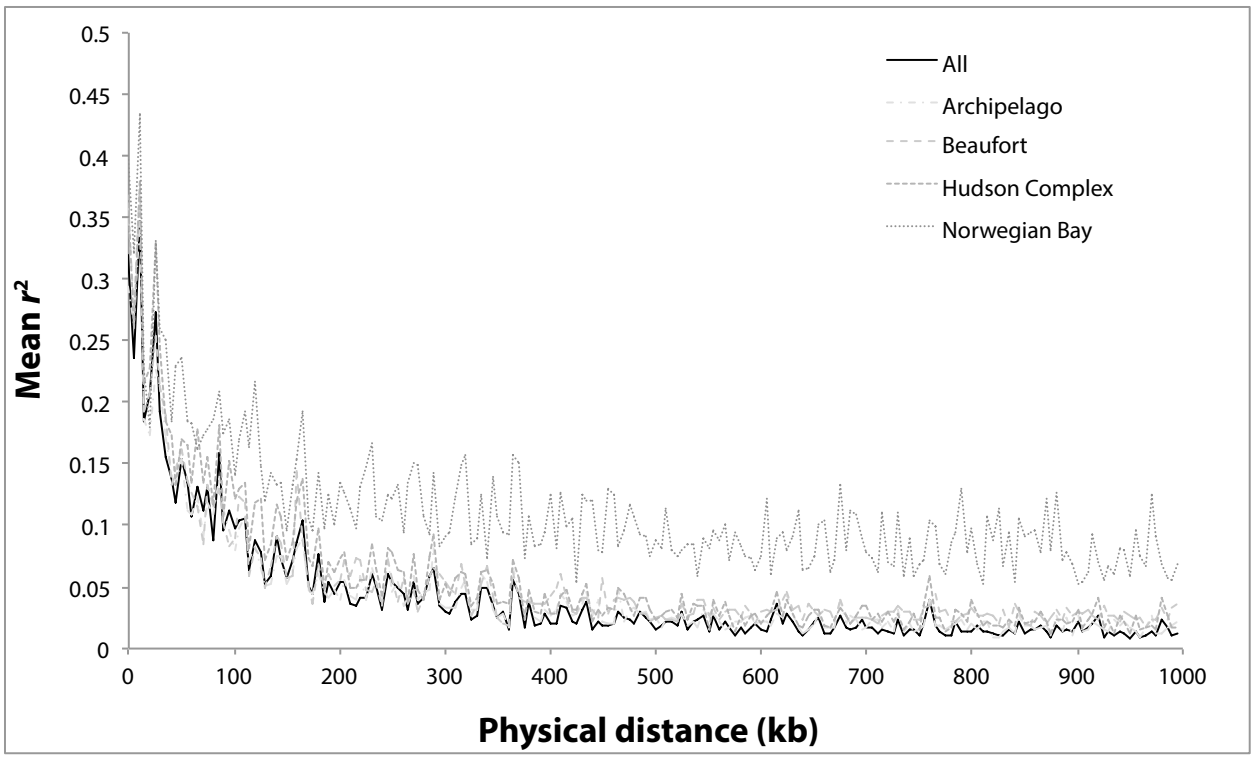

Figure 3.5. Linkage disequilibrium calculated for all filtered autosomal SNPs among all founder bears sampled (*N*=880, incl. 4 Arctic Basin bears), and for all bears sampled in each of the four major Canadian genetic clusters: the Arctic Archipelago (*N*=178), the Beaufort Sea (*N*=63), the Hudson Complex (incl. Labrador; *N*=604), and Norwegian Bay (*N*=31).

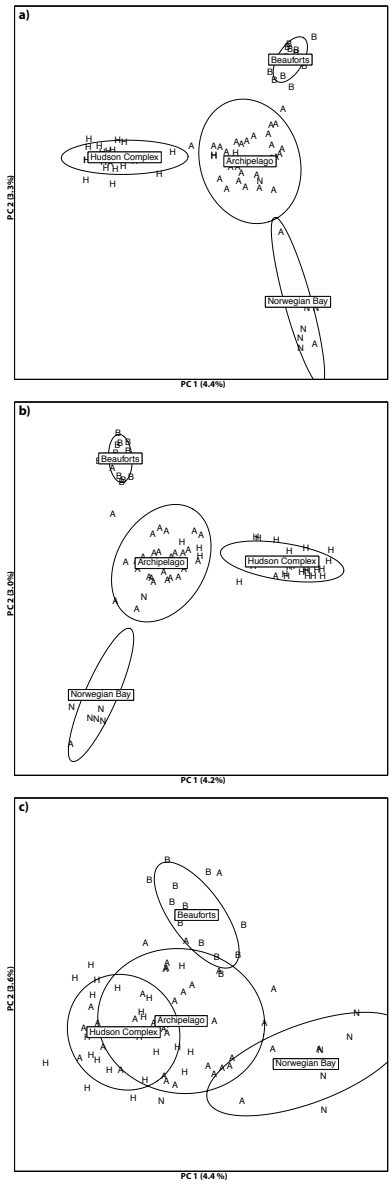

Figure 3.6. Principal component analyses of genetic variation among three randomly selected males and three randomly selected females drawn from each of Canada's 13 subpopulations, grouped into major genetic regions from Paetkau et al. (1999): the Arctic Archipelago (N=36), the Beauforts (N=12), the Hudson Complex (incl. Labrador; N=24), and Norwegian Bay (N=6). Shown are results for: a) 3046 LD-pruned RAD SNPs, b) 1778 LD-pruned transcriptomic SNPs, and c) 24 microsatellites. Individuals of each cluster are represented by the cluster's initial (i.e., 'A', 'B', 'H', 'N'). Inertia ellipses were drawn using default settings in ADEGENET, such that each ellipse contains approximately two-thirds of all data points for its respective group.

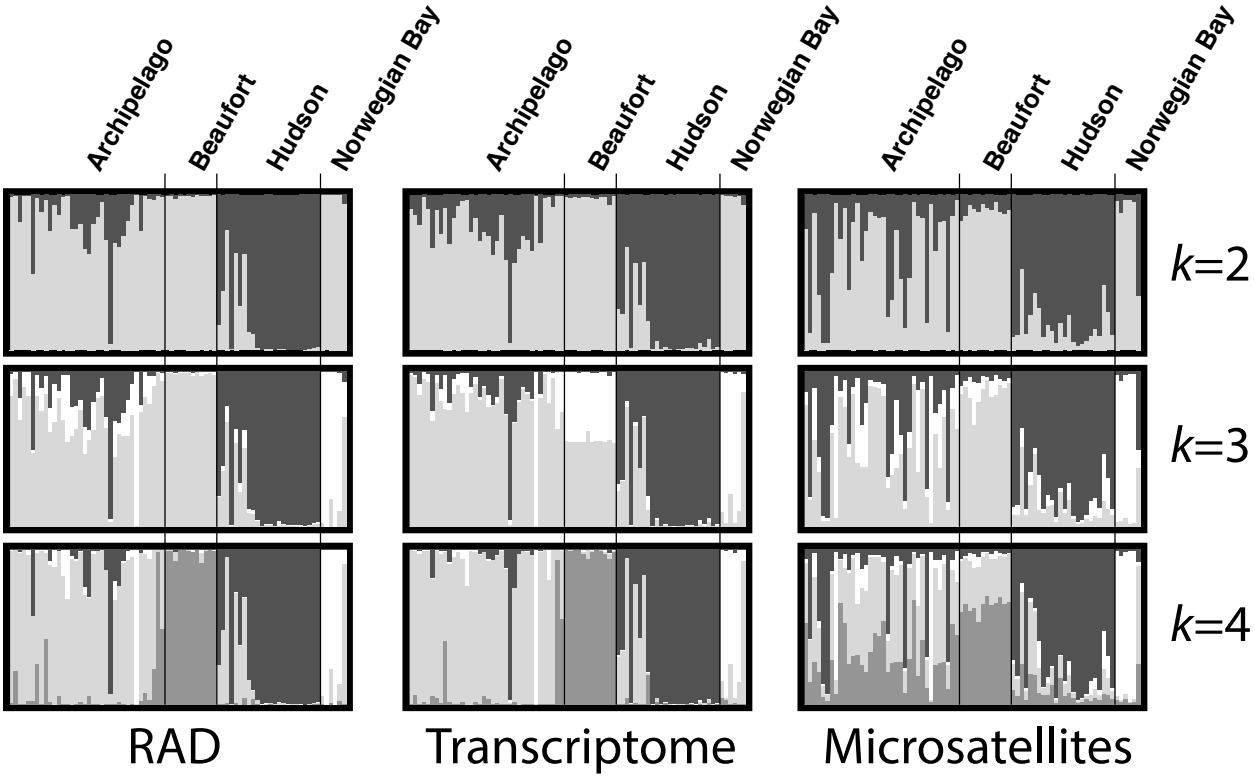

Figure 3.7. Admixture plots for 20 CLUMPP-averaged structure runs of three randomly selected males and three randomly selected females from each of Canada's 13 subpopulations, grouped into major genetic regions from Paetkau et al. (1999): the Arctic Archipelago (N=36), the Beauforts (N=12), Hudson Complex (incl. Labrador; N=24), and Norwegian Bay (N=6). Shown are results using 3046 LD-pruned RAD SNPs, 1778 LD-pruned transcriptomic SNPs, and 24 microsatellites. k=4 was selected for both SNP datasets using the Pritchard method, whereas k=2 was selected by the Evanno method. k=3 was selected for microsatellites using the Pritchard and Evanno methods.

Chapter 4: Population structure of Canadian polar bears determined using thousands of single-nucleotide polymorphisms

Abstract

Polar bears (*Ursus maritimus*) are highly dependent on sea ice for locomotion and mating, but despite observed changes to sea ice caused by Arctic warming, population structure has never been examined using using a high-resolution set of genetic markers. We genotyped 5441 single nucleotide polymorphisms (SNPs) and up to 24 microsatellites in ~30 individuals from each of Canada's 13 management units (MUs). Results from a suite of tests (incl. Bayesian clustering, *k*-means clustering, and AMOVA) confirm previous findings of four slightly–moderately differentiated (F_{CT} = 0.039) regions in Canada, which appear to have been populated from the northwest, and which correspond to the Beaufort Sea, the Arctic Archipelago, Norwegian Bay, and the Hudson Complex. North–south substructure within the Hudson Complex and east–west substructure within the Archipelago was also observed, and genetic clusters and subclusters are related to regional differences in sea-ice regime. All pairs of MUs are significantly differentiated except for the Northern Beaufort Sea and the Southern Beaufort Sea (F_{ST} = 0.001), suggesting that these two MUs may constitute a single panmictic population. Rarefaction analyses show that the Norwegian Bay cluster has suffered loss of genetic diversity owing to small effective population size ($N_e \approx 17.9$), and among the outlier loci that best distinguish this cluster are SNPs in PDLIM5 (associated with dilated cardiomyopathy) and near SLC15A5 (associated with visceral adipose tissue deposition), which could be related to unique ecological and physical characteristics of Norwegian Bay bears.

4.1 Introduction

Polar bears (*Ursus maritimus*) are Holarctic marine mammals, and are highly dependent on the sea ice as a platform for locomotion, hunting, and mating. They prefer areas of annual ice near the continental shelves, which support more productive ecosystems and whose leads provide easy access to their primary prey: ringed seals (*Pusa hispida*) and bearded seals (*Erignathus barbatus*). Before the advent of satellite tracking and genetics, polar bears were believed to be circumpolar wanderers, travelling with the ice in the polar currents (Pedersen 1945). However, because they exhibit broad-scale site fidelity (e.g., Taylor *et al.* 2001) and genetic clustering (Paetkau *et al.* 1999), this romantic view of polar bears as Arctic nomads is now known to be false. Currently, 20,000–31,000 individuals are thought to exist in 19 management units (MUs) worldwide; approximately 50–70% live in the 13 MUs lying partially or entirely within Canadian jurisdiction (Obbard *et al.* 2009; Wiig *et al.* 2015). MUs have been delineated based primarily on harvest and telemetry data; however, most studies have been based on the movements of females—male polar bears cannot easily be radio-collared for long-term tracking because their necks are broader than their heads (Amstrup *et al.* 2001), and consequently little is known about male movement.

Mating takes place on the ice in late spring or early summer, and in areas with a seasonal ice melt, individuals move ashore in late summer. Females den on land in most areas of the Arctic, and give birth in early winter before emerging with their cubs in spring. Polar bears exhibit broad-scale fidelity to oversummering and mating locations (e.g., Lone *et al.* 2013; Stirling *et al.* 2004) and there is limited long-distance migration between MUs (Taylor & Lee 1995), thereby giving rise to genetic population structure. The most comprehensive population genetics studies of polar bears to date have used only 14–21 microsatellite loci (Malenfant *et al.* 2016; Paetkau *et al.* 1999; Peacock *et al.* 2015b), and show four major genetic clusters of polar bears worldwide, represented in Canada by the Beaufort Sea, the Canadian Arctic Archipelago, Norwegian Bay, and the Hudson Complex (incl. Foxe Basin, Hudson Bay and the coasts of Labrador and Newfoundland). Other studies have detected a unique genetic cluster corresponding to James Bay at the southernmost reach of polar bear habitat (Crompton *et al.* 2008; Crompton *et al.* 2014; Viengkone 2015), east–west differentiation in the Canadian Arctic Archipelago (Malenfant *et al.* 2016), and genetic clusters corresponding to the Gulf of Boothia and M'Clintock Channel MUs (Campagna *et al.* 2013).

The four major genetic clusters of polar bears correspond roughly to the major Arctic sea-ice ecoregions comprising polar bear habitat (Amstrup *et al.* 2007). These ecoregions differ in expected response to future climate change, in annual patterns of ice formation and melting, productivity and community composition, and in observed differences in polar bear behaviour. Together with regional differences in diet (Thiemann *et al.* 2008b), these factors have been used to propose the existence of five "designatable units" for conservation and management purposes under Canadian law (Thiemann *et al.* 2008a). However—as these authors note—microsatellites reflect neutral genetic diversity, which may not correspond with the adaptive differentiation considered by the Committee on the Status of Endangered Wildlife in Canada as a criterion for establishing a designatable unit (COSEWIC 2012). Evidence of adaptive differentiation among polar bears is limited: although polar bears differ in morphology and reproductive characteristics throughout their range (e.g., Pertoldi *et al.* 2012; Taylor *et al.* 2009), these differences are not known to be heritable, and in the few studies of potentially adaptive variation conducted to date, polar bears have exhibited little variation in allozymes and in the major histocompatibility complex (Larsen *et al.* 1983; Weber *et al.* 2013).

In this study, we use a recently developed 9K Illumina BeadChip (Malenfant *et al.* 2015a) to reanalyse the population structure of Canadian polar bears. This chip comprises restriction-site associated DNA (RAD) SNPs—the majority of which are in non-coding DNA and are putatively neutral—and potentially adaptive transcriptomic SNPs developed from fat and blood. We use this assay to determine patterns of neutral genetic differentiation and test for adaptive genetic variation across the Canadian Arctic. This is the first comprehensive study of polar bear population genomics and is among the largest-scale SNP studies for any wild species.

4.2 Materials and methods

4.2.1 SNP chip development and genotyping

The SNP chip development process has been described by Malenfant *et al.* (2015a). In brief, we used high-throughput transcriptome and RAD sequencing to develop a 9K Infinium iSelect HD BeadChip. Transcriptomic SNPs were detected in blood and fat samples of 10 bears from Western Hudson Bay, whereas RAD SNPs were developed from 38 bears from across their circumpolar range. To reduce effects of ascertainment, RAD SNPs were selected without consideration of the frequency or population of origin of the SNP in the ascertainment sample. In

total, 3411 RAD SNPs and 2030 transcriptomic SNPs were found to be well-clustered and polymorphic. 107 SNPs displayed X-linked inheritance and were used to confirm the sex of all individuals. Genotypes were highly reliable: no errors were detected among 14 duplicate samples.

For this study, we genotyped 412 putatively unrelated polar bears sampled from across Canada, including ≥13 males and ≥13 females from each of Canada's 13 MUs (Table A4.1). Tissue samples were residual punches from ear-tagging (using procedures approved by Environment Canada, the Ontario Ministry of Natural Resources, or the University of Saskatchewan) or were collected by hunters as part of Canada's legal harvest. DNA was extracted using DNeasy® Blood & Tissue Kits (Qiagen, Hilden, Germany), and genotyping was conducted according to Illumina's recommended protocols. SNPs were called using GENOMESTUDIO® 2011.1 (Genotyping Module 1.9; Illumina), and 13 samples with call rates <0.9 were removed, leaving 399 samples for analysis. Geographical sampling was similar to the distribution of Canadian samples used in Paetkau *et al.* (1999), with the addition of Southern Hudson Bay and with more concentrated sampling on southern Baffin Island (in the Baffin Bay and Davis Strait MUs) and in Admiralty Inlet (in the Lancaster Sound MU). Collection dates for these 399 samples ranged from 1985 to 2012 (Figure A4.1), with >95% of samples having been collected subsequent to the last major assessment of polar bear population structure (Paetkau *et al.* 1999). For comparison with SNPs, we also attempted to genotype 24 microsatellites in all individuals for which there was any remaining DNA (Tables A4.2, A4.3).

We removed all X-linked SNPs and SNPs with call rate <0.9 or minor allele frequency (MAF) <0.01. Because Bayesian clustering methods assume that linkage disequilibrium (LD) is caused by population structure rather than background LD caused by physical linkage between loci (Corander & Marttinen 2006), we generated an "LD-pruned dataset" from the filtered RAD SNPs, using pairwise LD pruning in a customized version of PLINK 1.07 (Purcell *et al.* 2007) to remove one locus from each pair of loci with $r^2 > 0.5$ within a sliding window of 10 loci. All subsequent analyses used this LD-pruned RAD dataset unless otherwise indicated.

4.2.2 Genetic clustering: discriminant analysis of principal components and Bayesian cluster analysis

We used *k*-means clustering on all principal components (PCs), which identified four genetic clusters as optimal according to the Bayesian information criterion (BIC; Figure A4.2).

We then performed a discriminant analysis of principal components (DAPC; Jombart *et al.* 2010) using these clusters, retaining 13 PCs (determined using *optim.a.score()* on an initial run) and all three discriminant functions. All analyses were performed using ADEGENET 1.4-2 (Jombart 2008; Jombart & Ahmed 2011) in R 3.1.0.

We used a hierarchical approach to Bayesian cluster analysis, first analysing the full 399-individual LD-pruned dataset using BAPS 6.0 (Corander & Marttinen 2006). Mixture analysis (k_{max} = 16) detected four genetic clusters, which were subsequently used for admixture analysis (N_{min} = 5, N_{it} = 100, N_{ref} = 200, $N_{ref\,it}$ = 10). BAPS provides a posterior probability of assignment for each individual, and the 323 "well-assigned" individuals (i.e., non-admixed, $P \geq 0.95$) were used to create four cluster-specific datasets (N_1 = 141, N_2 = 66, N_3 = 94, N_4 = 22). As above, MAF-filtering and LD-pruning were performed independently on each cluster-specific dataset for subsequent analysis. Because STRUCTURE is more sensitive than BAPS at low levels of genetic differentiation (Rodriguez-Ramílo *et al.* 2009), we ran STRUCTURE on each of the four cluster-specific LD-pruned datasets using the admixture model with correlated allele frequencies (Falush *et al.* 2003) for 20 independent replicate runs of 200,000 iterations (incl. 100,000 burn-in iterations) for k=1 to 4–9 depending on the number of management units comprising each cluster. STRUCTURE outputs were assessed using STRUCTURE HARVESTER 0.6.93 (Earl & Vonholdt 2012), and assignment plots were created using CLUMPP 1.1.2 (Jakobsson & Rosenberg 2007) and DISTRUCT 1.1 (Rosenberg 2004). (See also Supplementary Methods and Results in Appendix 4.)

4.2.3 Current and historical migration rates

We performed an assignment test in GENODIVE (default settings, 200 permutations) to identify recent migrants. To examine historical divergence of MUs and subsequent migration among them, we used TREEMIX 1.12 (Pickrell & Pritchard 2012), exploring 0–6 migration events. We rooted the tree with the Beaufort Sea MUs based on results of an initial run that also included SNP genotypes for a single grizzly bear (*Ursus arctos horribilis*) (Supplementary Methods; Figure A4.8). Because this algorithm is sensitive to recent admixture and migration, we excluded all significantly admixed individuals and significant recent migrants, leaving 315 individuals for analysis. We performed 100 bootstrap replicates to assess confidence in population splits and estimated standard errors and *P*-values for all migration weights using 10-SNP blocks to account for any residual non-independence among LD-pruned SNPs.

4.2.4 Allelic diversity, linkage disequilibrium, and effective population sizes

We estimated the proportion of polymorphic loci and the proportion of private alleles for cluster-specific datasets using the rarefaction method implemented in ADZE 1.0 (Szpiech *et al.* 2008). Because these proportions are likely to be affected by the SNP ascertainment scheme, we also examined these proportions using microsatellite genotypes for each of the cluster-specific datasets, after removing 12 out of our 24 loci that had ≥5% missing data in at least one cluster. LD decay was estimated for each cluster using non-linear least squares fitting in a custom R script to calculate the Hill–Weir estimator of r^2 (Hill & Weir 1988) using MAF=0.01, 0.05, and 0.10. Effective population sizes for each cluster were calculated using the LD model with random mating in NeEstimator 2.01 (Do *et al.* 2014) with a critical MAF of 0.05.

4.2.5 Genetic differentiation and F_{ST} outliers

We characterized the genetic diversity of polar bears across their range using an analysis of molecular variance (AMOVA; Excoffier *et al.* 1992) in GenoDive 2.0b25 (Meirmans & Van Tienderen 2004), which—as a first step—uses *k*-means clustering of MUs to generate hierarchical structure (Meirmans 2012a). To test for sex-biased dispersal, AMOVAs were conducted for all 399 individuals as well as 197 females and 202 males separately. To determine pairwise genetic differentiation between MUs, we then used a modified version of EIGENSOFT 5.0.2 (Price *et al.* 2006) to calculate Hudson's F_{ST}, an unbiased measure for SNPs that is robust to unequal sample sizes (Bhatia *et al.* 2013). To examine the effects of ascertainment bias—if any—we also calculated pairwise Weir and Cockerham F_{ST} (Weir & Cockerham 1984) for microsatellites using SPAGeDi 1.4 (Hardy & Vekemans 2002). 95% confidence intervals (CIs) were generated from jackknifing of individual microsatellite loci or of 10-SNP blocks of loci. Significance of pairwise F_{ST} was assessed using 2000 permutations per pair. Unless otherwise stated, a significance level of $\alpha = 0.05$ was used for all tests, with a Holm correction (Holm 1979) for multiple tests where appropriate.

To test for F_{ST} outliers among all RAD and transcriptomic loci (with MAF≥0.05), we used BayeScan 2.1 (Foll & Gaggiotti 2008; prior odds=100) on the four genetic clusters identified by BAPS. For comparison, we also used three newer approaches to outlier identification: FLK (Bonhomme *et al.* 2010), X^TX (Bayenv 2; Günther & Coop 2013), and OutFLANK (Whitlock & Lotterhos 2015; pre-release version downloaded from GitHub on July 23, 2014). FLK and Bayenv

2 were parameterized using RAD SNPs as a putatively neutral set of loci. *P*-values were mapped onto NCBI's annotated polar bear genome (GCF_000687225.1) using the R package QQMAN 0.1.1 (Turner 2014), and significant SNPs were annotated with the closest gene within 50 kb; significance was assessed using a false-discovery rate (FDR) cut-off of $q<0.1$. We obtained gene ontology information from BioMart's (Kasprzyk 2011) ailMel1 gene set for panda (last accessed Sept. 4, 2014), and GO enrichment was assessed using SNP2GO 1.0.1 (FDR=0.1, extension=50,000; Szkiba *et al.* 2014) using outliers as candidate loci.

4.3 Results

4.3.1 SNP and microsatellite genotyping

After MAF-filtering and LD-pruning, 2946 RAD SNPs remained on 247 scaffolds representing 92.4% of the draft genome; their average call rate was 0.999 (Table 4.1). We obtained microsatellite genotypes for 360 of our 399 individuals, including 287 complete 24-locus genotypes. For an additional 18 individuals sampled prior to 1996, no remaining DNA was available, therefore genotypes for the 15 microsatellites from Paetkau *et al.* (1999) that were a subset of our 24 loci were used for these individuals.

4.3.2 Genetic clustering of individuals

We identified four genetic clusters as optimal under the Bayesian information criterion (Figure A4.2) using *k*-means clustering of 399 individuals in ADEGENET, corresponding roughly to the Hudson Complex (FB, SH, and WH), the Canadian Archipelago (BB, GB, KB, LS, MC), the Beaufort Sea (NB, SB), and Norwegian Bay (NW). Davis Strait (DS) was intermediate between the Archipelago and Hudson clusters, and Viscount Melville Sound (VM) was intermediate between the Archipelago and Beaufort clusters (Figure 4.1).

Four genetic clusters were similarly identified in BAPS (Figures 4.2, 4.3, A4.3). In all BAPS and STRUCTURE runs, Davis Strait was comprised of mostly Archipelago–Hudson admixed individuals, and considerable admixture was also present in Viscount Melville Sound (Archipelago–Beaufort), Gulf of Boothia (Archipelago–Hudson), and Norwegian Bay (Archipelago–High Arctic). To examine genetic substructure, we ran STRUCTURE on non-admixed individuals of each genetic cluster (Figures A4.6, A4.7). The Evanno method (Evanno *et al.* 2005) best supported $k=2$ in the Arctic Archipelago (with sub-clusters corresponding to the Western and Eastern Archipelago) and the Hudson Complex (with a distinct sub-cluster corresponding to James

Bay in the southernmost reaches of the Southern Hudson Bay MU), and k=3 in the Beaufort Sea and Norwegian Bay. However, the Evanno method cannot evaluate the possibility that k=1, and because STRUCTURE may also overestimate k if unknown familial relationships are present (Pritchard *et al.* 2010), we considered each k-value based on biological feasibility and prior knowledge of polar bear population structure, settling on k=1 for Norwegian Bay and the Beaufort Sea.

4.3.3 Current and historical migration rates

In an assignment test, 263/399 (=65.9%) of individuals assign to their home subpopulation, and 374/399 (=93.7%) assign to their home region. 15/399 individuals (=3.8%) were significantly identified as migrants, all but two of which were outside of their home region (Table 4.4). Except for a single long-distance migrant from SB to GB, all significant cross-population assignments were between adjacent pairs of MUs. Relatively more males than females were significant migrants, but this difference was not significant (♂= 9/202, ♀=6/197; G-test of independence with Williams' correction: G=0.534, d.f.=1, P=0.46). After removing significant migrants and admixed individuals, TREEMIX generated a tree showing dispersal from the Beaufort Sea to the Hudson Complex, having high bootstrap support (i.e., ≥70%) for the placement of all populations except GB (Figure 4.4). Four migration events were significant ($P < 1\times10^{-4}$) and compatible with this topology, and together explained 99.6% of the variance in the data (Table A4.4, Figure A4.9). All significant historical migrations were between adjacent MUs except for apparent gene flow between Davis Strait and the Beaufort Sea (weight = 0.124, $P = 1.36\times10^{-6}$).

4.3.4 Allelic diversity, linkage disequilibrium, and effective population sizes

Patterns of allelic diversity for SNPs and microsatellites were similar following rarefaction analysis: overall diversity was highest in the Archipelago, private allelic diversity was highest in the Beaufort Sea, and the lowest diversity was in Norwegian Bay (Figure 4.6). Patterns of LD decay (Figure A4.10) were similar to those calculated by Malenfant *et al.* (2015a), which show rapid LD decay (MAF=0.05: half-length ≈ 50kb) for all clusters but Norwegian Bay (MAF=0.05: half-length ≈ 250kb). Differences in LD decay were also reflected in calculations of effective population size (mean N_e, parametric 95% C.I.): Archipelago = 347.6 (342.0–353.4), Beaufort = 335.0 (324.6–346.0), Hudson = 494.6 (477.6–512.9), and Norwegian Bay = 17.9 (17.6–18.1).

4.3.5 Genetic differentiation and F_{ST} outliers

We identified four clusters (corresponding to geographic regions) as optimal using *k*-means clustering of MUs in GENODIVE under the pseudo-*F* criterion, concordant with clusters identified by BAPS/STRUCTURE and *k*-means clustering of individuals in ADEGENET: 1) FB, SH, WH; 2) BB, DS, GB, KB, LS, MC, VM; 3) NB, SB; 4) NW. Regions account for ~3.9% of total genetic variation (F_{CT} = 0.039) and MUs within regions account for ~1.2% total genetic variation (F_{SC} = 0.013). F_{CT} and F_{SC} values for males were 10–15% lower than for females, though 95% confidence intervals marginally overlap.

Pairwise SNP and microsatellite F_{ST} values for MUs were highly correlated in a remarkable 1:1 regression (r^2 = 0.91; Figure 4.5) and did not differ significantly overall (paired *t*-test: $m_{SNP-ms} = 6.8\times10^{-4}$, t = 0.82, d.f. = 77, P = 0.41). 95% CIs for microsatellites were extremely broad, and only two MU pairs did not have overlapping 95% CIs for SNPs and microsatellites (Table 4.3). Differences in pairwise F_{ST} were not attributable to differing methods of F_{ST} calculation for SNPs and microsatellites or by the use of a restricted subset of individuals for microsatellite F_{ST} calculations (Supplementary Material). Using microsatellites, 11 pairs of MUs were not significantly differentiated after a Holm correction; however, using LD-pruned RAD SNPs, all MU pairs were significantly differentiated except for the Northern and Southern Beaufort Sea (P = 0.051).

21 loci were significant outliers (FDR<0.1) using FLK, 18 of which were located within 50 kb of an annotated gene, and 10 of which also lie within the 1% tail of BAYENV's X^TX statistic (Figures 4.7, A4.11). Two loci were also significant outliers using OUTFLANK: a RAD SNP 34,296 bases upstream of the gene SLC15A5 (solute carrier family 15, member 5), and a transcriptomic SNP in the 3' UTR of the gene PDLIM5 (PDZ and LIM domain 5). Both loci display similar patterns of differentiation, with the globally minor allele being most common in Norwegian Bay (Figure 4.8). We found no significant outliers using BAYESCAN, nor any significant GO enrichment for any set of outlier loci using SNP2GO.

4.4 Discussion

4.4.1 Migration of polar bears into Canada

Polar bears diverged from brown bears ~400,000 years ago (Liu *et al.* 2014), however their current distribution in North America was only established after the last glacial maximum (LGM)

~20,000 years ago, which left most of the continent and the Arctic Basin uninhabitable (Bradley & England 2008). The range of polar bears during the LGM remains unknown. Presence of polar bears' primary prey—ringed seals—in caves of the Alaska Panhandle (Heaton & Grady 2003), as well as the presence of polar bear mitochondrial haplotypes and X-linked variants among some Panhandle brown bears (Cahill *et al.* 2013), suggest that polar bears used the Northeast Pacific as a refugium during this period. However, modern polar bears are more closely related to extinct Irish brown bears than to Panhandle brown bears (Edwards *et al.* 2011), and an Atlantic refugium is supported by polar bear subfossils from Scandinavia immediately predating and postdating the LGM (Ingólfsson & Wiig 2009), and winter sea ice as far south as Spain (de Vernal *et al.* 2005) may have allowed for colonization or gene flow across the Atlantic.

Our TREEMIX results suggest that polar bears populated Canada from the northwest, migrating from the Beaufort Sea through the Canadian Archipelago into the High Arctic and Baffin Bay, then south through Davis Strait and into the Hudson Complex. Based on the only known Canadian subfossil—undated Pleistocene remains from Baillie Island, Northwest Territories (Vincent 1989)—polar bears were present in the Beaufort Sea by the late Pleistocene (i.e., ≥11,700 years ago), and their subsequent migration pattern into Canada would be consistent with the breakup sequences of the Laurentide and Innuitian ice sheets (Dyke 2004). Ice sheets had receded in most of the Archipelago and Norwegian Bay 9500 years ago and in most of Hudson Bay by 8400 years ago (Dyke 2004), making the regions habitable for polar bears and their prey. TREEMIX also detected significant historical gene flow from Davis Strait into the Beaufort Sea, perhaps through Eurasia via the East Greenland MU with which Davis Strait abuts. However, this may be an artefact of incomplete geographical sampling or of genetic contribution to the Archipelago and Hudson Bay from an Atlantic refugium, and the matter should be investigated further with the addition of non-Canadian samples.

4.4.2 Genetic structure of Canadian polar bears

Our analyses with thousands of SNPs and modern techniques confirm the primary finding of previous population genetics studies of polar bears using low-resolution marker sets (Malenfant *et al.* 2016; Paetkau *et al.* 1999; Peacock *et al.* 2015b): *k*-means clustering of individuals in ADEGENET, Bayesian clustering of individuals in BAPS, and *k*-means clustering of MUs in GENODIVE each detected four major genetic clusters of polar bears in Canada, corresponding to

the Hudson Complex, the Canadian Arctic Archipelago, the Beaufort Sea, and Norwegian Bay. Overall, major regions were slightly–moderately differentiated (F_{CT} = 0.039), and demarcations align with geographical features—such as the presence of land—or differences in sea-ice regime, such as the predominant type of ice or the concentration of multiyear ice during the breeding season (Figure A4.12). Norwegian Bay is surrounded by islands to the north, south, and east, and by polynyas in the south and thick multiyear ice to the west, which greatly limit exchange with neighbouring MUs (Taylor *et al.* 2001). The Beaufort Sea and the Archipelago are separated by dense multiyear ice, which forms a barrier to movement (Bethke *et al.* 1996), though some Northern Beaufort and Viscount Melville individuals mix on the pack ice together (Taylor *et al.* 2001), providing for the admixture in Viscount Melville observed our study. The Hudson Complex is separated from the Archipelago by land to the north and east. Substantial Hudson–Archipelago admixture was observed on southern Baffin Island in the Davis Strait MU, corresponding to observed movements between southern and northern Davis Strait and between northern Davis Strait and Baffin Bay (Peacock *et al.* 2013).

Within the Hudson Complex, we detected a unique genetic sub-cluster concentrated in James Bay at the southern reaches of the Southern Hudson Bay MU, as previously reported (Crompton *et al.* 2008; Crompton *et al.* 2014; Viengkone 2015). James Bay is demarcated from Hudson Bay proper by a shift from medium to thick first-year ice, and recent satellite-collar data for Southern Hudson Bay and James Bay bears show little overlap in home ranges (Obbard & Middel 2012). Consequences of treating James Bay as its own management unit have been addressed in a companion study (Viengkone 2015). Within the Archipelago, we detected evidence of eastern and western sub-clusters, which has previously been reported at a more limited geographical scale (i.e., including only the M'Clintock Channel and Gulf of Boothia MUs) by Campagna *et al.* (2013). However, the genetic clusters here differ from those reported by Malenfant *et al.* (2016). Specifically, Malenfant *et al.* (2016) found that Lancaster Sound and M'Clintock Channel cluster with the Western Archipelago (Gulf of Boothia and Viscount Melville), whereas here we find that these MUs cluster with the Eastern Archipelago (Kane Basin and Baffin Bay). It is plausible that the clusters we observed in this study are due to sea-ice features: because of the presence of thick multiyear ice, eastern Viscount Melville and northern M'Clintock Channel tend to have bears only at very low densities (Taylor *et al.* 2001), which would restrict gene flow with Lancaster Sound. However, our sampling excludes a large part of

western Lancaster Sound and northern M'Clintock channel, and genetic clustering can be affected by such sampling discontinuities (Schwartz & McKelvey 2008). Disentangling these possibilities may require more even sampling throughout the Canadian Archipelago, which is more likely to come from scientific handling than from harvested samples, which are generally concentrated around Inuit settlements.

Notably, we did not detect any genetic contribution from the Polar Basin cluster (represented in our study by the Northern and Southern Beaufort Sea MUs) in the Eastern Archipelago (i.e., Kane Basin or Baffin Bay), suggesting that there is not substantial gene flow from the Eastern Polar Basin into the Canada. These results bolster the findings of Malenfant *et al.* (2016) over those of Peacock *et al.* (2015b), suggesting that there has not been large-scale movement of polar bears in response to recent climate-change-induced sea ice loss. However, the present study did not include samples from Svalbard or Eastern Greenland, and would be better tested by including samples from these regions.

Overall, SNP F_{ST} was highly correlated with microsatellite F_{ST}, and—perhaps because of extremely broad confidence intervals for microsatellites—we found no evidence of ascertainment bias. SNPs had narrow confidence intervals and high power to differentiate MUs based on F_{ST}, detecting significant differentiation between all but one pair of MUs, including 11 cases in which microsatellite-based F_{ST} was non-significant. Notably, we found that SNPs—but not microsatellites—significantly differentiated the Baffin Bay and Kane Basin MUs, which were previously found to have been undifferentiated and were speculated to have formed a source–sink pair (Paetkau *et al.* 1999), a suggestion which is not supported by GPS collar tracking, since the two MUs have distinct ranges (Taylor *et al.* 2001). Despite the greater power of our SNPs to detect population differentiation, we found no evidence of differentiation between the Northern and Southern Beaufort MUs. Although this may be related to our continuous sampling distribution across the MU boundary lines, the lack of distinction between these MUs is also supported by recent tracking data, which show no discontinuities in movements among adult females (Andrew Derocher, personal communication).

Although pedigree-based studies have suggested that dispersal may be slightly male-biased in the Barents Sea (Zeyl *et al.* 2009b) and possibly in Hudson Bay (Malenfant *et al.* 2015b; Richardson 2014), the issue has not been well-addressed in population genetics studies. A regional

comparison of microsatellite and mitochondrial DNA among polar bears of the Canadian Arctic Archipelago found no evidence of sex-biased dispersal (Campagna *et al.* 2013). At a range-wide level, Peacock *et al.* (2015b) suggested high levels of sex-biased dispersal; however, these results were likely erroneous due to the inclusion of incorrect F_{ST} values caused by small sample sizes and retention of loci with large amounts of missing data (Malenfant *et al.* 2016). In the present study, we found only marginal evidence for a male bias in movement. Proportionally more males than females were identified as migrants, though the difference was not significant with a sample size of 399 individuals. Likewise, 95% confidence intervals for *F*-values in sex-specific AMOVAs at both the level of genetic cluster and of MU overlap marginally. We detected a single long-distance disperser in our data, a male who migrated ~1800 km from the Southern Beaufort Sea to the Gulf of Boothia. Although we detected no long-distance female dispersal from our genetic data, long-distance migrations have been observed among collared females, including a single female who migrated 5256 km across the polar basin from Alaska to Greenland (Durner & Amstrup 1995). Thus, any male bias in movement appears to be limited.

4.4.3 Norwegian Bay

Although we detected both migrants and admixed individuals in Norwegian Bay, a genetic cluster concentrated in the northeast portion of the MU has remained divergent. Inuit harvesters have reported Norwegian Bay polar bears as being physically different from those of other subpopulations (Taylor *et al.* 2001), referring to them as "weasel bears", which appear to have narrower heads and bodies (Mitchell Taylor, personal communication). Possibly related to this, a SNP near the gene SLC15A5 was determined to be a Norwegian Bay-discriminating outlier using three methods of outlier detection, and—in humans—a SNP in this gene (rs10772915) has been previously associated with overall deposition of visceral adipose tissue (Fox *et al.* 2012; Table S2), which may be related to their skinnier appearance. Since their divergence with brown bears, cardiomyopathy-related genes have experienced the strongest selection in polar bears, possibly causing a reorganization of the circulatory system related to selective pressure for long-distance swimming (Liu *et al.* 2014). We found a Norwegian Bay-discriminating SNP in the 3' UTR of PDLIM5—a gene associated with dilated cardiomyopathy in mice (Cheng *et al.* 2010)—and many Norwegian Bay bears have retained the brown bear allele. Though this likely represents a founder effect or subsequent loss of genetic diversity owing to inbreeding and drift (as seen in rarefaction analyses), it is perhaps also attributable to lack of long-distance swimming in this MU: as an

isolated region characterized by thick multiyear ice, long-range swimming is generally unnecessary as most individuals restrict themselves to small bays, fiords, and coastal tide cracks in the east (Taylor *et al.* 2001; Taylor *et al.* 2009). Therefore—as opposed to elsewhere in their range—there may have been little selection in Norwegian Bay for genes related to the cardiovascular system.

Norwegian Bay is expected to be one of the "last ice areas" and may become a refugium for polar bears if climate change continues (Derocher 2012); however it has not been surveyed since 1997 (when our samples were collected), and the current status of this unique genetic cluster is unknown. With an effective population size of only ~17.9, this cluster will be subject to inbreeding depression and loss of evolutionary potential (Frankham *et al.* 2014). Because of rapid LD decay in polar bears, our limited scan for differentiated loci is unlikely to have captured the full array of potentially adaptive differences among subpopulations, and further tests using more extensive genomic data and more recent samples should be conducted to determine the degree to which the Norwegian Bay subpopulation is locally adapted or has merely been subject to loss of adaptive diversity.

Table 4.1. Summary statistics for 2946 LD-pruned SNPs in each of 13 Canadian management units (MUs). N = sample size after removal of low-quality samples; MAF = minor allele frequency for variable SNPs; H_O = observed heterozygosity; H_E = expected heterozygosity using MU-specific allele frequencies.

Management unit	N	Mean call rate	Proportion variable	Average MAF	H_O	H_E	F_{IS}
Baffin Bay (BB)	30	1.000	0.895	0.156	0.227	0.227	0.002
Davis Strait (DS)	33	1.000	0.890	0.156	0.225	0.226	0.004
Foxe Basin (FB)	33	1.000	0.851	0.152	0.217	0.220	0.009
Gulf of Boothia (GB)	30	0.996	0.904	0.158	0.228	0.229	0.005
Kane Basin (KB)	30	0.999	0.884	0.158	0.228	0.229	0.004
Lancaster Sound (LS)	31	1.000	0.906	0.157	0.225	0.228	0.009
M'Clintock Channel (MC)	29	0.998	0.844	0.156	0.224	0.224	0.002
Northern Beaufort Sea (NB)	31	1.000	0.883	0.157	0.228	0.229	0.001
Norwegian Bay (NW)	31	0.998	0.802	0.143	0.203	0.206	0.014
Southern Beaufort Sea (SB)	32	1.000	0.876	0.157	0.226	0.227	0.003
Southern Hudson Bay (SH)	31	1.000	0.798	0.151	0.213	0.216	0.014
Viscount Melville Sound (VM)	28	0.997	0.884	0.158	0.225	0.229	0.013
Western Hudson Bay (WH)	30	0.999	0.796	0.150	0.216	0.216	0.002

Table 4.2. Hierarchical AMOVA for 399 polar bears—and sex-specific AMOVAS for 202 males and 197 females—from 13 Canadian management units (MUs) grouped into four regions identified by *k*-means clustering of MUs in GENODIVE.

Variance component	*F*-statistic	% variance			*F*-value (95% C.I.)		
		All	Males	Females	All	Males	Females
Within individuals	F_{IT}	94.2%	94.3%	94.1%	0.058 (0.055–0.061)	0.057 (0.054–0.061)	0.059 (0.056–0.063)
Among individuals	F_{IS}	0.7%	0.9%	0.5%	0.008 (0.005–0.010)	0.010 (0.007–0.013)	0.006 (0.002–0.009)
Among MUs	F_{SC}	1.2%	1.2%	1.4%	0.013 (0.012–0.014)	0.012 (0.011–0.013)	0.014 (0.013–0.015)
Among clusters	F_{CT}	3.9%	3.6%	4.1%	0.039 (0.037–0.040)	0.036 (0.034–0.038)	0.041 (0.038–0.043)

Table 4.3. Pairwise Hudson's F_{ST} values for SNPs × 100 (below diagonal) and Weir and Cockerham F_{ST} values for microsatellites × 100 (above diagonal). Management unit (MU) abbreviations are as in Table 4.1. Significant values—as determined using 2000 permutations—are indicated with boldface. Shading indicates that SNP and microsatellite F_{ST} values differed significantly based on non-overlapping 95% confidence intervals from jackknifing of loci. A box encloses each of the four clusters identified by *k*-means clustering of MUs in GENODIVE using SNPs.

	SH	**WH**	**FB**	**DS**	**BB**	**KB**	**LS**	**GB**	**MC**	**VM**	**NW**	**NB**	**SB**
SH		0.6	0.4	**2.6**	**3.8**	**4.5**	**4.7**	**2.3**	**6.0**	**6.3**	**9.2**	**7.2**	**7.9**
WH	**0.8**		0.0	**2.5**	**3.3**	**3.9**	**4.0**	**2.1**	**4.9**	**5.8**	**8.7**	**6.3**	**6.8**
FB	**0.7**	**0.4**		**1.7**	**2.7**	**3.4**	**3.3**	**1.2**	**4.7**	**5.8**	**8.5**	**5.9**	**6.7**
DS	**2.6**	**2.4**	**1.4**		**1.3**	**2.3**	**2.7**	**1.6**	**3.4**	**3.9**	**7.0**	**5.0**	**6.0**
BB	**4.5**	**4.3**	**3.1**	**1.0**		0.5	0.7	0.7	**2.0**	**2.5**	**5.2**	**4.0**	**4.5**
KB	**5.1**	**5.0**	**3.8**	**1.6**	**0.8**		0.2	0.6	**2.4**	**2.5**	**4.0**	**3.4**	**3.8**
LS	**5.2**	**5.0**	**3.8**	**1.6**	**0.7**	**0.6**		0.8	**1.5**	**1.6**	**4.8**	**4.3**	**4.4**
GB	**3.8**	**3.5**	**2.4**	**1.1**	**0.8**	**1.1**	**0.6**		1.2	**2.3**	**5.8**	**3.4**	**3.8**
MC	**6.9**	**6.7**	**5.6**	**3.6**	**2.6**	**2.6**	**1.7**	**2.0**		**1.7**	**7.5**	**5.3**	**5.4**
VM	**6.6**	**6.4**	**5.4**	**3.2**	**2.4**	**2.4**	**1.7**	**2.2**	**1.9**		**7.7**	**3.2**	**3.4**
NW	**9.9**	**9.9**	**8.6**	**6.6**	**5.8**	**4.9**	**4.5**	**5.7**	**6.5**	**6.3**		**8.6**	**8.5**
NB	**7.2**	**7.2**	**6.0**	**4.0**	**3.6**	**3.7**	**3.3**	**3.5**	**4.4**	**2.0**	**7.7**		0.2
SB	**7.4**	**7.2**	**6.2**	**4.0**	**3.7**	**3.8**	**3.3**	**3.6**	**4.8**	**2.3**	**7.9**	0.1	

Table 4.4. Assignment test results. Each row represents the population in which an individual was sampled and each column represents their putative population of origin. Superscripts indicate the number of significantly cross-assigned individuals; where absent, none were significant. A box encloses each of the four clusters identified by *k*-means clustering of management units in GENODIVE.

	SH	WH	FB	DS	BB	KB	LS	GB	MC	VM	NW	NB	SB	Total
SH	20	5	6											31
WH	1	18	11											30
FB	2	8	19	3				$1^{(1)}$						33
DS	$1^{(1)}$		3	20	6		1	2						33
BB				1	23	2		3	1					30
KB					5	20	3	1			$1^{(1)}$			30
LS					3	4	19	3		$1^{(1)}$	$1^{(1)}$			31
GB			$2^{(2)}$		1		3	23					$1^{(1)}$	30
MC							3	$3^{(1)}$	23					29
VM							2		1	22		$3^{(2)}$		28
NW							$7^{(4)}$				24			31
NB										2		14	15	31
SB												14	18	32

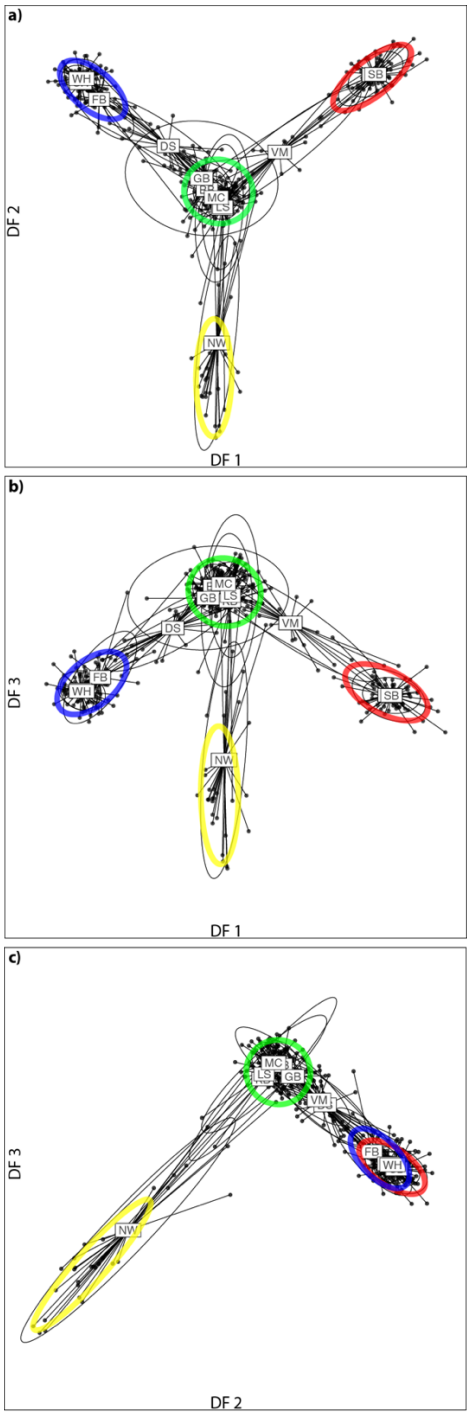

Figure 4.1. Discriminant analysis of principal components on 399 Canadian polar bears. Subpopulation abbreviations are as in Table 4.1. Names of some MUs may be obscured where centroids overlap.

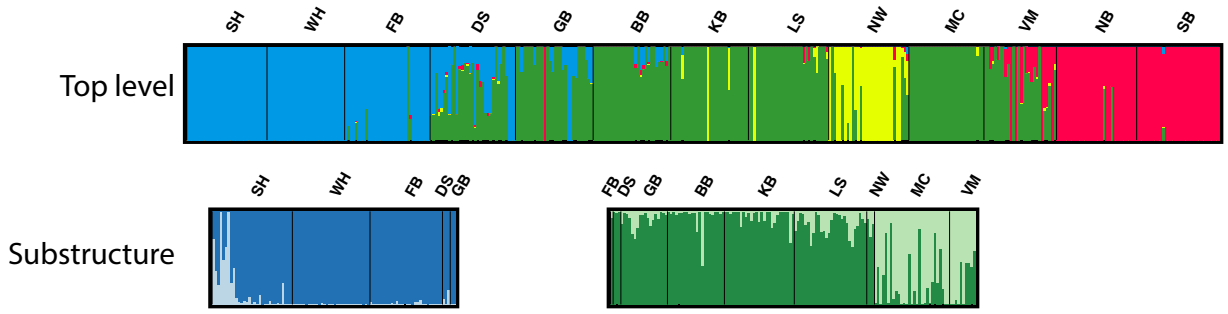

Figure 4.2. Admixture plots generated using BAPS (top level) and STRUCTURE (sublevels).

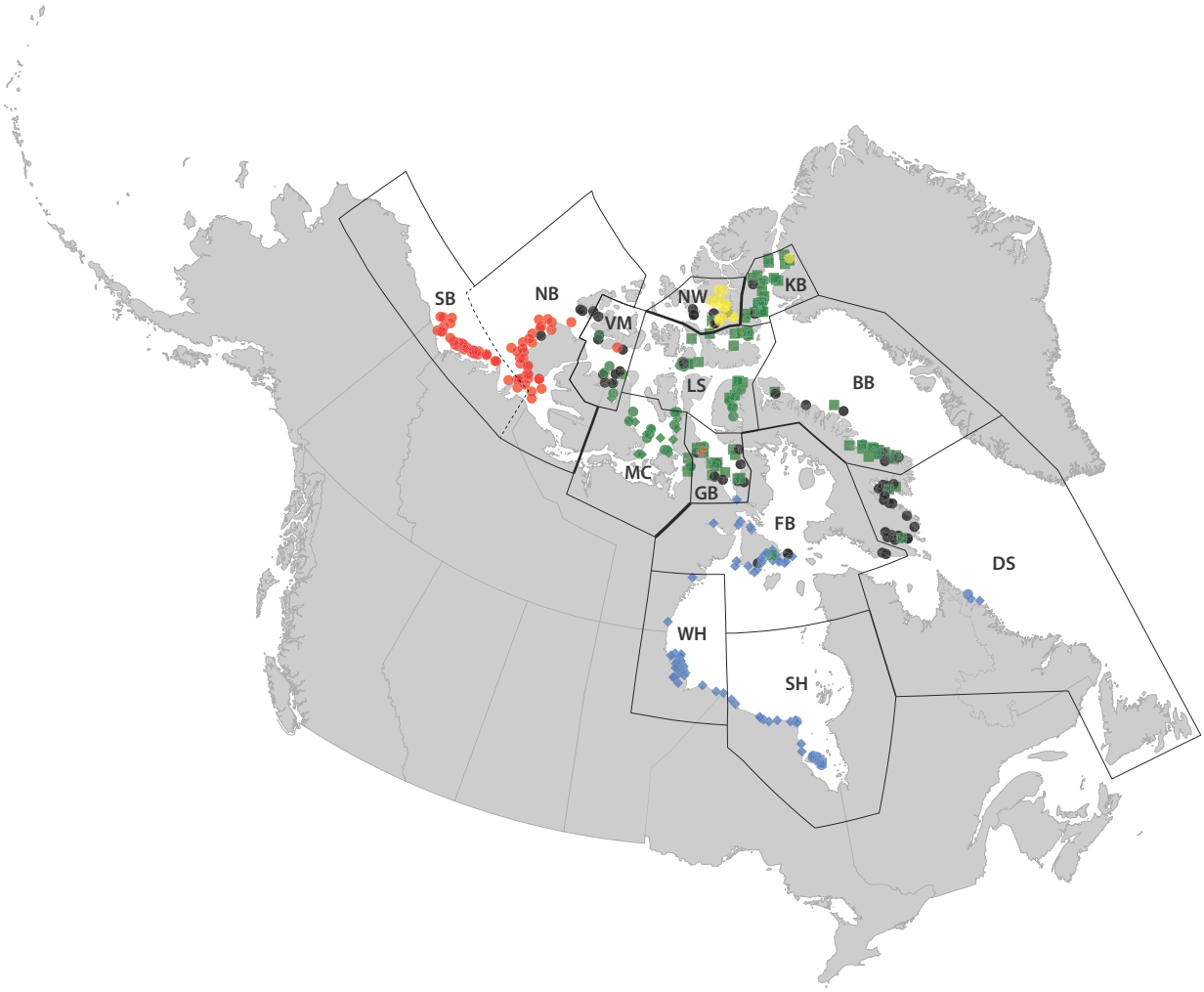

Figure 4.3. Map of Canadian polar bear management units (MUs) and 395 sampling sites. Each point represents a single individual, with colour corresponding to one of the major genetic clusters identified in BAPS. Significantly admixed individuals are displayed in black. Widths of borders between MUs are inversely proportional to the number of effective migrants expected under the island model of dispersal using pairwise Hudson's F_{ST} values from Table 4.2; a dashed line indicates non-significance. Sampling location was not available for four Viscount Melville Sound individuals, which are therefore not displayed in the Figure.

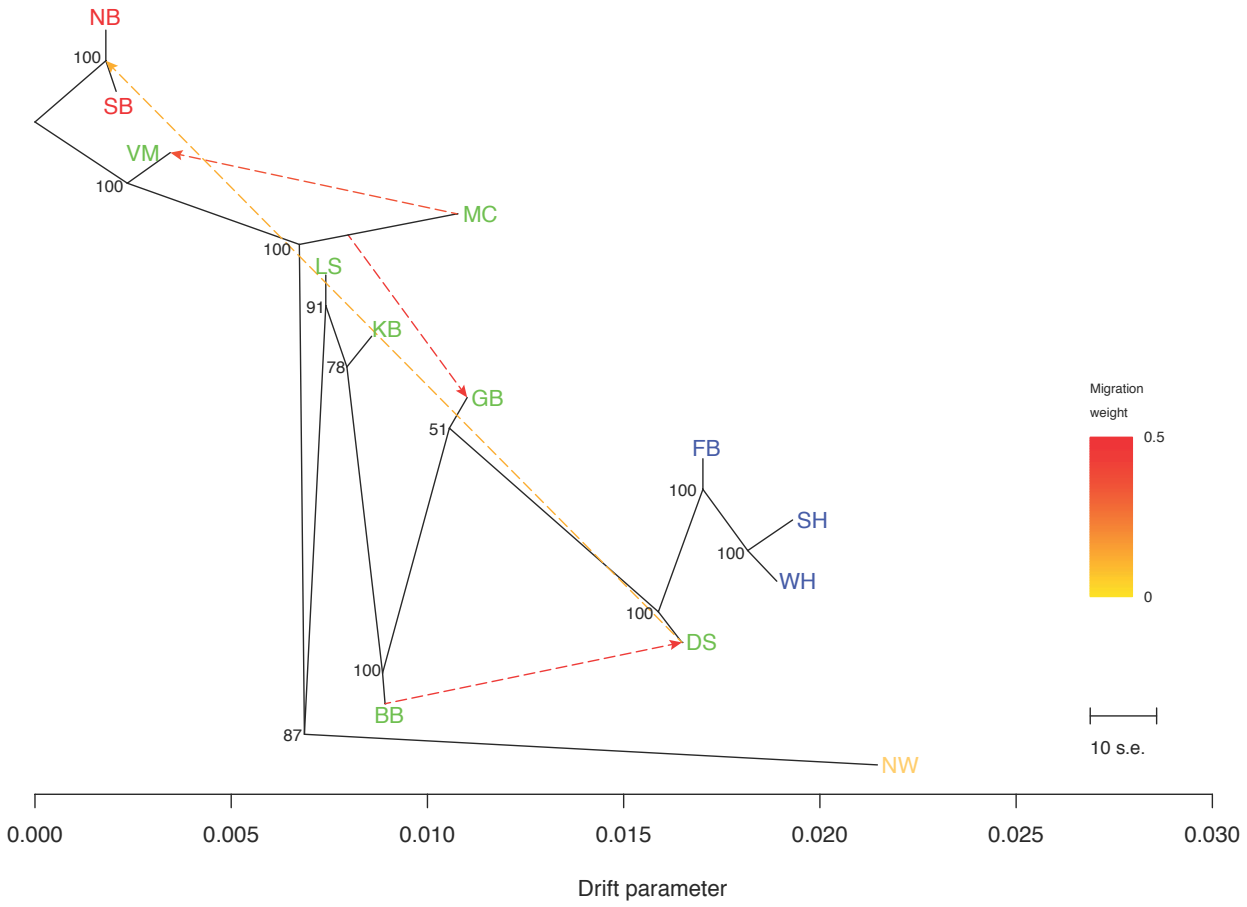

Figure 4.4. Maximum-likelihood tree of historical population splits (solid lines), allowing for four subsequent migration events (dashed lines) in TREEMIX, where migration weights are related to the proportion of alleles originating in the parental population. Population names are color-coded to match each of the four clusters identified by *k*-means clustering of MUs in GENODIVE. Numbers at internal nodes indicate support from 100 bootstrap replicates. The scale bar indicates ten times the average standard error.

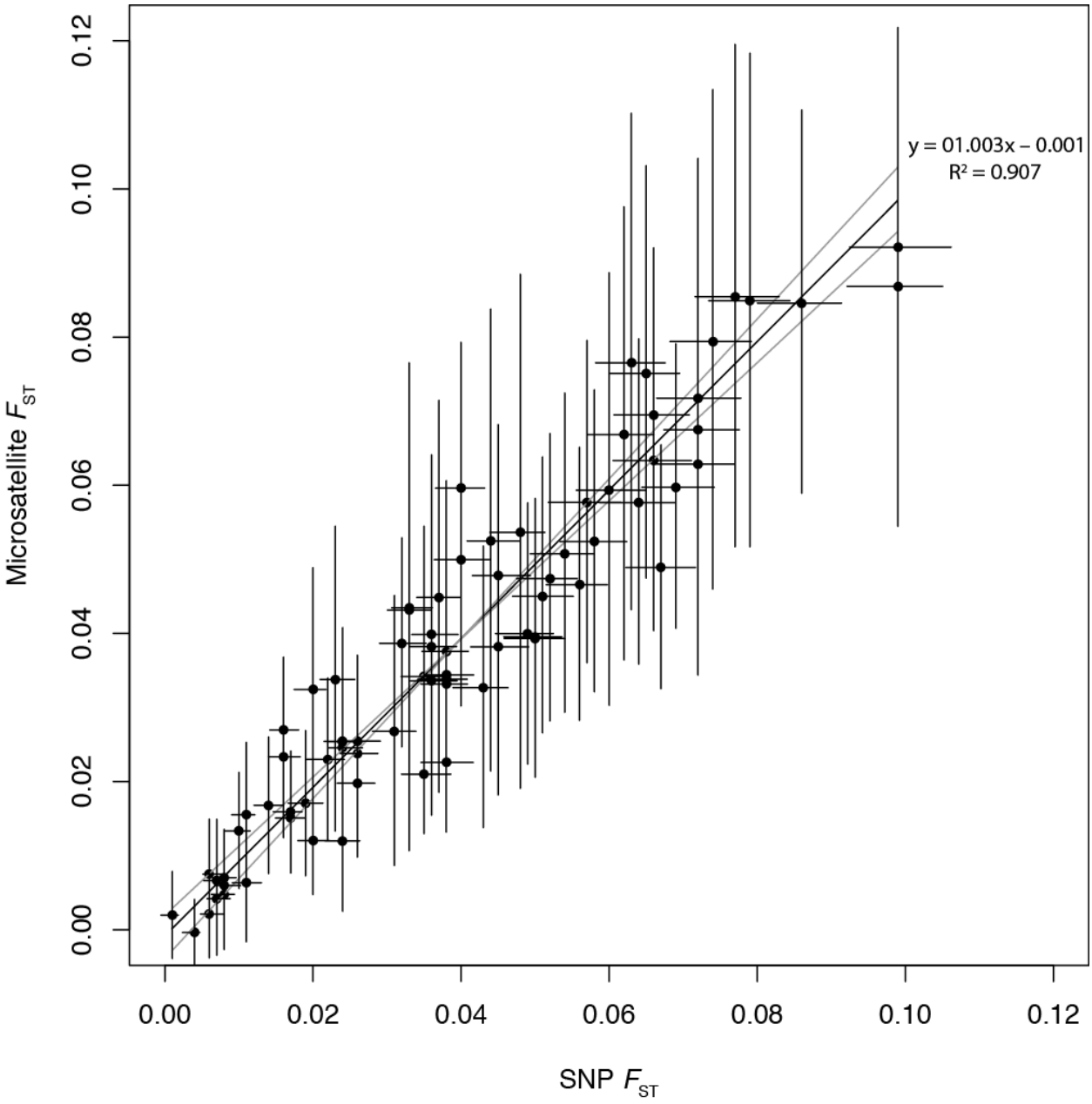

Figure 4.5. Pairwise F_{ST} values of 24 microsatellites and 2946 SNPs. Error bars give 95% confidence intervals obtained from jackknifing of loci (microsatellites) or blocks of 10 consecutive loci (SNPs). Lines indicate the slope of a major axis regression and its 95% confidence intervals.

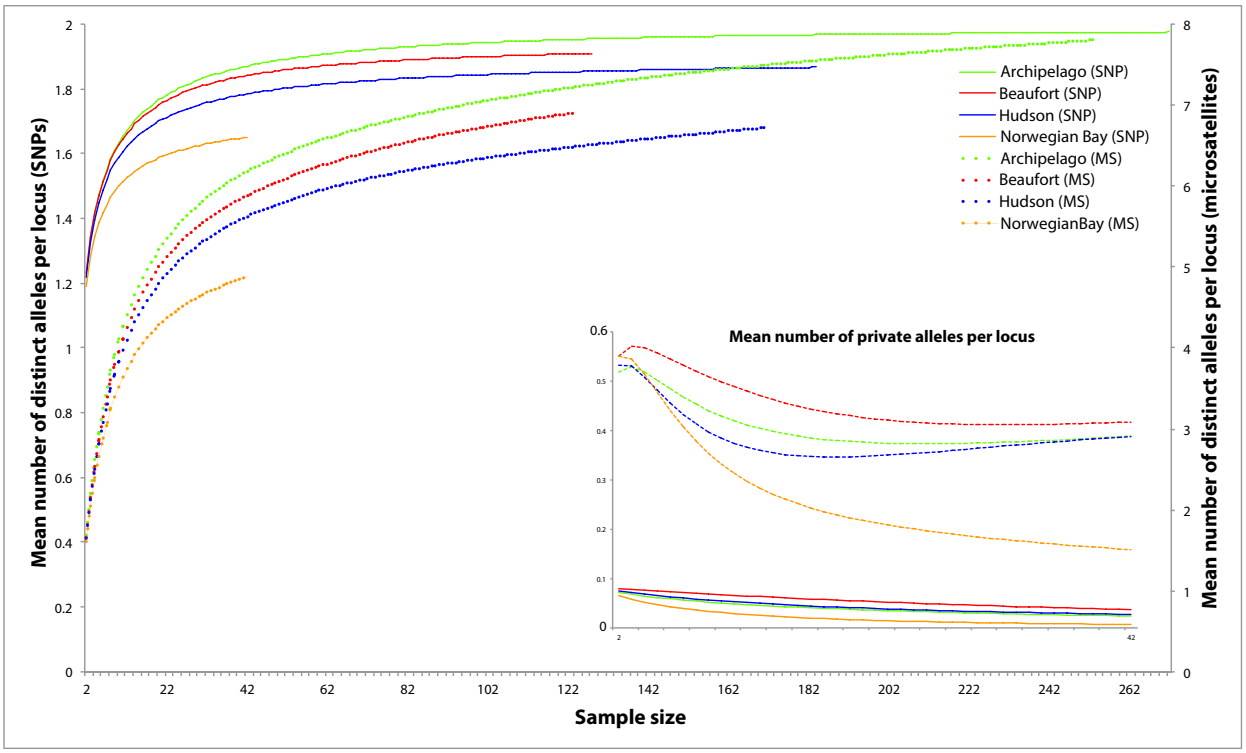

Figure 4.6. Rarefaction analyses for 2946 LD-pruned SNPs and 12 microsatellites for non-admixed individuals from each of the four main identified genetic clusters. The main plot shows the mean number of distinct alleles per locus; the inset shows allelic variation that is private to each of the four genetic clusters. In both graphs, the x-axis indicates subsample size in chromosomes.

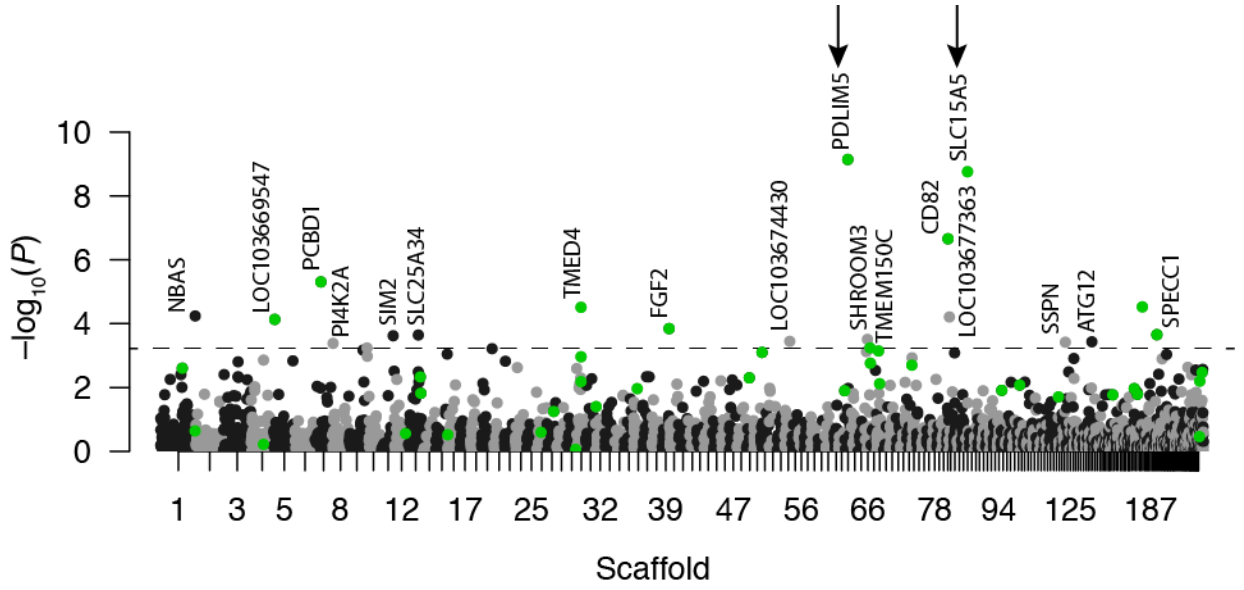

Figure 4.7. Manhattan plot of F_{ST} outliers using *P*-values calculated from FLK. The dashed line indicates a false-discovery rate (FDR) of 0.1. Green points lie within the 1% tail of X^TX values calculated in BAYENV 2. Arrows indicate significant (i.e., FDR<0.1) outliers in OUTFLANK. SNPs above FLK's line of significance are annotated with the names of the nearest known gene in the polar bear genome (within 50 kb). LOC103669547 and LOC103674430 are long non-coding RNAs; LOC103677363 produces an OX-2 membrane glycoprotein-like product.

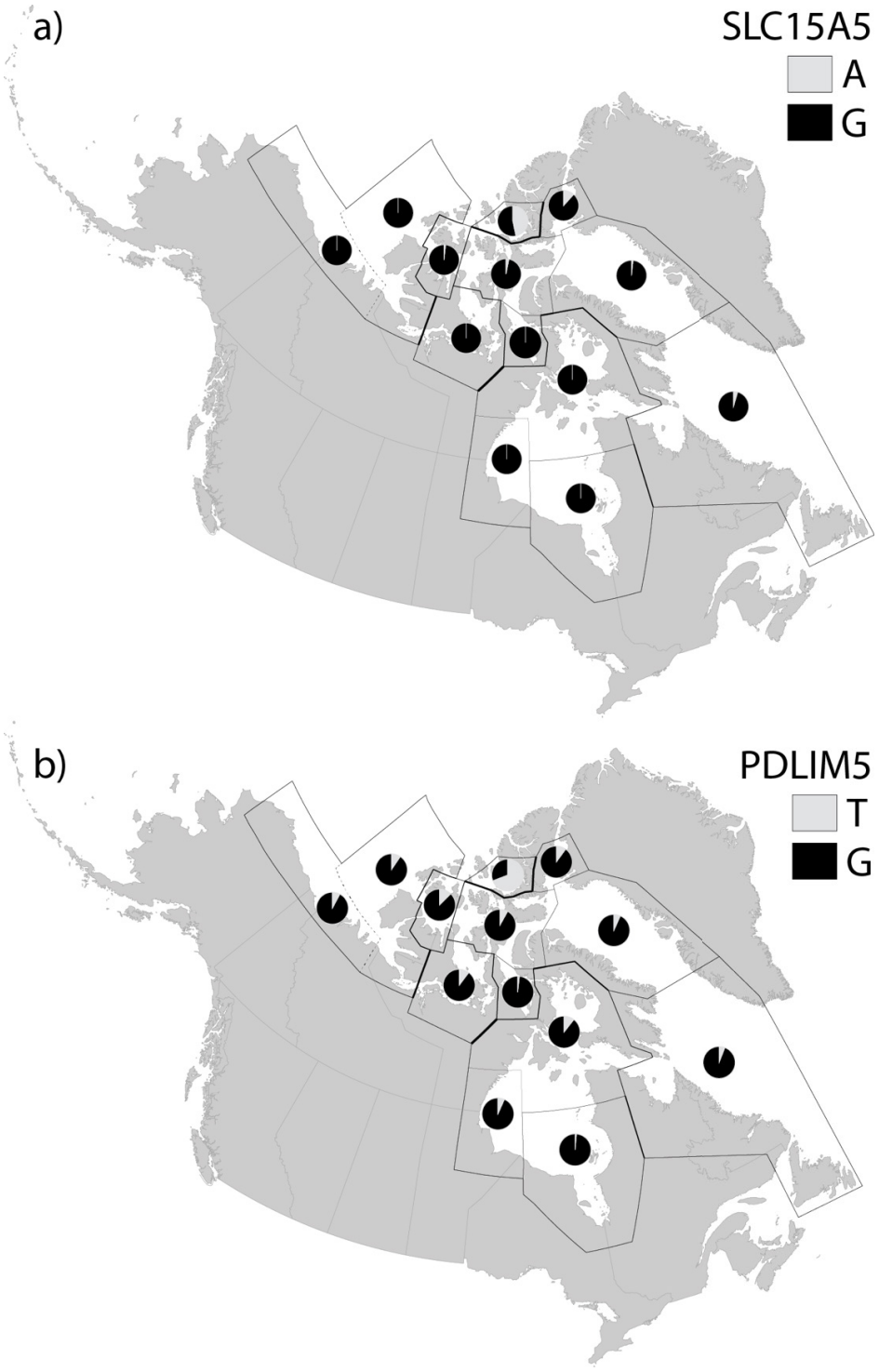

Figure 4.8. Map of allele frequencies for a) RAD SNP 75533_92 (near SLC15A5), and b) transcriptomic SNP scaffold62_6020088 (PDLIM5).

Chapter 5: Evidence of adoption, monozygotic twinning, and low inbreeding rates in a large genetic pedigree of polar bears

5.1 Abstract

Multigenerational pedigrees have been developed for free-ranging populations of many species, are frequently used to describe mating systems, and are used in studies of quantitative genetics. Here, we document the development of a 4449-individual pedigree for the Western Hudson Bay subpopulation of polar bears (*Ursus maritimus*), created from relationships inferred from field and genetic data collected over six generations of bears sampled between 1966 and 2011. Microsatellite genotypes for 22–25 loci were obtained for 2945 individuals, and parentage analysis was performed using the program FRANz, including additional offspring–dam associations known only from capture data. Parentage assignments for a subset of 859 individuals were confirmed using an independent medium-density set of single nucleotide polymorphisms. To account for unsampled males in our population, we performed half-sib–full-sib analysis to reconstruct males using the program COLONY, resulting in a final pedigree containing 2957 assigned maternities and 1861 assigned paternities with only one observed case of inbreeding between close relatives. During genotyping, we identified two independently captured two-year-old males with identical genotypes at all 25 loci, showing—for the first time—a case of monozygotic twinning among polar bears. In addition, we documented six new cases of cub adoption, which we attribute to cub misidentification or misdirected maternal care by a female bereaved of her young. Importantly, none of these adoptions could be attributed to reduced female vigilance caused by immobilization to facilitate scientific handling, as has previously been suggested.

5.2 Introduction

Multigenerational pedigrees are useful in studies describing mating systems and for quantitative genetics research (Pemberton 2008) and large pedigrees have been developed for wild populations of many species, including red deer (*Cervus elaphus*; Slate *et al.* 2002), bighorn sheep (*Ovis canadensis*; Poissant *et al.* 2010), song sparrows (*Melospiza melodia*; Reid *et al.* 2011), and American red squirrels (*Tamiasciurus hudsonicus*; Taylor *et al.* 2012). However, because of the great effort and expense of sampling large carnivores, few pedigrees have been developed for ursid species, with most parentage analyses containing no more than a few hundred individuals, which are typically sampled non-invasively (Cronin *et al.* 2005; De Barba *et al.* 2010; Itoh *et al.* 2012; Norman & Spong 2015; Onorato *et al.* 2004; however, cf. Bellemain et al. 2006; Moore et al. 2015; Proctor et al. 2004). To date, the largest parentage analysis of polar bears (*Ursus maritimus*) was based on 583 individuals in the Barents Sea (Zeyl *et al.* 2009a; Zeyl *et al.* 2009b), which showed that polar bears exhibit serial monogamy, male-biased dispersal, and that inbreeding between close relatives is rare.

Polar bears are large carnivores that occur at low densities throughout the circumpolar Arctic and subarctic regions. They have a polygynous mating system (Derocher *et al.* 2010), typically breeding between late March and June, with females giving birth to 1–3 cubs in November–December while overwintering in maternity dens. Females emerge from dens in early spring, and are the only providers of parental care until their cubs become independent—typically at about 2.5 years old (Ramsay & Stirling 1988). Though family groups tend to avoid other bears—perhaps to avoid cannibalism and other conspecific aggression (Taylor *et al.* 1985)—cases of adoption have been documented (Atkinson *et al.* 1996a; Belikov 1976; Derocher & Wiig 1999; Lunn *et al.* 2000; Saunders 2005; Vibe 1976). Although adoption has been known to occur in the Barents Sea subpopulation (Derocher & Wiig 1999), Zeyl *et al.* (2009a, 2009b) did not report any cases of adoption, perhaps because of the infrequency of occurrence, combined with the study's comparatively small sample size.

Adoption has been observed in more than 60 mammalian species (Gorrell *et al.* 2010), and its occurrence requires special explanation due to the extremely high cost of milk provision to adopted young (e.g., Clutton-Brock *et al.* 1989). Allonursing and adoption may be explained adaptively through kin selection, reciprocal altruism, evacuation of excess milk, or through a gain

in parenting experience (Roulin 2002). Alternately, adoption and allonursing may simply be the result of error, occurring especially when a reproductive individual is already hormonally or behaviourally primed to provide parental care and is bereaved of their young (Riedman 1982). Most empirical studies support the kin selection, milk evacuation, or misdirected parental care hypotheses (Roulin 2002). Amongst polar bears, adoption has been attributed to misdirected parental care caused by cub misidentification (Lunn *et al.* 2000), which may be caused by confusion due to the immobilization of adult females prior to scientific handling (Derocher & Wiig 1999).

Like adoption, monozygotic twinning is taxonomically widespread but infrequent, and although well described in humans (e.g., Bulmer 1970) and cattle (e.g., Silva del Río *et al.* 2006), few cases have been documented in wildlife species. Monozygotic quadruplets–dodectuplets are the normal mode of reproduction among some *Dasypus* armadillos (Hardy 1995), and monozygotic twins have been identified in lesser flat-headed bats (*Tylonycteris pachypus*; Hua *et al.* 2011), in wolves (*Canis lupus*; Carmichael *et al.* 2009), among some species of pinnipeds (Spotte 1982), including Antarctic fur seals (*Arctocephalus gazella*; Hoffman & Forcada 2009), and possibly in mule deer (*Odocoileus hemionus*; Anderson & Wallmo 1984). The apparent scarcity of monozygotic twins is partially attributable to the difficulty of identifying them, as this requires genetic or embryological confirmation. For instance, conjoined twins, which develop from monozygotic twins and are therefore far rarer, are phenotypically conspicuous, and at least 20 cases of conjoined twinning in wildlife species have been published (Kompanje & Hermans 2008). To our knowledge, identical twinning (or conjoined twinning) has never been reported for any species of bear, although no study has had a sample size large enough to reliably detect such a rare event.

In this paper, we present a large pedigree of polar bears comprising 4449 individuals from the Western Hudson Bay subpopulation sampled over six bear generations in northeastern Manitoba, Canada between 1966 and 2011. Western Hudson Bay is the best-studied of the 19 global management units of polar bears (Obbard *et al.* 2009), with extensive phenotypic data from scientific handling collected as part of a long-term mark–recapture study. Estimated population size has declined from 1185 individuals in 1987 to 806 individuals in 2011 (Lunn *et al.* 2016; however, cf. Stapleton *et al.* 2014), with an estimated long-term effective population size (N_e) of

approximately 200–400 individuals (R. Malenfant, unpublished data). During pedigree creation, we documented six new cases of cub adoption, and show—for the first time—an instance of monozygotic twinning among polar bears. Further, we find no cases of inbreeding between first-degree relatives. This pedigree is now being used to determine the mating system of polar bears (Richardson 2014), and in future studies, this pedigree will be used to determine the heritabilities of various body size metrics, some of which have been declining in this subpopulation for decades (Stirling & Derocher 2012).

5.3 Materials and methods

5.3.1 Sample collection

Most tissue samples were collected from bears that were immobilized and handled as part of long-term ecological studies of polar bears in Western Hudson Bay, Canada. However, a small number of samples were collected from bears captured by Manitoba Conservation staff near the community of Churchill as part of the Polar Bear Alert Program (Kearney 1989) or from polar bears harvested each year as part of a legal, regulated subsistence hunt by Inuit living along the coast of western Hudson Bay (Derocher *et al.* 1997; Taylor *et al.* 2008). Sampling locations are shown in Figure 5.1. During their first handling, each individual was assigned a unique ID applied as a permanent tattoo on the inside of the upper lip and affixed as a plastic tag in each ear. Skin samples were collected by retaining leftover pinnal tissue from ear-tagging or from adipose tissue samples collected using a 6-mm biopsy punch of superficial fat on the rump (Ramsay *et al.* 1992; Thiemann *et al.* 2008b). Blood samples were collected by drawing blood from a femoral vein into a sterile Vacutainer®. All samples were stored at –80°C until DNA extraction. If the age of a newly sampled individual was unknown (i.e., not a cub-of-the-year or a dependent yearling), a vestigial premolar tooth was extracted for age determination using measurement of cementum annulus deposition (Calvert & Ramsay 1998). All individuals handled by Environment and Climate Change Canada were sampled between mid-July and late December and were selected for handling indiscriminately of age or sex; however, in every year from 1980 onward (except for 1985 and 1986), a February/March sampling effort was also included, in which only adult females and their cubs-of-the-year—which had recently emerged from maternity dens—were handled.

5.3.2 DNA extraction and microsatellite genotyping

Total genomic DNA was extracted from fat, skin, or leukocytes recovered from ACK-lysed blood using DNeasy® Blood & Tissue Kits (Qiagen, Hilden, Germany). We genotyped 2945 individuals born between 1960 and 2011, including duplicate samples from 69 individuals included to estimate genotyping error rates. Individuals born before 2006 were genotyped at all 25 microsatellite loci (Table A5.1); however, because of changes to the genotyping protocol made in 2012 to streamline microsatellite multiplexing, individuals born from 2006 onward were genotyped at 24 loci (excluding CXX173). PCR products from microsatellite amplifications were resolved on an Applied Biosystems 377 DNA Sequencer, 3100-Avant DNA Analyzer, or a 3730 DNA Analyzer, and sized relative to GENESCAN size standards. Genotyping was performed using the programs GENOTYPER and GENEMAPPER (Applied Biosystems, Foster City, CA, USA).

5.3.3 Genetic diversity, tests of disequilibrium, and statistics

The number of observed alleles (N_A), observed heterozygosities (H_O), expected heterozygosities (H_E), probabilities of exclusion (P_{ex}), and probabilities of identity (P_{ID}) were calculated using GENALEX 6.501 (Peakall & Smouse 2006, 2012); P_{ex} was calculated using the formula for single unknown parent exclusion from Jamieson and Taylor (1997). Departures from Hardy–Weinberg equilibrium (HWE) and linkage disequilibrium (LD) were assessed with exact tests (Guo & Thompson 1992) and a Markov chain (dememorization number = 5000, number of batches = 1000, number of iterations per batch = 2000) using GENEPOP ON THE WEB 4.2 (Raymond & Rousset 1995; Rousset 2008). The total genotyping error rate (calculated as the sum of the allelic dropout rate (E1) and false allele rate (E2), Table A6.1) was calculated from duplicate samples using the program PEDANT 1.0 (Johnson & Haydon 2007) using 100,000 replicates. Unless otherwise indicated, all other statistics were calculated in R 3.1.3 (R Core Team 2015), and a significance level of α=0.05 was used for all tests.

5.3.4 Pedigree generation and adoption detection

We used the program FRANZ 2.0 (Riester *et al.* 2009, 2010) to generate an initial pedigree from our microsatellite data, using a sub-pedigree comprising known mother–cub relations from field data, individuals' years of birth (and death, if known) and the settings specified in Table 5.1. FRANZ generates a multigenerational pedigree in a single step, using simulations to determine expected parent–offspring mismatch rates, simulated annealing to estimate the maximum-

likelihood pedigree, and Metropolis-coupled Markov chain Monte Carlo sampling to calculate parentage posterior probabilities. As part of its simulation step, FRANZ uses the empirical distribution of parent–offspring mismatch rates to identify problematic parental assignments in the sub-pedigree (Figure 5.2), which we have classified here as putative adoptions. Although our field records contain no instances of females younger than four years old (or older than 28 years old) having successfully given birth, we specified a possible reproductive age range of 2–32 (at time of parturition) to account for outliers amongst unobserved maternities as well as possible errors in tooth aging (cf. Medill *et al.* 2009). For simplicity, we also used this same age range for males; males generally do not become reproductively active until at least their fifth or sixth year, though they may begin to produce spermatozoa at age two (Rosing-Asvid *et al.* 2002). The oldest female and male polar bears captured in the Western Hudson Bay subpopulation were 32 and 29 years old, respectively.

To detect the genetic mothers of adopted individuals, we removed their links from our field-data sub-pedigree and re-ran FRANZ. Then, to validate and error-correct the resultant pedigree, we used the program VIPER 1.01 (Paterson *et al.* 2012) to examine the inheritance of 4,475 single-nucleotide polymorphisms (SNPs) genotyped in a 859-individual subset of pedigreed bears. These SNPs were developed from transcriptomic and RAD sequencing and were genotyped with high fidelity in all individuals using a recently developed 9K Illumina BeadChip for polar bears (Malenfant *et al.* 2015a). We removed all pedigree links displaying more than one SNP inheritance error, which we determined as a cutoff based on the empirical distribution of inheritance errors.

Finally, to account for a lower proportion of males than females being sampled in our data (which led to proportionally fewer paternity than maternity assignments), we used the program COLONY 2.0 (Jones & Wang 2010) to generate hypothetical sires and differentiate between full siblings and maternal half siblings. To reduce false paternity assignments, we limited candidate offspring in this analysis to 760 individuals having unassigned sires but genetically assigned dams. All individuals were pooled in a single analysis irrespective of birth year to allow for the possibility that a hypothetical male had sired multiple offspring across years. We allowed for male and female polygamy, using maternal and paternal sibship priors of 3.655 and 2.968 respectively, which were

determined empirically from the pedigree. All pedigree statistics were calculated using the package PEDANTICS 1.5 (Morrissey & Wilson 2010).

5.3.5 Genetic relatedness

Asocial animals such as polar bears might choose to adopt nearby orphans if they are genetically related, as this can provide an inclusive fitness advantage to the foster parent (e.g., Gorrell *et al.* 2010). To determine if adopted cubs were genetically related to their foster mothers, we used the program COANCESTRY 1.0.1.2 (Wang 2011) to obtain the Queller-and-Goodnight (1989), Lynch-and-Ritland (1999), and Wang (2002) relatedness metrics using allele frequencies and error rates estimated from the full microsatellite dataset. Because all estimators gave similar results, only the Queller-and-Goodnight estimator results are presented. This estimator was designed for studies of kin selection and has the property that unrelated individuals are expected, on average, to have a relatedness of zero.

5.4 Results

5.4.1 Microsatellite genotypes

Complete 25-locus genotypes were obtained for 2418 individuals, 24-locus genotypes were obtained for 478 individuals, 23-locus genotypes were obtained for 34 individuals, and 22-locus genotypes were obtained for 15 individuals. The mean number of observed alleles (N_A) was 7.6 (range: 3–10), and mean observed (H_O) and expected (H_E) heterozygosities were both 0.672 (ranges: 0.112–0.847 and 0.112–0.840, respectively). Two loci, G1A and G10L, deviated from HWE (P_{G1A} = 0.0028, P_{G10L} = 0.0064) but were not significantly out of HWE following a strict Bonferroni correction for multiple tests ($\alpha_{corrected}$ = 0.002). Complete summary statistics for microsatellite loci are presented in Table A5.1. Thirty pairwise tests of LD were significant following strict Bonferroni correction, however, this was likely because our dataset contained many groups of related individuals. Combined probability of exclusion (P_{ex}) over all loci is 0.99991; this drops to 0.99988 if the locus CXX173—the locus that was not typed in individuals born from 2006 onward—is excluded. Combined probability of identity (P_{ID}) was 7.102×10^{-23} for unrelated individuals and 1.562×10^{-9} for full siblings; these increase to 5.020×10^{-22} and 3.551×10^{-9} respectively if CXX173 is excluded. Total genotyping error rate was estimated at 0.36%. Fourteen successfully genotyped individuals were removed prior to pedigree generation because their years of birth were unknown.

5.4.2 Pedigree statistics and inbreeding

We supplemented the remaining 2931 genotyped-and-aged individuals with 1225 individuals known only from field observation. FRANz assigned 2972 maternities using field and/or genetic data and 1105 paternities using genetic data alone. Based on SNP inheritance errors identified in VIPER, 4 offspring–sire links out of 163 (=2.5%) and 15 offspring–dam links out of 465 (=3.2%) were removed. In all 15 of these cases, offspring–dam relationships had been inferred using genetic data only (i.e., they were not based on field observations). COLONY reconstructed 293 sires, which collectively accounted for 760 paternal assignments (mean ± SD offspring per reconstructed sire = 2.6 ± 1.4), and brought the pedigree to 4449 individuals in total. Nine females aged 3 years or younger and nine males aged 2 years or younger (at time of conception) were assigned as parents in the final version of the pedigree, though the ages of 17 of these 18 individuals were uncertain as they were derived from tooth-aging estimates. The oldest dam and sire assigned in the pedigree were 28 and 30 respectively at the time of conception.

Including COLONY-reconstructed individuals, the pedigree contains 1381 founders (i.e., individuals of unknown parentage) and extends to six generations for some individuals. Of 382 recorded mating events in which the identities of dam, sire, and at least one grandparent on each side were known, only three individuals had non-zero inbreeding coefficients: X11088, X11089, and X11389. X11088 and X11089 are littermates born in 1989 to X10668 after mating with her half-brother X10497; X11389 was supposedly born to X09396 and her brother X09398 (however, cf. the Discussion regarding this mating). A graphical view of the pedigree and complete pedigree statistics and are given in Figure 5.3 and Table A5.2, respectively.

5.4.3 Monozygotic twinning

We detected one pair of identical twin males among 574 genotyped twin litters and 37 genotyped triplet litters: cubs X17324 and X17326 match at all 25 loci (Online Resource 2 at doi:10.1007/s00300-015-1871-0). Both individuals were independent two-year olds at the time of capture (November 10 and 11, 2003, respectively), and were handled ~3.5 km apart on opposite sides of the Churchill airport. They were known not to have been recaptures of the same individual because the second-captured individual (X17326) did not have a permanent tattoo or ear tags. If dizygotic, the probability of these cubs sharing genotypes at all 25 loci is 1.64×10^{-11}, as calculated from the full genotypes of both parents. To discount the possibility that these identical genotypes

were the result of sample mix-up, we reconfirmed the genotype of X17324 using a second tissue sample that was collected from the animal's subsequent harvest; unfortunately, a second sample for X17326 was not available. However, because these individuals were handled on different days, the probability of sample mix-up during fieldwork is extremely low.

5.4.4 Cases of adoption

We identified six previously undetected cases of adoption occurring between 1981 and 2004, and we identified four of the six genetic mothers (Table 5.2, Online Resource 2 at doi:10.1007/s00300-015-1871-0). In five of these cases, cubs were adopted during their first year of life; in the remaining case (X09059), it was unclear if the cub was adopted during its first or second year. In two cases, adoptive mothers were observed to have fostered cubs for at least a year, and from later capture and harvest records, it is known that at least five of the six adopted cubs survived to independence. The fate of X11097 is unknown. Although five of the six adopted cubs were female, there was no statistical evidence of preference to adopt females over males (binomial test of 1:1 ratio: $P = 0.22$). All adopted cubs appeared to be unrelated to their adoptive mothers: average adoptee–adopter relatedness is −0.038, and 95% confidence intervals for the Queller-and-Goodnight relatedness estimators were not significantly different from 0 in all cases. In two of the six adoption cases, females were also accompanied by their own genetic offspring.

5.5 Discussion

5.5.1 Inbreeding

Active inbreeding avoidance is often presumed to be common amongst animals because of reduced fitness of inbred offspring (Keller & Waller 2002), though tolerance of—or even preference for—inbreeding may occur because of inclusive fitness benefits (Szulkin *et al.* 2013). When inbreeding avoidance does occur, it is generally attributed to mate choice or sex-biased dispersal (Pusey & Wolf 1996). However, sex-biased dispersal may also occur for reasons unrelated to inbreeding, such as sex differences in the benefits of retaining a productive territory or avoidance of intersexual competition (Moore & Ali 1984). Little is known about inbreeding or sex-biased dispersal in polar bears, and primary among the motivations for developing this pedigree was the characterization of inbreeding in this subpopulation (Richardson *et al.* 2006).

We detected only two instances of incestuous mating: one between half-siblings X10668 and X10497 (producing X11088 and X11089), and another putative case between full-siblings

X09396 and X09398 (producing X11389). However, in this latter case, X09398 is almost certainly a false paternity assignment: X09396 is an ungenotyped dam that was assigned using only field data, probably causing X09398 to be incorrectly assigned as a father because of allele-sharing with his sister. Therefore, after excluding this case, inbreeding among close relatives appears to be extremely rare in the Western Hudson Bay subpopulation, occurring only once among the 382 mating events (=0.26%) in which it could have been observed, although this is a minimum estimate because of the incompleteness of the pedigree. For comparison, in a study of the Barents Sea subpopulation, a single instance of father–daughter inbreeding was detected amongst 22 matings between parents of known identity (Zeyl *et al.* 2009a), suggesting that the rate of mating between first-degree relatives was ~4.5%.

Polar bears exhibit low variation at major histocompatibility complex (MHC) loci (Weber *et al.* 2013), which are thought to play an important role in kin recognition (Villinger & Waldman 2012). Black bears seem to have poor kin recognition (Moore *et al.* 2015), and it has been suggested that polar bears have also undergone little selection for kin recognition because of low population densities (Lunn *et al.* 2000). If this is the case amongst polar bears, then kin recognition and mate choice are unlikely to explain low inbreeding rates. In contrast, our finding of little-to-no inbreeding in the Western Hudson Bay subpopulation may result from substantial dispersal and interbreeding between Western Hudson Bay and the adjacent Southern Hudson Bay and (southern) Foxe Basin management units (Richardson 2014), which are genetically similar to Western Hudson Bay (Crompton *et al.* 2014; Viengkone 2015). Studies of American black bears (*U. americanus*; Costello *et al.* 2008; however, cf. Moore et al. 2015) and brown bears (*U. arctos*; Bellemain *et al.* 2006) have found similar rates of close inbreeding, which were attributed to lack of opportunity resulting from low population density and male-biased dispersal. In another study, inbreeding avoidance was cited as the most likely cause of male natal dispersal among brown bears (Zedrosser *et al.* 2007). These findings are also likely to hold true for polar bears, which occur at even lower densities, and for which limited genetic evidence also suggests male-biased dispersal in some subpopulations (Zeyl *et al.* 2009b). However, because radio-telemetry data for male polar bears is scarce, little is known about dispersal patterns in male polar bears and further study is needed.

5.5.2 Monozygotic twinning

Inclusive fitness theory predicts the possible spread of genes for monozygotic twinning (Gleeson *et al.* 1994; Williams 1975), and though the reason for the rarity of monozygotic twinning is not well understood, it may be partially attributable to higher rates of spontaneous abortion for monozygotic twins (Livingston & Poland 1980) and lower survival of twins in species that normally bear only one offspring (e.g., Fricke 2001). Based on observed sex ratios of multi-cub litters, Ramsay and Stirling (1988) determined that monozygotic twinning was likely rare or absent among polar bears. Our study confirms that monozygotic polar bear twins are extremely rare, being found in less than 1/600 litters ($\lesssim$0.17%) in our data. To our knowledge, this is the first confirmed record of monozygotic twinning among polar bears or any other ursid, and previous genetics studies of bears (e.g., Bellemain *et al.* 2006; Proctor *et al.* 2004; Zeyl *et al.* 2009a) likely failed to detect twins because of smaller sample sizes. Slightly higher rates of monozygotic twinning have been found for humans (0.35–0.4%; Bulmer 1970) and for cattle (0.33%; Silva del Río *et al.* 2006). In part, the lower estimate for polar bears may result from discounting the "invisible fraction" (Grafen 1988) of identical twins that were never observed because at least one cub died prior to emergence from the maternity den.

5.5.3 Adoption

According to Hamilton's (1964) theory of kin selection, natural selection will favour a heritable predisposition for altruistic behaviour when $C < rB$, where C is the fitness cost to the altruist, B is the fitness benefit to recipient, and r is the relatedness between these individuals. Thus, kin selection requires greater-than-average relatedness between altruist and recipient, and relatedness must be particularly high to account for such energetically costly behaviours as adoption and nursing. Lunn *et al.* (2000) ruled out kin selection as an explanation for three previous cases of polar bear adoption based on low genetic relatedness. Our results reinforce the finding that adopted cubs and their foster mothers seem to be unrelated, and that kin selection does not appear to drive adoption in this subpopulation. Though reciprocal care of offspring has been observed in polar bears (Lunn 1986), given polar bears' low population densities and generally asocial nature, reciprocal altruism is also extremely unlikely to explain the observed adoptions, and no reciprocal cases of adoption were observed in our data.

Milk evacuation may explain allonursing behaviour in some pinnipeds (Riedman & Boeuf 1982) and bats (Wilkinson 1992); however, it is extremely unlikely to explain adoption in polar bears. Whereas it is beneficial for pinnipeds and bats to be leaner to increase diving or flight efficiency (Roulin 2002), lean polar bears lack the energy storage and thermal benefits (Pond *et al.* 1992), as well as the reproductive benefits (Stirling *et al.* 1999) associated with fatter body condition. This is particularly true in the Western Hudson Bay subpopulation, where mothers may fast for four or more months during the ice-free period each year. In this subpopulation, a female's ability to maintain pregnancy (Derocher *et al.* 1992) and the survival of her own cubs (Derocher & Stirling 1996) are mass-dependent, so that a female would gain no apparent benefit from milk evacuation. Since it appears that all six foster mothers had birthed genetic litters by the time of adoption, the parental experience hypothesis is also unlikely to account for any of these adoptions (Roulin 2002).

Adopted cubs were captured alone with their foster mother in four of six cases, and in all these cases, the adopted cub is known to have survived to independence, implying the provisioning of milk by the mother to the adoptive offspring, as has been observed directly in at least once instance of fostering (Belikov 1976). Because spontaneous lactation is not believed to occur in most species and has only been consistently demonstrated among dwarf mongooses (*Helogale parvula*) suckling close relatives (Creel *et al.* 1991), it is highly unlikely to explain allonursing of alien offspring among polar bears. This suggests that these cubs' adoptions coincided with the loss of the females' biological litters (either due to death or because of unintentional cub-swapping with another female), while females were biologically capable of suckling. In the remaining two adoption cases, cub misidentification is the most likely explanation, as adopted cubs were accompanied by the female's own biological offspring. Cub mixing sometimes occurs in both polar bears and brown bears (Glenn *et al.* 1976; Lunn 1986), and in any of these adoption cases, cub-swapping may have occurred due to simple misidentification during periods of high bear density, such as springtime den emergence or the autumn fasting period ashore (Derocher & Stirling 1990; Ramsay & Stirling 1988). We note that in one observed case of adoption, it has been proposed that a female with two cubs of her own adopted two of another female's cubs after she was killed in a fight (Vibe 1976); however, in all four cases in which we were able to infer an adopted cub's biological dam, the biological dam is known to have survived past the adoption

event based on field data or later pedigree assignments. Therefore, in at least four of our six cases, the adoption cannot be attributed to orphaning.

It has been suggested that scientific handling may increase the probability of cub abandonment or adoption if maternal vigilance is reduced during the time it takes to fully recover from immobilization (Derocher & Wiig 1999). Importantly, we found no evidence to support this hypothesis. We were able to identify four of the six genetic mothers, two of which had not been captured for five years prior to the adoption, and the remaining two of which were not captured until after the adoption. Likewise, none of the six foster mothers was captured in the period between the adopted cub's birth and their first observation together. This finding corresponds with a number of studies that have failed to find a significant negative correlation between scientific handling and litter size (Amstrup 1993; Lunn *et al.* 2004), cub survival (Ramsay & Stirling 1986a; Rode *et al.* 2014), or the cohesion of family groups (Messier 2000).

5.6 Ethical standards

All applicable international, national, and/or institutional guidelines for the care and use of animals were followed. Environment and Climate Change Canada's animal-handling procedures were approved annually by their Prairie and Northern Region Animal Care Committee, and all research was conducted under wildlife research permits issued by the Province of Manitoba and by Parks Canada Agency.

Table 5.1. Non-default settings used for pedigree generation in the program FRANz.

Parameter	Setting
Female reproductive age range	2–32
Male reproductive age range	2–32
Maximum number of candidate mothers	5,000
Maximum number of candidate fathers	5,000
Number of simulation iterations	1,000,000
Maximum number of simulated annealing iterations	1,000,000,000
Number of Metropolis–Hastings burn-in iterations	5,000,000
Number of Metropolis–Hastings iterations	30,000,000
Metropolis–Hastings sampling frequency	100

Table 5.2. New cases of polar bear adoption reported in this paper. P_M = proportion of loci mismatched between cub and candidate mother; r_{QG} = Queller-and-Goodnight relatedness between cub and the adoptive mother. In two cases (represented as "—"), the true dam could not be determined. Asterisks denote individuals whose genotypes could be confirmed by genetic assignment of their other observed offspring to them; most cubs' genotypes could not be confirmed in this manner because they are not known to have parented offspring.

Cub	Sex	Year of birth	Observed dam (P_M)	Date(s) observed together	Age of observed dam	Other cubs in litter	r_{QG} (95% CI)	Inferred dam (P_M)	Survived to independence
X09059*	Female	1980	X05562* (10/25)	Aug. 10, 1981	7	0	−0.19 (−0.36 – 0.03)	X09913* (0/25)	Yes
X10608	Female	1987	X10607* (5/25)	Sept. 24, 1987	8	0	−0.05 (−0.22 – 0.12)	—	Yes
X11097	Female	1989	X05668* (9/25)	Mar. 22, 1989	6	2	−0.07 (−0.35 – 0.14)	X11456* (0/25)	Unknown
X17069	Male	1998	X03318* (4/25)	Nov. 30, 1998	24	0	0.17 (0.00 – 0.36)	—	Yes
X17294*	Female	2003	X17082* (4/25)	Sept. 22, 2003 – Nov. 8, 2004	7–8	1	0.03 (−0.12 – 0.21)	X10688* (0/25)	Yes
X19939	Female	2004	X11940* (12/25)	Sept. 18, 2004 – Sept. 18, 2005	11–12	0	−0.12 (−0.38 – 0.10)	X12273* (1/25)	Yes

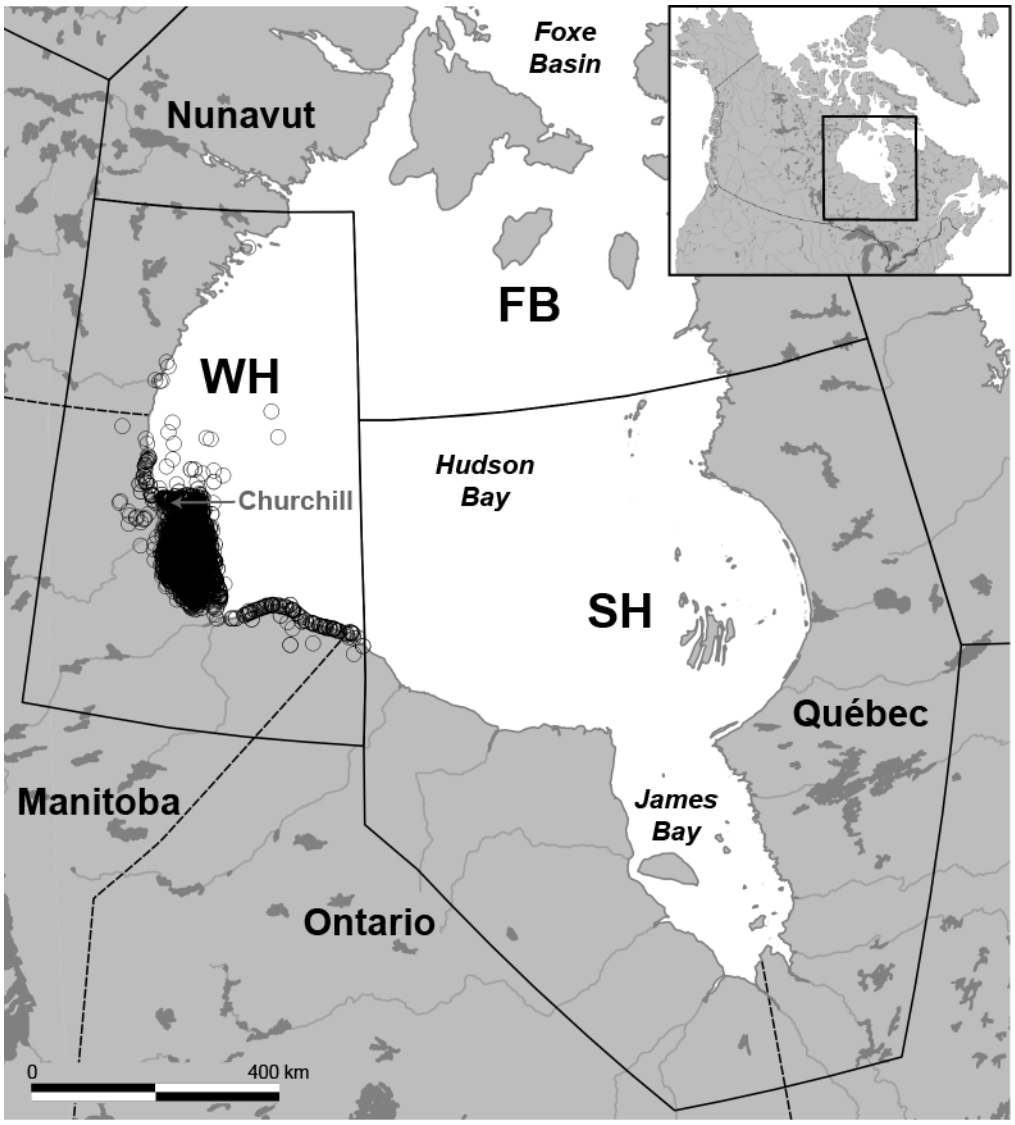

Figure 5.1. Sampling locations of bears included in the Western Hudson Bay pedigree. Solid lines indicate management unit borders (FB = Foxe Basin; SH = Southern Hudson Bay; WH = Western Hudson Bay); dashed lines indicate provincial or territorial borders.

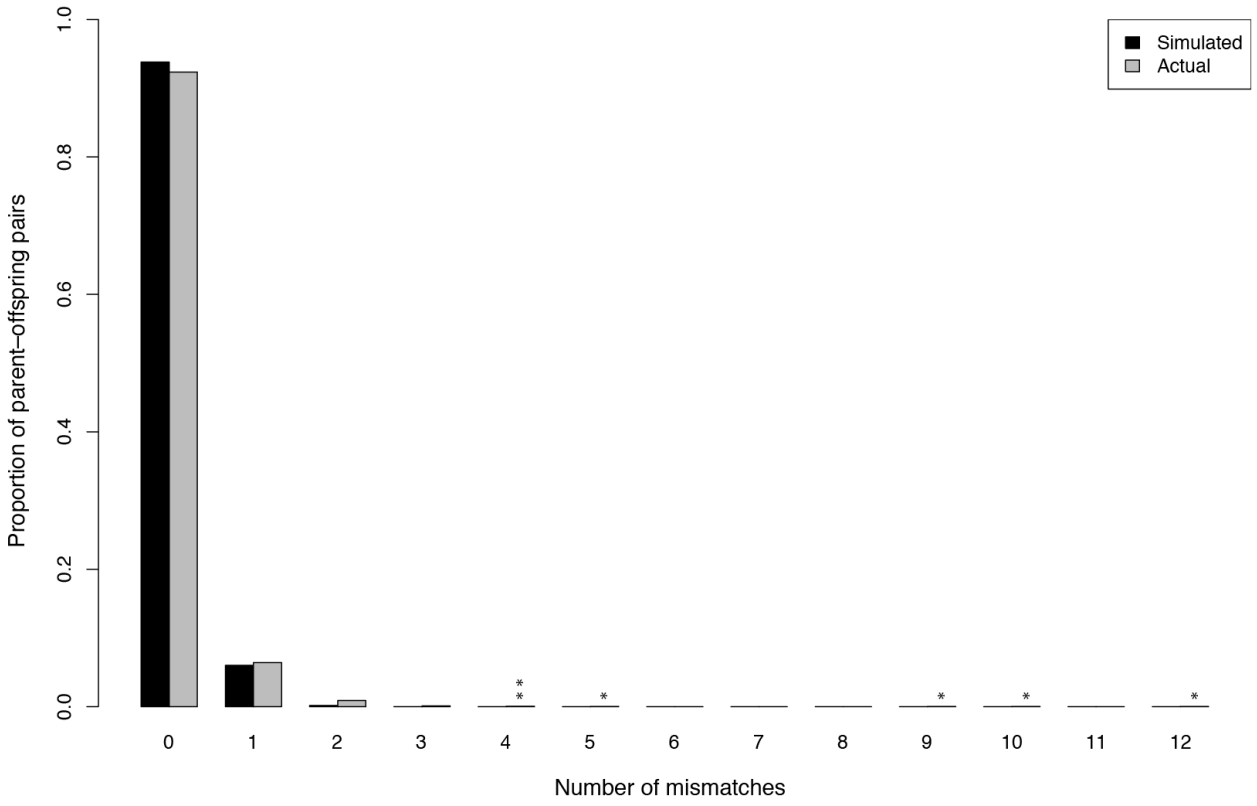

Figure 5.2. Number of mismatched microsatellite loci for simulated and actual parentage assignments. Simulation results represent 2,000,000 parent–offspring pairs generated in FRANz using empirically estimated error rates. Asterisks indicate putatively adopted individuals.

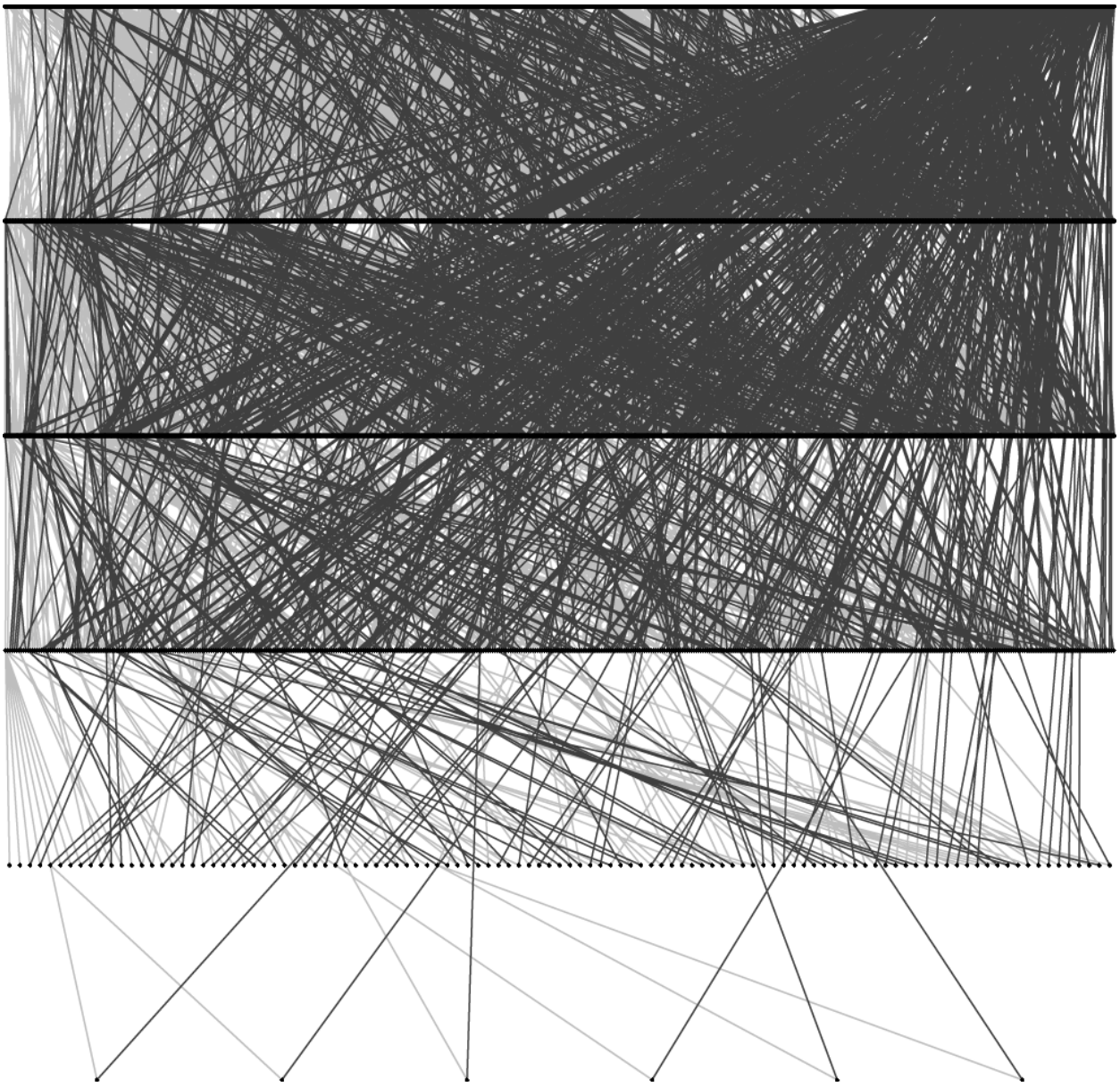

Figure 5.3. Graphical representation of the 4449-individual polar bear pedigree described in this paper. Each point is an individual bear. Maternities are represented by grey lines; paternities are represented by black lines.

Chapter 6: Heritability of body size in the polar bears of Western Hudson Bay

6.1 Abstract

Polar bears (*Ursus maritimus*) are the largest of all extant bears, and individual fitness is directly dependent on body size through males' abilities to win access to mates, females' abilities to provide for their young, and all bears' abilities to survive increasingly long fasting periods caused by climate-changed induced habitat loss. In the southerly Western Hudson Bay subpopulation (near Churchill, Manitoba, Canada), polar bears have been declining in body size and condition for decades; however, nothing is yet known about the contemporary genetic underpinnings of body size variation, which may be subject to natural selection based on these changes. Here, we combine two recently developed genetic resources for polar bears—a 4459-individual multigenerational pedigree and a medium-density single-nucleotide polymorphism (SNP) genotyping array—to provide the first estimates of contemporary genetic variation in fitness-related traits in polar bears. We used the animal model to generate estimates of heritability (h^2) from repeated measures recorded between 1966 and 2011, obtaining h^2 estimates of 0.34–0.48 for strictly skeletal traits and 0.17 for axillary girth (a measure that is also dependent on fatness). We genotyped 859 of these individuals with our SNP array to test for association with estimated breeding values for these traits, and combined p-values over genetic pathways using gene-set analysis. Results appear to be characteristic of polygenetic inheritance and suggest that variability in axillary girth may be partially attributable to variation in pathways related to growth-hormone signaling and the trefoil-factor pathway, which is expressed in gastrointestinal mucosa. Low evolvabilities suggest that the polar bears of Western Hudson Bay will be slow to adapt genetically to climate change.

6.2 Introduction

One of the primary aims of evolutionary biology is determining the nature of variation in fitness-related traits (Ellegren & Sheldon 2008), including the dissection of traits into variance components (Lynch & Walsh 1998), and the determination of the traits' genomic architectures (Slate *et al.* 2010). Typically, this is done using a multigenerational pedigree (Pemberton 2008), in order to obtain the expected genetic relatedness between all members of the population, which can be used in a linear mixed effects model known as the "animal model" to estimate heritability (Kruuk 2004; Wilson *et al.* 2010). In species for which high-density genotyping assays are available or for which next-generation sequencing of hundreds or thousands of individuals is economically feasible, pedigrees are beginning to lose currency for heritability estimation (Speed & Balding 2015). This is because constructing a pedigree data is burdensome, and because calculating heritability based on *actualized* relatedness directly from genetic markers as opposed to *expected* relatedness based on pedigree relationships can generate more accurate results when a large number of markers (i.e., ≥10,000) are used (Bérénos *et al.* 2014; Speed & Balding 2015; Visscher 2009). Regardless of the method of estimation, variation in morphological traits such as body size have generally been found to have moderate heritability (h^2) in wild populations (i.e., $\overline{h^2}$ = 0.56; Postma 2014) and coefficients of variation—which are mean-scaled and are therefore a better way of comparing multiple traits or populations (Houle 1992)—are typically less than 10% for adult size (Hill 2012). In model organisms, most of the genetic variance in complex traits is additive (Hill *et al.* 2008), and caused by large numbers of loci, mostly of small effect (Flint & Mackay 2009). This "infinitesimal model" is one of the key assumptions of classical quantitative genetics (Orr 2005).

In order to determine the genetic architecture of a trait, linkage-based quantitative trait locus (QTL) mapping has traditionally been used (e.g., Slate *et al.* 2002); however, as high-throughput genotyping has become affordable, there has been a recent shift a shift away from linkage mapping to association mapping (henceforth "genome-wide association studies"; GWAS), which use historical linkage disequilibrium as opposed to observed recombination events, which allows for finer-scale mapping of QTLs without the need for a pedigree (Mackay *et al.* 2009). Unfortunately, relatedness between individuals used in a GWAS is actually considered a confounding factor, which may result in false positives due to inflation of test statistics, and which

should be controlled for using any of a number of methods, including genomic control, principal component analysis (PCA), mixed models, or a combination of these (Price *et al.* 2010). With the greater availability of medium- and high-density single-nucleotide polymorphism (SNP) genotyping platforms and next-generation sequencing, genetic architecture has been examined in an increasing number of wild populations through GWAS and the related technique of genome partitioning (Yang *et al.* 2011b). Most have failed to find genes of large effect, suggesting that the traits are highly polygenic (e.g., Bérénos *et al.* 2015; Husby *et al.* 2015; Kardos *et al.* 2016; Miller 2015; Robinson *et al.* 2013; Santure *et al.* 2013; Wenzel *et al.* 2015; however, cf. Johnston et al. 2011), as indicated by a large number of weak associations that fail to reach genome-wide significance because of stringent post-correction α-values. Surprisingly, to our knowledge, all existing studies have stopped at this stage. None have applied recent techniques from human genetics such as gene-set analysis (de Leeuw *et al.* 2016; Wang *et al.* 2011), which can increase the power and interpretability of a GWAS by combining multiple SNP association statistics across genes and then across biological pathways.

Recently, polar bears (*Ursus maritimus*) have become a popular study species for wildlife genetics, though most studies have focused on phylogenetics and hybridization (e.g., Cahill *et al.* 2013; Cahill *et al.* 2015; Miller *et al.* 2012b). Polar bears diverged from brown bears (*U. arctos*) approximately 400,000 years ago (Liu *et al.* 2014), and they have experienced strong selection and rapid evolution in genes related to fat metabolism, energy production, and the cardiovascular system in response to changes in habitat and diet (Liu *et al.* 2014; Welch *et al.* 2014). Early studies of polar bear genetic variation using allozymes found very low intra- and inter-population genetic variation (Allendorf *et al.* 1979; Larsen *et al.* 1983), suggesting that little variation might remain after rapid evolution and subsequent bottlenecking during climatic fluctuations. Since the abandonment of allozymes for DNA markers, there have been few efforts to characterize the contemporary genetic variation of polar bears at potentially adaptive loci (however, cf. Bowen *et al.* 2015a; Weber *et al.* 2013), and there has never been an effort to characterize additive genetic variance or estimate heritability, despite their relevance to adaptability of populations in response to climate change (Gienapp & Brommer 2014).

In this paper, we use a recently developed pedigree of 4449 polar bears (*Ursus maritimus*) from the Western Hudson Bay subpopulation (Malenfant *et al.* 2015b) to estimate the heritability

of four routinely measured adult body size metrics using the animal model, specifically: straight-line body length, axillary girth (which is influenced by fatness), head length, and zygomatic breadth. These measures are variously related to fitness through the ability to win access to mates (Richardson 2014), to successfully birth and wean offspring (Derocher & Stirling 1996, 1998; Derocher *et al.* 1992), and to survive the annual fasting period (Molnár *et al.* 2010). After obtaining heritability estimates and the breeding value for each individual using best linear unbiased prediction (BLUP), we then used a medium-density SNP array (Malenfant *et al.* 2015a) to conduct a GWAS to look for markers and genes that may contribute to these breeding values. For comparison, we also include heritability estimates and a GWAS based on a recently published method that calculates heritability and marker associations directly from the genetic data without the need for a pedigree (Ronnegard *et al.* 2016). Finally, we use gene-set analysis in an attempt to render our results more interpretable. This study represents the first heritability estimates or examination of genetic architecture for any ursid.

6.3 Materials and methods

6.3.1 Data collection and quality control

Details of polar bear handling and sample collection in Western Hudson Bay are given by Malenfant *et al.* (2015b). In brief, polar bears have been handled by Environment and Climate Change Canada near Churchill, Manitoba, Canada between mid-July and late December indiscriminately of age or sex every year from 1966 to 2011, with additional sampling of adult females and their cubs-of-the-year in February and March in most years from 1980 onward. Western Hudson Bay is near the southern edge of the species' current distribution (IUCN/SSC Polar Bear Specialist Group 2015), and recent climate-change-induced loss of sea ice (Kowal *et al.* 2015) is thought to have resulted in smaller body sizes (Stirling & Parkinson 2006), possible changes to the morphometry–mass relationship (Thiemann *et al.* 2011), and a decline in population size (Lunn *et al.* 2016). Upon first capture, each individual was assigned a unique identifier using ear tags and a permanent tattoo on the inside of the upper lip. Leftover pinnal tissue was kept for genetic analysis. For individuals whose age could not be determined by visual inspection, a vestigial premolar tooth was extracted for age determination based on cementum annulus deposition (Calvert & Ramsay 1998). Each captured adult was measured for straight-line body length (from tip of nose to tip of tail) and axillary girth (i.e., body circumference measured under the armpits) using a tape measure. Since 1985, head length and zygomatic breadth have also been

estimated using callipers. Fatness is recorded on a subjective five-point scale (Stirling *et al.* 2008) that is not amenable to heritability estimation using ASREML and therefore was not considered here. Body mass is not usually measured for adult bears, though it can be estimated from body length and axillary girth (Thiemann *et al.* 2011). Environment and Climate Change Canada's animal-handling procedures were approved annually by their Prairie and Northern Region Animal Care Committee, and all research was conducted under wildlife research permits issued by the Province of Manitoba and by Parks Canada Agency.

Prior to estimation of heritability and genetic associations, we visually examined plots of growth curves and body-size ratios to detect and remove outliers. Outlying measurements were removed only if they were grossly incorrect; for instance, if a bear's head was recorded as having been wider than it was long, this suggested data-entry error and the point was removed (cf. Fig. A6.1). We also used preliminary runs of the program ASREML 3.0 (VSN International, Hemel Hempstead, UK) to identify and remove a small number of additional points identified as outliers when they could be confirmed as problematic by examining the original data. For instance, if a bear's adult length was measured three times as 234 cm, 263 cm, 235 cm, and the second measurement was identified as an outlier in ASREML, this point was removed as a probable data-entry error.

6.3.2 Heritability

We estimated the heritability of each body-size metric (and its standard error) independently, using restricted maximum-likelihood estimation of a univariate animal model in ASREML. For these analyses, we limited ourselves to examining only adult sizes, which are less likely to be influenced by maternal effects than juvenile traits (e.g., Réale *et al.* 1999). Although polar bears are highly sexually dimorphic (Derocher *et al.* 2005; Derocher *et al.* 2010), exploratory analyses suggested that cross-sex genetic correlations did not differ significantly from unity, so for all analyses in this chapter, we fitted univariate models (with sex as a fixed effect) in order to maximize sample sizes for the GWAS on breeding values. The significance of all fixed effects in our animal models were confirmed using conditional Wald tests. The significance of each random effect was assessed using a likelihood ratio-test (distributed as χ^2 with $d.f.$=1) comparing twice the log-likelihoods of the models with and without the effect. A significance level of α=0.05 was used for all tests unless otherwise indicated. The final models used are given in Table 6.1. Because

heritabilities are difficult to compare across traits or populations, we also calculated coefficients of variance and evolvabilities for each trait following Garcia-Gonzalez *et al.* (2012).

6.3.3 SNP genotyping and quality control

For SNP genotyping, we used a custom Illumina 9K BeadChip, the details of which are described by Malenfant *et al.* (2015a). Briefly, this array targets SNPs identified in restriction-site associated DNA (RAD) sequences from polar bears from across the Canadian Arctic and blood/fat transcriptomic SNPs identified in the polar bears of Western Hudson Bay. Whereas RAD SNPs were selected only to guarantee relatively even representation from the scaffolds of the draft polar bear genome, transcriptomic SNPs were selected for inclusion based on minor allele frequency in the ascertainment sample and their inclusion in at least one of a number of gene ontology categories, most of which we believed might be associated with differences in body size or other traits of interest (Malenfant *et al.* 2015a). The complete SNP dataset for Western Hudson Bay comprises 859 individuals genotyped for 5433 SNPs that passed our GENOMESTUDIO® quality controls (Malenfant *et al.* 2015a). To facilitate the possible future construction of a linkage map, the dataset includes many first-degree relatives. Individuals from our pedigree were selected for SNP genotyping so as to simultaneously maximize the number of parent–offspring links and the number of repeated measures, but without ascertainment with respect to any phenotypic trait.

For SNPs, we used a quality-control protocol based on those of Turner *et al.* (2001) and Anderson *et al.* (2010), using a custom version of PLINK 1.07 (Malenfant *et al.* 2015a; Purcell *et al.* 2007). Because of probable sample mix-up, prior to analysis we removed two individuals who were reported as being female based on field data but who were genetically male based on average heterozygosity for X-linked SNPs (cf. Malenfant *et al.* 2015a). X-linked SNPs were subsequently removed. We also removed individuals with abnormally high or low heterozygosity (i.e., population mean ± 3 SD) or having >2% missing data. We then used a modified version of EIGENSOFT 5.02 (Price *et al.* 2006) to perform a principal component analysis (PCA) on an LD-pruned dataset (using *--indep-pairwise 10 1 0.2* in PLINK) comprising 1416 quality-filtered bears from across Canada to detect and remove Western Hudson Bay individuals who appeared to be migrants or to be admixed based on visual examination of the first two principal components (PCs; Fig. A6.2). We then removed SNPs with a minor allele frequency (MAF) < 0.01 or >2% missing data. We flagged SNPs that were significantly out of Hardy–Weinberg equilibrium (HWE; α =

0.001) for further examination post-GWAS rather than discarding them because disequilibrium may be expected in the presence of a true association (Turner *et al.* 2001). SNPs with Mendelian inheritance errors based on pre-established pedigree relations were likewise flagged but retained, as they may represent phenotype-specific copy-number variants (Turner *et al.* 2001). Allele frequencies and HWE p-values were calculated using only the 374 founders within the SNP-genotyped data.

6.3.3 Genome-wide association study – estimation from breeding values

Traditional GWAS methods (e.g., PLINK, EMMAX, GCTA) cannot account for repeated measurements on a single individual (Husby *et al.* 2015), as is the case for body length and axillary girth in our data. One way to approach this problem is to use a pedigree to calculate the heritability of the trait and predict individuals' breeding values using BLUP. Individuals' predicted breeding values can then be used as singly measured traits in a GWAS (e.g., Johnston *et al.* 2011; Miller 2015). We adopted this approach, which we refer to as $GWAS_{Ped}$, for comparison with a newer approach—described below—that estimates the GWAS directly from repeated-measures data. We used the predicted breeding values from ASReml and discarded records for all individuals who were not measured at least once for the trait of interest. Therefore, our GWAS does not include any individuals whose breeding values were based solely on the predicted genetic merit of their relatives. We used these breeding values as response variables in a GWAS calculated using a modified version of GCTA 1.21 (Yang *et al.* 2011a). GCTA implements a mixed-linear-model-association (MLMA) analysis, in which a genetic relationship matrix (GRM) is calculated from the data and its contribution to phenotypic similarity is accounted for when testing each marker. By accounting for the actual structure in the data being used, this approach can result in both lower false positive rates and increased power (Yang *et al.* 2014). Specifically, we applied GCTA's "leave-one-chromosome-out" (MLMA-LOCO) approach, in which the chromosome—or in our case, scaffold—on which a SNP is located is omitted when the GRM used for the association test of that SNP is generated. This further increases the power to detect an association (Yang *et al.* 2014).

Whether population stratification has been correctly accounted for in a GWAS is generally determined by examination of a quantile–quantile plot (QQ plot) of p-values and the calculation of a genomic-inflation factor (λ). In the case that there is little population stratification and only a

few markers show association with the trait, then λ should be approximately equal to one (Devlin & Roeder 1999). If $\lambda > 1.05$, then test statistics from association analyses may be unacceptably inflated by the effects of population stratification (Price *et al.* 2010). Typically, this is addressed by adding eigenvectors from a principal component analysis (PCA) of genotype data as fixed effects in the GWAS to account for stratification (Price *et al.* 2006; Price *et al.* 2010; Stram 2014). However, in traits that are highly polygenic, as is likely to be the case for skeletal size and fatness (Lango Allen *et al.* 2010; Speliotes *et al.* 2010), QQ plots may indicate apparent genomic inflation even in the absence of population structure (Yang *et al.* 2011c). This is because a large number of the markers used are likely to capture *some* variation in the trait since many SNPs will be in LD with causal variants. Polygenicity and population stratification can be pieced apart by regressing the test statistics for SNPs on the SNPs' LD scores (Bulik-Sullivan *et al.* 2015); however, this requires high-density phased genotypes that are not available for polar bears.

Our initial QQ plots for $GWAS_{Ped}$ suggested substantial genomic inflation. Because we were unable to apply LD-score regression, we considered three versions of $GWAS_{Ped}$: one with no eigenvectors used as fixed effects, one with 10 eigenvectors (EIGENSOFT's default), and one with the top 127 eigenvectors, all of which were determined as being significant using Velicer's minimum average partial test (Velicer 1976), as implemented in the R code provided by Shriner (2011). For all GWAS, we calculated λ for p-values using the regression method in GENABEL 1.8-0 (GENABEL project developers 2013) and q-values (Storey 2002) in the R package QVALUE 2.2.2 (Storey *et al.* 2015). GWAS hits with $q<0.1$ were considered significant. Manhattan plots and QQ plots were generated using the R package QQMAN (Turner 2014) in R 3.2.3 (R Core Team 2015).

6.3.4 Genome-wide association study – direct estimation from repeated measures

Breeding values predicted using BLUP may be biased, which can lead to anticonservative results (Hadfield *et al.* 2010; Postma 2006). Therefore, as an alternate approach to $GWAS_{Ped}$, we also used a recently developed GWAS method implemented in the R package REPEATABEL 1.0 (Ronnegard *et al.* 2016) to simultaneously estimate trait heritability and SNP effects. We call this approach $GWAS_{Rep}$. REPEATABEL is explicitly designed for association analyses on repeated-measures traits for individuals that may be related. The method operates in three main steps: first, a linear mixed model is fitted (assuming no SNP effects) to estimate variance components (e.g.,

heritability) using a GRM as a correlation matrix for polygenic effects; second, a new response vector and design matrix are calculated for non-genetic fixed effects; finally, SNP effects are estimated using ordinary least squares and significance is computed using Wald tests. Because we were unable to get convergence with the ASREML models presented in Table 6.1, for these models, we fitted age as a covariate instead of a factor and include an age^2 term for axillary girth to account for senescence.

6.3.5 Gene-set analysis

We performed gene-set analysis on each the $GWAS_{Ped}$ results for each of the four traits using MAGMA 1.03 (default settings; de Leeuw *et al.* 2015). For this analysis, we extracted gene locations from NCBI's *Ursus maritimus* Annotation Release 100, and we tested the 1330 canonical pathways from the MSigDB Database (version 5.1; Subramanian *et al.* 2005). Following de Leeuw *et al.* (2015), we used a 10-kb window for SNP annotation by default; however, we tested the robustness of our results by seeing if they held when the program was set to 0-kb, 20-kb, and 50-kb windows. To account for multiple tests within each window-size setting, we used MAGMA's empirical p-value approach, using 10,000 permutations.

6.4 Results

6.4.1 Data collection and quality control

Plots of morphometric measurements as a function of age are shown in Fig. 6.1. Females approach asymptotic sizes at a younger age than males across all morphometrics except for zygomatic breadth, which appears to increase gradually throughout their lives. For axillary girth, which is partially dependent on body fatness, males display clear signs of senescence beginning in their late teens or early twenties. This is less apparent in females, likely because of the moderating effect of cub rearing of females during their peak reproductive years and the additional springtime sampling effort in which many females are captured post-parturition. The total number of individuals and measurements retained for pedigree-based heritability analysis of each adult trait is shown in Table 6.2.

For SNP-based analyses, six individuals were removed because of high/low heterozygosity, and three individuals were removed because of low genotyping success rates; total genotyping rate in the remaining individuals was >0.999. Seven individuals were removed because they appeared to be migrants or to be admixed based on visual examination of a scatterplot of PCs

1 and 2 (Fig. A6.2). In total, 841 Western Hudson Bay individuals passed all filtering criteria. Subsequently, four SNPs were removed because of missing data, and 861 SNPs were removed because of low MAF, leaving 4461 autosomal SNPs for downstream analysis. Two RAD SNPs and two transcriptomic SNPs were flagged as being significantly out of HWE. Six SNPs were flagged as containing either one or two Mendelian inheritance errors.

6.4.2 Heritability

Estimated variance components from ASREML are given in Tables 6.2 and 6.3; coefficients of additive genetic variation (CV_A) and univariate evolvabilities (I_A) are given in Table 6.4. All fixed and random effects included in the final models were significant, and all heritabilities were significantly greater than zero based on 95% CIs (calculated as 1.96×SE). Strictly skeletal traits (straight-line body length, head length, and zygomatic breadth) displayed moderate inheritance (h^2 = 0.34–0.48), while the heritability of axillary girth was substantially lower (h^2 = 0.17). In contrast, CV_A and I_A were greatest for axillary girth. Year was a substantial source of variance for body length (y^2 = 0.22) and axillary girth (y^2 = 0.16), but was almost insignificant for head length and zygomatic breadth ($y^2 \leq 0.02$), perhaps because measurement for these two traits only started in 1985, whereas measurement for body length and axillary girth have been estimated since the 1960s. Point estimates of heritabilities calculated in REPEATABEL were similar to those from ASREML though generally lower (Table A6.1), in all cases lying within the 95% confidence intervals of the pedigree-based estimates. Estimates of year effects for body length and axillary girth from REPEATABEL (y^2 = 0.06 and y^2 = 0.08, respectively) were substantially lower than those from ASREML, perhaps because samples genotyped on the array tended to be more recently collected.

6.4.3 GWAS and gene-set analysis

Manhattan plots for $GWAS_{Ped}$ results are shown in Fig. 6.2, and the corresponding QQ plots are shown in Fig. 6.3. In the absence of any additional correction for population stratification (i.e., PCs = 0), all GWAS appear to exhibit substantial genomic inflation (λ = 1.24–1.31). Inflation factors decreased only slightly when 10 PCs were used as covariates; they decreased substantially (i.e., to $\lambda < 1$) when all 127 significant PCs were used. Manhattan plots and QQ plots from $GWAS_{Rep}$ are given in Fig. 6.4. They most closely resemble the results from $GWAS_{Ped}$ when using all 127 PCs (i.e., $\lambda \approx 1$). Because it was not clear which of the four GWAS methods gave the most

accurate results, we summarized the significant GWAS hits from all four methods in Table 6.5. Effect sizes and p-values in Table 6.5 were taken from $GWAS_{Ped}$ using 0 PCs as covariates. No marker was significant over all four GWAS methods, and none of the SNPs that were flagged for HWE disequilibrium or Mendelian inheritance errors (displayed as green points in Figs. 6.2 and 6.4) were significantly associated with any of the traits we tested. None of the SNPs identified as F_{ST} outliers in Chapter 4 of this thesis were reidentified as contributing to any trait in our GWAS, nor were any in genes identified has having undergone the strongest selection in polar bears since their divergence with brown bears (Liu *et al.* 2014). Four of the five SNPs with the highest effect size were not located within 10 kb of any gene. Of the remainder of the significant SNPs, most were located in introns or other non-coding regions, and only a single non-synonymous SNP (in NFX1, a major histocompatibility complex repressor gene) was found to be a significant hit. Although there is high phenotypic correlation between all of the traits tested (cf. Fig A6.1), only one marker was a significant hit for multiple traits: a SNP in the proinflammatory cytokine gene IL18, which has been associated with a very large number of traits, including bone anabolism (Raggatt *et al.* 2008).

Significant competitive results from gene-set analysis based on $GWAS_{Ped}$ with 0 PCs as covariates (and using a 10-kb window around each SNP for gene annotation, as in de Leeuw *et al.* (2015)) are shown in Table 6.6. These represent biological pathways whose constituent genes are more strongly associated with the trait than are genes that are not members of the pathway. We found no significant associations for body length or zygomatic breadth. Head length was significantly associated with the immunity-related cytosolic DNA sensing pathway; however, this was driven largely by the strong association between head length and IL18 described above. Results for axillary girth were more interesting. Axillary girth was significantly associated with genes related to growth hormone signaling, the longevity pathway (which is related to growth hormone, insulin-like growth factor 1, and caloric intake), and the trefoil factor pathway (which is related to repair of the intestinal mucosa). However, it should be noted that none of these associations were robust to adjustments in window size (considering 0-kb, 20-kb and 50-kb windows) or to the GWAS method used (i.e., 10 PCs vs. 127 PCs vs. $GWAS_{Rep}$). Therefore, they should be considered highly tentative; however, they may demonstrate the potential benefit of gene-set analysis for GWAS of wild populations.

6.5 Discussion

6.5.1 Heritability and evolvability

In both pedigree- and marker-based analyses, all four morphological traits examined were significantly heritable, and—based on overlapping 95% confidence intervals—the heritabilities estimated from the two methods did not differ significantly, despite differing base populations, the incompleteness of the pedigree, and the small number of markers used to estimate relatedness compared to those used for human and agricultural genetics. Heritability and repeatability (estimated as the sum of heritability and permanent environmental effect) were lowest for axillary girth, and this measure also displayed the highest residual variance. This is likely because of the fluctuating nature of body condition, which depends upon partially stochastic factors such as hunting success. In addition, lower heritability and repeatability may also result from greater measurement error for axillary girth than for other traits: axillary girth is measured by sliding a tape measure under the chest of a prone, sedated bear. Since this portion of the tape measure cannot be seen, it is likely that individuals are not consistently measured across exactly the same point in their chest. Low repeatability and high residual variance for axillary girth suggest that it may benefit from additional repeated measurements. As expected, repeatability was highest for head length and zygomatic breadth, which are measured precisely with calipers. In contrast to its heritability, axillary girth had a slightly higher CV_A than did other traits. Lower heritability and a higher CV_A has regularly been documented in studies of mammals that have compared additive genetic variation for skeletal size and body mass (e.g., Coltman *et al.* 2001; Kruuk *et al.* 2000; Milner *et al.* 2000; Wilson *et al.* 2006). For mass, a higher CV_A is expected because—unlike axillary girth—it is a volumetric rather than a linear trait (Houle 1992). In our case, a slightly greater CV_A for axillary girth may reflect the fact that a larger number of genes underlie this trait: unlike strictly skeletal traits, axillary girth is directly dependent upon both skeletal size *and* fat deposition.

For comparison with other species, we calculated the median heritability, CV_A, and evolvability of morphological traits for mammals estimated in REML-based animal models using the supplementary data of Postma (2014). Heritabilities for polar bear body length, head length, and zygomatic breadth were commensurate with the median heritability (median $h^2 = 0.29$); though the heritability for axillary girth in our study was much lower. The coefficients of additive genetic variance and evolvabilities for all four of the traits considered in this study were lower than the

medians from Postma (2014) (median CV_A= 4.1; median I_A= 0.17). This suggests that any evolutionary response to selection of body size in Western Hudson Bay polar bears would be comparatively slow. To our knowledge, this is the first estimate of a potential evolutionary response in polar bears. This is particularly relevant in the face of declining sea ice in Western Hudson Bay (Kowal *et al.* 2015), which has caused increased fasting time ashore, and is thought to have caused in declines in body mass (Stirling & Parkinson 2006). Although these likely represent non-adaptive, plastic changes as opposed to adaptive genetic responses (Boutin & Lane 2014), the amenability of polar bear body size to selection was previously unknown.

6.5.2 GWAS and gene-set results

GWAS identified a number of candidate genes that may contribute to body size variation in polar bears, although the extent to which the significance of these results may have been inflated is unclear since some apparent genomic inflation is expected for polygenic traits (Yang *et al.* 2011c). The particularly high genomic inflation factors for $GWAS_{Ped}$ with 0 PCs may have been caused by our hybrid RAD–transcriptome approach in which our transcriptomic SNPs were selected specifically to be in genes that could be associated with body size based on gene ontology categories (Malenfant *et al.* 2015a). In fact, because of this design choice, results of $GWAS_{Ped}$ using 127 PCs as covariates and results of $GWAS_{Rep}$ seem overly conservative (i.e., $\lambda \lesssim 1$), since it stands to reason that there should be *some* inflation based on the large number of potentially relevant transcriptomic loci used. Although 127 PCs were significant under Velicer's minimum average partial test (and a similar number were significant using EIGENSOFT's Tracy–Widom statistic), it seems likely that with so many covariates, the model is simply fitting noise. And since REPEATABEL uses genomic relatedness to estimate polygenic effects and obtain heritability estimates *before* the program performs the GWAS, some of the SNP effects will be captured by the random polygenic effect (Ronnegard *et al*. 2016). (Although this should result in a slight overestimate in heritability, most of our SNP-based heritability estimates from REPEATABEL were actually slightly lower than the equivalent pedigree-based estimates from ASREML.) Ultimately, the only safe conclusion is that there is little evidence for genes that contribute very strongly to body size in this dataset, since the only SNP that was significant in both $GWAS_{Rep}$ and $GWAS_{Ped}$ was located in an unannotated region.

With the caveat that BLUP-based breeding values are not ideal as response variables in a GWAS because they can reduce power, increase the false positive rate, and misestimate QTL effect sizes (Ekine *et al.* 2014), we suggest that unadjusted $GWAS_{Ped}$ results may be the most sensible representation of the genetic architectures of these traits. Unadjusted $GWAS_{Ped}$ was also the least stringent GWAS, and because this is an exploratory study and we are merely trying to identify *putative* associations, these are the results we discuss now. Four of the five top hits for $GWAS_{Ped}$ were RAD SNPs that were not located within 10 kb of a gene. This is a frequent finding in GWAS studies: a substantial fraction of associations for complex traits are in noncoding regions and may represent undiscovered genes or noncoding RNAs (Flint & Mackay 2009; Rockman 2012). Perhaps more likely, these may be false positives caused by the "winner's curse" (Bazerman & Samuelson 1983), meaning that the most significant hits in a GWAS are also likely to be those whose effects were the most overestimated. Considered individually, it is easy to justify many of the remaining genes identified as containing significant QTLs in $GWAS_{Ped}$. For instance, all three of the annotated significant hits for straight-line body length can be associated with growth or metabolism: SLC39A11 has been associated with visceral fat deposition in women (Fox *et al.* 2012); CA2 is a metabolic gene belonging to the gene ontology categories for bone resorption and osteoclast differentiation; and C4A has been associated with type-1 diabetes (Thomsen *et al.* 1988). Unfortunately, since these are exactly the kinds of transcriptomic SNPs we chose to put on the array in the first place, it is not surprising that the GWAS generates plausible associations, and therefore the plausibility of the results does little to reassure us that these are not false positives. This is a significant drawback of a candidate-gene approach, which was unfortunately necessary in our study because of the dual-purposes of the medium-density SNP array, which was designed both for population genomics and association studies (Malenfant *et al.* 2015a).

Although individual GWAS hits are difficult to interpret, gene-set analysis results are tantalizing though tenuous. Even though growth hormone receptor was not a significant hit in any GWAS, we found evidence that variance in axillary girth may be significantly associated with various biological pathways related to growth hormone, including the trefoil-factor pathway, which is related to repair of the intestinal mucosa. This is because gene-set analysis aggregates associations over genes and then over pathways in order to increase power. However, these results only held for unadjusted $GWAS_{Ped}$ using a window size of 10 kb (cf. de Leeuw *et al.* 2015); when

window size was adjusted or other GWAS methods were used, this association no longer held true. To our knowledge, this is the first application of gene-set analysis to a wild population.

In humans, quantitative traits related to skeletal size and fatness such as height (Lango Allen *et al.* 2010) and BMI (Speliotes *et al.* 2010) are highly polygenic. Low power is likely to be the rule for quantitative traits if the infinitesimal model is correct (Jensen *et al.* 2014), and in large populations, genotyping thousands of individuals using extremely high-density arrays (or next-generation sequencing) may be needed in order even to detect variants of relatively large effect (Kardos *et al.* 2016). Indeed, even though a typical human GWAS may include tens or hundreds of thousands of individuals genotyped for a million SNPs or more, most variation in quantitative traits remains unaccounted for and is believed to lie in rare alleles or small-effect QTL that are in weak LD with the markers genotyped for GWAS (Hill 2012). Therefore, in our medium-density GWAS using only 841 individuals, we will have unquestionably missed the vast majority of causative variants. Is it possible that QTL of large effect do exist and we missed them? Because of rapid LD decay among Hudson Bay polar bears (Malenfant *et al*. 2015a; Fig. A4.10), our "GWAS" does not truly capture genome-wide variation, and it is possible that some QTL of large effect were missed because they were located in untagged regions. The polygenicity of a trait can be examined using genome partitioning (Robinson *et al*. 2013; Yang *et al*. 2011b); however this requires an adequate number of markers per chromosome in order to estimate relatedness (e.g., ≥60; Santure *et al*. 2013). Unfortunately, the polar bear genome is segmented into scaffolds, and there are only 10 scaffolds having ≥60 SNPs on our chip. We attempted to perform genome partitioning (data not shown); however, results were dependent on the inclusion of a single influential point: when scaffold 1 (the longest scaffold) was included, there was a significant positive correlation between scaffold length and heritability explained; when this scaffold was removed, the correlation was no longer significant. The question of polygenicity should be examined again after the construction of a linkage map (or additional sequencing data) allows scaffolds to be grouped together into putative chromosomes.

6.5.3 Conclusion

Polar bears exhibit moderate heritabilities (h^2 = 0.34–0.48) for strictly skeletal traits (body length, head length, and zygomatic breadth), and low heritability (h^2 = 0.17) for axillary girth, which is also dependent on fatness. Coefficients of additive genetic variance (1.9–2.9) and

evolvabilities (0.038–0.082) are comparatively low, suggesting that any genetic response to selection on body size will be slow. Results from genome-wide association studies are ambiguous; however, all traits are likely to be highly polygenic and there is no conclusive evidence of variants in any one gene contributing strongly to body size variation. Quantitative genetics studies of polar bears will benefit from construction of a linkage map, the application of higher-resolution genotyping technologies, and typing additional individuals.

Table 6.1. Animal models used to estimate heritabilities of each trait in pedigree-based analyses. All models were implemented in ASREML 3.0. μ indicates the intercept. Age and Year were fitted as numerical factors, whereas DayOfYear refers to the ordinal date, which was fitted as a covariate (scaled and centred to $\mu = 0$, $\sigma = 1$). "Animal" refers to an individual's entry in the additive genetic relatedness matrix, whereas "ID" gives permanent environmental effects specific to each individual. For axillary girth—which varies throughout the year because it is affected by fatness—some effects were included only for females only, since only females are associated with cubs and only females are handled during both the autumn and springtime handling periods. Asterisks indicate that both main effects and their interaction were included in the model.

Response	Fixed effects	Random effects
Body length	μ, Sex*Age	Animal, ID, Year
Axillary girth	μ, Sex*Age, DayOfYear ♀: NumberOfCubs Season*DayOfYear	Animal, ID, Year
Head length	μ, Sex*Age	Animal, ID, Year
Zygomatic breadth	μ, Sex*Age	Animal, ID, Year

Table 6.2. Means, variances, and estimated random-effect sizes for pedigree-based animal models of adult polar bear body size characters. N_{Ind} and N_{Rec} indicate the number of individuals and the number of records used in each model. V_{Obs} is the observed variance in the original phenotypic data; V_P is the total phenotypic variance after fitting fixed effects, obtained by summing the variance components estimated for each model in ASREML 3.0. Variance components: V_A = additive genetic; V_{PE} = permanent environmental; V_Y = year; V_R = residual. Values in parentheses represent standard deviations (SD) or standard errors (SE).

Trait	N_{Ind}	N_{Rec}	Mean (SD)	V_{Obs}	V_P (SE)	V_A	V_{PE}	V_Y	V_R
Body length (cm)	1489	3509	211.9 (18.8)	353.8	55.7 (3.9)	18.8	14.4	12.0	10.5
Axillary girth (cm)	1475	3576	137.1 (20.4)	414.9	88.9 (4.4)	15.4	11.2	14.4	47.9
Head length (mm)	1307	2963	374.6 (31.7)	1003.0	135.3 (5.0)	52.9	45.5	1.6	35.3
Zygomatic breadth (mm)	1306	2971	225.9 (28.0)	780.6	60.1 (2.3)	28.6	20.9	0.9	9.7

Table 6.3. Random-effect sizes for pedigree-based animal models of adult polar bear body size characters, displayed as proportions of phenotypic variation (V_P) attributable to each source of variation. Values in parentheses represent standard errors. h^2 = heritability; c^2 = permanent environmental; y^2= year; ε^2 = residual. These correspond to V_A, V_{PE}, V_Y, and V_R in Table 6.2, respectively.

Trait	h^2	c^2	y^2	ε^2
Body length	0.34 (0.05)	0.26 (0.05)	0.22 (0.05)	0.19 (0.01)
Axillary girth	0.17 (0.04)	0.13 (0.04)	0.16 (0.04)	0.54 (0.03)
Head length	0.39 (0.06)	0.34 (0.06)	0.01 (0.00)	0.26 (0.01)
Zygomatic breadth	0.48 (0.06)	0.35 (0.06)	0.02 (0.01)	0.16 (0.01)

Table 6.4. Coefficients of variance for pedigree-based animal models of adult polar bear body size characters. Coefficients of phenotypic (CV_P), additive genetic (CV_A), and residual (CV_R) variance and their standard errors were calculated as given in equations (1) and (5) of Garcia-Gonzalez *et al.* (2012) respectively. I_A is the mean-standardized additive variance, a measure of evolvability that indicates the expected proportional change under a unit of selection; the measure and its standard error were calculated according to equations (2) and (6) of Garcia-Gonzalez *et al.* (2012) respectively. Results are multiplied by 100 and expressed as percentages according to convention; values in parentheses represent standard errors.

Trait	$\boldsymbol{CV_P}$	$\boldsymbol{CV_A}$	$\boldsymbol{CV_R}$	$\boldsymbol{I_A}$
Body length	3.5 (0.1)	2.0 (0.2)	1.5 (0.0)	0.042 ($6.4\text{x}10^{-3}$)
Axillary girth	6.9 (0.2)	2.9 (0.3)	5.0 (0.1)	0.082 ($2.0\text{x}10^{-2}$)
Head length	3.1 (0.1)	1.9 (0.2)	1.6 (0.0)	0.038 ($6.1\text{x}10^{-3}$)
Zygomatic breadth	3.4 (0.1)	2.4 (0.2)	1.4 (0.0)	0.056 ($7.7\text{x}10^{-3}$)

Table 6.5. Significant associations (q < 0.1) in GWAS. p-values and effect sizes (b ± standard error) shown were obtained from the $GWAS_{Ped}$ that used 0 PCs (eigenvectors) as fixed effects. Checkmarks in the rightmost columns indicate whether a SNPs was significant for a given GWAS. SLen = straight-line body length; AxG = axillary girth; HdLen = head length; ZBrd = zygomatic breadth. "—" indicates that there was no gene annotation within 10,000 bp.

Trait	Scaffold	Position	Gene	p-value	b (SE)	PCs=0	PCs=10	PCs=127	$GWAS_{Rep}$
SLen	28	15,746,352	—	2.25×10^{-6}	1.55 (0.33)	✓	✓		✓
	32	10,726,153	SLC39A11 (intron)	3.21×10^{-7}	–0.76 (0.15)	✓	✓	✓	
	48	7,563,163	CA2 (3' UTR)	8.83×10^{-5}	0.53 (0.14)	✓			
	232	789,045	C4A (intron)	1.28×10^{-5}	–2.02 (0.46)	✓	✓	✓	
AxG	60	11,460,413	—	5.47×10^{-6}	–1.28 (0.31)	✓	✓		
	67	10,412,075	GNPTAB (synonymous)	1.23×10^{-6}	–0.45 (0.11)	✓			
	67	10,441,201	CHPT1 (intron)	1.11×10^{-5}	–0.45 (0.11)	✓	✓		
HdLen	31	10,208,507	IL18 (intron)	2.22×10^{-5}	1.06 (0.25)	✓			
	94	830,916	MLLT3 (3' UTR)	2.38×10^{-5}	1.00 (0.24)	✓			
ZBrd	22	4,837,027	—	7.14×10^{-5}	1.72 (0.43)	✓			
	26	18,150,402	CMAH (synonymous)	6.42×10^{-5}	0.75 (0.19)	✓	✓		
	30	15,420,508	—	2.55×10^{-4}	–1.74 (0.48)	✓			
	31	10,150,488	SDHD (intron)	4.07×10^{-5}	0.73 (0.18)	✓	✓		
	31	10,208,507	IL18 (intron)	4.38×10^{-6}	0.86 (0.19)	✓	✓		
	71	9,191,812	NFX1 (non-synonymous)	3.09×10^{-5}	0.74 (0.18)	✓			
	82	5,773,591	PARD3 (5' UTR)	1.07×10^{-4}	0.65 (0.17)	✓			
	87	3,932,193	TERF2 (synonymous)	1.22×10^{-5}	–0.76 (0.17)	✓			
	88	1,835,142	—	2.69×10^{-4}	0.70 (0.19)	✓			
	123	1,534,948	ARHGEF10 (5' – 423 bp)	1.14×10^{-4}	0.67 (0.17)	✓			

Table 6.6. Significant results of gene-set analysis using MAGMA on $GWAS_{Ped\ (PC=0)}$. p_{self} is the p-value associated with the null hypothesis that none of the genes in the set is associated with the trait; p_{comp} is the p-value associated with the null hypothesis that the genes in the gene set are not more strongly associated with the trait than genes outside the set; p_{FWER} represents p_{comp} values corrected for multiple testing using the permutation procedure. Trait abbreviations are as in Table 6.5.

Trait	Gene set	No. of genes	p_{self}	p_{comp}	p_{FWER}
SLen	—	—	—	—	—
AxG	Growth hormone signaling pathway	15	1.21×10^{-4}	1.28×10^{-5}	0.0185
	Growth hormone receptor signaling pathway	9	1.27×10^{-2}	1.10×10^{-5}	0.0163
	Longevity pathway	8	2.62×10^{-3}	2.08×10^{-6}	0.0039
	Trefoil factor pathway	11	3.23×10^{-4}	2.89×10^{-5}	0.0383
HdLen	Cytosolic DNA sensing pathway	17	7.00×10^{-3}	5.20×10^{-7}	0.0021
ZBrd	—	—	—	—	—

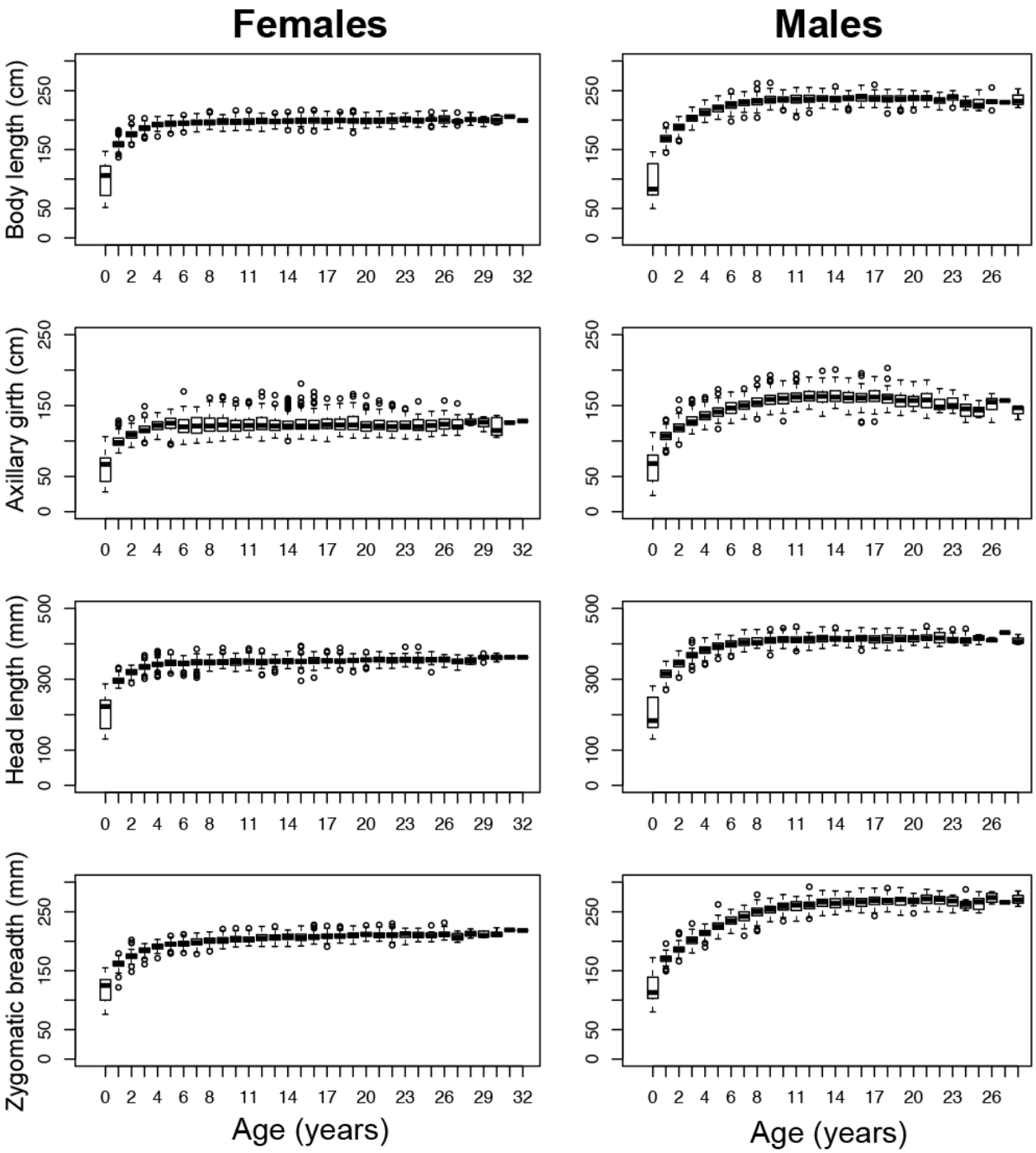

Figure 6.1. Plots of female and male body size metrics as a function of age. High variation in aged-0 individuals is a result of many (fast-growing) cubs of the year having been captured both in springtime and again in autumn.

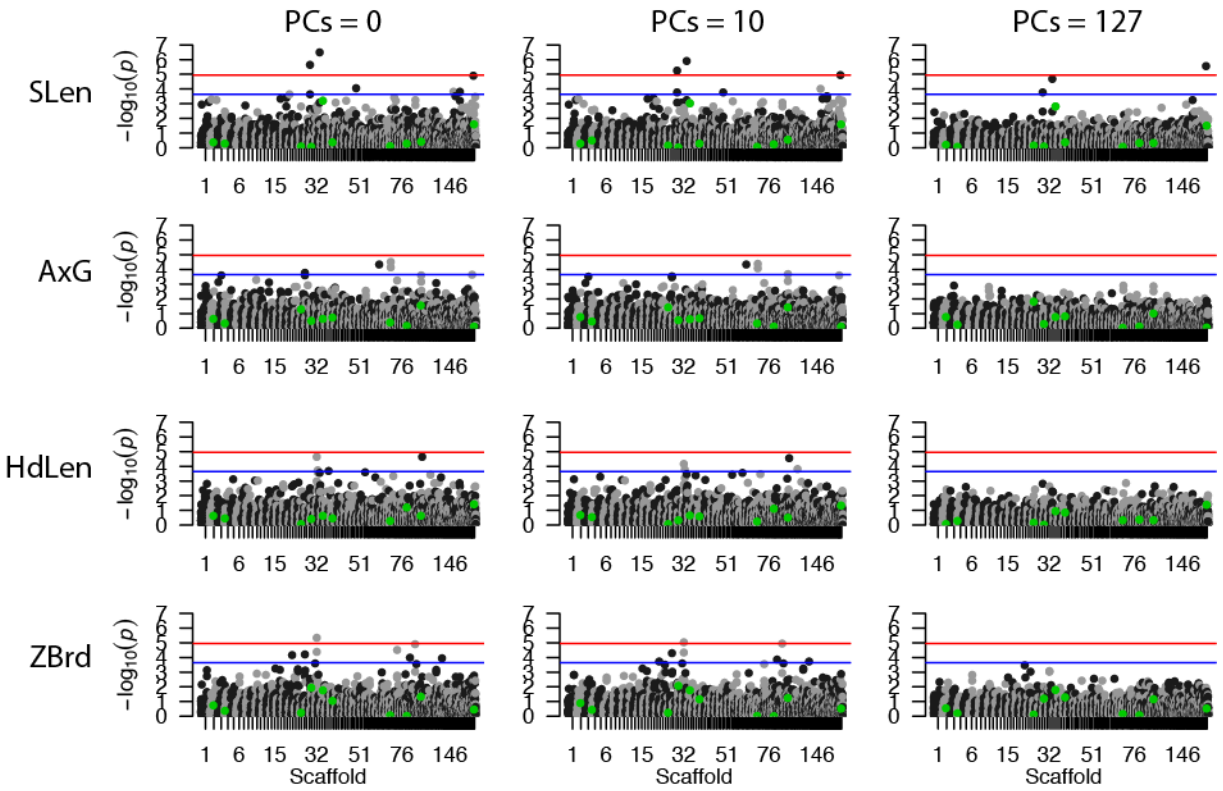

Figure 6.2. Manhattan plots for *GWAS*$_{Ped}$, genome-wide association analyses for breeding values calculated using the animal model in ASREML. Plots are shown using 0, 10, and 127 principal components (eigenvectors) as fixed effects. Red lines denote the cutoff for significant association using a strict Bonferroni correction for the number of loci (i.e., $\alpha = 0.05$/number of loci); blue lines denote the cutoff for suggestive association (i.e., $\alpha = 1$/number of loci). Green points indicate the SNPs flagged for being significantly out of Hardy–Weinberg equilibrium or having Mendelian inheritance errors. SLen = straight-line body length; AxG = axillary girth; HdLen = head length; ZBrd = zygomatic breadth.

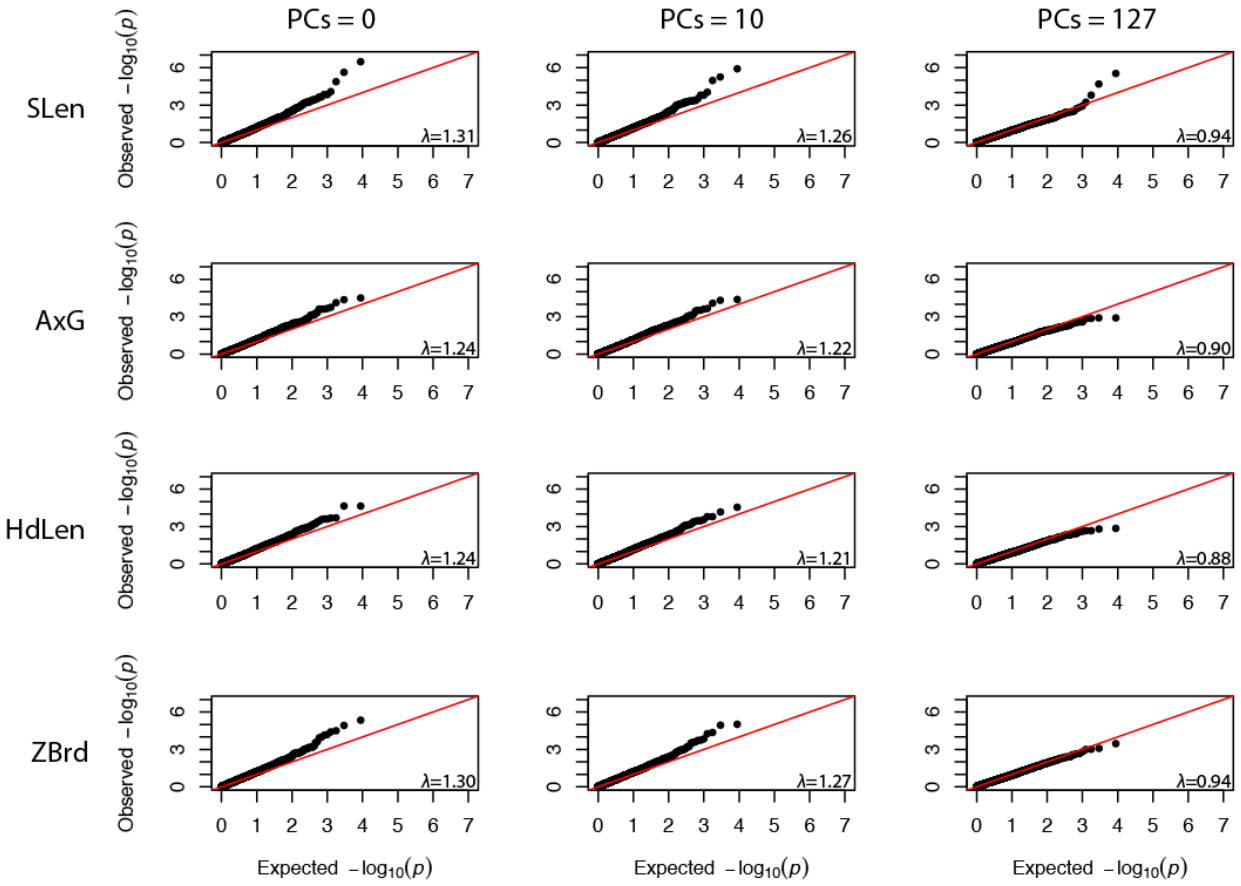

Figure 6.3. Quantile–quantile plots for the genome-wide association studies ($GWAS_{Ped}$) presented in Fig. 6.2. Red lines denote a 1:1 slope. λ denotes the genomic inflation factor. SLen = straight-line body length; AxG = axillary girth; HdLen = head length; ZBrd = zygomatic breadth.

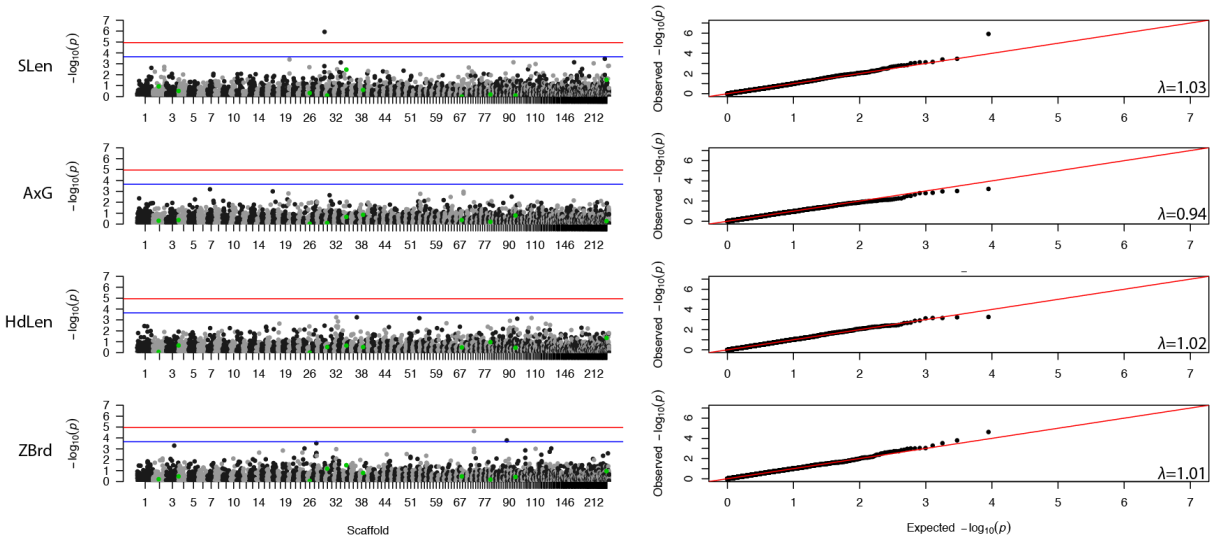

Figure 6.4. Manhattan plots (left) and quantile–quantile plots (right) for $GWAS_{Rep}$, the genome-wide association study using REPEATABEL. In Manhattan plots, red lines denote the cutoff for significant association using a strict Bonferroni correction for the number of loci (i.e., α = 0.05/number of loci); blue lines denote the cutoff for suggestive association (i.e., α = 1/number of loci). Green points indicate the SNPs flagged for being significantly out of Hardy–Weinberg equilibrium or having Mendelian inheritance errors. In quantile-quantile plots, red lines denote a 1:1 slope. λ denotes the genomic inflation factor. Trait abbreviations are as in Fig. 6.2.

Chapter 7: Conclusion

The goal of my doctoral research was to combine established genetic methods such as microsatellite genotyping with more recent approaches such as medium-density SNP genotyping in order to determine the population structure and genomic architecture of quantitative traits in polar bears (*Ursus maritimus*). I used single-nucleotide polymorphisms (SNPs) from restriction-site associated DNA (RAD) and transcriptomic sequencing to develop a medium-density SNP array for highly reliable genotyping of polar bears. In multiple studies, I used these SNPs, together with other new and previously published genetic resources, to reanalyse the global and Canadian population structure and gene flow of polar bears. I then generated a large pedigree of polar bears from the Western Hudson Bay management unit, and generated the first estimates of heritability for any trait for any species of bear. Breeding values from this analysis were then used as traits for association analyses using the SNP array.

In **Chapter 2**, I reanalysed the population structure of polar bears from across their circumpolar range using nuclear microsatellites and mitochondrial DNA previously published by (Peacock *et al.* 2015b). After identifying and correcting a number of methodological shortcomings, I showed that many of the major findings of the original publication were not supported by their data. Specifically, I demonstrated that: (1) as previously reported—and as confirmed in Chapters 3 and 4 using newly collected samples and higher-resolution marker sets—Norwegian Bay forms a unique genetic cluster of polar bears in the Canadian High Arctic near Canada's expected last sea-ice refugium, (2) the original publication's estimates of highly directional gene flow in response to climate change appear to have been caused by inadequate sample sizes and non-convergence of the program BAYESASS, and (3) there is little genetic evidence for strong male-biased dispersal in polar bears. These findings have important implications for the management of polar bears, especially in the face of ongoing climate-change-induced habitat loss.

In **Chapter 3**, I designed a SNP array for polar bears from next-generation sequencing data, which was among the first applications of this technology to non-model, non-agroeconomic species. Using a small subset of individuals, I showed that SNPs identify known genetic structure where a typical number of microsatellites fail. In addition, I showed the utility of this array for sex determination, and that harvested bears were significantly more likely to be mis-sexed than

scientifically sampled bears, possibly because of misreporting or inferior recordkeeping. Although the design of this SNP array was a success, it contained a high number of monomorphic loci (=32.3% of successfully printed loci). I attributed these failed loci to errors in next-generation sequencing, which were compounded by a low minor allele count cutoff for RAD data, and the use of a naïve SNP-calling script for transcriptomic data. These lessons will prove invaluable for future SNP array design.

In **Chapter 4**, I used the SNP array to re-examine the population structure of Canadian polar bears, which comprise approximately 50–70% of the global population. Although the SNP array provided higher resolution than the handful of microsatellites used in previous studies (e.g., Malenfant *et al.* 2016), it reconfirmed the finding of four moderately differentiated clusters of polar bears in the Canadian Arctic, corresponding to the Hudson Complex, the Canadian Arctic Archipelago, the Beaufort Sea, and Norwegian Bay, with additional substructure detected in the Hudson Complex and the Archipelago. TREEMIX analyses suggested one way in which polar bears may have entered Canada after the last ice age: entry from the Beaufort Sea with additional contribution to Hudson Bay and the Archipelago from an Atlantic refugium via Davis Strait. Based on the RAD and transcriptomic SNPs printed on the chip, there was limited evidence for adaptive genetic differentiation between clusters, with the exception of two loci for which the globally minor allele was the most frequent allele in Norwegian Bay. These loci affect fat deposition and the circulatory system. It is easy to construct "just-so stories" (Gould 1978) in which these loci are related to the unique ecological and morphological characteristics of the bears in Norwegian Bay; further study with a higher-resolution marker set is required to see if genetic pathways related to metabolism or dilated cardiomyopathy are truly differentiated.

In **Chapter 5**, I developed a multigenerational pedigree of polar bears, comprising 4449 individuals from the Western Hudson Bay management unit. Relationships were inferred from field data and multi-locus microsatellite genotypes from samples collected between 1966 and 2011. The pedigree is among the largest ever created for a large mammal, and includes 2957 assigned maternities and 1861 assigned paternities, yet contains only a single observed case of inbreeding between first-degree relatives. We attributed this low rate of inbreeding to interbreeding with neighbouring management units, rather than to active avoidance, as other bear species are believed to have poor kin recognition, and MHC diversity—which is used for kin recognition and

mate choice in mammals—is known to be low among polar bears. Poor kin recognition may also have been responsible for the six new cases of cub adoption I identified in this chapter. Notably, none of these adoptions could be attributed to reduced vigilance caused by drugging of females as a prerequisite to scientific handling, and our study joins others that have shown little ill effect of scientific handling on polar bears.

In **Chapter 6**, I combined the Western Hudson Bay pedigree and the SNP array to produce the first heritability estimates for polar bears. I found moderate heritability (h^2 = 0.34–0.48) for strictly skeletal traits (i.e., straight-line body length, head length, and zygomatic breadth) and lower heritability (h^2 = 0.17) for axillary girth, which is partially dependent on fatness. Similar results were obtained when heritabilities were estimated directly from the genetic relatedness matrix calculated using the SNP array. An association study on breeding values exhibited substantial genomic inflation; however, this is expected for polygenetic traits, especially if using a partial candidate-gene approach as in our mixed RAD–transcriptomic SNP array. Most significant SNPs were located in non-coding regions of genes, with no obvious associations with genes previously shown to have been under selection in polar bears, nor any of our F_{ST} outliers from Chapter 4. However, gene-set analysis on association results for axillary girth revealed a significant association in pathways related to growth-hormone signaling and the trefoil-factor pathway expressed in the intestinal mucosa. Unfortunately, this finding was not robust to adjustment of program parameters such as SNP window size—which represents a "researcher degree of freedom" (Simmons *et al.* 2011)—and the obtained p-values are unlikely to survive any correction for multiple-hypothesis testing.

As documented in Appendix 1, sample collection for the transcriptomics portion of this project was conducted in 2009. At this time, next-generation sequencing had yet to be broadly applied within molecular ecology, and was just beginning to emerge (Ekblom & Galindo 2011). In fact, the protocol behind RAD sequencing—which we also employed in this project—had only been published the year before (Baird *et al.* 2008). Other SNP arrays of this scale (e.g., Hagen *et al.* 2013; Kawakami *et al.* 2014a; van Bers *et al.* 2012) had yet to be published for any non-model, non-agroeconomic species when our SNP array was ordered from Illumina in 2012. The polar bear genome—which was released online in 2011 but was not officially annotated until three years later (Liu *et al.* 2014)—did not yet exist, and the most advanced polar bear genetics studies to date had

relied strictly upon microsatellites (Paetkau *et al.* 1999) or mitochondrial DNA (Delisle & Strobeck 2002).

To my knowledge, the blood and fat transcriptome assemblies presented in Appendix 1 formed the first publicly available annotation for the polar bear genome (Genomic Resources Development Consortium *et al.* 2014). The SNP array presented in Chapter 3 was among the first to be constructed for a non-model, non-agroeconomic species. The population genetic analyses in Chapters 2 and 4 provide new benchmarks for global and Canadian estimates of population structure, along with the first major attempts to find adaptive genetic variation among populations since the switch from allozymes to DNA markers. The pedigree presented in Chapter 5 is the largest ever constructed for any population of polar bears and includes the first-ever known pair of identical polar bear twins. The natural adoptions detected when assembling this pedigree contradict a previous hypothesis that adoptions may be caused by scientific handling (Derocher & Wiig 1999), and add to a list of evidence that physical capture–mark–recapture studies do not seem to negatively affect the species. The heritability estimates calculated from our pedigree in Chapter 6 are another first for polar bears—and to my knowledge represent the first quantitative genetics study or association study ever conducted for any ursid.

Collectively, the chapters of this thesis represent a major contribution to our knowledge of polar bears: they are the most comprehensive analyses of polar bear genetic variation that have ever been conducted, both within Western Hudson Bay, and at the national and circumpolar levels. Proper management of polar bears—both under Canadian law and internationally—will require an increased understanding of how the populations differ with respect to adaptive genetic variation. Future studies should focus on reanalysing global population structure and the genomic architecture of traits using higher-resolution marker sets that truly capture genome-wide variation. For inter-population research, this will be aided by careful consideration of sampling scheme (Lotterhos & Whitlock 2015; Schwartz & McKelvey 2008), which may only be possible to obtain using scientifically collected rather than harvested samples that tend to be concentrated near settlements. Intra-population research such as association studies may require a vastly larger number of genetic markers and genotyped individuals than are currently available for polar bears in order to reliably detect quantitative trait loci (e.g., Kardos *et al.* 2016). Until such resources become available for polar bears, I recommend the lines of research below.

First, I recommend the extension of quantitative genetics work to include additional traits such as fatness (Stirling *et al.* 2008), energy stores (Molnár *et al.* 2009), and cub mass (Derocher & Stirling 1996), as well as the sex-specific examination of maternal effects, which are believed to more greatly affect adult females than adult males (Atkinson *et al.* 1996b). Second, bivariate animal models (e.g., Coltman *et al.* 2005) should be used to determine genetic covariance between morphometric traits and genetic lines of least resistance in response to selection (Schluter 1996). Bivariate models should also be used to examine cross-sex genetic correlations and sex-specific additive genetic variances, which may influence polar bear sexual dimorphism (Derocher *et al.* 2005; Derocher *et al.* 2010). Third, genomic inbreeding coefficients can be used to determine any effects of inbreeding depression on phenotypic or life-history traits (e.g., Huisman *et al.* 2016). Fourth, the pedigree should be used to link scaffolds of the draft polar bear genome into putative chromosomes by constructing a linkage map, which would enable the use of genome partitioning (Robinson *et al.* 2013; Yang *et al.* 2011b) to more reliably examine the polygenicity of traits. Finally, because Western Hudson Bay is an open population, our pedigree is too incomplete to reliably use gene-dropping simulations (e.g., Gratten *et al.* 2012; Johnston *et al.* 2013) to determine if a change in allele frequency can be attributed to selection as opposed to drift. Therefore, I suggest using the unfortunately named "BDSM" technique (birth date selection mapping; Decker *et al.* 2012; Walsh & Lynch 2014) to search for alleles that have undergone recent selection. This method flips a typical association study on its head and uses year of birth as the response variable rather than a covariate in order to detect significant changes in allele frequency over time. Although this technique is extremely promising if deep pedigree data is available (Walsh & Lynch 2014), it has not yet been applied to wild populations.

In truth, I have already conducted many of these analyses, but that's a story for another day.

References

Albrechtsen A, Nielsen FC, Nielsen R (2010) Ascertainment biases in SNP chips affect measures of population divergence. *Molecular Biology and Evolution* **27**, 2534–2547.

Allendorf FW, Christiansen FB, Dobson T, Eanes WF, Frydenberg O (1979) Electrophoretic variation in large mammals: I. The polar bear, *Thalarctos maritimus*. *Hereditas* **91**, 19–22.

Altschul SF, Madden TL, Schaffer AA*, et al.* (1997) Gapped BLAST and PSI-BLAST: a new generation of protein database search programs. *Nucleic Acids Research* **25**, 3389–3402.

Alvarez M, Schrey AW, Richards CL (2015) Ten years of transcriptomics in wild populations: what have we learned about their ecology and evolution? *Molecular Ecology* **24**, 710–725.

Amstrup SC (1993) Human disturbances of denning polar bears in Alaska. *Arctic* **46**, 246–250.

Amstrup SC, Durner GM, McDonald TL, Mulcahy DM, Garner GW (2001) Comparing movement patterns of satellite-tagged male and female polar bears. *Canadian Journal of Zoology-Revue Canadienne De Zoologie* **79**, 2147–2158.

Amstrup SC, Durner GM, Stirling I, McDonald TL (2010) Allocating harvests among polar bear stocks in the Beaufort Sea. *Arctic* **58**, 247–259.

Amstrup SC, Gardner C (1994) Polar bear maternity denning in the Beaufort Sea. *Journal of Wildlife Management* **58**, 1–10.

Amstrup SC, Marcot BG, Douglas DC (2007) Forecasting the Range-wide Status of Polar Bears at Selected Times in the 21st Century. U.S. Geological Survey, Reston, VA.

Anderson AE, Wallmo OC (1984) *Odocoileus hemionus*. *Mammalian Species* **219**, 1–9.

Anderson CA, Pettersson FH, Clarke GM, Cardon LR, Morris AP, Zondervan KT (2010) Data quality control in genetic case-control association studies. *Nature Protocols* **5**, 1564–1573.

Anderson EC, Dunham KK (2008) The influence of family groups on inferences made with the program Structure. *Molecular Ecology Resources* **8**, 1219–1229.

Andrews KR, Good JM, Miller MR, Luikart G, Hohenlohe PA (2016) Harnessing the power of RADseq for ecological and evolutionary genomics. *Nature Reviews Genetics* **17**, 81–92.

Ashburner M, Ball CA, Blake JA*, et al.* (2000) Gene Ontology: tool for the unification of biology. *Nature Genetics* **25**, 25–29.

Atkinson SN, Cattet MRL, Polischuk SC, Ramsay MA (1996a) A case of offspring adoption in free-ranging polar bears (*Ursus maritimus*). *Arctic* **49**, 94–96.

Atkinson SN, Stirling I, Ramsay MA (1996b) Growth in early life and relative body size among adult polar bears (*Ursus maritimus*). *Journal of Zoology* **239**, 225–234.

Baird NA, Etter PD, Atwood TS*, et al.* (2008) Rapid SNP discovery and genetic mapping using sequenced RAD markers. *PLoS ONE* **3**, e3376.

Ball AD, Stapley J, Dawson DA, Birkhead TR, Burke T, Slate J (2010) A comparison of SNPs and microsatellites as linkage mapping markers: lessons from the zebra finch (*Taeniopygia guttata*). *BMC Genomics* **11**, 218.

Bazerman MH, Samuelson WF (1983) I won the auction but don't want the prize. *Journal of Conflict Resolution* **27**, 618–634.

Beerli P (2009) How to use Migrate or why are Markov chain Monte Carlo programs difficult to use? In: *Population Genetics for Animal Conservation* (eds. Bertorelle G, Bruford MW, Hauffe HC, Rizzoli A, Vernesi C), pp. 42–79. Cambridge University Press, Cambridge, UK.

Belikov SE (1976) Behavioral aspects of the polar bear, *Ursus maritimus*. *Bears: Their Biology and Management* **3**, 37–40.

Bellemain E, Zedrosser A, Manel S, Waits LP, Taberlet P, Swenson JE (2006) The dilemma of female mate selection in the brown bear, a species with sexually selected infanticide. *Proceedings of the Royal Society B-Biological Sciences* **273**, 283–291.

Bérénos C, Ellis PA, Pilkington JG, Lee SH, Gratten J, Pemberton JM (2015) Heterogeneity of genetic architecture of body size traits in a free-living population. *Molecular Ecology* **24**, 1810–1830.

Bérénos C, Ellis PA, Pilkington JG, Pemberton JM (2014) Estimating quantitative genetic parameters in wild populations: a comparison of pedigree and genomic approaches. *Molecular Ecology* **23**, 3434–3451.

Bermingham ML, Bishop SC, Woolliams JA*, et al.* (2014) Genome-wide association study identifies novel loci associated with resistance to bovine tuberculosis. *Heredity* **112**, 543–551.

Bethke R, Taylor M, Amstrup S, Messier F (1996) Population delineation of polar bears using satellite collar data. *Ecological Applications* **6**, 311–317.

Bhatia G, Patterson N, Sankararaman S, Price AL (2013) Estimating and interpreting F_{ST}: the impact of rare variants. *Genome Research* **23**, 1514–1521.

Bidon T, Frosch C, Eiken HG*, et al.* (2013) A sensitive and specific multiplex PCR approach for sex identification of ursine and tremarctine bears suitable for non-invasive samples. *Molecular Ecology Resources* **13**, 362–368.

Bidon T, Janke A, Fain SR*, et al.* (2014) Brown and polar bear Y chromosomes reveal extensive male-biased gene flow within brother lineages. *Molecular Biology and Evolution* **31**, 1353–1363.

Bidon T, Schreck N, Hailer F, Nilsson MA, Janke A (2015) Genome-wide search identifies 1.9 Mb from the polar bear Y chromosome for evolutionary analyses. *Genome Biology and Evolution* **7**, 2010–2022.

Bohling JH, Adams JR, Waits LP (2013) Evaluating the ability of Bayesian clustering methods to detect hybridization and introgression using an empirical red wolf data set. *Molecular Ecology* **22**, 74–86.

Bonhomme M, Chevalet C, Servin B*, et al.* (2010) Detecting selection in population trees: the Lewontin and Krakauer test extended. *Genetics* **186**, 241–262.

Boutin S, Lane JE (2014) Climate change and mammals: evolutionary versus plastic responses. *Evolutionary Applications* **7**, 29–41.

Bowen L, Keith Miles A, Stott J, Waters S, Atwood T (2015a) Enhanced biological processes associated with alopecia in polar bears (*Ursus maritimus*). *Science of the Total Environment* **529**, 114–120.

Bowen L, Miles AK, Waters S, Meyerson R, Rode K, Atwood T (2015b) Gene transcription in polar bears (*Ursus maritimus*) from disparate populations. *Polar Biology* **38**, 1413–1427.

Bradley RS, England JH (2008) The Younger Dryas and the sea of ancient ice. *Quaternary Research* **70**, 1–10.

Brumfield RT, Beerli P, Nickerson DA, Edwards SV (2003) The utility of single nucleotide polymorphisms in inferences of population history. *Trends in Ecology & Evolution* **18**, 249–256.

Bulik-Sullivan BK, Loh P-R, Finucane HK*, et al.* (2015) LD Score regression distinguishes confounding from polygenicity in genome-wide association studies. *Nature Genetics* **47**, 291–295.

Bulmer MG (1970) *The Biology of Twinning in Man* Clarendon Press, Oxford, UK.

Cahill JA, Green RE, Fulton TL*, et al.* (2013) Genomic evidence for island population conversion resolves conflicting theories of polar bear evolution. *PLoS Genetics* **9**, e1003345.

Cahill JA, Stirling I, Kistler L*, et al.* (2015) Genomic evidence of geographically widespread effect of gene flow from polar bears into brown bears. *Molecular Ecology* **24**, 1205–1217.

Calvert W, Ramsay MA (1998) Evaluation of age determination of polar bears by counts of cementum growth layer groups. *Ursus* **10**, 449–453.

Campagna L, Van Coeverden de Groot PJ, Saunders BL*, et al.* (2013) Extensive sampling of polar bears (*Ursus maritimus*) in the Northwest Passage (Canadian Arctic Archipelago) reveals population differentiation across multiple spatial and temporal scales. *Ecology and Evolution* **3**, 3152–3165.

Carmichael L, Nagy JA, Strobeck C (2009) Monozygotic twin wolves with divergent life histories. *Arctic* **61**, 329–331.

Cheng H, Kimura K, Peter AK*, et al.* (2010) Loss of enigma homolog protein results in dilated cardiomyopathy. *Circulation Research* **107**, 348–356.

Cheng L, Connor T, Aanensen D, Spratt B, Corander J (2011) Bayesian semi-supervised classification of bacterial samples using MLST databases. *BMC Bioinformatics* **12**, 302.

Cherry SG, Derocher AE, Thiemann GW, Lunn NJ (2013) Migration phenology and seasonal fidelity of an Arctic marine predator in relation to sea ice dynamics. *Journal of Animal Ecology* **82**, 912–921.

Chesser RK, Baker RJ (1996) Effective sizes and dynamics of uniparentally and diparentally inherited genes. *Genetics* **144**, 1225–1235.

Clutton-Brock TH, Albon SD, Guinness FE (1989) Fitness costs of gestation and lactation in wild mammals. *Nature* **337**, 260–262.

Coates BS, Sumerford DV, Miller NJ*, et al.* (2009) Comparative performance of single nucleotide polymorphism and microsatellite markers for population genetic analysis. *Journal of Heredity* **100**, 556–564.

Coltman DW, O'Donoghue P, Hogg JT, Festa-Bianchet M (2005) Selection and genetic (co)variance in sheep. *Evolution* **59**, 1372–1382.

Coltman DW, Pilkington J, Kruuk LEB, Wilson K, Pemberton JM (2001) Positive genetic correlation between parasite resistance and body size in a free-living ungulate population. *Evolution* **55**, 2116–2125.

Conesa A, Götz S, García-Gómez JM, Terol J, Talón M, Robles M (2005) Blast2GO: a universal tool for annotation, visualization and analysis in functional genomics research. *Bioinformatics* **21**, 3674–3676.

Corander J, Marttinen P (2006) Bayesian identification of admixture events using multilocus molecular markers. *Molecular Ecology* **15**, 2833–2843.

Corander J, Marttinen P, Mäntyniemi S (2006) A Bayesian method for identification of stock mixtures from molecular marker data. *Fishery Bulletin* **104**, 550–558.

Corander J, Marttinen P, Siren J, Tang J (2008a) Enhanced Bayesian modelling in BAPS software for learning genetic structures of populations. *BMC Bioinformatics* **9**, 539.

Corander J, Sirén J, Arjas E (2008b) Bayesian spatial modeling of genetic population structure. *Computational Statistics* **23**, 111–129.

COSEWIC (2012) *Guidelines for Recognizing Designatable Units*. Committee on the Status of Endangered Wildlife in Canada, Ottawa, Canada. http://www.cosewic.gc.ca/eng/sct2/sct2_5_e.cfm

Costello CM, Creel SR, Kalinowski ST, Vu NV, Quigley HB (2008) Sex-biased natal dispersal and inbreeding avoidance in American black bears as revealed by spatial genetic analyses. *Molecular Ecology* **17**, 4713–4723.

Creel SR, Monfort SL, Wildt DE, Waser PM (1991) Spontaneous lactation is an adaptive result of pseudopregnancy. *Nature* **351**, 660–662.

Crompton AE, Obbard ME, Petersen SD, Wilson PJ (2008) Population genetic structure in polar bears (*Ursus maritimus*) from Hudson Bay, Canada: implications of future climate change. *Biological Conservation* **141**, 2528–2539.

Crompton AE, Obbard ME, Petersen SD, Wilson PJ (2014) Corrigendum to "Population genetic structure in polar bears (*Ursus maritimus*) from Hudson Bay, Canada: Implications of future climate change" [Biol. Conserv. 141(10) (2008) 2528–2539]. *Biological Conservation* **179**, 152.

Cronin MA, Amstrup SC, Scribner KT (2006) Microsatellite DNA and mitochondrial DNA variation in polar bears (*Ursus maritimus*) from the Beaufort and Chukchi seas, Alaska. *Canadian Journal of Zoology-Revue Canadienne De Zoologie* **84**, 655–660.

Cronin MA, Amstrup SC, Talbot SL, Sage GK, Amstrup KS (2009) Genetic variation, relatedness, and effective population size of polar bears (*Ursus maritimus*) in the southern Beaufort Sea, Alaska. *Journal of Heredity* **100**, 681–690.

Cronin MA, Macneil MD (2012) Genetic relationships of extant brown bears (*Ursus arctos*) and polar bears (*Ursus maritimus*). *Journal of Heredity* **103**, 873–881.

Cronin MA, Rincon G, Meredith RW*, et al.* (2014) Molecular phylogeny and SNP variation of polar bears (*Ursus maritimus*), brown bears (*U. arctos*), and black bears (*U. americanus*) derived from genome sequences. *Journal of Heredity* **105**, 312–323.

Cronin MA, Shideler R, Waits L, Nelson RJ (2005) Genetic variation and relatedness on grizzly bears in the Prudhoe Bay region and adjacent areas in northern Alaska. *Ursus* **16**, 70–84.

Cullingham CI, Cooke JEK, Dang S, Coltman DW (2013) A species-diagnostic SNP panel for discriminating lodgepole pine, jack pine, and their interspecific hybrids. *Tree Genetics & Genomes* **9**, 1119–1127.

Darriba D, Taboada GL, Doallo R, Posada D (2012) jModelTest 2: more models, new heuristics and parallel computing. *Nature Methods* **9**, 772.

Dawson E, Abecasis GR, Bumpstead S*, et al.* (2002) A first-generation linkage disequilibrium map of human chromosome 22. *Nature* **418**, 544–548.

Day-Richter J, Harris MA, Haendel M, Group TGOO-EW, Lewis S (2007) OBO-Edit—an ontology editor for biologists. *Bioinformatics* **23**, 2198–2200.

De Barba M, Waits LP, Garton EO*, et al.* (2010) The power of genetic monitoring for studying demography, ecology and genetics of a reintroduced brown bear population. *Molecular Ecology* **19**, 3938–3951.

de Leeuw CA, Mooij JM, Heskes T, Posthuma D (2015) MAGMA: Generalized gene-set analysis of GWAS data. *PLoS Computational Biology* **11**, e1004219.

de Leeuw CA, Neale BM, Heskes T, Posthuma D (2016) The statistical properties of gene-set analysis. *Nature Reviews Genetics*, In press.

de Vernal A, Eynaud F, Henry M*, et al.* (2005) Reconstruction of sea-surface conditions at middle to high latitudes of the Northern Hemisphere during the Last Glacial Maximum (LGM) based on dinoflagellate cyst assemblages. *Quaternary Science Reviews* **24**, 897–924.

Decker JE, Vasco DA, McKay SD*, et al.* (2012) A novel analytical method, Birth Date Selection Mapping, detects response of the Angus (*Bos taurus*) genome to selection on complex traits. *BMC Genomics* **13**, 1–14.

Delisle I, Strobeck C (2002) Conserved primers for rapid sequencing of the complete mitochondrial genome from carnivores, applied to three species of bears. *Molecular Biology and Evolution* **19**, 357–361.

DePristo MA, Banks E, Poplin R*, et al.* (2011) A framework for variation discovery and genotyping using next-generation DNA sequencing data. *Nature Genetics* **43**, 491–498.

Derocher AE (2012) *Polar Bears: A Complete Guide to Their Biology and Behavior* Johns Hopkins University Press, Baltimore.

Derocher AE, Andersen M, Wiig Ø (2005) Sexual dimorphism of polar bears. *Journal of Mammalogy* **86**, 895–901.

Derocher AE, Andersen M, Wiig Ø, Aars J (2010) Sexual dimorphism and the mating ecology of polar bears (*Ursus maritimus*) at Svalbard. *Behavioral Ecology and Sociobiology* **64**, 939–946.

Derocher AE, Lunn NJ, Stirling I (2004) Polar bears in a warming climate. *Integrative and Comparative Biology* **44**, 163–176.

Derocher AE, Stirling I (1990) Distribution of polar bears (*Ursus maritimus*) during the ice-free period in western Hudson Bay. *Canadian Journal of Zoology-Revue Canadienne De Zoologie* **68**, 1395–1403.

Derocher AE, Stirling I (1996) Aspects of survival in juvenile polar bears. *Canadian Journal of Zoology-Revue Canadienne De Zoologie* **74**, 1246–1252.

Derocher AE, Stirling I (1998) Maternal investment and factors affecting offspring size in polar bears (*Ursus maritimus*). *Journal of Zoology* **245**, 253–260.

Derocher AE, Stirling I, Andriashek D (1992) Pregnancy rates and serum progesterone levels of polar bears in western Hudson Bay. *Canadian Journal of Zoology-Revue Canadienne De Zoologie* **70**, 561–566.

Derocher AE, Stirling I, Calvert W (1997) Male-biased harvesting of polar bears in western Hudson Bay. *Journal of Wildlife Management* **61**, 1075–1082.

Derocher AE, Wiig Ø (1999) Observation of adoption in polar bears (*Ursus maritimus*). *Arctic* **52**, 413–415.

Devlin B, Roeder K (1999) Genomic control for association studies. *Biometrics* **55**, 997–1004.

Do C, Waples RS, Peel D, Macbeth GM, Tillett BJ, Ovenden JR (2014) NeEstimator v2: re-implementation of software for the estimation of contemporary effective population size (N_e) from genetic data. *Molecular Ecology Resources* **14**, 209–214.

Doupé JP, England JH, Furze M, Paetkau D (2009) Most northerly observation of a grizzly bear (*Ursus arctos*) in Canada: photographic and DNA evidence from Melville Island, Northwest Territories. *Arctic* **60**, 271–276.

Drummond CS, Hamilton MB (2007) Hierarchical components of genetic variation at a species boundary: population structure in two sympatric varieties of *Lupinus microcarpus* (Leguminosae). *Molecular Ecology* **16**, 753–769.

Durbin R, Li H, Handsaker B*, et al.* (2009) The Sequence Alignment/Map format and SAMtools. *Bioinformatics* **25**, 2078–2079.

Durner GM, Amstrup SC (1995) Movements of a polar bear from northern Alaska to northern Greenland. *Arctic* **48**, 338–341.

Dyke AS (2004) An outline of North American deglaciation with emphasis on central and northern Canada. In: *Developments in Quaternary Sciences* (eds. Ehlers J, Gibbard PL), pp. 373–424. Elsevier, Boston.

Earl DA, Vonholdt BM (2012) STRUCTURE HARVESTER: a website and program for visualizing STRUCTURE output and implementing the Evanno method. *Conservation Genetics Resources* **4**, 359–361.

Edwards CJ, Suchard MA, Lemey P*, et al.* (2011) Ancient hybridization and an Irish origin for the modern polar bear matriline. *Current Biology* **21**, 1251–1258.

Ekblom R, Galindo J (2011) Applications of next generation sequencing in molecular ecology of non-model organisms. *Heredity* **107**, 1–15.

Ekine CC, Rowe SJ, Bishop SC, de Koning D-J (2014) Why breeding values estimated using familial data should not be used for genome-wide association studies. *G3: Genes|Genomes|Genetics* **4**, 341–347.

Ellegren H, Sheldon BC (2008) Genetic basis of fitness differences in natural populations. *Nature* **452**, 169–175.

Evanno G, Regnaut S, Goudet J (2005) Detecting the number of clusters of individuals using the software STRUCTURE: a simulation study. *Molecular Ecology* **14**, 2611–2620.

Excoffier L, Lischer HEL (2010) Arlequin suite ver 3.5: a new series of programs to perform population genetics analyses under Linux and Windows. *Molecular Ecology Resources* **10**, 564–567.

Excoffier L, Smouse PE, Quattro JM (1992) Analysis of molecular variance inferred from metric distances among DNA haplotypes: application to human mitochondrial DNA restriction data. *Genetics* **131**, 479–491.

Falush D, Stephens M, Pritchard JK (2003) Inference of population structure using multilocus genotype data: Linked loci and correlated allele frequencies. *Genetics* **164**, 1567–1587.

Faubet P, Waples RS, Gaggiotti OE (2007) Evaluating the performance of a multilocus Bayesian method for the estimation of migration rates. *Molecular Ecology* **16**, 1149–1166.

Ferguson SH, Taylor MK, Born EW, Rosing-Asvid A, Messier F (1999) Determinants of home range size for polar bears (*Ursus maritimus*). *Ecology Letters* **2**, 311–318.

Fetterer F, Savoie M, Helfrich S, Clemente-Colón P (2010, updated daily) masie_ice_r00_v01_2008106_4km In: *Multisensor Analyzed Sea Ice Extent – Northern Hemisphere* (ed. Center NSaID). National Ice Center (NIC) and NSIDC, Boulder, Colorado USA.

Flint J, Mackay TFC (2009) Genetic architecture of quantitative traits in mice, flies, and humans. *Genome Research* **19**, 723–733.

Foll M, Gaggiotti O (2008) A genome-scan method to identify selected loci appropriate for both dominant and codominant markers: a Bayesian perspective. *Genetics* **180**, 977–993.

Fox CS, Liu Y, White CC*, et al.* (2012) Genome-wide association for abdominal subcutaneous and visceral adipose reveals a novel locus for visceral fat in women. *PLoS Genetics* **8**, e1002695.

Frankham R, Bradshaw CJA, Brook BW (2014) Genetics in conservation management: revised recommendations for the 50/500 rules, Red List criteria and population viability analyses. *Biological Conservation* **170**, 56–63.

Frazer KA, Ballinger DG, Cox DR*, et al.* (2007) A second generation human haplotype map of over 3.1 million SNPs. *Nature* **449**, 851–861.

Fricke PM (2001) Review: twinning in dairy cattle. *The Professional Animal Scientist* **17**, 61–67.

Garcia-Gonzalez F, Simmons LW, Tomkins JL, Kotiaho JS, Evans JP (2012) Comparing evolvabilities: common errors surrounding the calculation and use of coefficients of additive genetic variation. *Evolution* **66**, 2341–2349.

GenABEL project developers (2013) GenABEL: genome-wide SNP association analysis.

Genomic Resources Development Consortium, Coltman DW, Davis CS, Lunn NJ, Malenfant RM, Richardson ES (2014) Genomic Resources Notes accepted 1 August 2013–30 September 2013. *Molecular Ecology Resources* **14**, 219.

Gibbs RA, Taylor JF, Van Tassell CP*, et al.* (2009) Genome-wide survey of SNP variation uncovers the genetic structure of cattle breeds. *Science* **324**, 528–532.

Gienapp P, Brommer JE (2014) Evolutionary dynamics in response to climate change. In: *Quantitative Genetics in the Wild* (eds. Charmantier A, Garant D, Kruuk LEB). Oxford University Press, Oxford, UK.

Gilbert KJ, Andrew RL, Bock DG*, et al.* (2012) Recommendations for utilizing and reporting population genetic analyses: the reproducibility of genetic clustering using the program STRUCTURE. *Molecular Ecology* **21**, 4925–4930.

Gleeson SK, Clark AB, Dugatkin LA (1994) Monozygotic twinning: an evolutionary hypothesis. *Proceedings of the National Academy of Sciences* **91**, 11363–11367.

Glenn LP, Lentfer JW, Faro JB, Miller LH (1976) Reproductive biology of female brown bears (*Ursus arctos*), McNeil River, Alaska. *Bears: Their Biology and Management* **3**, 381–390.

Gorrell JC, McAdam AG, Coltman DW, Humphries MM, Boutin S (2010) Adopting kin enhances inclusive fitness in asocial red squirrels. *Nature Communications* **1**, 22.

Goudet J, Perrin N, Waser P (2002) Tests for sex-biased dispersal using bi-parentally inherited genetic markers. *Molecular Ecology* **11**, 1103–1114.

Gould SJ (1978) Sociobiology: the art of storytelling. *New Scientist* **80**, 530–533.

Grafen A (1988) On the Uses of Data on Lifetime Reproductive Success. In: *Reproductive Success* (ed. Clutton-Brock TH), pp. 454–471. Univeristy of Chicago Press, Chicago, IL.

Gratten J, Pilkington JG, Brown EA, Clutton-Brock TH, Pemberton JM, Slate J (2012) Selection and microevolution of coat pattern are cryptic in a wild population of sheep. *Molecular Ecology* **21**, 2977–2990.

Gray MM, Granka JM, Bustamante CD*, et al.* (2009) Linkage disequilibrium and demographic history of wild and domestic canids. *Genetics* **181**, 1493–1505.

Guichoux E, Lagache L, Wagner S*, et al.* (2011) Current trends in microsatellite genotyping. *Molecular Ecology Resources* **11**, 591–611.

Guindon S, Gascuel O (2003) A simple, fast, and accurate algorithm to estimate large phylogenies by maximum likelihood. *Systematic Biology* **52**, 696–704.

Gunderson KL (2009) Whole-Genome Genotyping on Bead Arrays. In: *DNA Microarrays for Biomedical Research* (ed. Dufva M), pp. 197–213. Humana Press, New York.

Günther T, Coop G (2013) Robust identification of local adaptation from allele frequencies. *Genetics* **195**, 205–220.

Guo SW, Thompson EA (1992) Performing the exact test of Hardy-Weinberg proportion for multiple alleles. *Biometrics* **48**, 361–372.

Hadfield JD, Wilson AJ, Garant D, Sheldon BC, Kruuk LEB (2010) The misuse of BLUP in ecology and evolution. *American Naturalist* **175**, 116–125.

Hagen IJ, Billing AM, Rønning B*, et al.* (2013) The easy road to genome-wide medium density SNP screening in a non-model species: development and application of a 10 K SNP-chip for the house sparrow (*Passer domesticus*). *Molecular Ecology Resources* **13**, 429–439.

Hailer F, Kutschera VE, Hallstrom BM*, et al.* (2012) Nuclear genomic sequences reveal that polar bears are an old and distinct bear lineage. *Science* **336**, 344–347.

Hale ML, Burg TM, Steeves TE (2012) Sampling for microsatellite-based population genetic studies: 25 to 30 individuals per population is enough to accurately estimate allele frequencies. *PLoS ONE* **7**, e45170.

Hamilton SG, Castro de la Guardia L, Derocher AE, Sahanatien V, Tremblay B, Huard D (2014) Projected polar bear sea ice habitat in the Canadian Arctic Archipelago. *PLoS ONE* **9**, e113746.

Hamilton WD (1964) The genetical evolution of social behaviour. I. *Journal of Theoretical Biology* **7**, 1–16.

Hardy ICW (1995) Protagonists of polyembryony. *Trends in Ecology & Evolution* **10**, 179–180.

Hardy OJ, Charbonnel N, Fréville H, Heuertz M (2003) Microsatellite allele sizes: a simple test to assess their significance on genetic differentiation. *Genetics* **163**, 1467–1482.

Hardy OJ, Vekemans X (2002) SPAGeDi: a versatile computer program to analyse spatial genetic structure at the individual or population levels. *Molecular Ecology Notes* **2**, 618–620.

Hauser L, Baird M, Hilborn R, Seeb LW, Seeb JE (2011) An empirical comparison of SNPs and microsatellites for parentage and kinship assignment in a wild sockeye salmon (*Oncorhynchus nerka*) population. *Molecular Ecology Resources* **11**, 150–161.

Heaton TH, Grady F (2003) The Late Wisconsin vertebrate history of Prince of Wales Island, Southeast Alaska. In: *Ice Age Cave Faunas of North America* (eds. Schubert BW, Mead JI, Graham RW), pp. 17–53. Indiana University Press, Bloomington.

Heidelberger P, Welch PD (1983) Simulation run length control in the presence of an initial transient. *Operations Research* **31**, 1109–1144.

Hill WG (2012) Quantitative genetics in the genomics era. *Current Genomics* **13**, 196–206.

Hill WG, Goddard ME, Visscher PM (2008) Data and theory point to mainly additive genetic variance for complex traits. *PLoS Genetics* **4**, e1000008.

Hill WG, Weir BS (1988) Variances and covariances of squared linkage disequilibria in finite populations. *Theoretical Population Biology* **33**, 54–78.

Hoffman JI, Forcada J (2009) Genetic analysis of twinning in Antarctic fur seals (*Arctocephalus gazella*). *Journal of Mammalogy* **90**, 621–628.

Hoffman JI, Tucker R, Bridgett SJ, Clark MS, Forcada J, Slate J (2012) Rates of assay success and genotyping error when single nucleotide polymorphism genotyping in non-model organisms: a case study in the Antarctic fur seal. *Molecular Ecology Resources* **12**, 861–872.

Holm S (1979) A simple sequentially rejective multiple test procedure. *Scandinavian Journal of Statistics* **6**, 65–70.

Houle D (1992) Comparing evolvability and variability of quantitative traits. *Genetics* **130**, 195–204.

Hua P, Zhang L, Zhu G, Jones G, Zhang S, Rossiter SJ (2011) Hierarchical polygyny in multiparous lesser flat-headed bats. *Molecular Ecology* **20**, 3669–3680.

Hubisz MJ, Falush D, Stephens M, Pritchard JK (2009) Inferring weak population structure with the assistance of sample group information. *Molecular Ecology Resources* **9**, 1322–1332.

Huisman J, Kruuk LE, Ellis PA, Clutton-Brock T, Pemberton JM (2016) Inbreeding depression across the lifespan in a wild mammal population. *Proceedings of the National Academy of Sciences* **113**, 3585–3590.

Hurvich CM, Tsai C-L (1989) Regression and time series model selection in small samples. *Biometrika* **76**, 297–307.

Husby A, Kawakami T, Rönnegård L, Smeds L, Ellegren H, Qvarnström A (2015) Genome-wide association mapping in a wild avian population identifies a link between genetic and phenotypic variation in a life-history trait. *Proceedings of the Royal Society of London B: Biological Sciences* **282**, 20150156.

Ingólfsson Ó, Wiig Ø (2009) Late Pleistocene fossil find in Svalbard: the oldest remains of a polar bear (*Ursus maritimus* Phipps, 1744) ever discovered. *Polar Research* **28**, 455–462.

Itoh T, Sato Y, Kobayashi K, Mano T, Iwata R (2012) Effective dispersal of brown bears (*Ursus arctos*) in eastern Hokkaido, inferred from analyses of mitochondrial DNA and microsatellites. *Mammal Study* **37**, 29–41.

IUCN/SSC Polar Bear Specialist Group (2015) *2014 Polar Bear Status Table.* http://pbsg.npolar.no/en/status/status-table.html

Jakobsson M, Rosenberg NA (2007) CLUMPP: a cluster matching and permutation program for dealing with label switching and multimodality in analysis of population structure. *Bioinformatics* **23**, 1801–1806.

Jamieson A, Taylor SS (1997) Comparisons of three probability formulae for parentage exclusion. *Animal Genetics* **28**, 397–400.

Jensen H, Szulkin M, Slate J (2014) Molecular quantitative genetics. In: *Quantitative Genetics in the Wild* (eds. Charmantier A, Garant D, Kruuk LEB). Oxford University Press, Oxford, UK.

Johnson PCD, Haydon DT (2007) Maximum-likelihood estimation of allelic dropout and false allele error rates from microsatellite genotypes in the absence of reference data. *Genetics* **175**, 827–842.

Johnston SE, Gratten J, Berenos C*, et al.* (2013) Life history trade-offs at a single locus maintain sexually selected genetic variation. *Nature* **502**, 93–95.

Johnston SE, McEwan JC, Pickering NK*, et al.* (2011) Genome-wide association mapping identifies the genetic basis of discrete and quantitative variation in sexual weaponry in a wild sheep population. *Molecular Ecology* **20**, 2555–2566.

Jombart T (2008) adegenet: a R package for the multivariate analysis of genetic markers. *Bioinformatics* **24**, 1403–1405.

Jombart T, Ahmed I (2011) adegenet 1.3-1: new tools for the analysis of genome-wide SNP data. *Bioinformatics* **27**, 3070–3071.

Jombart T, Devillard S, Balloux F (2010) Discriminant analysis of principal components: a new method for the analysis of genetically structured populations. *BMC Genetics* **11**, 94.

Jones OR, Wang J (2010) COLONY: a program for parentage and sibship inference from multilocus genotype data. *Molecular Ecology Resources* **10**, 551–555.

Jorgenson E, Witte JS (2007) Microsatellite markers for genome-wide association studies. *Nature Reviews Genetics* **8**.

Kalinowski ST (2009) How well do evolutionary trees describe genetic relationships among populations? *Heredity* **102**, 506–513.

Kalinowski ST (2011) The computer program STRUCTURE does not reliably identify the main genetic clusters within species: simulations and implications for human population structure. *Heredity* **106**, 625–632.

Kardos M, Husby A, McFarlane SE, Qvarnstrom A, Ellegren H (2016) Whole-genome resequencing of extreme phenotypes in collared flycatchers highlights the difficulty of detecting quantitative trait loci in natural populations. *Molecular Ecology Resources* **16**, 727–741.

Karl SA, Toonen RJ, Grant WS, Bowen BW (2012) Common misconceptions in molecular ecology: echoes of the modern synthesis. *Molecular Ecology* **21**, 4171–4189.

Kasprzyk A (2011) BioMart: driving a paradigm change in biological data management. *Database* **2011**, bar049.

Katoh K, Misawa K, Kuma Ki, Miyata T (2002) MAFFT: a novel method for rapid multiple sequence alignment based on fast Fourier transform. *Nucleic Acids Research* **30**, 3059–3066.

Kawakami T, Backstrom N, Burri R*, et al.* (2014a) Estimation of linkage disequilibrium and interspecific gene flow in Ficedula flycatchers by a newly developed 50k single-nucleotide polymorphism array. *Molecular Ecology Resources* **14**, 1248–1260.

Kawakami T, Smeds L, Backström N*, et al.* (2014b) A high-density linkage map enables a second-generation collared flycatcher genome assembly and reveals the patterns of avian recombination rate variation and chromosomal evolution. *Molecular Ecology* **23**, 4035–4058.

Kearney SR (1989) The Polar Bear Alert Program at Churchill, Manitoba. In: *Bear–People Conflicts: Proceedings of a Symposium on Management Strategies* (ed. Bromley M), pp. 83–92. Northwest Territories Department of Renewable Resources, Yellowknife, Northwest Territories, Canada.

Keller LF, Waller DM (2002) Inbreeding effects in wild populations. *Trends in Ecology & Evolution* **17**, 230–241.

Kijas JW, Lenstra JA, Hayes B*, et al.* (2012) Genome-wide analysis of the world's sheep breeds reveals high levels of historic mixture and strong recent selection. *PLoS Biology* **10**, e1001258.

Kinnard C, Zdanowicz CM, Fisher DA, Isaksson E, de Vernal A, Thompson LG (2011) Reconstructed changes in Arctic sea ice over the past 1,450 years. *Nature* **479**, 509–512.

Kitahara E, Isagi Y, Ishibashi Y, Saitoh T (2000) Polymorphic microsatellite DNA markers in the Asiatic black bear *Ursus thibetanus*. *Molecular Ecology* **9**, 1661–1662.

Koboldt DC, Chen K, Wylie T*, et al.* (2009) VarScan: variant detection in massively parallel sequencing of individual and pooled samples. *Bioinformatics* **25**, 2283–2285.

Kompanje EJO, Hermans JJ (2008) Cephalopagus conjoined twins in a leopard cat (*Prionailurus bengalensis*). *Journal of Wildlife Diseases* **44**, 177–180.

Kopelman NM, Mayzel J, Jakobsson M, Rosenberg NA, Mayrose I (2015) Clumpak: a program for identifying clustering modes and packaging population structure inferences across K. *Molecular Ecology Resources* **15**, 1179–1191.

Kowal S, Gough WA, Butler K (2015) Temporal evolution of Hudson Bay sea ice (1971–2011). *Theoretical and Applied Climatology*, 1–8.

Kruuk LEB (2004) Estimating genetic parameters in natural populations using the 'animal model'. *Philosophical Transactions of the Royal Society B-Biological Sciences* **359**, 873–890.

Kruuk LEB, Clutton-Brock TH, Slate J, Pemberton JM, Brotherstone S, Guinness FE (2000) Heritability of fitness in a wild mammal population. *Proceedings of the National Academy of Sciences of the United States of America* **97**, 698–703.

Kutschera VE, Bidon T, Hailer F, Rodi JL, Fain SR, Janke A (2014) Bears in a forest of gene trees: Phylogenetic inference is complicated by incomplete lineage sorting and gene flow. *Molecular Biology and Evolution* **31**, 2004–2017.

Kutschera VE, Frosch C, Janke A*, et al.* (2016) High genetic variability of vagrant polar bears illustrates importance of population connectivity in fragmented sea ice habitats. *Animal Conservation*, In press.

Kwok R, Rothrock DA (2009) Decline in Arctic sea ice thickness from submarine and ICESat records: 1958–2008. *Geophysical Research Letters* **36**, L15501.

Lachance J, Tishkoff SA (2013) SNP ascertainment bias in population genetic analyses: Why it is important, and how to correct it. *Bioessays* **35**, 780–786.

Laidre KL, Born EW, Gurarie E, Wiig Ø, Dietz R, Stern H (2013) Females roam while males patrol: divergence in breeding season movements of pack-ice polar bears (*Ursus maritimus*). *Proceedings of the Royal Society B-Biological Sciences* **280**, 20122371.

Lan T, Cheng J, Ratan A*, et al.* (2016) Genome-wide evidence for a hybrid origin of modern polar bears. *biorXiv*.

Langmead B, Trapnell C, Pop M, Salzberg SL (2009) Ultrafast and memory-efficient alignment of short DNA sequences to the human genome. *Genome Biology* **10**, R25.

Lango Allen H, Estrada K, Lettre G*, et al.* (2010) Hundreds of variants clustered in genomic loci and biological pathways affect human height. *Nature* **467**, 832–838.

Larsen T, Tegelström H, Juneja RK, Taylor MK (1983) Low protein variability and genetic similarity between populations of the polar bear (*Ursus maritimus*). *Polar Research* **1**, 97–106.

Latch EK, Dharmarajan G, Glaubitz JC, Rhodes OE (2006) Relative performance of Bayesian clustering software for inferring population substructure and individual assignment at low levels of population differentiation. *Conservation Genetics* **7**, 295–302.

Li B, Zhang G, Willersleve E, Wang J, Wang J (2011) Genomic data from the polar bear (*Ursus maritimus*). *GigaScience*.

Li H, Ruan J, Durbin R (2008) Mapping short DNA sequencing reads and calling variants using mapping quality scores. *Genome Research* **18**, 1851–1858.

Lindblad-Toh K, Wade CM, Mikkelsen TS*, et al.* (2005) Genome sequence, comparative analysis and haplotype structure of the domestic dog. *Nature* **438**, 803–819.

Lindqvist C, Schuster SC, Sun Y*, et al.* (2010) Complete mitochondrial genome of a Pleistocene jawbone unveils the origin of polar bear. *Proceedings of the National Academy of Sciences* **107**, 5053–5057.

Liu NJ, Chen L, Wang S, Oh CG, Zhao HY (2005) Comparison of single-nucleotide polymorphisms and microsatellites in inference of population structure. *BMC Genetics* **6**, S26.

Liu S, Lorenzen Eline D, Fumagalli M*, et al.* (2014) Population genomics reveal recent speciation and rapid evolutionary adaptation in polar bears. *Cell* **157**, 785–794.

Livingston JE, Poland BJ (1980) A study of spontaneoulsy aborted twins. *Teratology* **21**, 139–148.

Lone K, Aars J, Ims R (2013) Site fidelity of Svalbard polar bears revealed by mark-recapture positions. *Polar Biology* **36**, 27–39.

Lotterhos KE, Whitlock MC (2015) The relative power of genome scans to detect local adaptation depends on sampling design and statistical method. *Molecular Ecology* **24**, 1031–1046.

Lunn NJ (1986) Observations of nonaggressive behavior between polar bear family groups. *Canadian Journal of Zoology-Revue Canadienne De Zoologie* **64**, 2035–2037.

Lunn NJ, Paetkau D, Calvert W, Atkinson S, Taylor M, Strobeck C (2000) Cub adoption by polar bears (*Ursus maritimus*): determining relatedness with microsatellite markers. *Journal of Zoology* **251**, 23–30.

Lunn NJ, Servanty S, Regehr EV, Converse SJ, Richardson E, Stirling I (2016) Demography of an apex predator at the edge of its range – impacts of changing sea ice on polar bears in Hudson Bay. *Ecological Applications*, In press.

Lunn NJ, Stirling I, Andriashek D, Richardson E (2004) Selection of maternity dens by female polar bears in western Hudson Bay, Canada and the effects of human disturbance. *Polar Biology* **27**, 350–356.

Lynch M, Ritland K (1999) Estimation of pairwise relatedness with molecular markers. *Genetics* **152**, 1753–1766.

Lynch M, Walsh B (1998) *Genetics and Analysis of Quantitative Traits* Sinauer, Sunderland, Mass.

Mackay TFC, Stone EA, Ayroles JF (2009) The genetics of quantitative traits: challenges and prospects. *Nature Reviews Genetics* **10**, 565–577.

Malenfant RM, Coltman DW, Davis CS (2015a) Design of a 9K Illumina BeadChip for polar bears (*Ursus maritimus*) from RAD and transcriptome sequencing. *Molecular Ecology Resources* **15**, 587–600.

Malenfant RM, Coltman DW, Richardson ES*, et al.* (2015b) Evidence of adoption, monozygotic twinning, and low inbreeding rates in a large genetic pedigree of polar bears. *Polar Biology*, In press.

Malenfant RM, Davis CS, Cullingham CI, Coltman DW (2016) Circumpolar genetic structure and recent gene flow of polar bears: a reanalysis. *PLoS ONE* **11**, e0148967.

Matishov GG, Chelintsev NG, Goryaev YI, Makarevich PR, Ishkulov DG (2014) Assessment of the amount of polar bears (*Ursus maritimus*) on the basis of perennial vessel counts. *Doklady Earth Sciences* **458**, 1312–1316.

Matukumalli LK, Lawley CT, Schnabel RD*, et al.* (2009) Development and characterization of a high density SNP genotyping assay for cattle. *PLoS ONE* **4**, e5350.

Mauritzen M, Derocher AE, Pavlova O, Wiig Ø (2003) Female polar bears, *Ursus maritimus*, on the Barents Sea drift ice: walking the treadmill. *Animal Behaviour* **66**, 107–113.

Mauritzen M, Derocher AE, Wiig Ø (2001) Space-use strategies of female polar bears in a dynamic sea ice habitat. *Canadian Journal of Zoology-Revue Canadienne De Zoologie* **79**, 1704–1713.

McCue ME, Bannasch DL, Petersen JL*, et al.* (2012) A high density SNP array for the domestic horse and extant Perissodactyla: utility for association mapping, genetic diversity, and phylogeny studies. *PLoS Genetics* **8**, e1002451.

Meacham F, Boffelli D, Dhahbi J, Martin DI, Singer M, Pachter L (2011) Identification and correction of systematic error in high-throughput sequence data. *BMC Bioinformatics* **12**, 451.

Medill S, Derocher AE, Stirling I, Lunn N, Moses RA (2009) Estimating cementum annuli width in polar bears: identifying sources of variation and error. *Journal of Mammalogy* **90**, 1256–1264.

Meirmans PG (2012a) AMOVA-based clustering of population genetic data. *Journal of Heredity* **103**, 744–750.

Meirmans PG (2012b) The trouble with isolation by distance. *Molecular Ecology* **21**, 2839–2846.

Meirmans PG (2014) Nonconvergence in Bayesian estimation of migration rates. *Molecular Ecology Resources* **14**, 726–733.

Meirmans PG (2015) Seven common mistakes in population genetics and how to avoid them. *Molecular Ecology* **24**, 3223–3231.

Meirmans PG, Van Tienderen PH (2004) GENOTYPE and GENODIVE: two programs for the analysis of genetic diversity of asexual organisms. *Molecular Ecology Notes* **4**, 792–794.

Messier F (2000) Effects of capturing, tagging and radio-collaring polar bears for research and management purposes in Nunavut and Northwest Territories, p. 64. Department of Biology, University of Saskatchewan, Saskatoon, SK, Canada.

Michalakis Y, Excoffier L (1996) A generic estimation of population subdivision using distances between alleles with special reference for microsatellite loci. *Genetics* **142**, 1061–1064.

Miller JM (2015) *Development and Application of Genomic Resources for Bighorn Sheep (Ovis canadensis)* Dissertation, University of Alberta.

Miller JM, Kijas JW, Heaton MP, McEwan JC, Coltman DW (2012a) Consistent divergence times and allele sharing measured from cross-species application of SNP chips developed for three domestic species. *Molecular Ecology Resources* **12**, 1145–1150.

Miller JM, Malenfant RM, David P*, et al.* (2013) Estimating genome-wide heterozygosity: effects of demographic history and marker type. *Heredity* **112**, 240–247.

Miller W, Schuster SC, Welch AJ*, et al.* (2012b) Polar and brown bear genomes reveal ancient admixture and demographic footprints of past climate change. *Proceedings of the National Academy of Sciences* **109**, E2382–E2390.

Milner JM, Pemberton JM, Brotherstone S, Albon SD (2000) Estimating variance components and heritabilities in the wild: a case study using the 'animal model' approach. *Journal of Evolutionary Biology* **13**, 804–813.

Molnár PK, Derocher AE, Thiemann GW, Lewis MA (2010) Predicting survival, reproduction and abundance of polar bears under climate change. *Biological Conservation* **143**, 1612–1622.

Molnár PK, Klanjscek T, Derocher AE, Obbard ME, Lewis MA (2009) A body composition model to estimate mammalian energy stores and metabolic rates from body mass and body length, with application to polar bears. *Journal of Experimental Biology* **212**, 2313–2323.

Moore J, Ali R (1984) Are dispersal and inbreeding avoidance related? *Animal Behaviour* **32**, 94–112.

Moore JA, Xu R, Frank K, Draheim H, Scribner KT (2015) Social network analysis of mating patterns in American black bears (*Ursus americanus*). *Molecular Ecology* **24**, 4010–4022.

Morin PA, Luikart G, Wayne RK, SNP Workshop Grp (2004) SNPs in ecology, evolution and conservation. *Trends in Ecology & Evolution* **19**, 208–216.

Morrissey MB, Wilson AJ (2010) PEDANTICS: an R package for pedigree-based genetic simulation and pedigree manipulation, characterization and viewing. *Molecular Ecology Resources* **10**, 711–719.

Nakamura K, Oshima T, Morimoto T*, et al.* (2011) Sequence-specific error profile of Illumina sequencers. *Nucleic Acids Research* **39**, e90.

Nei M (1978) Estimation of average heterozygosity and genetic distance from a small number of individuals. *Genetics* **89**, 583–590.

Nei M (1987) *Molecular Evolutionary Genetics* Columbia University Press, New York.

Nei M, Tajima F, Tateno Y (1983) Accuracy of estimated phylogenetic trees from molecular data. *Journal of Molecular Evolution* **19**, 153–170.

Nielsen R, Signorovitch J (2003) Correcting for ascertainment biases when analyzing SNP data: applications to the estimation of linkage disequilibrium. *Theoretical Population Biology* **63**, 245–255.

Norman AJ, Spong G (2015) Single nucleotide polymorphism-based dispersal estimates using noninvasive sampling. *Ecology and Evolution* **5**, 3056–3065.

Obbard ME, Middel KR (2012) Bounding the Southern Hudson Bay polar bear subpopulation. *Ursus* **23**, 134–144.

Obbard ME, Thiemann GW, Peacock E, DeBruyn TD (2009) Polar Bears: Proceedings of the 15th Working Meeting of the IUCN/SSC Polar Bear Specialist Group, vii + 235 pp.

Oksanen J, Blanchet FG, Kindt R*, et al.* (2015) vegan: Community Ecology Package.

Onorato DP, Hellgren EC, Van Den Bussche RA, Skiles JR (2004) Paternity and relatedness of American black bears recolonizing a desert montane island. *Canadian Journal of Zoology-Revue Canadienne De Zoologie* **82**, 1201–1210.

Orr HA (2005) The genetic theory of adaptation: a brief history. *Nature Reviews Genetics* **6**, 119–127.

Ostrander EA, Sprague GF, Rine J (1993) Identification and characterization of dinucleotide repeat $(CA)_n$ markers for genetic mapping in dog. *Genomics* **16**, 207–213.

Paetkau D, Amstrup SC, Born EW*, et al.* (1999) Genetic structure of the world's polar bear populations. *Molecular Ecology* **8**, 1571–1584.

Paetkau D, Calvert W, Stirling I, Strobeck C (1995) Microsatellite analysis of population structure in Canadian polar bears. *Molecular Ecology* **4**, 347–354.

Paetkau D, Shields GF, Strobeck C (1998) Gene flow between insular, coastal and interior populations of brown bears in Alaska. *Molecular Ecology* **7**, 1283–1292.

Paetkau D, Strobeck C (1994) Microsatellite analysis of genetic variation in black bear populations. *Molecular Ecology* **3**, 489–495.

Pagano AM, Durner GM, Amstrup SC, Simac KS, York GS (2012) Long-distance swimming by polar bears (*Ursus maritimus*) of the southern Beaufort Sea during years of extensive open water. *Canadian Journal of Zoology-Revue Canadienne De Zoologie* **90**, 663–676.

Paterson T, Graham M, Kennedy J, Law A (2012) VIPER: a visualisation tool for exploring inheritance inconsistencies in genotyped pedigrees. *BMC Bioinformatics* **13**, 16.

Peacock E, Derocher AE, Lunn NJ, Obbard ME (2010) Polar Bear Ecology and Management in Hudson Bay in the Face of Climate Change. In: *A Little Less Arctic: Top Predators in the World's Largest Northern Inland Sea, Hudson Bay* (eds. Ferguson SH, Loseto LL, Mallory ML), pp. 93–115. Springer, New York.

Peacock E, Sonsthagen SA, Obbard ME*, et al.* (2015a) Correction: Implications of the circumpolar genetic structure of polar bears for their conservation in a rapidly warming Arctic. *PLoS ONE* **10**, e0136126.

Peacock E, Sonsthagen SA, Obbard ME*, et al.* (2015b) Implications of the Circumpolar Genetic Structure of Polar Bears for Their Conservation in a Rapidly Warming Arctic. *PLoS ONE* **10**, e112021.

Peacock E, Taylor MK, Laake J, Stirling I (2013) Population ecology of polar bears in Davis Strait, Canada and Greenland. *Journal of Wildlife Management* **77**, 463–476.

Peakall R, Smouse PE (2006) GENALEX 6: genetic analysis in Excel. Population genetic software for teaching and research. *Molecular Ecology Notes* **6**, 288–295.

Peakall R, Smouse PE (2012) GenAlEx 6.5: genetic analysis in Excel. Population genetic software for teaching and research-an update. *Bioinformatics* **28**, 2537–2539.

Pedersen A (1945) *The Polar Bear: Its Distribution and Way of Life* Aktieselskabet E. Bruun & Co., Copenhagen, Denmark.

Pemberton JM (2008) Wild pedigrees: the way forward. *Proceedings of the Royal Society B-Biological Sciences* **275**, 613–621.

Pertoldi C, Sonne C, Wiig Ø, Baagøe HJ, Loeschcke V, Bechshøft TØ (2012) East Greenland and Barents Sea polar bears (*Ursus maritimus*): adaptive variation between two populations using skull morphometrics as an indicator of environmental and genetic differences. *Hereditas* **149**, 99–107.

Picardi E, Pesole G (2013) REDItools: high-throughput RNA editing detection made easy. *Bioinformatics* **29**, 1813–1814.

Pickrell JK, Pritchard JK (2012) Inference of population splits and mixtures from genome-wide allele frequency data. *PLoS Genetics* **8**, e1002967.

Poissant J, Hogg JT, Davis CS, Miller JM, Maddox JF, Coltman DW (2010) Genetic linkage map of a wild genome: genomic structure, recombination and sexual dimorphism in bighorn sheep. *BMC Genomics* **11**, 524.

Polyak L, Alley RB, Andrews JT*, et al.* (2010) History of sea ice in the Arctic. *Quaternary Science Reviews* **29**, 1757–1778.

Pond CM, Mattacks CA, Colby RH, Ramsay MA (1992) The anatomy, chemical composition, and metabolism of adipose tissue in wild polar bears (*Ursus maritimus*). *Canadian Journal of Zoology-Revue Canadienne De Zoologie* **70**, 326–341.

Pop M, Salzberg SL (2008) Bioinformatics challenges of new sequencing technology. *Trends in Genetics* **24**, 142–149.

Pop M, Salzberg SL (2015) Use and mis-use of supplementary material in science publications. *BMC Bioinformatics* **16**, 237.

Postma E (2006) Implications of the difference between true and predicted breeding values for the study of natural selection and micro-evolution. *Journal of Evolutionary Biology* **19**, 309–320.

Postma E (2014) Four decades of estimating heritabilities in wild vertebrate populations: improved methods, more data, better estimates? In: *Quantitative Genetics in the Wild* (eds. Charmantier A, Garant D, Kruuk LEB). Oxford University Press, Oxford, UK.

Price AL, Patterson NJ, Plenge RM, Weinblatt ME, Shadick NA, Reich D (2006) Principal components analysis corrects for stratification in genome-wide association studies. *Nature Genetics* **38**, 904–909.

Price AL, Zaitlen NA, Reich D, Patterson N (2010) New approaches to population stratification in genome-wide association studies. *Nature Reviews Genetics* **11**, 459–463.

Pritchard JK, Stephens M, Donnelly P (2000) Inference of population structure using multilocus genotype data. *Genetics* **155**, 945–959.

Pritchard JK, Wen X, Falush D (2010) Documentation for *structure* software: Version 2.3. University of Chicago, Chicago, USA.

Proctor MF, McLellan BN, Strobeck C, Barclay RMR (2004) Gender-specific dispersal distances of grizzly bears estimated by genetic analysis. *Canadian Journal of Zoology-Revue Canadienne De Zoologie* **82**, 1108–1118.

Prugnolle F, de Meeus T (2002) Inferring sex-biased dispersal from population genetic tools: a review. *Heredity* **88**, 161–165.

Purcell S, Neale B, Todd-Brown K*, et al.* (2007) PLINK: a tool set for whole-genome association and population-based linkage analyses. *American Journal of Human Genetics* **81**, 559–575.

Pusey A, Wolf M (1996) Inbreeding avoidance in animals. *Trends in Ecology & Evolution* **11**, 201–206.

Putman AI, Carbone I (2014) Challenges in analysis and interpretation of microsatellite data for population genetic studies. *Ecology and Evolution* **4**, 4399–4428.

Queller DC, Goodnight KF (1989) Estimating relatedness using genetic markers. *Evolution* **43**, 258–275.

R Core Team (2015) R: A Language and Environment for Statistical Computing. R Foundation for Statistical Computing, Vienna, Austria.

Raggatt LJ, Qin L, Tamasi J*, et al.* (2008) Interleukin-18 Is regulated by parathyroid hormone and is required for its bone anabolic actions. *Journal of Biological Chemistry* **283**, 6790–6798.

Ramos AM, Crooijmans RPMA, Affara NA*, et al.* (2009) Design of a high density SNP genotyping assay in the pig using SNPs identified and characterized by next generation sequencing technology. *PLoS ONE* **4**, e6524.

Ramsay MA, Mattacks CA, Pond CM (1992) Seasonal and sex differences in the structure and chemical composition of adipose tissue in wild polar bears (*Ursus maritimus*). *Journal of Zoology* **228**, 533–544.

Ramsay MA, Stirling I (1986a) Long-term effects of drugging and handling free-ranging polar bears. *Journal of Wildlife Management* **50**, 619–626.

Ramsay MA, Stirling I (1986b) On the mating system of polar bears. *Canadian Journal of Zoology-Revue Canadienne De Zoologie* **64**, 2142–2151.

Ramsay MA, Stirling I (1988) Reproductive biology and ecology of female polar bears (*Ursus maritimus*). *Journal of Zoology* **214**, 601–634.

Raymond M, Rousset F (1995) GENEPOP (Version 1.2): population genetics software for exact tests and ecumenicism. *Journal of Heredity* **86**, 248–249.

Réale D, Festa-Bianchet M, Jorgenson JT (1999) Heritability of body mass varies with age and season in wild bighorn sheep. *Heredity* **83**, 526–532.

Reich D, Thangaraj K, Patterson N, Price AL, Singh L (2009) Reconstructing Indian population history. *Nature* **461**, 489–494.

Reid JM, Arcese P, Sardell RJ, Keller LF (2011) Additive genetic variance, heritability, and inbreeding depression in male extra-pair reproductive success. *American Naturalist* **177**, 177–187.

Richardson E, Branigan M, Calvert W*, et al.* (2006) Research on polar bears in Canada 2001–2004. In: *Polar Bears: Proceedings of the 14th Working Meeting of the IUCN/SSC Polar Bear Specialist Group, 20–24 June 2005, Seattle, Washington, USA*. (eds. Aars J, Lunn NJ, Derocher AE), pp. 117–132. IUCN, Gland, Switzerland.

Richardson ES (2014) *The Mating System and Life History of the Polar Bear* Dissertation, University of Alberta.

Riedman ML (1982) The evolution of alloparental care and adoption in mammals and birds. *Quarterly Review of Biology* **57**, 405–435.

Riedman ML, Boeuf BJ (1982) Mother-pup separation and adoption in northern elephant seals. *Behavioral Ecology and Sociobiology* **11**, 203–215.

Riester M, Stadler PF, Klemm K (2009) FRANz: reconstruction of wild multi-generation pedigrees. *Bioinformatics* **25**, 2134–2139.

Riester M, Stadler PF, Klemm K (2010) Reconstruction of pedigrees in clonal plant populations. *Theoretical Population Biology* **78**, 109–117.

Robinson MR, Santure AW, DeCauwer I, Sheldon BC, Slate J (2013) Partitioning of genetic variation across the genome using multimarker methods in a wild bird population. *Molecular Ecology* **22**, 3963–3980.

Rockman MV (2012) The QTN program and the alleles that matter for evolution: all that's gold does not glitter. *Evolution* **66**, 1–17.

Rode KD, Pagano AM, Bromaghin JF*, et al.* (2014) Effects of capturing and collaring on polar bears: findings from long-term research on the southern Beaufort Sea population. *Wildlife Research* **41**, 311–322.

Rode KD, Robbins CT, Nelson L, Amstrup SC (2015) Can polar bears use terrestrial foods to offset lost ice-based hunting opportunities? *Frontiers in Ecology and the Environment* **13**, 138–145.

Rodriguez-Ramílo ST, Toro MA, Fernández J (2009) Assessing population genetic structure via the maximisation of genetic distance. *Genetics Selection Evolution* **41**, 49.

Rodriguez-Ramilo ST, Wang JL (2012) The effect of close relatives on unsupervised Bayesian clustering algorithms in population genetic structure analysis. *Molecular Ecology Resources* **12**, 873–884.

Ronnegard L, McFarlane SE, Husby A, Kawakami T, Ellegren H, Qvarnstrom A (2016) Increasing the power of genome wide association studies in natural populations using repeated measures: evaluation and implementation. *Methods in Ecology and Evolution*.

Rosenberg NA (2004) DISTRUCT: a program for the graphical display of population structure. *Molecular Ecology Notes* **4**, 137–138.

Rosing-Asvid A, Born E, Kingsley M (2002) Age at sexual maturity of males and timing of the mating season of polar bears (*Ursus maritimus*) in Greenland. *Polar Biology* **25**, 878–883.

Roulin A (2002) Why do lactating females nurse alien offspring? A review of hypotheses and empirical evidence. *Animal Behaviour* **63**, 201–208.

Rousset F (2000) Genetic differentiation between individuals. *Journal of Evolutionary Biology* **13**, 58–62.

Rousset F (2008) GENEPOP'007: a complete re-implementation of the GENEPOP software for Windows and Linux. *Molecular Ecology Resources* **8**, 103–106.

Sahanatien V, Derocher AE (2010) Foxe Basin Polar Bear Project 2010 Interim Report – Part 1: Movements, Habitat, Population Delineation & Inuit Qaujimajatugangnit, p. 29. Nunavut Department of Environment, Iqaluit, Canada.

Santure AW, De Cauwer I, Robinson MR, Poissant J, Sheldon BC, Slate J (2013) Genomic dissection of variation in clutch size and egg mass in a wild great tit (*Parus major*) population. *Molecular Ecology* **22**, 3949–3962.

Saunders BL (2005) *The Mating System of Polar Bears in the Central Canadian Arctic* M.Sc. Thesis, Queen's University.

Schliep KP (2011) phangorn: phylogenetic analysis in R. *Bioinformatics* **27**, 592–593.

Schluter D (1996) Adaptive radiation along genetic lines of least resistance. *Evolution* **50**, 1766–1774.

Schuler GD (1997) Sequence mapping by electronic PCR. *Genome Research* **7**, 541–550.

Schwartz MK, McKelvey KS (2008) Why sampling scheme matters: the effect of sampling scheme on landscape genetic results. *Conservation Genetics* **10**, 441–452.

Shriner D (2011) Investigating population stratification and admixture using eigenanalysis of dense genotypes. *Heredity* **107**, 413–420.

Silva del Río N, Kirkpatrick BW, Fricke PM (2006) Observed frequency of monozygotic twinning in Holstein dairy cattle. *Theriogenology* **66**, 1292–1299.

Simmons JP, Nelson LD, Simonsohn U (2011) False-positive psychology: undisclosed flexibility in data collection and analysis allows presenting anything as significant. *Psychological Science* **22**, 1359–1366.

Slate J, Santure AW, Feulner PGD*, et al.* (2010) Genome mapping in intensively studied wild vertebrate populations. *Trends in Genetics* **26**, 275–284.

Slate J, Visscher PM, MacGregor S, Stevens D, Tate ML, Pemberton JM (2002) A genome scan for quantitative trait loci in a wild population of red deer (*Cervus elaphus*). *Genetics* **162**, 1863–1873.

Slatkin M (1995) A measure of population subdivision based on microsatellite allele frequencies. *Genetics* **139**, 457–462.

Smith BJ (2007) boa: An R Package for MCMC Output Convergence Assessment and Posterior Inference Journal of Statistical Software. *Journal of Statistical Software* **21**, 1–37.

Spalding MD, Fox HE, Halpern BS*, et al.* (2007) Marine ecoregions of the world: a bioregionalization of coastal and shelf areas. *Bioscience* **57**, 573–583.

Speed D, Balding DJ (2015) Relatedness in the post-genomic era: is it still useful? *Nature Reviews Genetics* **16**, 33–44.

Speliotes EK, Willer CJ, Berndt SI*, et al.* (2010) Association analyses of 249,796 individuals reveal 18 new loci associated with body mass index. *Nature Genetics* **42**, 937–948.

Spencer CCA, Su Z, Donnelly P, Marchini J (2009) Designing genome-wide association studies: sample size, power, imputation, and the choice of genotyping chip. *PLoS Genetics* **5**, e1000447.

Spotte S (1982) The incidence of twins in pinnipeds. *Canadian Journal of Zoology-Revue Canadienne De Zoologie* **60**, 2226–2233.

Stapleton S, Atkinson S, Hedman D, Garshelis D (2014) Revisiting Western Hudson Bay: using aerial surveys to update polar bear abundance in a sentinel population. *Biological Conservation* **170**, 38–47.

Stirling I, Andriashek D, Latour P, Calvert W (1975) The Distribution and Abundance of Polar Bears in the Eastern Beaufort Sea. Canadian Wildlife Service, Edmonton, AB.

Stirling I, Derocher AE (2012) Effects of climate warming on polar bears: a review of the evidence. *Global Change Biology* **18**, 2694–2706.

Stirling I, Lunn NJ, Iacozza J (1999) Long-term trends in the population ecology of polar bears in western Hudson Bay in relation to climatic change. *Arctic* **52**, 294–306.

Stirling I, Lunn NJ, Iacozza J, Elliott C, Obbard M (2004) Polar bear distribution and abundance on the southwestern Hudson Bay coast during open water season, in relation to population trends and annual ice patterns. *Arctic* **57**, 15–26.

Stirling I, Parkinson CL (2006) Possible effects of climate warming on selected populations of polar bears (*Ursus maritimus*) in the Canadian Arctic. *Arctic* **59**, 261–275.

Stirling I, Spencer C, Andriashek D (1989) Immobilization of polar bears (*Ursus maritimus*) with Telazol in the Canadian Arctic. *Journal of Wildlife Diseases* **25**, 159–168.

Stirling I, Thiemann GW, Richardson E (2008) Quantitative support for a subjective fatness index for immobilized polar bears. *Journal of Wildlife Management* **72**, 568–574.

Storey JD (2002) A direct approach to false discovery rates. *Journal of the Royal Statistical Society: Series B (Statistical Methodology)* **64**, 479–498.

Storey JD, Bass AJ, Dabney A, Robinson D (2015) qvalue: Q-value estimation for false discovery rate control.

Stram DO (2014) *Design, Analysis, and Interpretation of Genome-wide Association Scans* Springer, New York.

Subramanian A, Tamayo P, Mootha VK*, et al.* (2005) Gene set enrichment analysis: a knowledge-based approach for interpreting genome-wide expression profiles. *Proceedings of the National Academy of Sciences* **102**, 15545–15550.

Szkiba D, Kapun M, von Haeseler A, Gallach M (2014) SNP2GO: functional analysis of genome-wide association studies. *Genetics* **197**, 285–289.

Szpiech ZA, Jakobsson M, Rosenberg NA (2008) ADZE: a rarefaction approach for counting alleles private to combinations of populations. *Bioinformatics* **24**, 2498–2504.

Szulkin M, Stopher KV, Pemberton JM, Reid JM (2013) Inbreeding avoidance, tolerance, or preference in animals? *Trends in Ecology & Evolution* **28**, 205–211.

Taberlet P, Camarra JJ, Griffin S*, et al.* (1997) Noninvasive genetic tracking of the endangered Pyrenean brown bear population. *Molecular Ecology* **6**, 869–876.

Takezaki N, Nei M (1996) Genetic distances and reconstruction of phylogenetic trees from microsatellite DNA. *Genetics* **144**, 389–399.

Takezaki N, Nei M, Tamura K (2014) POPTREEW: web version of POPTREE for constructing population trees from allele frequency data and computing some other quantities. *Molecular Biology and Evolution* **31**, 1622–1624.

Talbot SL, Shields GF (1996) Phylogeography of brown bears (*Ursus arctos*) of Alaska and paraphyly within the Ursidae. *Molecular Phylogenetics and Evolution* **5**, 477–494.

Tamura K, Nei M (1993) Estimation of the number of nucleotide substitutions in the control region of mitochondrial DNA in humans and chimpanzees. *Molecular Biology and Evolution* **10**, 512–526.

Taylor M, Larsen T, Schweinsburg RE (1985) Observations of intraspecific aggression and cannibalism in polar bears (*Ursus maritimus*). *Arctic* **38**, 303–309.

Taylor M, Lee J (1995) Distribution and abundance of Canadian polar bear populations: a management perspective. *Arctic* **48**, 147–154.

Taylor MK, Akeeagok S, Andriashek D*, et al.* (2001) Delineating Canadian and Greenland polar bear (*Ursus maritimus*) populations by cluster analysis of movements. *Canadian Journal of Zoology-Revue Canadienne De Zoologie* **79**, 690–709.

Taylor MK, Laake J, McLoughlin PD, Cluff HD, Messier F (2009) Mark–recapture and stochastic population models for polar bears of the High Arctic. *Arctic* **61**, 143–152.

Taylor MK, McLoughlin PD, Messier F (2008) Sex-selective harvesting of polar bears *Ursus maritimus*. *Wildlife Biology* **14**, 52–60.

Taylor RW, Boon AK, Dantzer B*, et al.* (2012) Low heritabilities, but genetic and maternal correlations between red squirrel behaviours. *Journal of Evolutionary Biology* **25**, 614–624.

Thiemann GW, Derocher AE, Stirling I (2008a) Polar bear *Ursus maritimus* conservation in Canada: an ecological basis for identifying designatable units. *Oryx* **42**, 504–515.

Thiemann GW, Iverson SJ, Stirling I (2008b) Polar bear diets and arctic marine food webs: insights from fatty acid analysis. *Ecological Monographs* **78**, 591–613.

Thiemann GW, Lunn NJ, Richardson ES, Andriashek DS (2011) Temporal change in the morphometry–body mass relationship of polar bears. *Journal of Wildlife Management* **75**, 580–587.

Thomsen M, Mølvig J, Zerbib A*, et al.* (1988) The susceptibility to insulin-dependent diabetes mellitus bis associated with C4 allotypes independently of the association with HLA-DQ alleles in HLA-DR3, 4 heterozygotes. *Immunogenetics* **28**, 320–327.

Tosser-Klopp G, Bardou P, Bouchez O*, et al.* (2014) Design and characterization of a 52K SNP chip for goats. *PLoS ONE* **9**, e86227.

Trapnell C, Pachter L, Salzberg SL (2009) TopHat: discovering splice junctions with RNA-Seq. *Bioinformatics* **25**, 1105–1111.

Trapnell C, Williams BA, Pertea G*, et al.* (2010) Transcript assembly and quantification by RNA-Seq reveals unannotated transcripts and isoform switching during cell differentiation. *Nature Biotechnology* **28**, 511–515.

Tsui C, Coleman LE, Griffith JL*, et al.* (2003) Single nucleotide polymorphisms (SNPs) that map to gaps in the human SNP map. *Nucleic Acids Research* **31**, 4910–4916.

Turner S, Armstrong LL, Bradford Y*, et al.* (2001) Quality Control Procedures for Genome-Wide Association Studies. In: *Current Protocols in Human Genetics*. John Wiley & Sons, Inc.

Turner SD (2014) qqman: an R package for visualizing GWAS results using Q-Q and manhattan plots. *biorXiv*, doi: 10.1101/005165.

van Bers NEM, Santure AW, Van Oers K*, et al.* (2012) The design and cross-population application of a genome-wide SNP chip for the great tit *Parus major*. *Molecular Ecology Resources* **12**, 753–770.

van Oers K, Santure AW, De Cauwer I*, et al.* (2014) Replicated high-density genetic maps of two great tit populations reveal fine-scale genomic departures from sex-equal recombination rates. *Heredity* **112**, 307–316.

Velicer WF (1976) Determining the number of components from the matrix of partial correlations. *Psychometrika* **41**, 321–327.

Vibe C (1976) Preliminary Report on the Second Danish Polar Bear Expedition to North East Greenland, 1974. In: *Proceedings of the Fifth Working Meeting of the Polar Bear Specialist Group*, pp. 91–97. IUCN, Morges, Switzerland.

Viengkone M (2015) *Population Structure and Space-use of Polar Bears (Ursus maritimus) in Hudson Bay* M.Sc. Thesis, University of Alberta.

Villinger J, Waldman B (2012) Social discrimination by quantitative assessment of immunogenetic similarity. *Proceedings of the Royal Society B-Biological Sciences* **279**, 4368–4374.

Vincent J-S (1989) Quaternary geology of the northern Canadian Interior Plains. In: *Quaternary Geology of Canada and Greenland* (ed. Fulton RJ), pp. 100–137. Geological Survey of Canada, Ottawa, Canada.

Visscher PM (2009) Whole genome approaches to quantitative genetics. *Genetica* **136**, 351–358.

Wahlund S (1928) Zusammensetzung von Populationen und Korrelationserscheinungen vom Standpunkt der Vererbungslehre aus betrachtet. *Hereditas* **11**, 65–106.

Wall JD, Tang LF, Zerbe B*, et al.* (2014) Estimating genotype error rates from high-coverage next-generation sequence data. *Genome Research* **24**, 1734–1739.

Walsh B, Lynch M (2014) Using molecular data to detect selection: signatures from recent single events. In: *Evolution and Selection of Quantitative Traits: I. Foundations*.

Wang C, Zöllner S, Rosenberg NA (2012) A quantitative comparison of the similarity between genes and geography in worldwide human populations. *PLoS Genetics* **8**, e1002886.

Wang J (2015) Does G_{ST} underestimate genetic differentiation from marker data? *Molecular Ecology* **24**, 3546–3458.

Wang JL (2002) An estimator for pairwise relatedness using molecular markers. *Genetics* **160**, 1203–1215.

Wang JL (2011) COANCESTRY: a program for simulating, estimating and analysing relatedness and inbreeding coefficients. *Molecular Ecology Resources* **11**, 141–145.

Wang L, Jia P, Wolfinger RD, Chen X, Zhao Z (2011) Gene set analysis of genome-wide association studies: Methodological issues and perspectives. *Genomics* **98**, 1–8.

Waples RS (2015) Testing for Hardy–Weinberg proportions: have we lost the plot? *Journal of Heredity* **106**, 1–19.

Waples RS, Gaggiotti O (2006) What is a population? An empirical evaluation of some genetic methods for identifying the number of gene pools and their degree of connectivity. *Molecular Ecology* **15**, 1419–1439.

Weber DS, Van Coeverden De Groot PJ, Peacock E*, et al.* (2013) Low MHC variation in the polar bear: implications in the face of Arctic warming? *Animal Conservation* **16**, 671–683.

Weir BS, Cockerham CC (1984) Estimating F-statistics for the analysis of population structure. *Evolution* **38**, 1358–1370.

Welch AJ, Bedoya-Reina OC, Carretero-Paulet L, Miller W, Rode KD, Lindqvist C (2014) Polar bears exhibit genome-wide signatures of bioenergetic adaptation to life in the Arctic environment. *Genome Biology and Evolution* **6**, 433–450.

Wenzel MA, James MC, Douglas A, Piertney SB (2015) Genome-wide association and genome partitioning reveal novel genomic regions underlying variation in gastrointestinal nematode burden in a wild bird. *Molecular Ecology* **24**, 4175–4192.

Whitlock MC, Lotterhos KE (2015) Reliable detection of loci responsible for local adaptation: inference of a null model through trimming the distribution of F_{ST}. *American Naturalist* **186**, S24–S36.

Wiig Ø, Amstrup S, Atwood T*, et al.* (2015) *Ursus maritimus.* IUCN. http://dx.doi.org/10.2305/IUCN.UK.2015-4.RLTS.T22823A14871490.en

Wilkinson GS (1992) Communal nursing in the evening bat, *Nycticeius humeralis*. *Behavioral Ecology and Sociobiology* **31**, 225–235.

Williams GC (1975) *Sex and Evolution* Princeton University Press, Princeton, NJ.

Willing EM, Dreyer C, van Oosterhout C (2012) Estimates of genetic differentiation measured by F_{ST} do not necessarily require large sample sizes when using many SNP markers. *PLoS ONE* **7**, e42649.

Wilson AJ, Pemberton JM, Pilkington JG, Clutton-Brock TH, Coltman DW, Kruuk LEB (2006) Quantitative genetics of growth and cryptic evolution of body size in an island population. *Evolutionary Ecology* **21**, 337–356.

Wilson AJ, Réale D, Clements MN*, et al.* (2010) An ecologist's guide to the animal model. *Journal of Animal Ecology* **79**, 13–26.

Wilson DE (1976) Cranial variation in polar bears. In: *Third International Conference on Bears* (eds. Pelton MR, Lentfer JW, Folk GE). International Union for Conservation of Nature and Natural Resources, Binghamton, New York.

Wilson GA, Rannala B (2003) Bayesian inference of recent migration rates using multilocus genotypes. *Genetics* **163**, 1177–1191.

Wilson GA, Rannala B (2005) Documentation for BayesAss 1.3. University of California Berkeley, Berkeley, CA.

Xu J, Zhao Z, Zhang X*, et al.* (2014) Development and evaluation of the first high-throughput SNP array for common carp (*Cyprinus carpio*). *BMC Genomics* **15**, 307.

Yan J, Shah T, Warburton ML, Buckler ES, McMullen MD, Crouch J (2009) Genetic characterization and linkage disequilibrium estimation of a global maize collection using SNP markers. *PLoS ONE* **4**, e8451.

Yang J, Lee SH, Goddard ME, Visscher PM (2011a) GCTA: A tool for genome-wide complex trait analysis. *The American Journal of Human Genetics* **88**, 76–82.

Yang J, Manolio TA, Pasquale LR*, et al.* (2011b) Genome partitioning of genetic variation for complex traits using common SNPs. *Nature Genetics* **43**, 519–525.

Yang J, Weedon MN, Purcell S*, et al.* (2011c) Genomic inflation factors under polygenic inheritance. *European Journal of Human Genetics* **19**, 807–812.

Yang J, Zaitlen NA, Goddard ME, Visscher PM, Price AL (2014) Advantages and pitfalls in the application of mixed-model association methods. *Nature Genetics* **46**, 100–106.

Zedrosser A, Støen O-G, Sæbø S, Swenson JE (2007) Should I stay or should I go? Natal dispersal in the brown bear. *Animal Behaviour* **74**, 369–376.

Zerbino DR, Birney E (2008) Velvet: algorithms for de novo short read assembly using de Bruijn graphs. *Genome Research* **18**, 821–829.

Zeyl E, Aars J, Ehrich D, Bachmann L, Wiig Ø (2009a) The mating system of polar bears: a genetic approach. *Canadian Journal of Zoology-Revue Canadienne De Zoologie* **87**, 1195–1209.

Zeyl E, Aars J, Ehrich D, Wiig Ø (2009b) Families in space: relatedness in the Barents Sea population of polar bears (*Ursus maritimus*). *Molecular Ecology* **18**, 735–749.

Zink RM, Barrowclough GF (2008) Mitochondrial DNA under siege in avian phylogeography. *Molecular Ecology* **17**, 2107–2121.

Appendices

Appendix 1: Polar bear (*Ursus maritimus*) transcriptome assembly and SNP discovery

A1.1 Introduction

Polar bears (*Ursus maritimus*) are an iconic Arctic species and often used as the poster species for climate change. The ecological consequences of climate change on polar bears have been well characterized thanks to long-term monitoring projects in select subpopulations. Polar bears in the Western Hudson Bay subpopulation have been declining in size and body condition for decades because of earlier sea ice breakup, reduced hunting time on the ice, and an increasingly long fasting season (Atkinson *et al.* 1996b; Stirling & Parkinson 2006). Maternal body condition is among the best known predictors of cub survival (Derocher & Stirling 1996), and as Western Hudson Bay females have decreased in size, rates of litter production and average litter size have also decreased, while cub mortality and average time to independence have increased (Stirling & Derocher 2012). Although these morphological changes have potential evolutionary consequences, little is yet known about whether there is any genetic variation in body size or fat accumulation that would provide the potential for adaptation.

To date, most polar bear genetics research has used mitochondrial DNA (e.g., Talbot & Shields 1996) or putatively neutral microsatellites originally developed for polar bears (Paetkau *et al.* 1995), other ursids (Kitahara *et al.* 2000; Paetkau *et al.* 1998; Paetkau & Strobeck 1994; Taberlet *et al.* 1997), or dogs (Ostrander *et al.* 1993). Since the announcement of the polar bear nuclear genome (Li *et al.* 2011), single-nucleotide polymorphisms (SNPs) have been increasingly used, though primarily in studies of polar bear–brown bear divergence and interbreeding (e.g., Cahill *et al.* 2013; Miller *et al.* 2012b). No attempts have been made to develop and deploy the high-density genetic markers necessary to extensively examine within-population morphometric variation or microevolution.

In this study, we used high-throughput Illumina sequencing to develop SNPs from pooled blood and fat transcriptomes, using samples from five adult female polar bears and five (unrelated) dependent cubs. In total, we generated 371,258 transcripts of which 36,755 were deemed to be "full length" (i.e., covered more than 90% of their best BLAST hit), and we identified 63,020

SNPs. Since this study was conducted, we have used a subset of these SNPs—together with SNPs identified from RAD sequencing—to develop an Illumina BeadChip for quantitative genetics research in Western Hudson Bay.

A1.2 Data access

- *Sequence files* – Sequence files can be found on the NCBI Sequence Read Archive under project number PRJNA193538. See Table A1.2 for individual accession numbers.
- *Reference file* – All SNP positions in the .vcf file are given relative to the draft polar bear genome (Li *et al.* 2011), available online at http://gigadb.org/dataset/100008 (last accessed Aug. 19, 2013).
- *Sequence assembly* – The duplicate-pruned alignment files used for SNP calling can be found on the NCBI Sequence Read Archive under project number PRJNA193538. See Table A1.2 for individual accession numbers.
- *Transcriptomic contigs* – A FASTA file representing full-length transcriptomic contigs has been deposited at GenBank, and is available under the accession GAJD00000000. The version described in this paper is the first version, GAJD01000000, with individual accession numbers GAJD01000001–GAJD01036755. An additional annotation file including a putative identity and gene ontology terms for each transcript is available as annotations.annot under DRYAD accession: doi:10.5061/dryad.606j6
- *Putative SNP data* – A VCF file representing SNP data pooled/merged across libraries is available as pb_syscallsnps.vcf.txt under DRYAD accession: doi:10.5061/dryad.606j6
- *Scripts used in the assembly – getsnpsfrompileup.pl* (Perl) – We found that existing SNP-calling software such as SAMTOOLS (Durbin *et al.* 2009) and VARSCAN (Koboldt *et al.* 2009) behaved poorly on our data because RefSkip characters ("<" and ">")—used to indicate a splice—were incorrectly interpreted as sequence data. Therefore, we wrote a Perl script to implement a simple frequency-based method of SNP calling for spliced data. This program takes as input the output from SAMTOOLS mpileup and outputs SNP calls in GFF3 format. By default, it will only call a SNP if the following criteria are met: coverage ≥ 10, frequency of minor allele ≥ 0.2, read support for minor allele ≥ 3, number of alleles = 2. It requires that each allele be supported by forward- and reverse-aligned reads, and it ignores all SNPs in indels and within seven bases of a putative splice site. If the reference genome

has been lower-case masked, it will also ignore SNPs in masked regions. This script is available on DRYAD under accession: doi:10.5061/dryad.606j6

A1.3 Meta-information

- *Sequencing center* – Illumina FastTrack Genotyping Services (San Diego, CA, USA)
- *Platform and model* – Illumina HiSeq 2000
- *Design description* – The goal of this study was to identify SNPs in the coding DNA of polar bears for future quantitative genetics analysis, using an established pedigree of more than 4,000 Western Hudson Bay bears (E. Richardson, unpublished data). Because we were interested primarily in polymorphisms in genes affecting cub fatness, growth, and maternal performance, we sampled blood and fat of five adult females and five dependent cubs. All individuals were unrelated and were captured within the management boundaries of the Western Hudson Bay subpopulation (Taylor & Lee 1995).
- Analysis type – cDNA
- *Run dates* – June 2011

A1.4 Library

- *Strategy* – Next-gen automated DNA sequencing (Illumina) of normalized cDNA
- Taxon – *Ursus maritimus*
- Sex, location, etc. – Table A1.1
- *Tissues* – Table A1.2
- *Sample handling* – All bears were located from a Bell 206B JetRanger helicopter and immobilized by remote injection of Telazol® prior to capture and handling (Stirling *et al.* 1989). Adipose tissue samples were then collected using a 6-mm biopsy punch from a superficial depot of fat on the rump, approximately 15 cm lateral to the tail (Ramsay *et al.* 1992; Thiemann *et al.* 2008b) and were placed into sterile tubes containing RNA*later*. From each individual, blood was drawn from a femoral vein into a sterile Vacutainer® and then immediately preserved in RNA*later*. All animal handling procedures were approved by Environment and Climate Change Canada's Prairie and Northern Region Animal Care Committee and all research was conducted under wildlife research permits issued by the Province of Manitoba and by Parks Canada Agency.

- *Selection* – Total RNA was duplex-specific thermostable nuclease (DSN) normalized according to a proprietary Illumina protocol (available at: http://tinyurl.com/illuminadsn; last accessed April 11, 2013).
- *Layout* – paired (2×100 nt reads); insert size = 280 nt, SD = 73 nt
- *Library construction protocol* – Each of our four libraries was constructed from the pooled (non-barcoded) DSN-normalized total RNA of five individuals, using the Illumina TruSeq Total RNA Sample Preparation Kit, according to the manufacturer's recommended protocol. Base calling was performed via the Illumina CASAVA 1.7 pipeline.

A1.5 Processing

- *Pipeline*: Because a high-quality draft version of the polar bear genome is available online (Li *et al.* 2011) for sequence alignment, all reads that passed Illumina's proprietary chastity filter were retained for subsequent analyses without additional data-quality filtering.

To assemble the transcriptome, we used the BOWTIE 0.12.7–TOPHAT 1.3.2–CUFFLINKS 1.1.0 suite (Langmead *et al.* 2009; Trapnell *et al.* 2009; Trapnell *et al.* 2010). For each of our four libraries, we first splice-aligned the sequencing reads to the genome using TOPHAT. To increase sensitivity, we enabled the 'coverage search', 'closure search', 'microexon search', and 'butterfly search' options. For all other settings, default values were used. We then ran CUFFLINKS (with default values) on the outputted .bam file to convert the read alignments into .gtf gene annotations of the genome. To produce the final transcripts, we used CUFFLINKS' CUFFMERGE utility to merge the .gtf files produced for each tissue type into a single annotation and its gffread utility to convert the annotation to a FASTA file.

To determine the identity of each transcript, we performed a BLAST (Altschul *et al.* 1997) search (blastx 2.2.24+; max. number of hits = 20; e-value threshold = 10^{-5}; default values for other settings) against a custom database comprising all mammalian RefSeq protein sequences. Polar bear transcripts were only annotated if they were defined as "full length" (i.e., if their best BLAST hit covered ≥90% of the RefSeq sequence). Finally, we annotated each of these full-length transcripts with gene ontology information using BLAST2GO 2.5.0 (Conesa *et al.* 2005) with default values.

To detect SNPs, we used the .bam alignment files created as part of the TOPHAT alignment. We first used the MarkDuplicates feature of PICARDTOOLS 1.60 (http://picard.sourceforge.net) to remove PCR duplicates from each .bam file. We then used PICARDTOOLS' MergeSamFiles feature to merge the fat and blood assemblies by age class, giving "merged adult" and "merged cub" assemblies. We used a custom Perl script (*getsnpsfrompileup.pl*; described above) to call SNPs within each of these merged assemblies and then merged the resultant SNP lists. Finally, to remove putative SNPs that may have been caused by systematic Illumina error, we used the program SYSCALL (Meacham *et al.* 2011) under its default settings to retain SNPs only if their posterior probability of being truly variant was greater than 0.95.

- *Runs*: Four runs were uploaded to NCBI's Sequence Read Archive in FASTQ format and were converted to SRA format by NCBI. Runs are accessible from BioProject PRJNA193538 under the accessions provided in Table A1.2.

A1.6 Results

- Alignment statistics – Table A1.3
- Quality scoring system – phred+64
- Quality scoring ASCII character range – "@" to "h"

Table A1.1. Sample descriptions.

Sample	Age class	Sex	Latitude	Longitude	Collection date
X10676	Adult	Female	58.06	–92.84	2009-09-10
X11005	Adult	Female	58.25	–93.10	2009-09-09
X11226	Adult	Female	58.12	–93.73	2009-09-08
X12208	Adult	Female	58.4	–93.90	2009-09-13
X19187	Adult	Female	58.37	–93.26	2009-09-09
X33053	Cub (COY*)	Male	58.04	–93.14	2009-09-10
X33055	Cub (COY)	Female	57.77	–93.34	2009-09-10
X33062	Cub (COY)	Male	58.36	–93.70	2009-09-08
X33065	Cub (Yearling)	Female	58.53	–93.39	2009-09-09
X33300	Cub (Yearling)	Female	58.31	–92.99	2009-09-11

*COY = cub of the year.

Table A1.2. NCBI Sequencing Read Archive (SRA) accessions for raw Illumina reads (*.fastq) and duplicate-pruned alignments to the polar bear genome (*.bam).

Age class	Tissue	SRA experiment accession	SRA reads accession	SRA alignment accession
Adult	Blood	SRX254432	SRR791842	SRR950076
Adult	Fat	SRX254508	SRR792293	SRR950077
Cub	Blood	SRX254512	SRR792903	SRR950074
Cub	Fat	SRX254514	SRR796171	SRR950075

Table A1.3. Alignment statistics.

Pool	Total number of reads	Number of reads aligned at full length	Number of spliced reads realigned (bases 1–25)	Number of spliced reads realigned (bases 26–50)	Number of spliced reads realigned (bases 51–75)	Number of spliced reads realigned (bases 76–100)
Adult blood	384,468,909	231,559,440	85,592,650	86,289,467	86,192,677	82,788,589
Adult fat	392,856,243	236,984,736	99,792,791	100,670,928	99,796,252	95,018,628
Cub blood	382,867,555	206,802,992	88,664,725	88,795,661	88,405,732	83,389,541
Cub fat	386,017,300	233,669,983	97,661,164	98,401,309	97,912,104	93,450,221

Appendix 2: Supplementary material for "Circumpolar genetic structure and recent gene flow of polar bears: a reanalysis"

Table A2.1. Individuals retained for all main analyses in this paper (except for BAYESASS estimates of migration rates). For a few individuals, there were discrepancies in the subpopulation designations between the list provided in Table S11 of Peacock *et al.*, 2015 and the listed provided in the microsatellite dataset on Dryad (doi:10.5061/dryad.v2j1r). These were assumed to represent individuals who were sampled multiple times across population boundaries (i.e., temporary or permanent migrants) or individuals whose subpopulation designations were changed according to Supporting Information S1 of Peacock *et al.*, 2015. Where these discrepancies existed, we have used the populations of origin from the microsatellite dataset. These are indicated by the first two characters in each individual ID, and correspond to the abbreviations in Table 2.1.

ID	ID	ID	ID	ID	ID	ID	ID	ID
BB14216	BS7922	DS18893	FB28223	KB13558	LS13690	NB10461	SB20424	VM13057
BB14411	BS7926	DS30620	FB28234	KB13560	LS13713	NB10468	SB20457	VM13061
BB14436	BS7935	DS30814	FB28249	KB13561	LS14154	NB10744	SB20580	VM13067
BB14459	BS7997	DS35017	FB28252	KB13564	LS14166	NB12020	SB20668	VM13130
BB14801	BS98398	DS35208	FB28253	KB13720	LS14175	NB12021	SB20735	VM13133
BB18293	CS121	DS35235	FB28254	KB13792	LS14178	NB12026	SB20764	VM13137
BB18299	CS138	DS35237	FB28258	KB13795	LS14334	NB12027	SB20886	VM13140
BB18305	CS139	DS35514	FB28261	KB13796	LS14503	NB12030	SB20987	VM13141
BB18327	CS20688	DS35711	FB28266	KB14488	LS25670	NB12031	SB20988	VM13144
BB18333	CS21058	DS35774	FB28270	KB14581	LS28036	NB12034	SB20990	VM13148
BB18348	CS21098	EG14416	FB28276	KB14582	LS28041	NB12035	SB21002	VM13151
BB23848	CS21106	EG14417	FB30602	KB14583	LS28056	NB12036	SB21219	VM13154
BB23864	CS21120	EG14418	FB30606	KB14591	LS28073	NB12038	SB21221	VM13155
BB23870	CS21137	EG14419	FB35163	KB14592	LS28078	NB12041	SB2525	VM13158
BB23871	CS21160	EG14420	FB35800	KB14607	LS28079	NB12042	SB32260	VM13242
BB23872	CS21170	EG14421	GB13674	KB14616	LS28086	NW04142	SB32267	VM13245
BB23875	CS21182	EG14422	GB13675	KB14617	LS28111	NW13340	SB6020	VM13249
BB35026	CS21183	EG14423	GB13678	KB14626	LS28112	NW13344	SB6098	VM13251
BB35076	CS21491	EG14425	GB14261	KB14627	LS28115	NW13345	SB6538	VM13252
BB35079	CS21494	EG14426	GB14262	KB15269	LS28117	NW13351	SB6545	VM13255
BB35082	CS21496	EG14427	GB14364	KS20035	LS28120	NW13502	SH16834	VM13257
BB35092	CS21497	EG14428	GB18125	KS20036	LS28121	NW13700	SH16866	VM13259
BB35098	CS21503	EG14429	GB19235	KS20037	LS28122	NW13701	SH16868	VM13272
BB35641	CS21508	EG14430	GB20821	KS20038	LS28124	NW13704	SH16888	VM13274
BB35646	CS21512	EG14431	GB20864	KS20043	LS28125	NW13716	SH16912	VM13276
BB35649	CS21521	EG14432	GB20866	KS20050	LS29150	NW13719	SH16914	WH00563
BB35652	CS57	EG7119	GB21562	KS20051	MC13465	NW14024	SH16916	WH04151
BB35664	CS6575	EG7120	GB21567	KS20052	MC13466	NW14029	SH16918	WH04198
BB35739	CS6738	EG7121	GB21615	KS20056	MC13666	NW14515	SH16920	WH05990
BB35745	CS6865	EG7123	GB21617	KS20057	MC13668	NW14516	SH16925	WH10565
BS23016	CS6875	EG7124	GB27786	KS20060	MC14975	NW14517	SH16940	WH10575
BS23060	CS6881	EG7125	GB27875	KS20061	MC14976	NW14519	SH16983	WH10602
BS23174	CS6950	EG7127	GB27882	KS7980	MC14977	NW14521	SH16987	WH10614
BS23177	CS6974	EG7128	GB27923	KS7982	MC14978	NW14522	SH30576	WH10631
BS23294	CS6980	EG7129	GB27924	KS7984	MC14979	NW14523	SH30889	WH10650
BS23357	DS18043	EG7131	GB27926	KS7986	MC21393	NW14524	SH30936	WH10651
BS23441	DS18069	EG7132	GB27927	KS7988	MC21396	NW14529	SH37004	WH11134
BS23460	DS18141	EG7133	GB27963	LP105	MC21551	NW14530	SH37009	WH11138
BS23479	DS18256	EG7351	GB27964	LP129	MC21927	NW14536	SH37010	WH11345
BS23497	DS18279	EG7352	GB27966	LP130	MC21928	NW14537	SH37012	WH12380
BS23513	DS18292	FB17541	GB27976	LP132	NB02573	NW14540	SH37013	WH17447
BS23538	DS18320	FB17545	GB28023	LP145	NB03541	NW14613	SH37014	WH19210
BS23616	DS18366	FB18528	GB28024	LP20044	NB09876	NW15285	SH37015	WH19962
BS23625	DS18395	FB18529	GB28297	LP20045	NB10000	NW15287	SH37016	WH25818
BS23683	DS18407	FB18839	GB28733	LP20046	NB10025	NW15299	SH37018	WH25859
BS23703	DS18451	FB18978	KB13167	LP20047	NB10046	SB06488	SH37022	WH27803
BS23707	DS18475	FB18987	KB13168	LP6985	NB10050	SB06835	SH37023	WH27859
BS23744	DS18624	FB18990	KB13175	LP6989	NB10051	SB09823	SH37037	WH27863
BS23750	DS18641	FB18997	KB13329	LP6990	NB10168	SB09837	SH37046	WH27865
BS23760	DS18648	FB22062	KB13335	LP6993	NB10299	SB09958	SH37047	WH27871
BS23822	DS18656	FB22068	KB13336	LP6994	NB10300	SB09970	VM02807	WH27872
BS23845	DS18783	FB22069	KB13337	LS03888	NB10303	SB10413	VM08677	WH27873
BS7815	DS18811	FB28209	KB13554	LS08543	NB10307	SB20184	VM08919	WH28093
BS7837	DS18852	FB28213	KB13556	LS13687	NB10448	SB20206	VM08958	WH28097
BS7914	DS18878	FB28222	KB13557	LS13688	NB10460	SB20334	VM13052	WH28098

Table A2.2. Significance of pairwise genic differentiation (below diagonal) and genotypic differentiation (above diagonal) as calculated for nuclear microsatellites in GENEPOP. Significant values after a Holm correction for the number of tests are indicated with "+", non-significant tests are indicated with a "-". For a description of boxes and shading, see the main manuscript. Values for the Laptev Sea are not shown as this MU was significantly out of Hardy–Weinberg equilibrium.

	SH	WH	FB	DS	BB	KB	LS	GB	MC	VM	NW	NB	SB	CS	LP	KS	BS	EG
SH		-	+	+	+	+	+	+	+	+	+	+	+	+		+	+	+
WH	-		-	+	+	+	+	+	+	+	+	+	+	+		+	+	+
FB	+	-		-	+	+	+	+	+	+	+	+	+	+		+	+	+
DS	+	+	-		-	+	+	+	+	+	+	+	+	+		+	+	+
BB	+	+	+	-		-	+	+	+	+	+	+	+	+		+	+	+
KB	+	+	+	+	-		+	+	+	+	+	+	+	+		+	+	+
LS	+	+	+	+	+	+		-	-	-	+	+	+	+		+	+	+
GB	+	+	+	+	+	+	-		+	+	+	+	+	+		+	+	+
MC	+	+	+	+	+	+	-	+		-	+	+	+	+		+	+	+
VM	+	+	+	+	+	+	-	+	-		+	+	+	+		+	+	+
NW	+	+	+	+	+	+	+	+	+	+		+	+	+		+	+	+
NB	+	+	+	+	+	+	+	+	+	+	+		-	-		-	+	+
SB	+	+	+	+	+	+	+	+	+	+	+	-		-		-	+	+
CS	+	+	+	+	+	+	+	+	+	+	+	-	-			-	+	+
LP																		
KS	+	+	+	+	+	+	+	+	+	+	+	-	+	+			-	-
BS	+	+	+	+	+	+	+	+	+	+	+	+	+	+		-		-
EG	+	+	+	+	+	+	+	+	+	+	+	+	+	+		-	-	

Table A2.3. Significance of exact test of population differentiation (below diagonal) and pairwise F_{ST} (above diagonal) as calculated for mitochondrial DNA haplotypes in ARLEQUIN. Significant values after a Holm correction for the number of tests are indicated with "+", non-significant tests are indicated with a "-". For a description of boxes and shading, see the main manuscript. Values for the Laptev Sea are not shown as this MU was significantly out of Hardy–Weinberg equilibrium. Values for M'Clintock Channel, Norwegian Bay, and Viscount Melville are not shown because sample sizes were inadequate to estimate haplotype frequencies (i.e., N≤3). All other rows/columns missing data were not genotyped for mitochondrial DNA.

	SH	**WH**	**FB**	**DS**	**BB**	**KB**	**LS**	**GB**	**MC**	**VM**	**NW**	**NB**	**SB**	**CS**	**LP**	**KS**	**BS**	**EG**
SH		+	-	+	+		+	-					+	+		+	+	
WH	+		+	+	+		+	+					+	+		+	+	
FB	-	+		-	-		+	-					+	+		+	+	
DS	+	+	-		+		+	-					+	+		+	+	
BB	+	+	+	+			-	-					+	+		+	+	
KB																		
LS	+	+	+	+	-			-					+	+		+	+	
GB	-	+	-	-	-		-						+	+		+	+	
MC																		
VM																		
NW																		
NB																		
SB	+	+	+	+	+		+	+						+		-	+	
CS	-	+	+	+	+		+	-					+			+	+	
LP																		
KS	+	+	+	+	+		+	+					-	-			-	
BS	+	+	+	+	+		+	+					+	+		-		
EG																		

Table A2.4. Sampling scheme used for BAYESASS analyses. We attempted to obtain 150 samples per cluster (min. 100) such that each management unit (MU) was proportionally represented according to its population size. Population sizes are estimated with broad confidence intervals, and many estimated population sizes (indicated with question marks below) are rough guesses that have not been accepted by the IUCN Polar Bear Specialist Group. Individuals were selected blindly (i.e., without viewing their cluster membership) while trying to obtain geographically representative sampling within each MU. We note that although Foxe Basin makes up approximately 50% of the Hudson cluster, sampling in the northern part of this MU (i.e., Foxe Basin *sensu stricto*) is poor in the original dataset. Therefore, we used additional samples from the Hudson Strait portion of this MU in their place. Polar bears from Hudson Strait appear to be genetically similar to northern Foxe Basin (and southern Davis Strait) (Viengkone 2015).

		3 out of 4 clusters					**4 out of 5 clusters (PC2015)**					**5 out of 6 clusters**				
MU	**Population size**	**Cluster**	**Proportion of cluster**	**Samples to use**	**Actually used**	**Mean YoC**	**Cluster**	**Proportion of cluster**	**Samples to use**	**Actually used**	**Mean YoC**	**Cluster**	**Proportion of cluster**	**Samples to use**	**Actually used**	**Mean YoC**
WH	1030 (IUCN/SSC Polar Bear Specialist Group 2015)	Hudson	0.20	30	30	1996	Hudson	0.20	30	30	1996	Hudson	0.20	30	30	1996
SH	951 (IUCN/SSC Polar Bear Specialist Group 2015)	Hudson	0.19	28	28	2008	Hudson	0.19	28	28	2008	Hudson	0.19	28	28	2008
FB	2580 (IUCN/SSC Polar Bear Specialist Group 2015)	Hudson	0.50	76	76	1999	Hudson	0.50	76	76	1999	Hudson	0.50	76	76	1999
sDS	557 (Peacock *et al.* 2013)	Hudson	0.11	16	16	2004	Hudson	0.11	16	16	2004	Hudson	0.11	16	16	2004
nDS	1602 (Peacock *et al.* 2013)	Archipelago	0.20	30	30	2007	Archipelago	0.20	30	30	2007	E. Archipelago	0.48	73	73	2005
BB	1546 (IUCN/SSC Polar Bear Specialist Group 2015)	Archipelago	0.20	29	29	1998	Archipelago	0.20	29	29	1998	E. Archipelago	0.47	70	70	2000
KB	164 (IUCN/SSC Polar Bear Specialist Group 2015)	Archipelago	0.02	3	3	1995	Archipelago	0.02	3	3	1995	E. Archipelago	0.05	7	7	1994
LS	2541 (IUCN/SSC Polar Bear Specialist Group 2015)	Archipelago	0.32	48	48	2001	Archipelago	0.32	48	48	2001	W. Archipelago	0.56	83	65	2001
MC	284 (IUCN/SSC Polar Bear Specialist Group 2015)	Archipelago	0.04	5	5	1996	Archipelago	0.04	5	5	1996	W. Archipelago	0.06	9	7	1996
GB	1592 (IUCN/SSC Polar Bear Specialist Group 2015)	Archipelago	0.20	30	30	2000	Archipelago	0.20	30	30	2000	W. Archipelago	0.35	52	37	2000
VM	161 (IUCN/SSC Polar Bear Specialist Group 2015)	Archipelago	0.02	3	3	1992	Archipelago	0.02	3	3	1992	W. Archipelago	0.04	5	4	1992
NB	980 (IUCN/SSC Polar Bear Specialist Group 2015)	Basin	0.06	10	10	1989	W. Basin	0.17	25	25	1989	W. Basin	0.17	25	25	1989
SB	907 (IUCN/SSC Polar Bear Specialist Group 2015)	Basin	0.06	9	9	1994	W. Basin	0.15	23	23	1996	W. Basin	0.15	23	23	1996
CS	3500? (IUCN/SSC Polar Bear Specialist Group 2015; Paetkau *et al.* 1999)	Basin	0.23	34	34	1991	W. Basin	0.59	89	89	1990	W. Basin	0.59	89	89	1990
wLP	500? (IUCN/SSC Polar Bear Specialist Group 2015; Paetkau *et al.* 1999)	Basin	0.03	5	5	2004	W. Basin	0.08	13	9	2001	W. Basin	0.08	13	9	2001
eLP	500? (IUCN/SSC Polar Bear Specialist Group 2015; Paetkau *et al.* 1999)	Basin	0.03	5	5	1994	E. Basin	0.05	8	4	1994	E. Basin	0.05	8	4	1994
KS	3200? (Matishov *et al.* 2014)	Basin	0.21	32	17	1994	E. Basin	0.34	51	17	1994	E. Basin	0.34	51	17	1994
BS	2644 (IUCN/SSC Polar Bear Specialist Group 2015)	Basin	0.17	26	26	2001	E. Basin	0.28	42	49	2001	E. Basin	0.28	42	49	2001
EG	3000? (Paetkau *et al.* 1999)	Basin	0.20	30	30	1990	E. Basin	0.32	48	30	1990	E. Basin	0.32	48	30	1990
	Missing data	**14-locus dataset: 0%; 21-locus dataset: 11.8%**					**14-locus dataset: 0.03%; 21-locus dataset: 11.4%**					**14-locus dataset: 0.02%; 21-locus dataset: 11.7%**				

Table A2.5. Proportions of migrant and non-migrant ancestry from BAYESASS for K=4 (minus Norwegian Bay). Each cell indicates the per-generation fraction of individuals from the population named in that *row* who are migrants from the population named in that *column*. Diagonals indicate the proportion of non-migrants. Numbers in parentheses indicate standard errors. Settings used to obtain good mixing (i.e., acceptance ratios of 0.2–0.6) were: Δ_A=0.15, Δ_M=0.1, Δ_F=0.2.

	Archipelago	**Polar Basin**	**Hudson Complex**
Archipelago	0.9394 (0.0190)	0.0114 (0.0096)	0.0492 (0.0164)
Polar Basin	0.0184 (0.0128)	0.9744 (0.0134)	0.0072 (0.0055)
Hudson Complex	0.0211 (0.0102)	0.0088 (0.0060)	0.9701 (0.0113)

Table A2.6. Proportions of migrant and non-migrant ancestry from BAYESASS for K=5 (minus Norwegian Bay). This population grouping corresponds roughly to the four-population grouping presented in PC2015, with the exception that Norwegian Bay has been removed from the Archipelago, and the Eastern/Western Polar Basin have been split at the large sampling discontinuity in the Laptev Sea. Each cell indicates the per-generation fraction of individuals from the population named in that *row* who are migrants from the population named in that *column*. Diagonals indicate the proportion of non-migrants. Numbers in parentheses indicate standard errors. Settings used to obtain good mixing (i.e., acceptance ratios of 0.2–0.6) were: Δ_A=0.15, Δ_M=0.1, Δ_F=0.25

	Archipelago	**Eastern Basin**	**Hudson Complex**	**Western Basin**
Archipelago	0.9350 (0.0183)	0.0046 (0.0043)	0.0500 (0.0161)	0.0104 (0.0082)
Eastern Basin	0.0095 (0.0083)	0.6734 (0.0074)	0.0048 (0.0045)	0.3123 (0.0123)
Hudson Complex	0.0207 (0.0101)	0.0040 (0.0038)	0.9673 (0.0113)	0.0080 (0.0056)
Western Basin	0.0064 (0.0056)	0.0055 (0.0049)	0.0027 (0.0026)	0.9855 (0.0077)

Table A2.7. Proportions of migrant and non-migrant ancestry from BAYESASS for K=6 (minus Norwegian Bay). Each cell indicates the per-generation fraction of individuals from the population named in that *row* who are migrants from the population named in that *column*. Diagonals indicate the proportion of non-migrants. Numbers in parentheses indicate standard errors. Settings used to obtain good mixing (i.e., acceptance ratios of 0.2–0.6) were: Δ_A=0.2, Δ_M=0.1, Δ_F=0.25.

	Eastern Archipelago	Eastern Basin	Hudson Complex	Western Archipelago	Western Basin
Eastern Archipelago	0.6770 (0.0100)	0.0032 (0.0031)	0.0568 (0.0199)	0.2581 (0.00216)	0.0049 (0.0042)
Eastern Basin	0.0047 (0.0046)	0.6738 (0.0081)	0.0050 (0.0047)	0.0102 (0.0087)	0.3063 (0.0136)
Hudson Complex	0.0281 (0.0131)	0.0037 (0.0035)	0.9529 (0.0145)	0.0081 (0.0063)	0.0071 (0.0050)
Western Archipelago	0.0106 (0.0081)	0.0054 (0.0051)	0.0134 (0.0095)	0.9554 (0.0156)	0.0153 (0.0102)
Western Basin	0.0038 (0.0035)	0.0052 (0.0047)	0.0027 (0.0027)	0.0055 (0.0050)	0.9829 (0.0079)

Table A2.8. Proportions of migrant and non-migrant ancestry from BAYESASS for K=5 (minus Norwegian Bay) with the additional removal of all samples from the Laptev Sea. Each cell indicates the per-generation fraction of individuals from the population named in that *row* who are migrants from the population named in that *column*. Diagonals indicate the proportion of non-migrants. Numbers in parentheses indicate standard errors. Settings used to obtain good mixing (i.e., acceptance ratios of 0.2–0.6) were: Δ_A=0.15, Δ_M=0.1, Δ_F=0.25.

	Archipelago	Eastern Basin	Hudson Complex	Western Basin
Archipelago	0.9354 (0.0189)	0.0048 (0.0045)	0.0496 (0.0165)	0.0102 (0.0082)
Eastern Basin	0.0102 (0.0088)	0.6726 (0.0062)	0.0056 (0.0053)	0.3117 (0.0119)
Hudson Complex	0.0207 (0.0102)	0.0039 (0.0037)	0.9672 (0.0116)	0.0082 (0.0057)
Western Basin	0.0073 (0.0062)	0.0054 (0.0048)	0.0029 (0.0029)	0.9845 (0.0082)

Table A2.9. Pairwise F_{ST} values for nuclear microsatellites recalculated in ARLEQUIN using the complete dataset from PC2015. Values above the diagonal were calculated using a missing data cutoff of 0.05, which resulted in the exclusion of the same seven loci described in the main manuscript. Values below the diagonal were calculated using a missing data cutoff of 1 (i.e., including all 21 loci), which results in many highly negative F_{ST} values. Values below the diagonal are identical to those presented in Table S5 of PC2015, except that they are shifted up by one. For instance, in PC2015, –0.113 corresponds to the F_{ST} for BB and CS, rather than for BB and BS. This suggests that—in addition to miscalculation of F_{ST} caused by large amounts of missing data—the F_{ST} values in PC2015 are also incorrect due to copy–paste error.

	BB	**BS**	**CS**	**DS**	**EG**	**FB**	**GB**	**KB**	**KS**	**LP**	**LS**	**MC**	**NB**	**NW**	**SB**	**SH**	**VM**	**WH**
BB		0.031	0.042	0.007	0.028	0.019	0.017	0.004	0.031	0.045	0.009	0.015	0.033	0.031	0.039	0.036	0.026	0.043
BS	–0.113		0.017	0.039	0.004	0.056	0.047	0.034	0.002	0.017	0.037	0.027	0.016	0.057	0.017	0.083	0.036	0.076
CS	0.018	–0.177		0.052	0.022	0.072	0.051	0.052	0.009	0.006	0.046	0.033	0.004	0.068	0.004	0.099	0.043	0.092
DS	0.004	–0.113	0.027		0.039	0.005	0.025	0.019	0.038	0.058	0.020	0.026	0.042	0.040	0.046	0.023	0.034	0.025
EG	–0.058	–0.126	–0.124	–0.075		0.055	0.045	0.027	0.008	0.018	0.031	0.026	0.016	0.053	0.021	0.086	0.039	0.081
FB	0.017	–0.080	0.041	0.001	–0.023		0.034	0.030	0.054	0.079	0.030	0.039	0.059	0.049	0.062	0.011	0.045	0.010
GB	–0.013	–0.064	–0.004	–0.022	0.020	0.008		0.024	0.050	0.057	0.012	0.013	0.039	0.046	0.046	0.044	0.026	0.051
KB	–0.086	–0.073	–0.087	–0.101	0.030	–0.054	0.003		0.038	0.056	0.008	0.014	0.035	0.026	0.047	0.050	0.023	0.052
KS	0.010	–0.263	0.008	0.014	–0.161	0.027	–0.005	–0.112		0.012	0.037	0.022	0.010	0.065	0.009	0.083	0.032	0.075
LP	0.030	–0.190	0.003	0.038	–0.107	0.059	0.016	–0.055	0.004		0.056	0.050	0.019	0.079	0.010	0.112	0.059	0.101
LS	–0.010	–0.081	0.020	–0.012	–0.014	0.012	0.011	–0.039	0.017	0.042		–0.001	0.030	0.026	0.043	0.049	0.010	0.049
MC	–0.077	–0.078	–0.106	–0.098	0.029	–0.049	–0.007	0.012	–0.130	–0.065	–0.050		0.025	0.043	0.033	0.061	0.010	0.057
NB	–0.054	–0.111	–0.142	–0.072	0.014	–0.020	0.015	0.038	–0.157	–0.107	–0.016	0.028		0.050	0.005	0.086	0.026	0.080
NW	–0.060	–0.042	–0.071	–0.081	0.055	–0.036	0.024	0.023	–0.086	–0.032	–0.024	0.038	0.051		0.062	0.067	0.036	0.066
SB	0.045	–0.135	–0.025	0.049	–0.064	0.066	0.013	–0.034	–0.021	–0.005	0.026	–0.048	–0.080	–0.020		0.086	0.038	0.079
SH	0.000	–0.146	0.087	–0.008	–0.081	–0.028	–0.018	–0.119	0.070	0.082	0.013	–0.113	–0.082	–0.105	0.056		0.064	0.009
VM	–0.063	–0.077	–0.100	–0.083	0.038	–0.037	0.004	0.025	–0.130	–0.062	–0.037	0.011	0.026	0.035	–0.047	–0.108		0.059
WH	0.018	–0.027	0.051	–0.013	0.052	–0.010	0.053	0.021	0.042	0.076	0.050	0.021	0.049	0.035	0.061	–0.042	0.028	

Table A2.10. Examples of locus-by-locus AMOVAs calculated in ARLEQUIN using a 5% missing data cutoff for 21 microsatellites. Significance was determined using 1000 permutations. Note that many potential population groupings such as the ones below were discounted in PC2015 because of apparently incorrectly calculated AMOVAs, which often included negative percentage variance explained for F_{SC}. We were unable to replicate these results; rather, all *F*-values are highly significant.

Hypothesis	Source of variation	% variance	*F*-statistic	*F*-value	*P*-value
Proposed Canadian Conservation Units (Hypothesis D of PC2015, Table S7)	Within individuals	96.04%	F_{IT}	0.040	0
	Among individuals in MUs	0.84%	F_{IS}	0.009	0.001
	Among MUs in clusters	1.18%	F_{SC}	0.012	0
	Among clusters	1.95%	F_{CT}	0.019	0
Proposed Canadian Conservation Units (including a separate cluster for Norwegian Bay)	Within individuals	95.96%	F_{IT}	0.040	0
	Among individuals in MUs	0.86%	F_{IS}	0.009	0.002
	Among MUs in clusters	1.18%	F_{SC}	0.012	0
	Among clusters	2.00%	F_{CT}	0.020	0

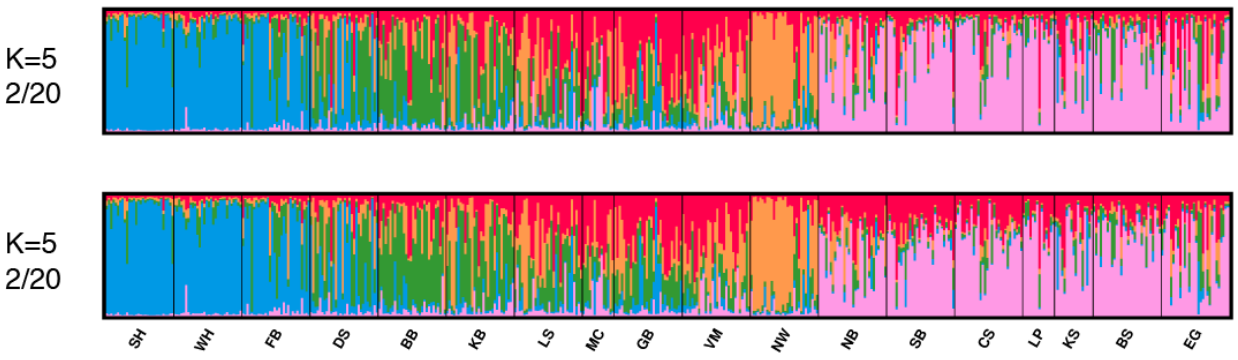

Figure A2.1. CLUMPAK-averaged minority modes for K=5. The majority mode is shown in Figure 2.2.

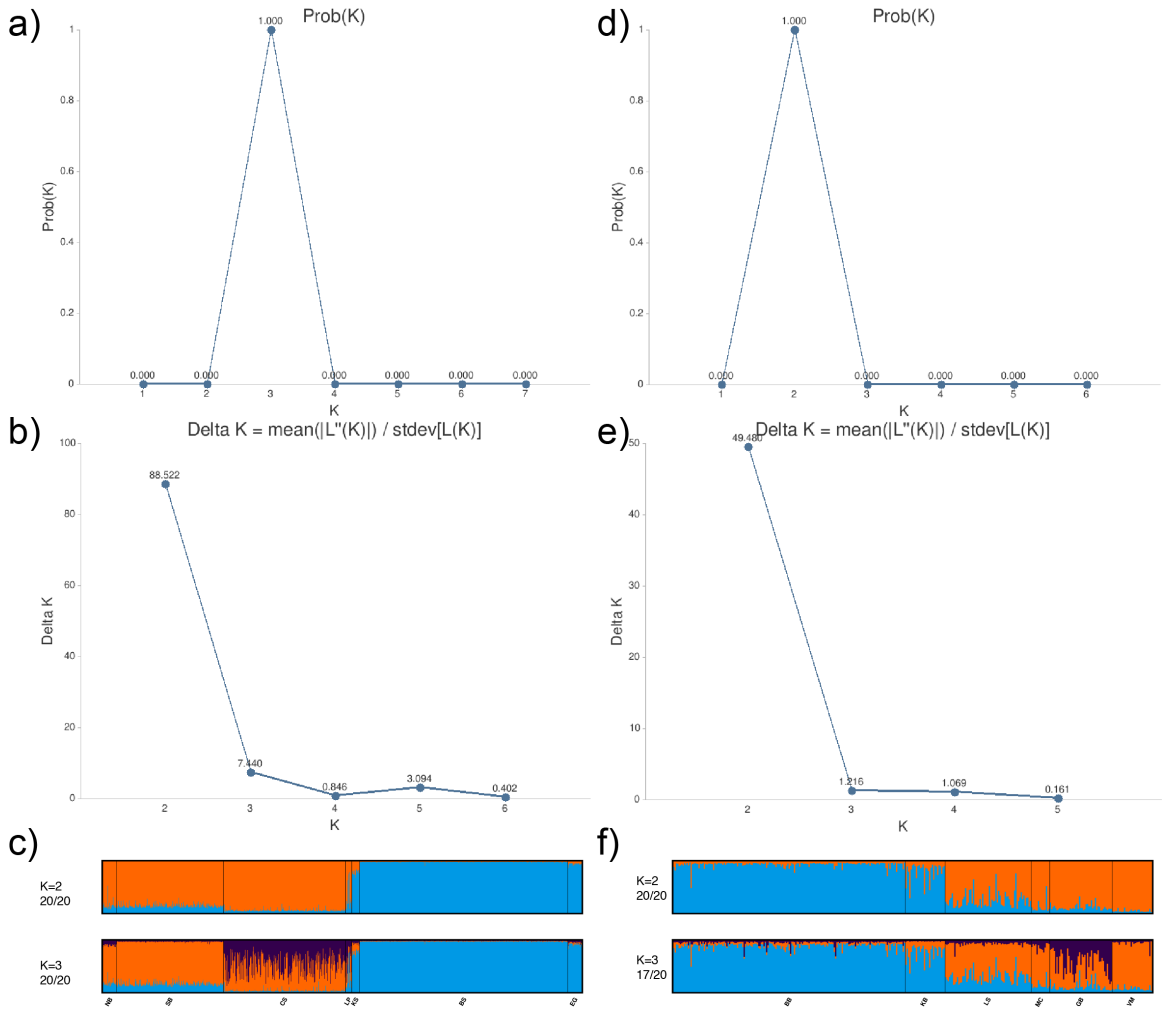

Figure A2.2. CLUMPAK output for STRUCTURE runs using LOCPRIOR=1 for the complete set of samples from: a–c) the Polar Basin cluster, and d–f) the Canadian Arctic Archipelago. a) and d) show the preferred number of clusters using the Pritchard method; b) and e) show the preferred number of clusters according to the Evanno method; c) and f) show the majority modes for the preferred number of clusters. Both show east–west differentiation in the preferred number of clusters. In f), the results for K=3 are also plotted (though they are not preferred by either method), as they show potential differentiation of the Gulf of Boothia from the neighbouring M'Clintock Channel management unit, as has previously been reported (Campagna *et al.* 2013). Note that Davis Strait samples have been excluded from the run for the Canadian Arctic Archipelago, because of their sheer number and because Davis Strait represents an admixture zone between the Archipelago and the Hudson Complex.

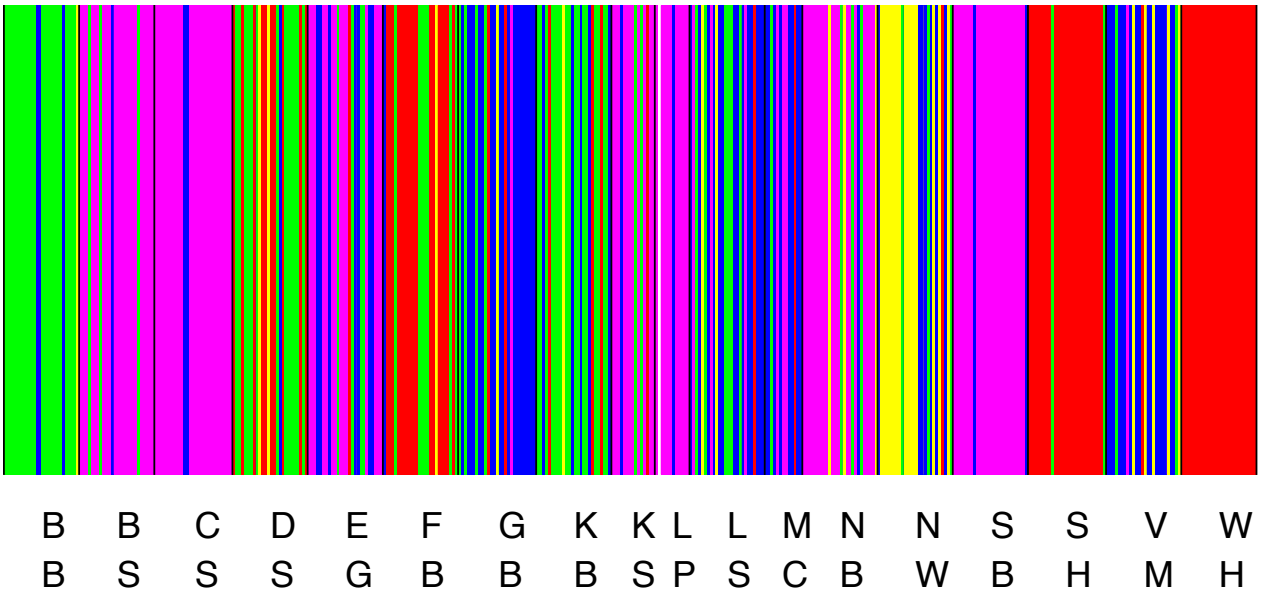

Figure A2.3. Admixture plot produced by BAPS for *K*=6. A single individual in LP with four missing loci (displayed here in white) was placed in its own genetic cluster during mixture clustering and was removed prior to admixture analysis, leaving five major genetic clusters. Management unit abbreviations are as in Table 2.1.

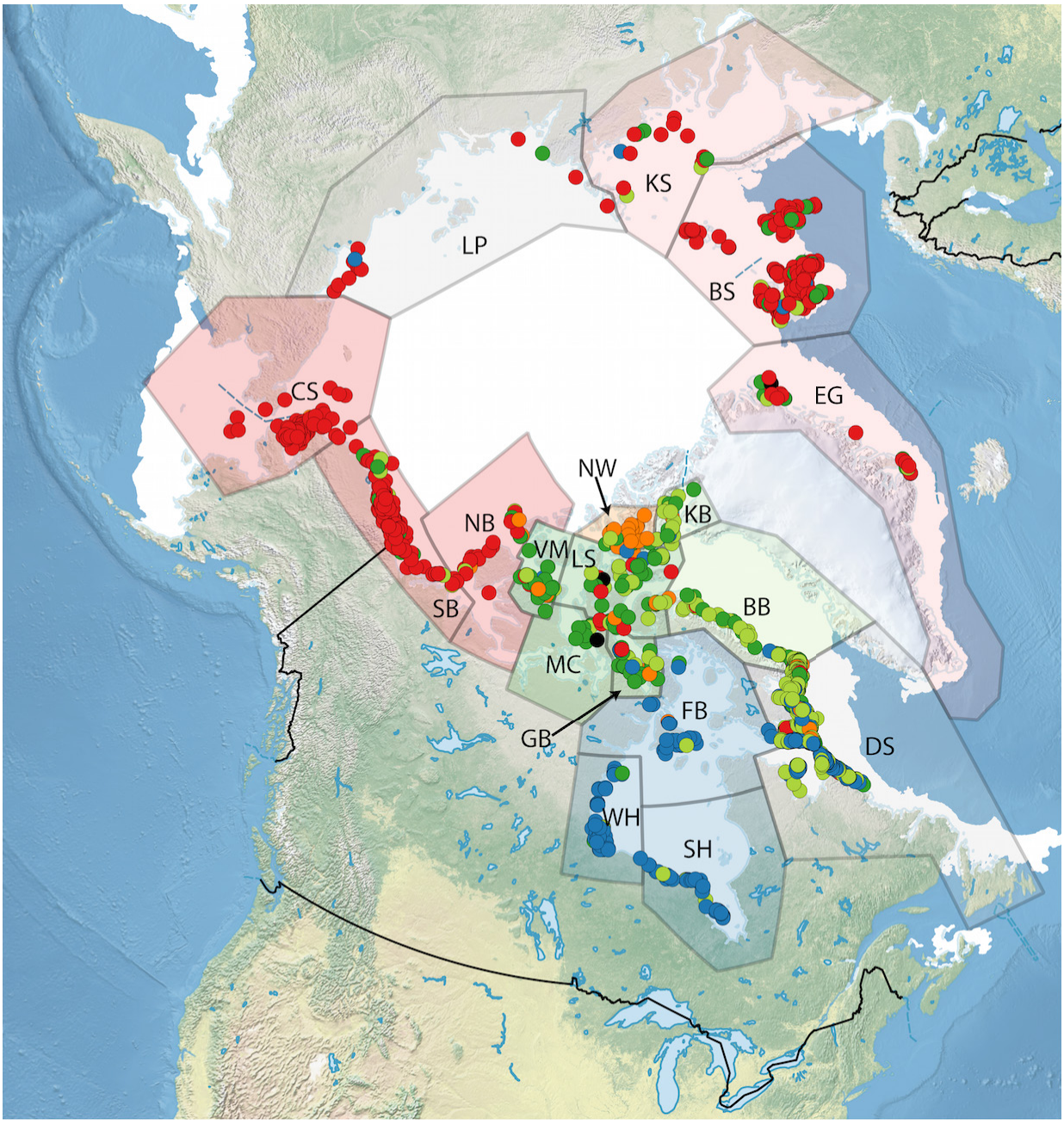

Figure A2.4. Genetic cluster memberships for all individuals with microsatellite genotypes included in the original study of Peacock *et al.*, 2015. Individuals in Figure A2.2 who were "highly assigned" (i.e., posterior probability of non-admixture > 0.05) to one of the five major clusters identified by BAPS were retained as a training set with which to cluster all other individuals. Significantly admixed individuals are shown displayed in black. Management unit abbreviations are as in Table 2.1. As in Figure 2.6, sea ice extent during the breeding season is approximated using measurements for April 15, 2008. Colours are as in Figure 2.4 of the main manuscript.

Figure A2.5. Pollock plot showing PCAs (axes: x = PC1, y = PC2) of 100 independent random subsamples of ≤30 individuals per management unit from the complete 2748-individual polar bear dataset. Only individuals who were fully genotyped for the fourteen loci listed in the main paper were included. Management units are colour-coded as in the main manuscript. In cases where four major clusters cannot clearly be distinguished, they usually become apparent by viewing the third PC (Figure A2.6).

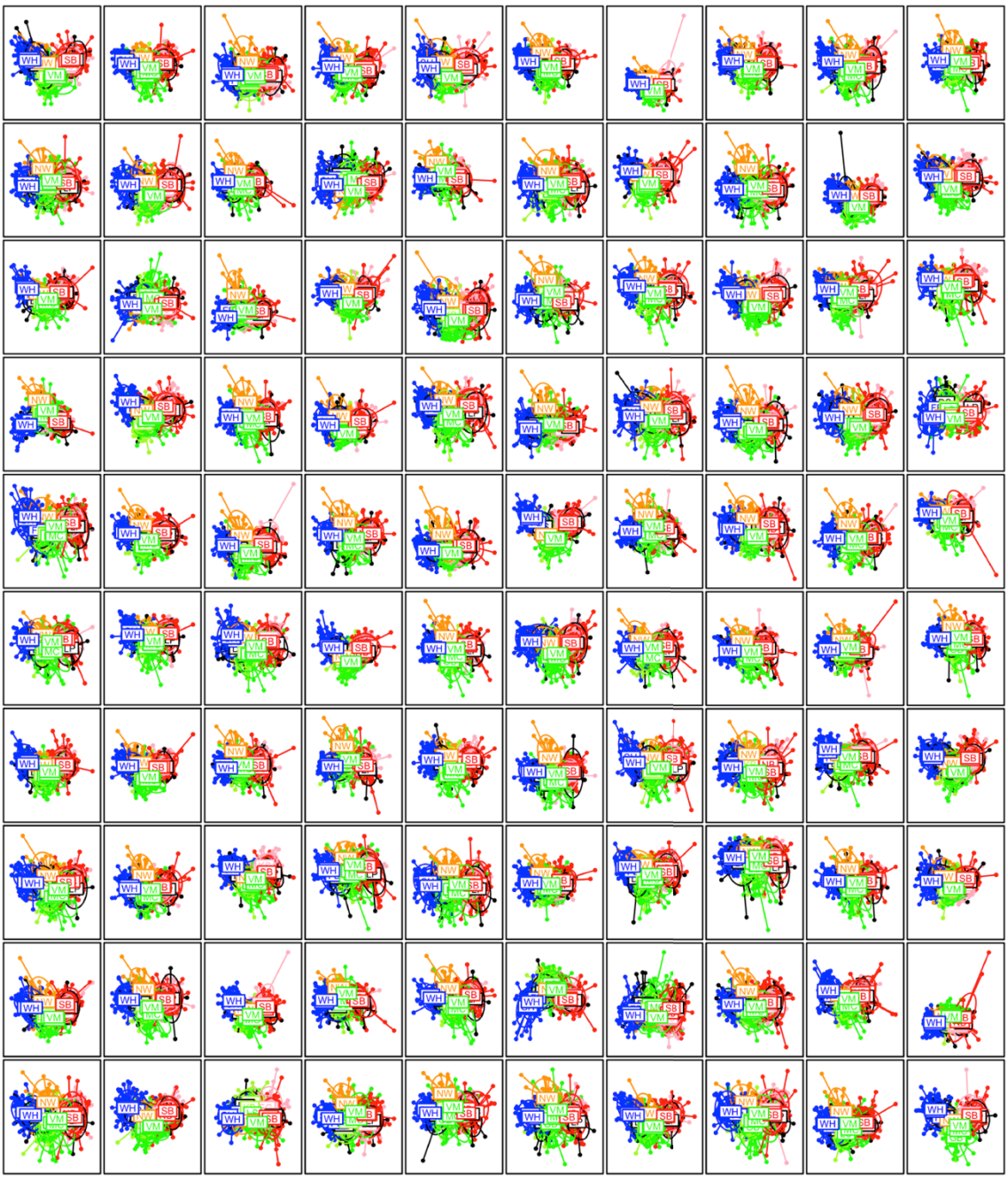

Figure A2.6. Pollock plot showing PCAs (axes: x = PC1, y = PC3) of 100 independent random subsamples of ≤30 individuals per management unit from the complete 2748-individual polar bear dataset. These are the same random subsets as used in Figure A2.5. Only individuals who were fully genotyped for the fourteen loci listed in the main paper were included. Management units are colour-coded as in the main manuscript.

Appendix 3: Supplementary material for "Design of a 9K Illumina BeadChip for polar bears (*Ursus maritimus*) from RAD and transcriptome sequencing"

Table A3.1. RAD sequencing sample information. "Chukchi Sea" was a pool of two individuals' DNA. "Russia" is a joint name for the present-day Laptev Sea and Kara Sea polar bear subpopulations, and was a pool of three individuals' DNA. Coverage-related values in columns 7 and 8 are given for the 22,978 filtered (i.e., SNP-chip-printable) RAD contigs only.

Individual	Subpopulation	Sex	Year sampled	Lane	Reads	Number of RAD clusters with 5×–500× coverage	Median depth	Per-contig coverage (mean ± SD)	Number of contigs with zero coverage
1	Baffin Bay	Female	1994	1	12,400,297	146,412	58	41.1 ± 44.3	839
2	Baffin Bay	Female	1994	1	5,976,995	126,293	32	16.4 ± 22.3	3220
3	Barents Sea	Female	1996	4	11,077,660	129,655	57	41.7 ± 50.9	1522
4–5	Chukchi Sea	N/A	1986–1994	1	11,837,700	144,331	57	39.5 ± 45.3	871
6	Davis Strait	Male	1994	2	18,651,113	157,848	76	65.3 ± 71.4	463
7	Davis Strait	Female	1991	3	6,244,268	126,057	35	22.2 ± 28.1	2500
8	Davis Strait	Male	1993	3	10,618,216	137,008	51	38.0 ± 46.0	915
9	Foxe Basin	Female	2007	1	10,697,827	140,970	51	36.0 ± 43.2	1004
10	Foxe Basin	Female	2007	1	6,005,258	127,317	26	16.4 ± 22.3	4322
11	Foxe Basin	Male	2007	1	22,152,302	163,340	82	72.8 ± 81.4	182
12	Gulf of Boothia	Male	2003	1	17,357,827	149,908	58	53.6 ± 70.7	835
13	Gulf of Boothia	Male	2003	2	9,447,019	130,202	43	33.7 ± 44.9	2495
14	Kane Basin	Male	1995	2	13,194,935	147,775	58	46.4 ± 57.1	1009
15	Kane Basin	Male	1992	2	11,488,608	141,404	53	40.8 ± 47.7	1269
16	Lancaster Sound	Male	1999	3	12,413,270	129,016	59	45.0 ± 57.2	1353
17	Lancaster Sound	Female	1996	3	31,106,709	151,301	84	111.6 ± 132.7	133
18	M'Clintock Channel	Male	1996	3	15,670,792	121,540	64	57.1 ± 78.5	2425
19	M'Clintock Channel	Male	1999	3	5,885,013	101,243	35	21.1 ± 31.3	4935
20	Northern Beaufort	Male	1987	3	24,163,746	149,046	102	87.4 ± 95.7	11
21	Northern Beaufort	Male	1986	4	17,017,030	138,979	80	65.0 ± 75.4	265
22	Northern Beaufort	Male	1986	4	6,720,002	120,369	35	25.6 ± 36.7	3218
23	Norwegian Bay	Female	1995	5	34,199,726	191,462	86	110.7 ± 119.0	29
24	Norwegian Bay	Female	1995	5	5,497,363	126,683	29	18.3 ± 23.4	3817
25–27	"Russia"	N/A	1994–1996	4	20,083,869	144,494	96	75.5 ± 82.4	100
28	Southern Beaufort	Female	2010	4	12,864,269	130,194	64	50.3 ± 61.0	945
29	Southern Beaufort	Female	2010	4	8,574,299	121,671	43	33.7 ± 43.1	2115
30	Southern Beaufort	Female	2010	4	4,632,888	85,544	29	18.9 ± 32.8	7952
31	Southern Hudson Bay	Female	2008	5	8,620,982	139,922	43	28.9 ± 32.9	1462
32	Southern Hudson Bay	Male	2009	5	10,924,093	149,692	48	35.8 ± 41.7	1018
33	Southern Hudson Bay	Female	2009	5	20,724,185	168,543	78	66.9 ± 68.8	176
34	Viscount Melville Sound	Female	1992	5	10,701,991	146,564	50	35.4 ± 40.4	965
35	Viscount Melville Sound	Female	1992	5	34,078,087	189,731	73	114.2 ± 134.0	38
36	Western Hudson Bay	Male	1991	2	13,151,433	147,591	58	46.8 ± 55.1	1074
37	Western Hudson Bay	Male	1987	2	19,466,365	158,174	79	68.7 ± 75.4	397
38	Western Hudson Bay	Male	1987	2	16,655,404	153,977	69	58.4 ± 69.4	699

Table A3.2. Gene ontology terms used for inclusion of transcriptomic SNPs.

ID	Term
GO:0007568	aging
GO:0048856	anatomical structure development
GO:0007610	behavior
GO:0005975	carbohydrate metabolic process
GO:0009758	carbohydrate utilization
GO:0090345	cellular organohalogen metabolic process
GO:0006952	defense response
GO:0007586	digestion
GO:0035240	dopamine binding
GO:0042417	dopamine metabolic process
GO:0015872	dopamine transport
GO:0097009	energy homeostasis
GO:0006094	gluconeogenesis
GO:0015758	glucose transport
GO:0040007	growth
GO:0042197	halogenated hydrocarbon metabolic process
GO:0005179	hormone activity
GO:0042562	hormone binding
GO:0002376	immune system process
GO:0055088	lipid homeostasis
GO:0010876	lipid localization
GO:0006629	lipid metabolic process
GO:0050958	magnetoreception
GO:0006582	melanin metabolic process
GO:0007275	multicellular organismal development
GO:0033555	multicellular organismal response to stress
GO:0018941	organomercury metabolic process
GO:0043473	pigmentation
GO:0009791	post-embryonic development
GO:0090066	regulation of anatomical structure size
GO:0010468	regulation of gene expression
GO:0040008	regulation of growth
GO:0010817	regulation of hormone levels
GO:0048583	regulation of response to stimulus
GO:0032225	regulation of synaptic transmission, dopaminergic
GO:0000003	reproduction
GO:0046686	response to cadmium ion
GO:0009743	response to carbohydrate stimulus
GO:0060992	response to fungicide
GO:0070848	response to growth factor stimulus
GO:0009635	response to herbicide
GO:0009725	response to hormone stimulus
GO:0017085	response to insecticide
GO:0010288	response to lead ion
GO:0033993	response to lipid
GO:0046689	response to mercury ion
GO:0051597	response to methylmercury
GO:0031667	response to nutrient levels
GO:0014070	response to organic cyclic compound
GO:0019236	response to pheromone
GO:0010269	response to selenium ion
GO:0009266	response to temperature stimulus
GO:0010043	response to zinc ion
GO:0048511	rhythmic process
GO:0007608	sensory perception of smell
GO:0051378	serotonin binding
GO:0042428	serotonin metabolic process
GO:0004993	serotonin receptor activity
GO:0007210	serotonin receptor signaling pathway
GO:0006837	serotonin transport
GO:0007587	sugar utilization
GO:0001963	synaptic transmission, dopaminergic
GO:0001659	temperature homeostasis

Table A3.3. Microsatellite summary statistics using three males and three females from each of Canada's 13 polar bear subpopulations. Scaffold numbers and approximate positions (±20 bp) were obtained using e-PCR; a "?" indicates that there were no results. N_A = number of alleles, H_O = observed heterozygosity, H_E = expected heterozygosity. All statistics were calculated using GENALEX. *CXX110 and UarMU50 are linked on scaffold 1; G10X and MSUT-2 are linked on scaffold 2.

Locus	Reference	Scaffold	Position	N_A	H_O	H_E
CXX20	Ostrander *et al.* (1993)	49	9592050	9	0.808	0.753
CXX110	Ostrander *et al*. (1993)	1*	60083750	12	0.705	0.761
G1A	Paetkau and Strobeck (1994)	69	9503000	6	0.513	0.613
G10B	Paetkau and Strobeck (1994)	230	268800	7	0.769	0.792
G1D	Paetkau and Strobeck (1994)	78	7224540	6	0.615	0.634
G10L	Paetkau and Strobeck (1994)	62	7576860	6	0.295	0.351
G10C	Paetkau *et al.* (1995)	28	5463890	7	0.577	0.563
G10M	Paetkau *et al.* (1995)	73	10570700	9	0.782	0.811
G10P	Paetkau *et al.* (1995)	?	?	9	0.679	0.750
G10X	Paetkau *et al.* (1995)	2*	11301030	10	0.756	0.835
UarMU05	Taberlet *et al.* (1997)	30	17752400	9	0.705	0.762
UarMU10	Taberlet *et al.* (1997)	3	11957700	8	0.615	0.681
UarMU23	Taberlet *et al.* (1997)	146	1246100	3	0.115	0.110
UarMU26	Taberlet *et al.* (1997)	7	26674790	8	0.769	0.861
UarMU50	Taberlet *et al.* (1997)	1*	41759660	8	0.808	0.807
UarMU51	Taberlet *et al.* (1997)	31	9252560	8	0.795	0.800
UarMU59	Taberlet *et al*. (1997)	147	2841890	10	0.795	0.837
G10H	Paetkau *et al.* (1998)	64	9471820	11	0.821	0.809
G10J	Paetkau *et al.* (1998)	45	4997650	3	0.603	0.553
G10U	Paetkau *et al.* (1998)	48	6639120	6	0.551	0.632
MSUT-1	Kitahara *et al.* (2000)	160	1628230	9	0.744	0.756
MSUT-2	Kitahara *et al.* (2000)	2*	11882860	7	0.667	0.726
MSUT-6	Kitahara *et al.* (2000)	?	?	3	0.269	0.373
MSUT-8	Kitahara *et al.* (2000)	132	2048750	6	0.705	0.771

Table A3.4. Logistic regressions of successful SNP printing and polymorphism among 1450 chip-genotyped individuals. "Individuals with minor allele" indicates the number of RAD samples (*N*=35 total) that contained at least one copy of the minor allele. Minor allele frequency (MAF) was estimated for transcriptomic SNPs using read counts from normalized RNA sequences of 10 sequenced individuals. VCF quality could not be modeled for transcriptomic SNPs, as they were called using an in-house program that did not output such a score. All predictors were fitted using a single degree of freedom.

	Predictor	***β***	**SE(*β*)**	***z***	***P***
SNP printing	Intercept	1.666	0.720	2.316	0.021
	Design score	0.475	0.741	0.641	0.521
RAD polymorphism	Intercept	–0.380	0.160	–2.376	0.018
	VCF quality	–0.008	0.002	–3.998	<0.001
	Depth	5.21×10^{-4}	8.89×10^{-5}	5.858	<0.001
	Individuals with minor allele	0.369	0.018	20.078	<0.001
Transcriptome polymorphism	Intercept	–1.138	0.195	–5.839	<0.001
	Depth	0.005	6.19×10^{-4}	8.722	<0.001
	MAF	5.764	0.594	9.699	<0.001

Table A3.5. Polar bear genomic scaffolds putatively forming part of the X-chromosome based on SNP clustering patterns (males always homozygous; females are either hetero- or homozygous). Scaffolds are denoted with "Cahill *et al.* (2013)" if this reference had already determined that the scaffold forms part of the X-chromosome. *1 of the 6 SNPs on scaffold 141 displays autosomal clustering.

Scaffold	Length (bp)	Proportion of filtered SNPs on scaffold with X-like clustering	Note
20	22,125,386	24/24	Cahill *et al.* (2013)
100	7,247,181	3/3	Cahill *et al.* (2013)
105	6,717,304	6/6	Cahill *et al.* (2013)
113	5,763,424	5/5	Cahill *et al.* (2013)
115	5,608,078	11/11	Cahill *et al.* (2013)
122	5,365,856	6/6	Cahill *et al.* (2013)
134	4,672,454	4/4	Cahill *et al.* (2013)
138	4,565,711	3/3	
141	4,364,041	5*/6	Cahill *et al.* (2013)
151	3,892,759	1/1	
166	3,286,445	2/2	
167	3,219,439	4/4	Cahill *et al.* (2013)
170	3,171,380	2/2	Cahill *et al.* (2013)
179	2,860,456	4/4	Cahill *et al.* (2013)
184	2,589,123	1/1	Cahill *et al.* (2013)
186	2,578,405	2/2	
201	2,055,564	1/1	
211	1,757,200	2/2	
228	1,315,073	3/3	
231	1,265,343	4/4	
248	947,286	1/1	
253	821,078	2/2	
260	777,269	1/1	
274	629,757	3/3	
286	468,345	1/1	
290	437,882	1/1	
292	425,832	1/1	
294	409,113	1/1	
313	276,930	1/1	
323	216,535	1/1	

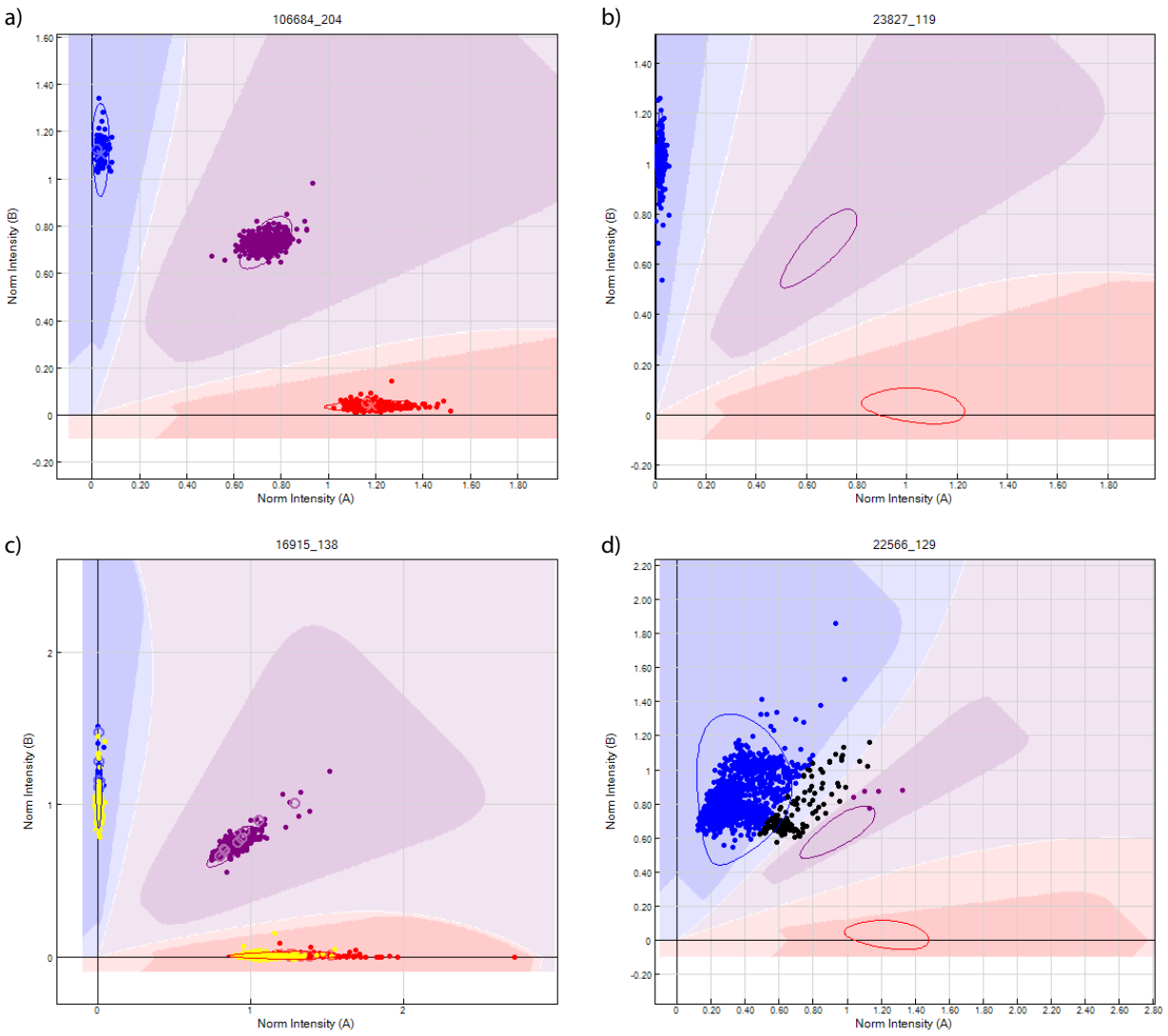

Figure A3.1. GENOMESTUDIO clustering plots showing normalized allelic intensities for allele A (x-axis) and allele B (y-axis) for each of four individual SNPs genotyped in 1427 individuals. a) RAD locus 106684_204: an example of a well-clustering SNP. b) RAD locus 106684_204: example of a monomorphic locus. c) X-chromosome SNP. Male samples—which are consistently homozygous—have been selected and are highlighted in yellow. Non-highlighted samples are female and comprise all three genotype classes. d) RAD locus 22566_129: an example of a problematic locus with poor clustering.

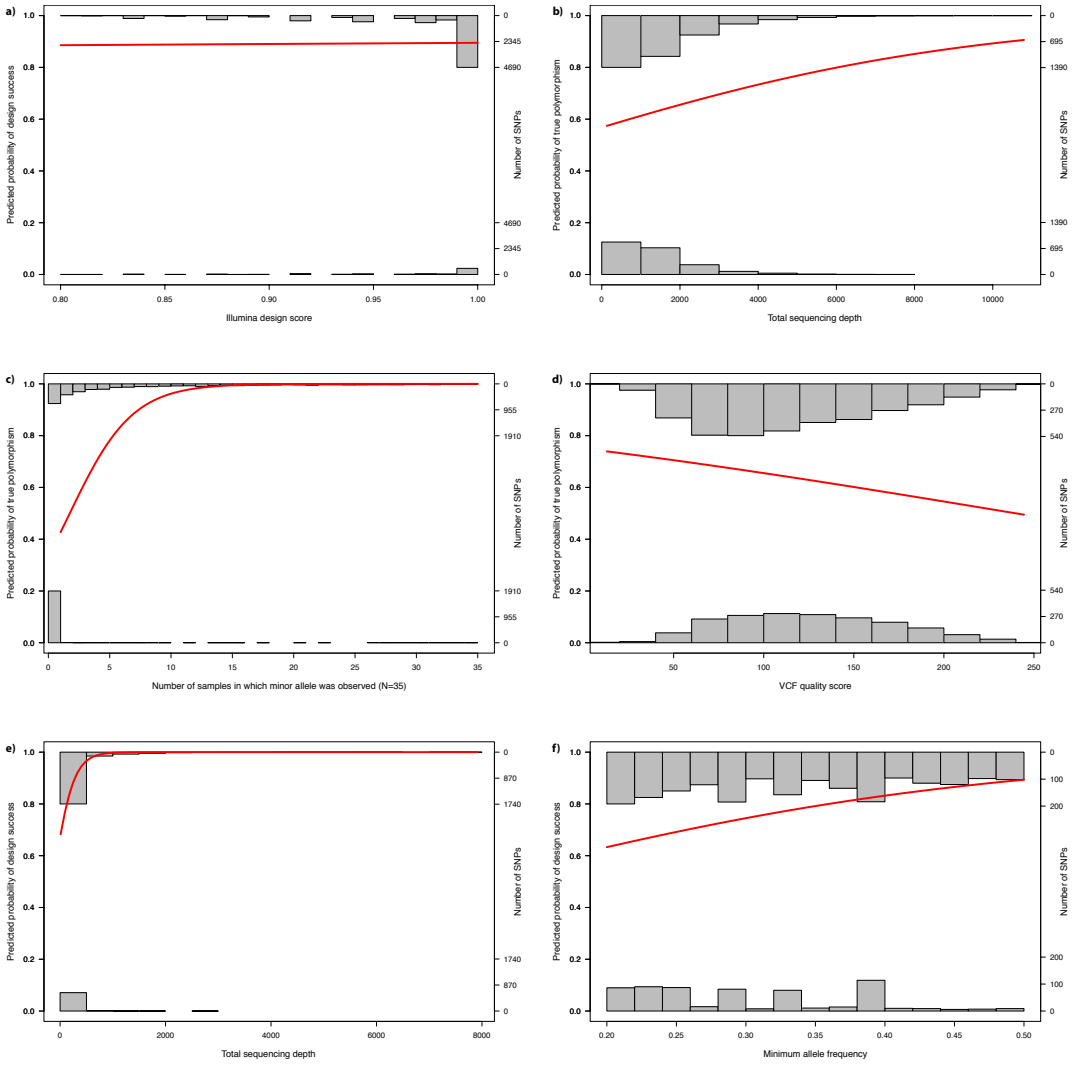

Figure A3.2. Logistic regressions of SNP chip printing or genotyping success. SNPs binned along the top axis were successfully printed or genotyped on the chip; SNPs binned along the bottom axis were not. Regression lines are shown in red. a) Logistic regression of successful SNP printing on Illumina design score. b–d) Logistic regression of a RAD SNP being truly polymorphic on: b) total sequencing depth for the RAD tag; c) number of the 35 RAD ascertainment samples in which the minor allele was observed; and d) VCF quality score. e–f) Logistic regression of a transcriptomic SNP being truly polymorphic on: e) total sequencing coverage for the transcriptomic SNP; and f) estimated minor allele frequency based on read counts in the ascertainment sample. Though b–d) and e–f) were conducted as multiple logistic regressions, plots shown here were generated from simple logistic regressions in the R package POPBIO. All predictor variables were significant ($P < 0.001$) except for design score ($P = 0.521$).

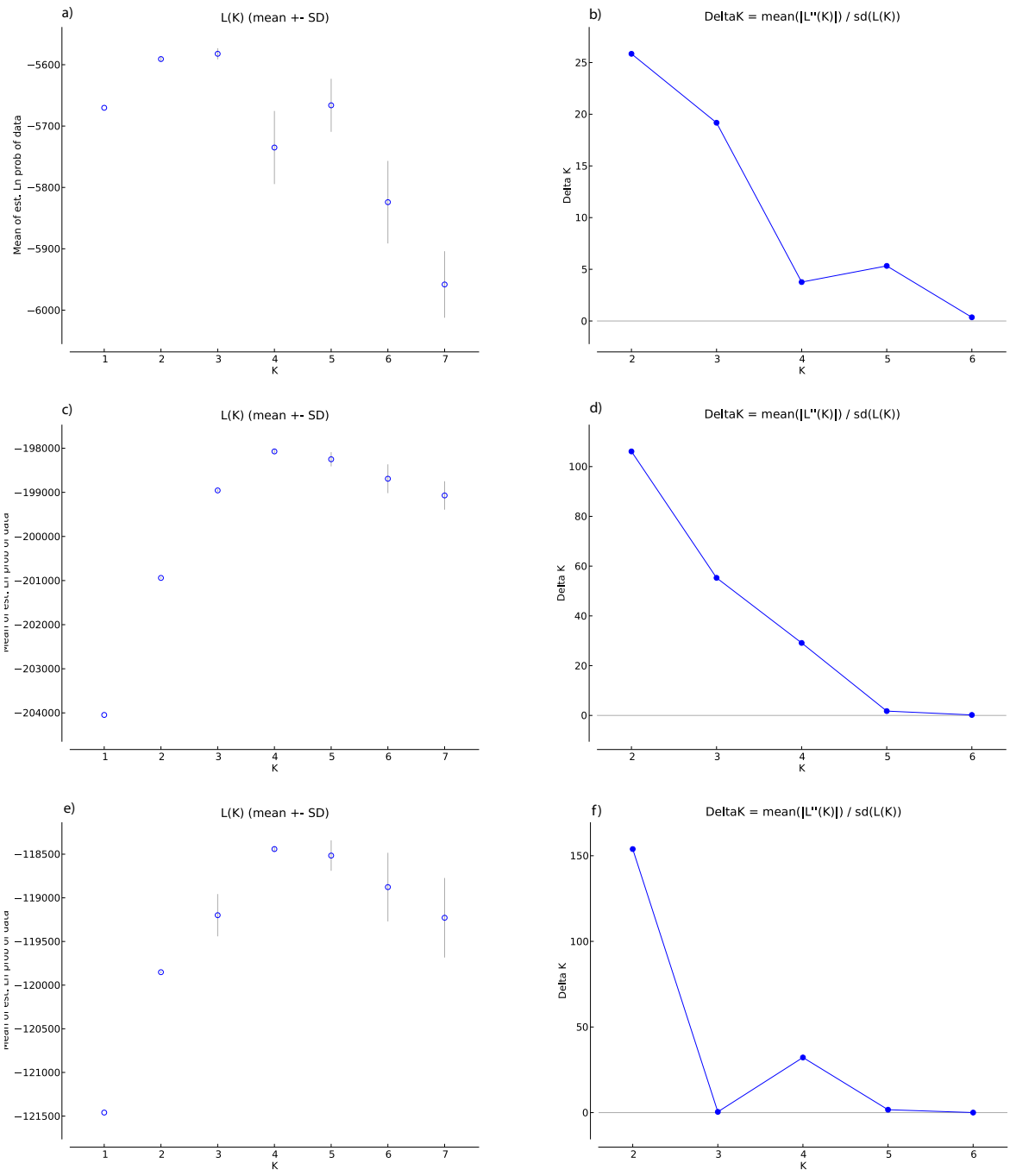

Figure A3.3. STRUCTURE HARVESTER output showing likelihood and Δ*K* values calculated for 20 replicates of STRUCTURE runs for *k*=1–7 for: 24 microsatellites (a & b), 3046 LD-pruned RAD SNPs (c & d), and 1778 LD-pruned transcriptomic SNPs (e & f).

Appendix 4: Supplementary material for "Population structure of Canadian polar bears determined using thousands of single-nucleotide polymorphisms"

A4.1 Canada-wide STRUCTURE analyses

For comparison with BAPS, Structure was also run on the full 399-individual dataset for k=1–16, using 20 independent runs of 200,000 iterations (incl. 100,000 burn-in iterations). Because Structure's default value for the concentration parameter of the Dirichlet distribution of allele frequencies (λ=1) may be inappropriate for SNPs with low minor allele frequencies (Pritchard et al. 2010), λ was estimated independently for the dataset using a trial run with k=1. We also used empirically estimated λ-values for all runs described in the main manuscript.

Results of STRUCTURE admixture analysis for k=4 (Figure A4.4) were virtually identical to those obtained from BAPS shown in the main manuscript. Though the Evanno method (Evanno *et al.* 2005) on Canada-wide STRUCTURE results indicates that k=2 is the best-supported clustering (Figure A4.5), this method may underperform in the case of weak genetic differentiation (Waples & Gaggiotti 2006); therefore, k=4 was again assumed to best represent the top hierarchical level of population structure, as this matches results of BAPS, GENODIVE, and ADEGENET.

A4.2 Grizzly genotyping and initial TREEMIX run

To obtain a root for a tree of Canadian polar bear subpopulations, we SNP-chip genotyped a grizzly bear (*Ursus arctos horribilis*)—a subspecies of brown bear (*U. arctos*)—from Kootenay National Park, British Colombia, Canada. Brown bears are the sister species to polar bears: the two species diverged ~400,000 years ago (Liu *et al.* 2014), and although interspecific hybridization has occurred in the past (e.g., Cahill *et al.* 2013; Edwards *et al.* 2011; Miller *et al.* 2012b) and sometimes still occurs (e.g., Doupé *et al.* 2009), there is no evidence of substantive interspecific gene flow among extant populations (Cronin & Macneil 2012). Of the 5333 well-clustering polymorphic SNPs on the chip (incl. 1984 transcriptomic SNPs), 5281 SNPs (≈99%) were successfully called in the grizzly, and 739 SNPs (≈14%) were heterozygous.

We generated a manually rooted tree by adding genotypes from grizzly to the subset of LD-pruned RAD SNPs described in the main manuscript. We manually rooted the tree with grizzly, disallowing migration/admixture and sample-size correction using 10-SNP blocks using TREEMIX's options: `-k 10 -m 0 -root Grizzly -noss`. Results are shown in Figure A4.8.

Perhaps because of small sample size for grizzly bears, runs that included grizzlies and allowed for migration/admixture suggested gene flow from grizzlies into the Hudson Complex. Although grizzlies are found in the area north of Churchill, Manitoba and the historical range of grizzlies extends to the southern reaches of James Bay, this admixture event was not supported by a three-population test (Reich *et al.* 2009), and therefore we excluded grizzly bears from the final TREEMIX analysis presented in the paper.

Table A4.1. Numbers of male and female samples from each subpopulation. Numerators indicate the number of samples successfully genotyped (call rate ≥ 0.9); denominators indicate the number of samples obtained. 399 out of 412 samples were successfully genotyped in total. Asterisks indicate the presence of incorrectly sexed individuals, as determined using patterns of heterozygosity among 108 X-linked loci. Two individuals (L29384 from Baffin Bay and X32579 from the Northern Beaufort Sea) were supplied as allegedly male samples but were genetically determined to be female; four individuals (L29393 from Baffin Bay, L29403 from Baffin Bay, L28775 from Foxe Basin, and L29571 from Lancaster Sound) were supplied as allegedly male samples but were genetically determined to be female. Where relevant the genetically determined sexes of individuals were used for all analysis (e.g., in sex-specific AMOVAs).

Management unit	Males	Females	Source
Baffin Bay (BB)*	14/15	16/17	Harvest (NU)
Davis Strait (DS)	17/17	16/16	Harvest (NU, NL)
Foxe Basin (FB)*	17/16	16/17	Harvest (NU)
Gulf of Boothia (GB)	16/16	14/15	Harvest (NU)
Kane Basin (KB)	16/17	14/15	Harvest & sampling (NU)
Lancaster Sound (LS)*	16/16	15/16	Harvest (NU)
M'Clintock Channel (MC)	16/17	13/14	Harvest & sampling (NU)
Northern Beaufort Sea (NB)*	17/18	14/13	Sampling (EC)
Norwegian Bay (NW)	14/15	17/17	Harvest & sampling (NU)
Southern Beaufort Sea (SB)	15/15	17/17	Sampling (EC)
Southern Hudson Bay (SH)	17/17	14/14	Sampling (ON)
Viscount Melville Sound (VM)	12/13	16/16	Sampling (NT), harvest (NU)
Western Hudson Bay (WH)	15/16	15/17	Sampling (EC)

Table A4.2. Microsatellites genotyped for the present study. N_A = total number of alleles observed among 378 genotyped individuals.

Locus	Reference	N_A	Proportion missing
CXX20	Ostrander *et al.* (1993)	11	0.003
CXX110	Ostrander *et al.* (1993)	13	0.000
G1A	Paetkau and Strobeck (1994)	7	0.013
G10B	Paetkau and Strobeck (1994)	8	0.005
G1D	Paetkau and Strobeck (1994)	6	0.026
G10L	Paetkau and Strobeck (1994)	7	0.003
G10C	Paetkau *et al.* (1995)	8	0.019
G10M	Paetkau *et al.* (1995)	10	0.024
G10P	Paetkau *et al.* (1995)	10	0.008
G10X	Paetkau *et al.* (1995)	12	0.003
UarMU05	Taberlet *et al.* (1997)	10	0.045
UarMU10	Taberlet *et al.* (1997)	8	0.045
UarMU23	Taberlet *et al.* (1997)	3	0.053
UarMU26	Taberlet *et al.* (1997)	10	0.045
UarMU50	Taberlet *et al.* (1997)	10	0.008
UarMU51	Taberlet *et al.* (1997)	9	0.048
UarMU59	Taberlet *et al.* (1997)	12	0.024
G10H	Paetkau *et al.* (1998)	11	0.040
G10J	Paetkau *et al.* (1998)	3	0.003
G10U	Paetkau *et al.* (1998)	7	0.003
MSUT-1	Kitahara *et al.* (2000)	10	0.077
MSUT-2	Kitahara *et al.* (2000)	8	0.050
MSUT-6	Kitahara *et al.* (2000)	6	0.098
MSUT-8	Kitahara *et al.* (2000)	6	0.048

Table A4.3. Microsatellite genotype summary statistics for each management unit (MU). N, Males and Females give the total proportion of SNP-genotyped individuals from each management unit that were also successfully microsatellite genotyped. A = allelic richness, H_O = observed heterozygosity, H_E = expected heterozygosity using MU-specific allele frequencies. MU abbreviations are as in Table A4.1.

Management unit	N	Males	Females	A (±SD)	H_O	H_E	F_{IS}
BB	28/30	12/12	16/18	6.021±1.865	0.659	0.663	0.010
DS	29/33	13/17	16/16	6.068±1.963	0.682	0.677	–0.010
FB	29/33	15/16	14/17	5.947±1.914	0.658	0.668	0.021
GB	24/30	10/16	14/14	6.255±1.708	0.690	0.699	0.020
KB	30/30	16/16	14/14	6.123±1.757	0.669	0.689	0.019
LS	30/31	14/15	16/16	6.261±1.705	0.676	0.688	0.035
MC	28/29	15/16	13/13	5.882±1.886	0.652	0.664	0.027
NB	31/31	17/17	14/14	5.883±1.722	0.648	0.654	0.005
NW	31/31	14/14	17/17	5.400±1.779	0.597	0.624	0.056
SB	29/32	15/15	14/17	6.010±1.936	0.650	0.668	0.027
SH	31/31	17/17	14/14	5.474±1.599	0.656	0.645	–0.015
VM	28/28	12/12	16/16	5.956±1.677	0.628	0.668	0.060
WH	30/30	15/15	15/15	5.860±1.793	0.682	0.675	–0.011

Table A4.4. Summary information for TREEMIX runs for 0–6 migration events (m).

m	Log likelihood	Variance explained
0	557.353	97.8%
1	621.955	99.0%
2	659.013	99.3%
3	674.591	99.5%
4	683.513	99.6%
5	687.476	99.6%
6	690.918	99.7%

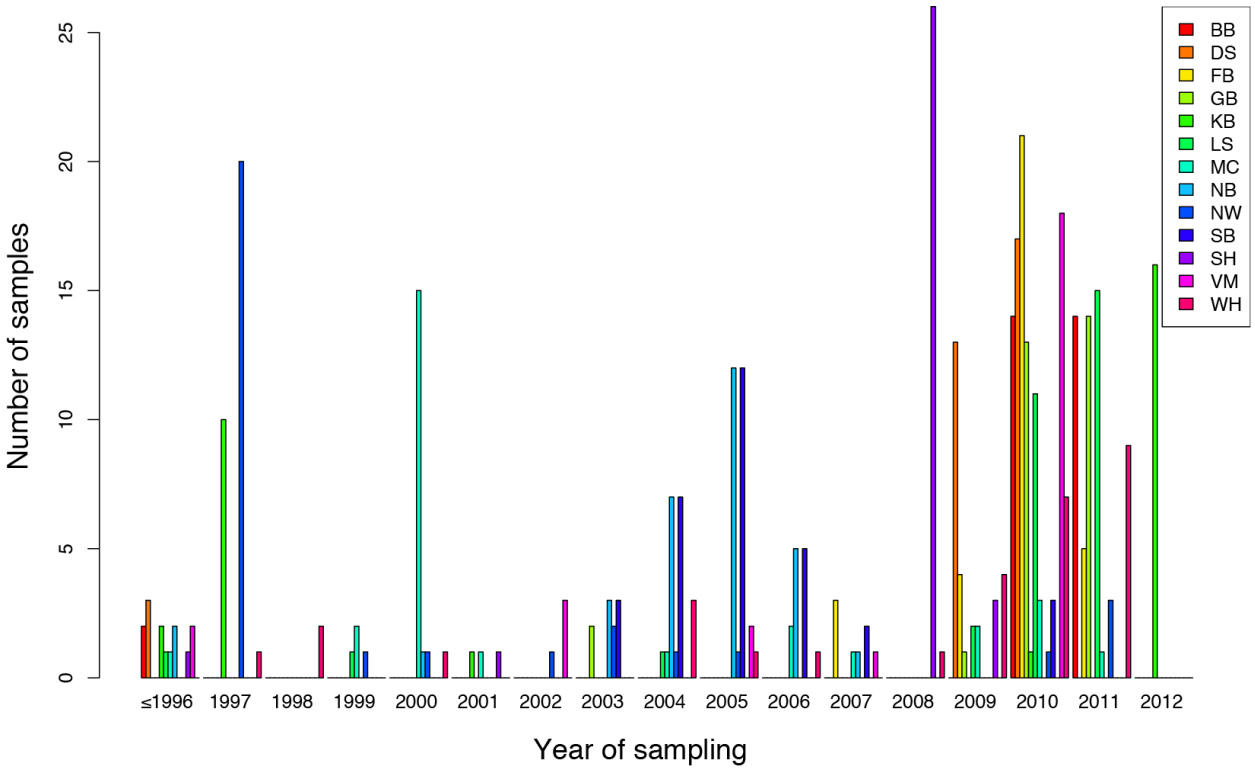

Figure A4.1. Histogram of sample collection years in each of the 13 management units (MUs). MU abbreviations are as in Table A4.1.

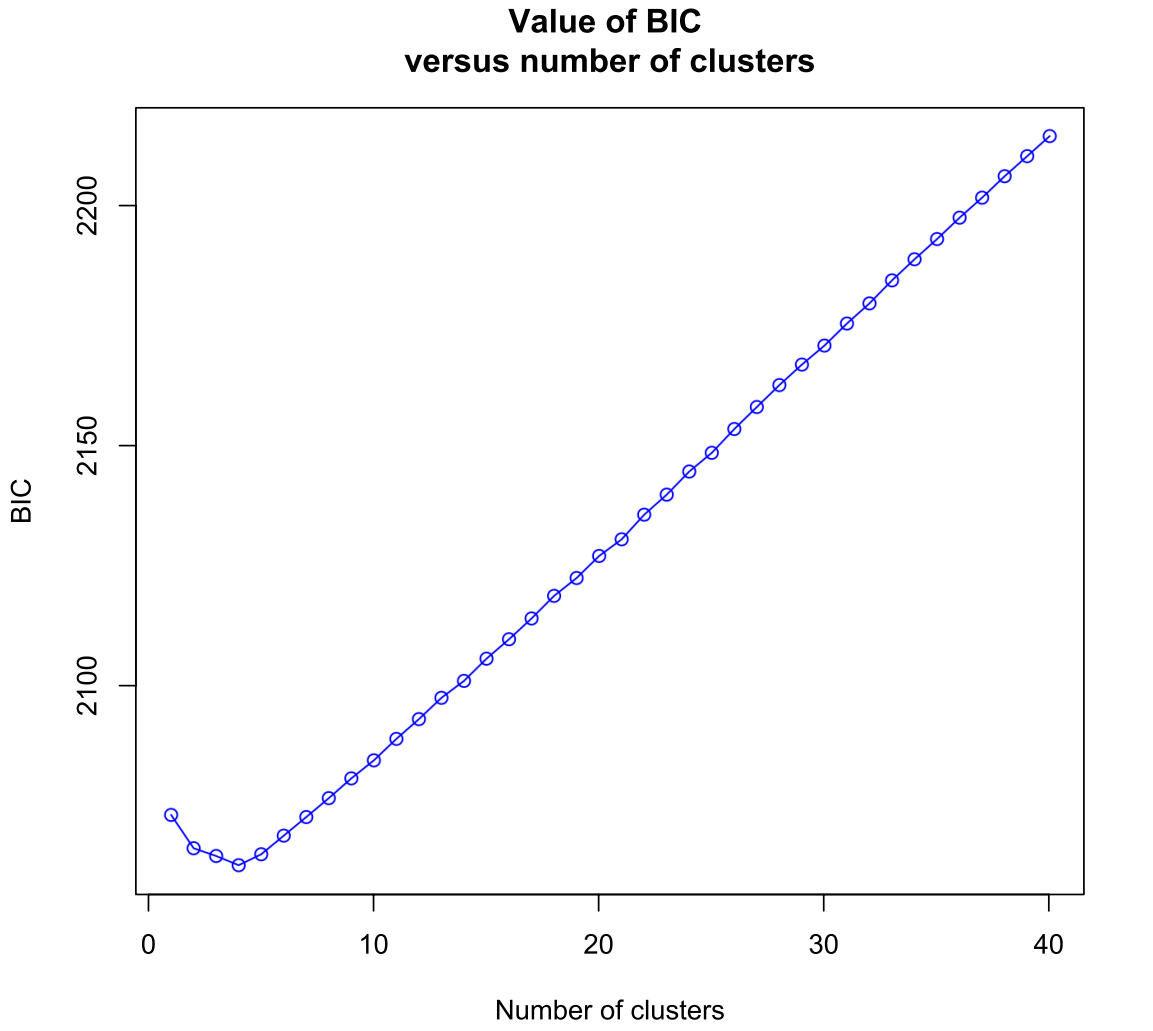

Figure A4.2. Bayesian information criterion (BIC) values for a given number of clusters as implemented in *k*-means clustering in ADEGENET 1.4-2 (Jombart 2008; Jombart & Ahmed 2011).

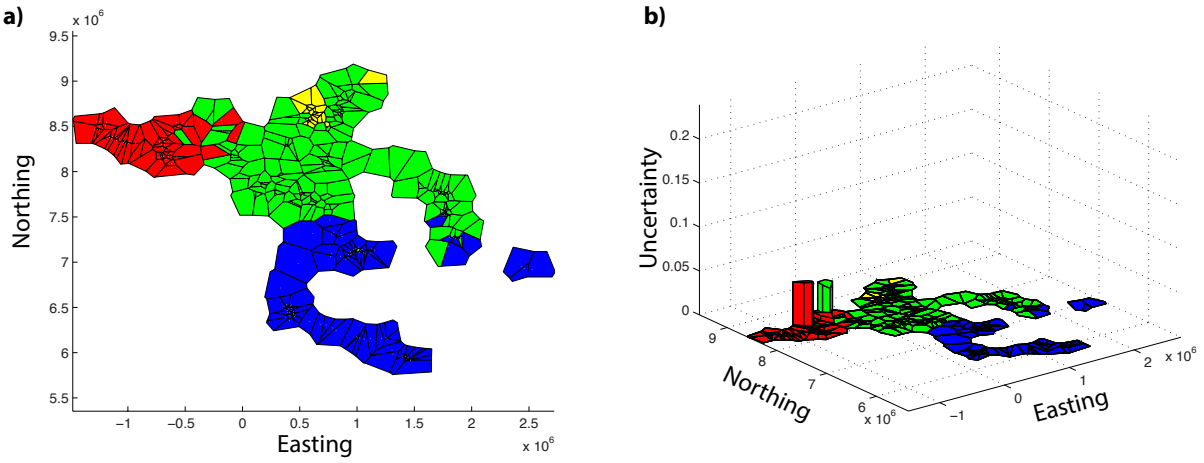

Figure A4.3. a) Voronoi tesselation resulting from automated spatial mixture clustering in BAPS 6.0 (Corander *et al.* 2008b) for k=1–16, which recognized four clusters. b) Local uncertainty in posterior mode tessellation.

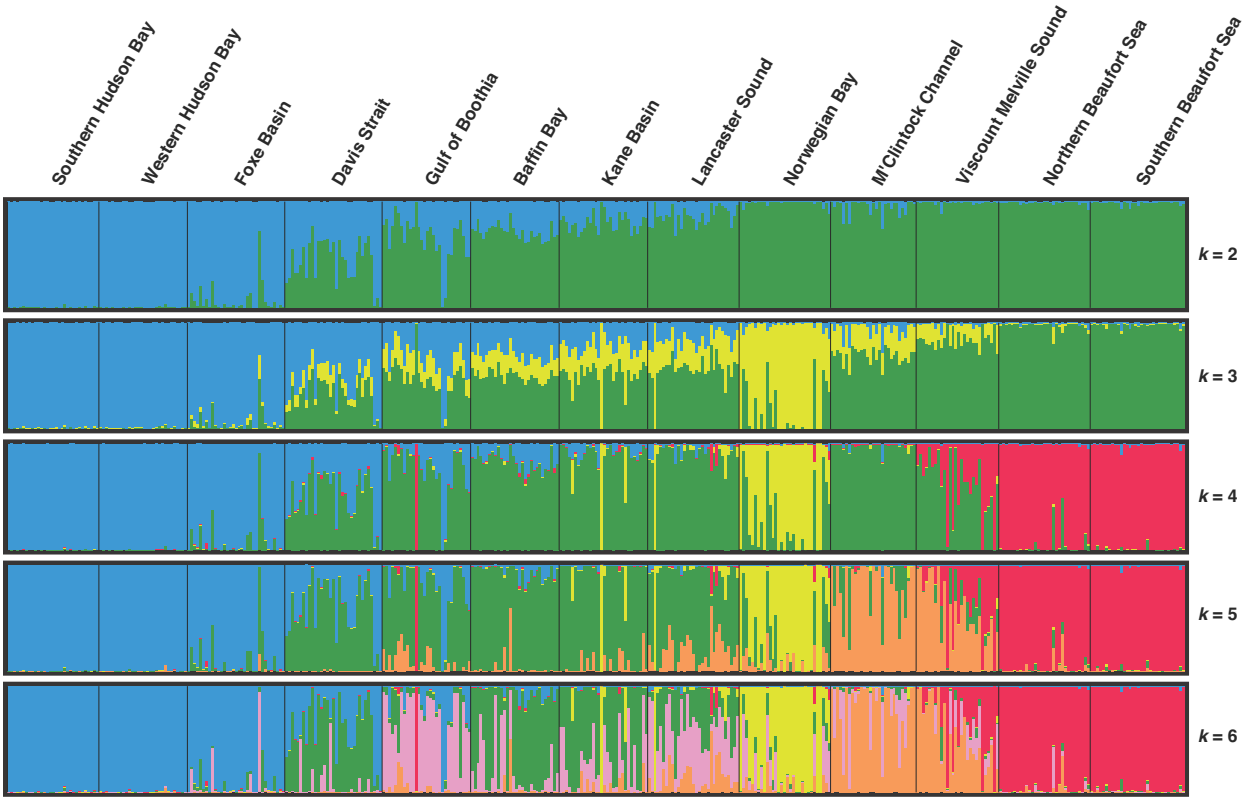

Figure A4.4. Canada-wide STRUCTURE analyses for 399 individuals for *k*=2–6. Though *k*=2 is best supported by the Evanno method, and *k*=16 is best supported by the Pritchard method, both DAPC and BAPS analyses suggest that *k*=4. The numbers under each *k*-value indicates the proportion of runs (out of 20) that converged to a similar solution as determined by CLUMPAK. Only minor modes with support from more than two runs are presented.

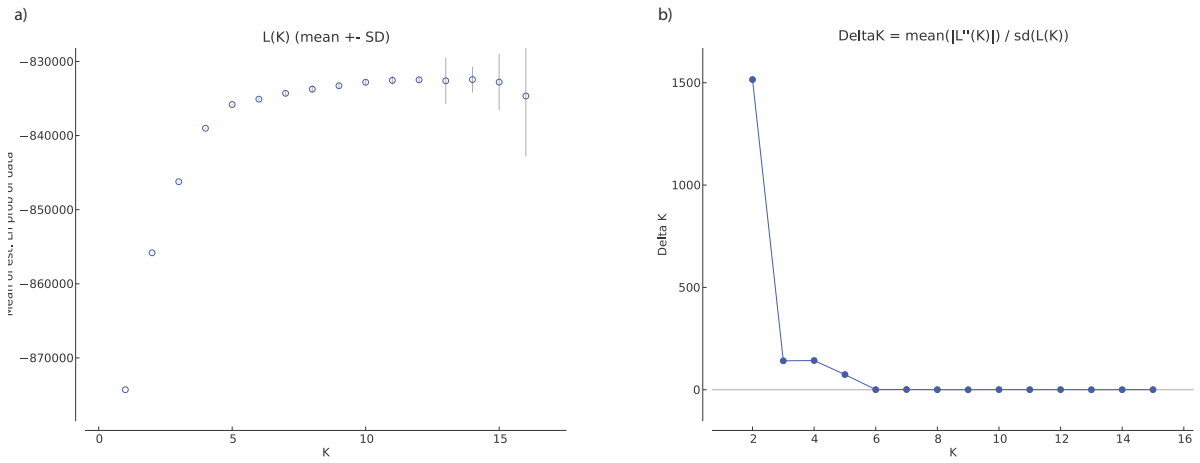

Figure A4.5. Pr(*K*|*X*), Δ*K*, and Prob K values from STRUCTURE for *k*=1–16.

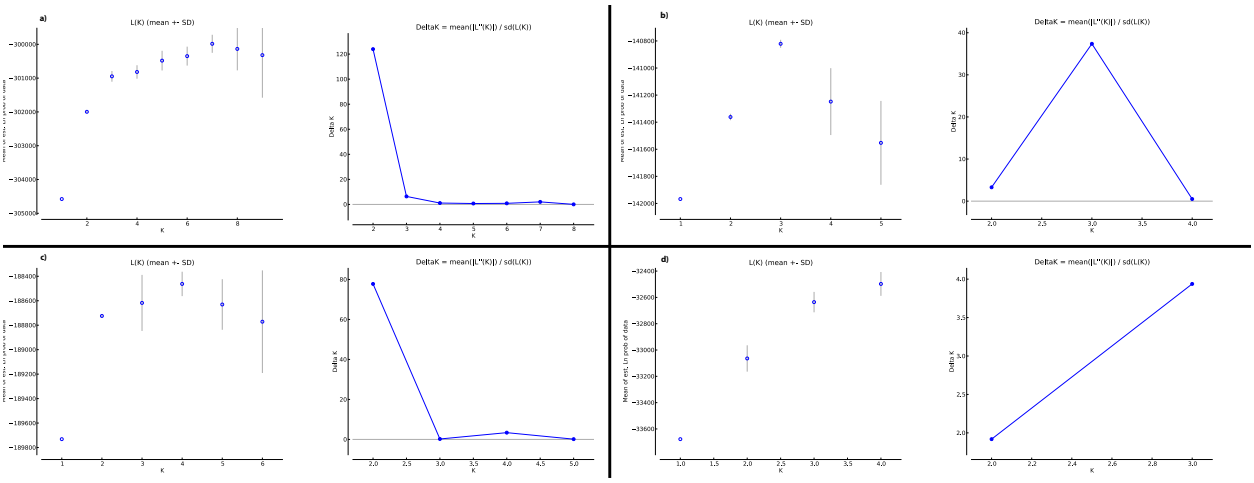

Figure A4.6. Pr($K|X$) and ΔK values from STRUCTURE for non-admixed individuals belonging to each of four genetic clusters identified by BAPS that are roughly coincident with: a) the Arctic Archipelago ($N = 141$), b) the Beaufort Sea ($N = 66$), c) the Hudson Complex (incl. Labrador; $N = 94$), and d) Norwegian Bay ($N = 22$).

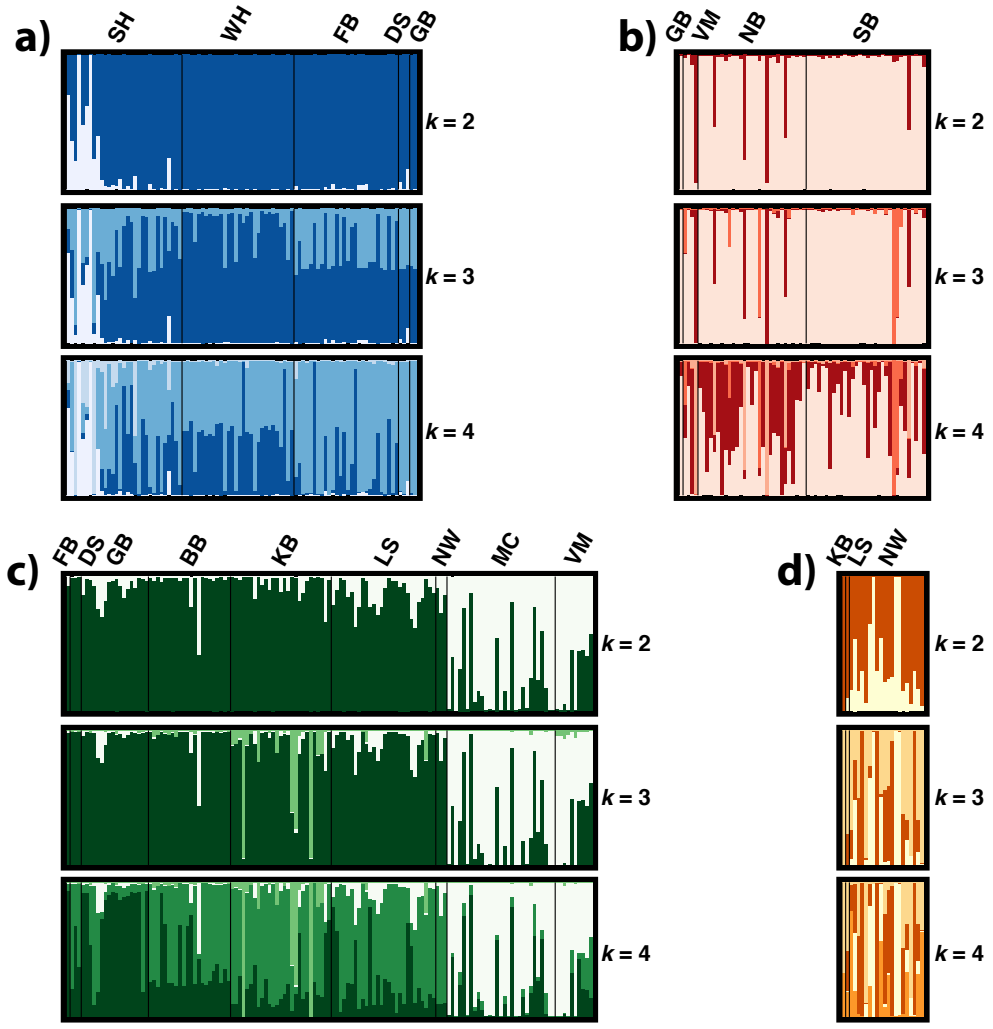

Figure A4.7. STRUCTURE results for k=1–4 for non-admixed individuals belonging to each of four genetic clusters identified by BAPS that are roughly coincident with: a) the Hudson Complex (incl. Labrador; N = 94), b) the Beaufort Sea (N = 66), c) the Arctic Archipelago (N = 141), and d) Norwegian Bay (N = 22).

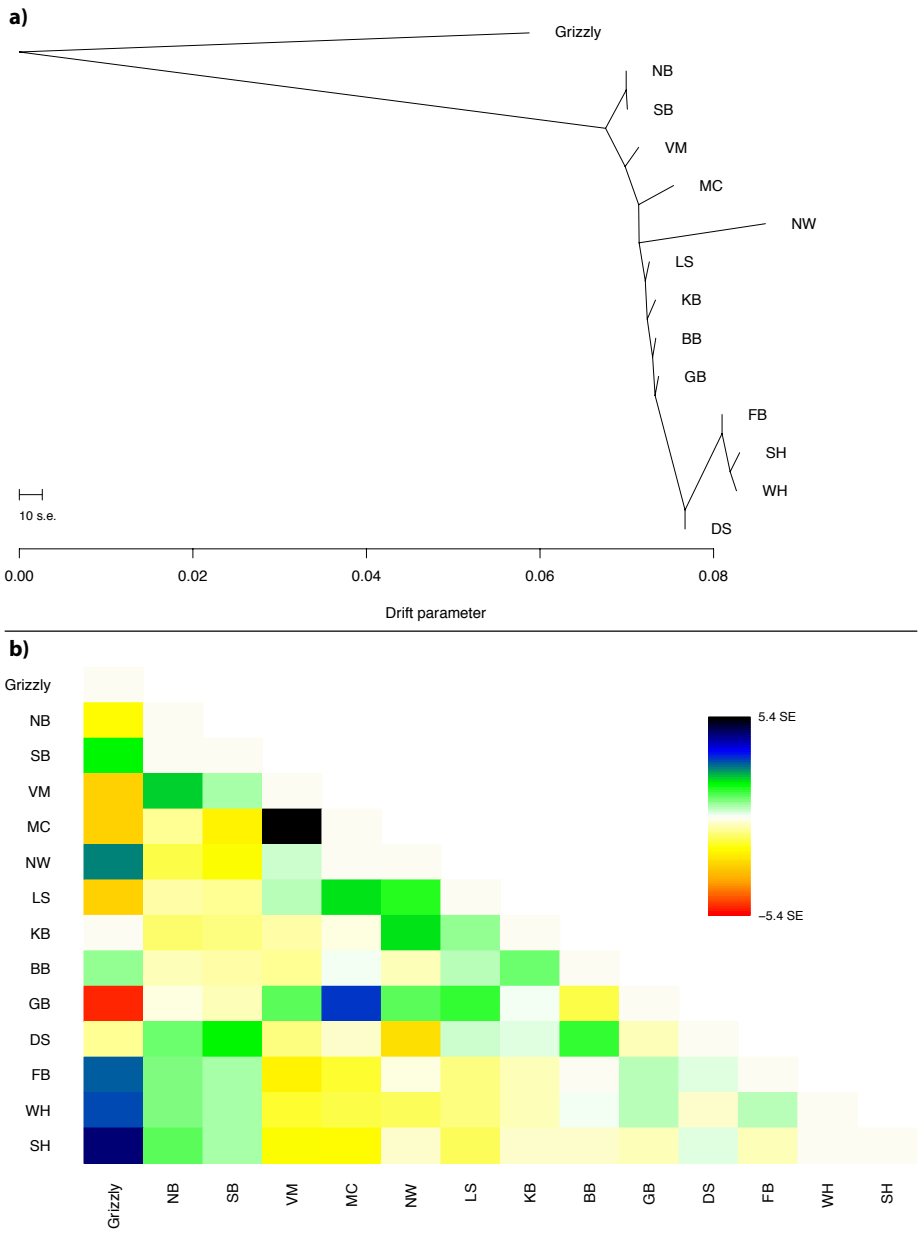

Figure A4.8. a) Maximum-likelihood tree of historical population splits, allowing for zero migration events in TREEMIX. The scale bar indicates ten times the average standard error. b) Scaled residual fit for each pair of populations under the maximum likelihood TREEMIX tree with four migration events shown in the main paper. Positive residuals indicate candidates for additional admixture events, as the current tree underestimates their relatedness. Negative residuals indicate population pairs that are more distantly related in the data than in the tree.

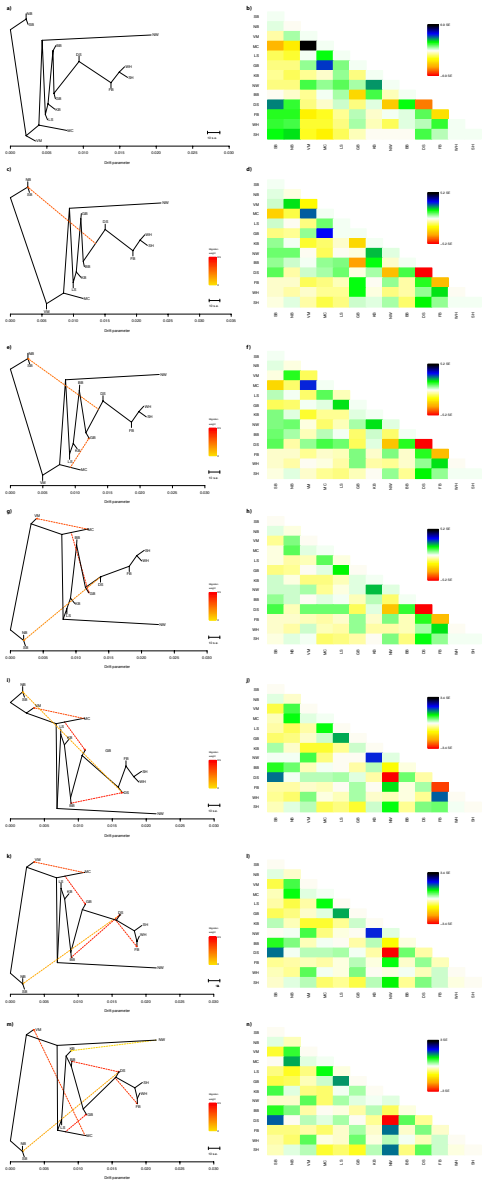

Figure A4.9. a,c,e,g,i,k) Maximum-likelihood trees of historical population splits (solid lines), allowing for 0–5 subsequent migration events (dashed lines) in TREEMIX, where migration weights are related to the proportion of alleles originating in the parental population. The scale bar indicates ten times the average standard error. b,d,f,h,j,l) Scaled residual fits for each pair of populations under the maximum likelihood TREEMIX tree with 0–5 migration events. Positive residuals indicate candidates for additional admixture events, as the current tree underestimates their relatedness. Negative residuals indicate population pairs that are more distantly related in the data than in the tree.

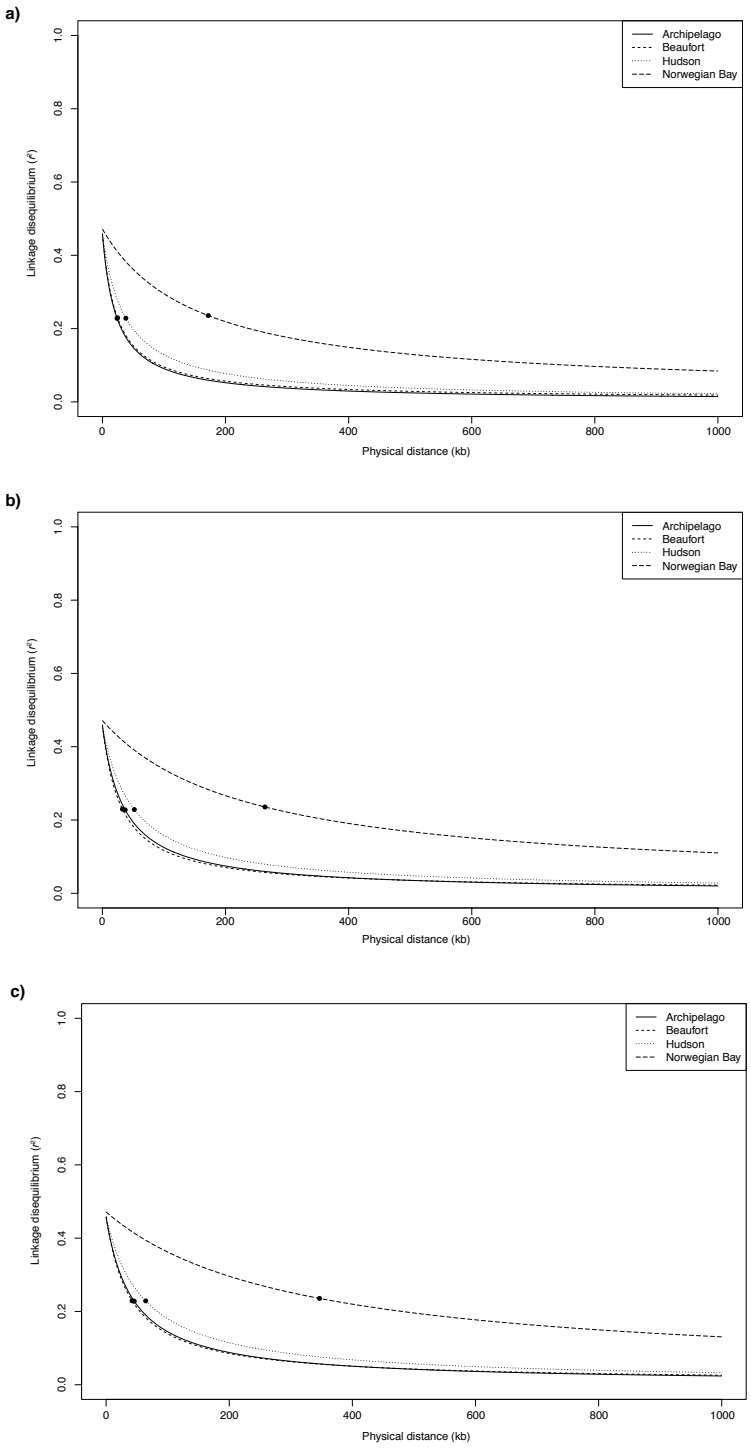

Figure A4.10. Linkage disequilibrium decay over physical distance for non-admixed individuals belonging to each of four genetic clusters of polar bears. a) Minor allele frequency (MAF) = 0.01; b) MAF = 0.05; c) MAF = 0.10.

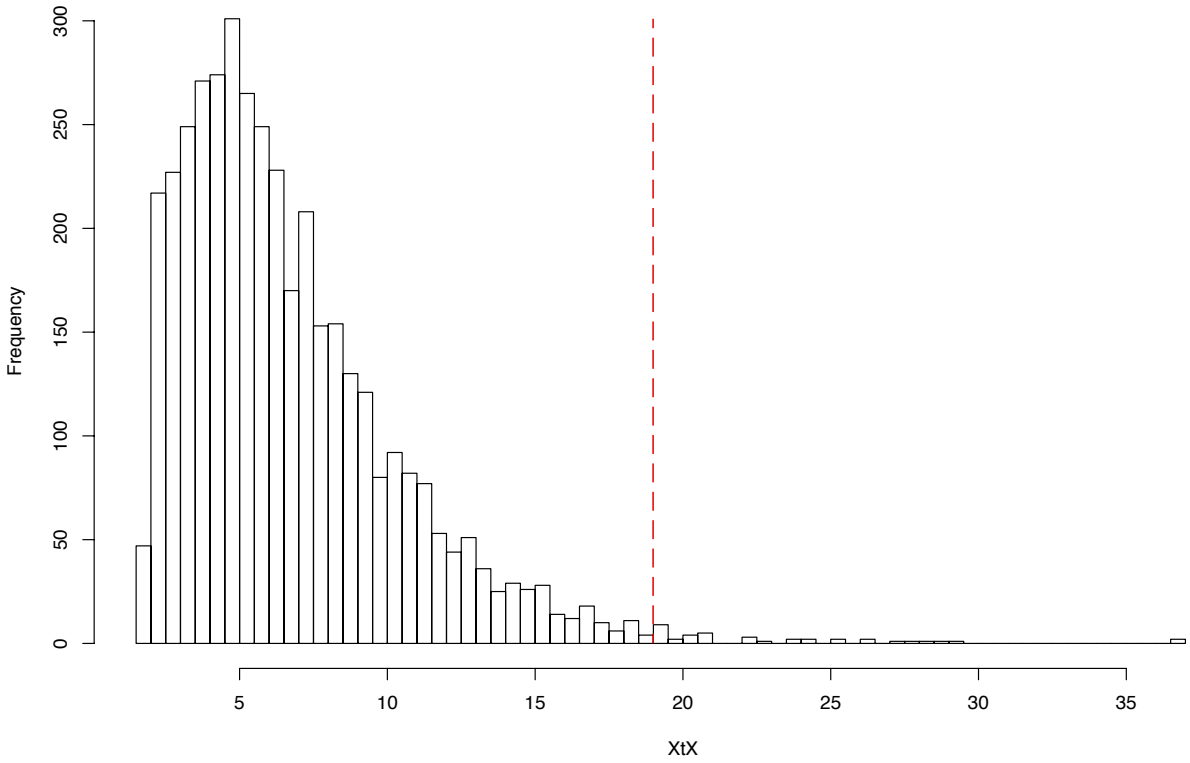

Figure A4.11. Histogram of XtX values calculated in BAYENV 2. The dashed red line indicates the 1% tail.

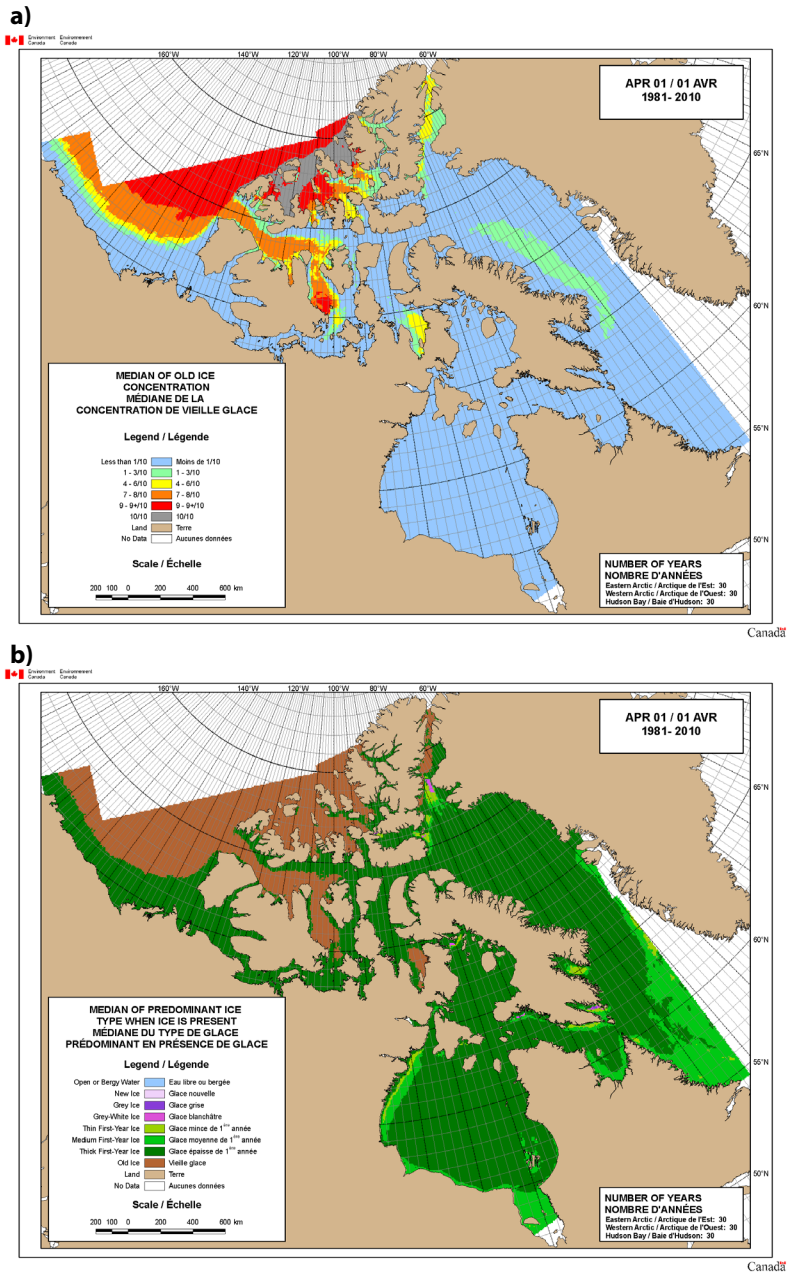

Figure A4.12. a) 30-year median of old-ice concentration for April 1 from 1981 to 2010. b) 30-year median of predominant ice type when ice is present on April 1 from 1981 to 2010. Copied with permission from *Climatic Ice Atlas 1981–2010*, (Copyright Canadian Ice Service, Environment Canada, 2011). This figure includes copies of official works published by the Government of Canada, and its reproduction here does not indicate affiliation with or endorsement of the Government of Canada.

Appendix 5: Supplementary material for "Evidence of adoption, monozygotic twinning, and low inbreeding rates in a large genetic pedigree of polar bears"

Table A5.1. Summary statistics for microsatellites used for pedigree creation and adoption detection. E_1 = allelic dropout rate, E_2 = false allele rate, N_A = number of alleles, H_O = observed heterozygosity, H_E = expected heterozygosity, P_{ex} = probability of exclusion for a single unknown parent, P_{ID} = probability of identity for unrelated individuals. For details on how each of these numbers was calculated, consult the main manuscript.

Locus	Reference	E_1	E_2	N_A	H_O	H_E	P_{ex}	P_{ID}
CXX20	Ostrander *et al.* (1993)	0	0.012	9	0.787	0.795	0.427	0.070
CXX110	Ostrander *et al.* (1993)	0	0	10	0.590	0.600	0.223	0.180
CXX173	Ostrander *et al.* (1993)	0.009	0.007	6	0.694	0.691	0.276	0.141
G1A	Paetkau and Strobeck (1994)	0	0	8	0.531	0.540	0.158	0.252
G10B	Paetkau and Strobeck (1994)	0	0	7	0.601	0.607	0.217	0.184
G1D	Paetkau and Strobeck (1994)	0	0	6	0.626	0.634	0.222	0.182
G10L	Paetkau and Strobeck (1994)	0	0	6	0.432	0.427	0.096	0.356
G10C	Paetkau *et al.* (1995)	0	0	8	0.674	0.681	0.270	0.146
G10M	Paetkau *et al.* (1995)	0	0.013	9	0.789	0.797	0.433	0.068
G10P	Paetkau *et al.* (1995)	0	0	9	0.743	0.749	0.363	0.093
G10X	Paetkau *et al.* (1995)	0	0	9	0.746	0.728	0.326	0.114
UarMU05	Taberlet *et al.* (1997)	0	0	10	0.785	0.771	0.403	0.077
UarMU10	Taberlet *et al.* (1997)	0	0	7	0.638	0.643	0.236	0.176
UarMU23	Taberlet *et al.* (1997)	0	0	3	0.112	0.112	0.006	0.791
UarMU26	Taberlet *et al.* (1997)	0	0	9	0.837	0.840	0.510	0.045
UarMU50	Taberlet *et al.* (1997)	0	0	9	0.788	0.781	0.393	0.082
UarMU51	Taberlet *et al.* (1997)	0.010	0	8	0.798	0.801	0.435	0.067
UarMU59	Taberlet *et al.* (1997)	0	0	10	0.847	0.831	0.496	0.050
G10H	Paetkau *et al.* (1998)	0	0	10	0.766	0.767	0.383	0.086
G10J	Paetkau *et al.* (1998)	0	0	4	0.639	0.628	0.201	0.209
G10U	Paetkau *et al.* (1998)	0.039	0	7	0.569	0.574	0.186	0.215
MSUT-1	Kitahara *et al.* (2000)	0	0	8	0.749	0.738	0.326	0.113
MSUT-2	Kitahara *et al.* (2000)	0	0	9	0.765	0.775	0.395	0.082
MSUT-6	Kitahara *et al.* (2000)	0	0	3	0.520	0.524	0.137	0.298
MSUT-8	Kitahara *et al.* (2000)	0	0	6	0.767	0.771	0.377	0.088

Table A5.2. Summary statistics for the final pedigree, including genetic parentage assignments and maternal relationships derived from field data. All statistics were calculated using the R package PEDANTICS 1.5 (Morrissey & Wilson 2010).

Records	4449
Maternities	2957
Paternities	1861
Full sibships	551
Maternal sibships	6403
Maternal half-sibships	5852
Paternal sibships	3009
Paternal half-sibships	2458
Maternal grandmothers	1401
Maternal grandfathers	739
Paternal grandmothers	487
Paternal grandfathers	329
Maximum pedigree depth	5
Founders (tier 1)	1381
N (tier 2)	1381
N (tier 3)	1075
N (tier 4)	497
N (tier 5)	109
N (tier 6)	6
Mean maternal sibship size	3.66
Mean paternal sibship size	2.81
Non-zero F	3
$F > 0.125$	0
Mean pairwise relatedness	7.90×10^{-4}
Pairwise relatedness ≥ 0.125	2.94×10^{-3}
Pairwise relatedness ≥ 0.25	1.72×10^{-3}
Pairwise relatedness ≥ 0.5	5.43×10^{-4}

Appendix 6: Supplementary material for "Heritability of body size in the polar bears of Western Hudson Bay"

Table A6.1. Point estimates of random effect sizes (h^2, c^2, y^2, and ε^2) calculated in REPEATABEL. Variance components: h^2 = heritability; c^2 = permanent environmental; y^2= year; ε^2 = residual.

Trait	$\boldsymbol{h^2}$	$\boldsymbol{c^2}$	$\boldsymbol{y^2}$	$\boldsymbol{\varepsilon^2}$
Straight-line body length	0.36	0.29	0.06	0.28
Axillary girth	0.11	0.13	0.08	0.67
Head length	0.35	0.32	0.01	0.31
Zygomatic breadth	0.40	0.27	0.01	0.32

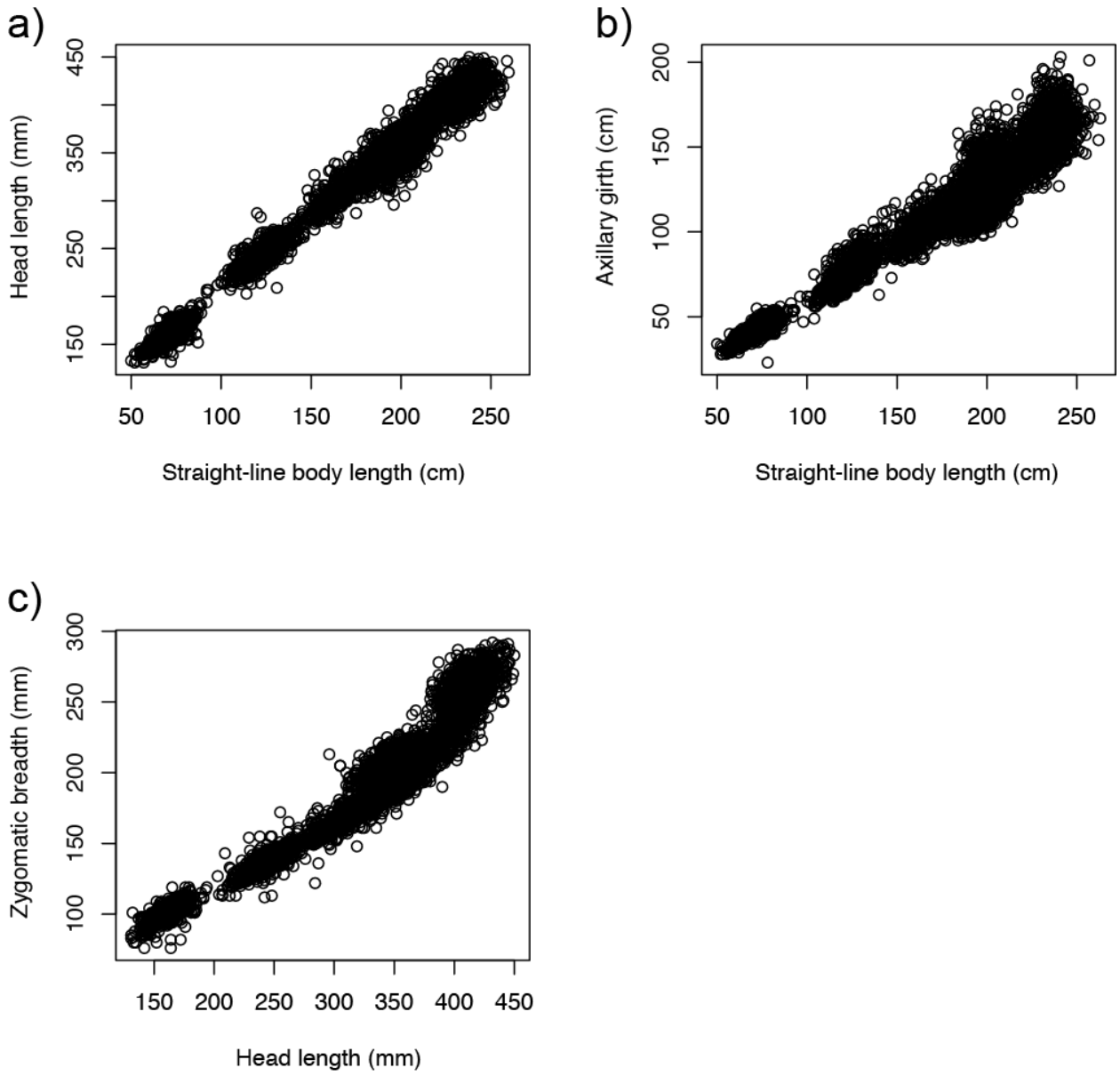

Figure A6.1. Scatterplots of various pairs of body-size measurements. a) Head length vs. body length, b) axillary girth vs. body length, c) zygomatic breadth vs. head length.

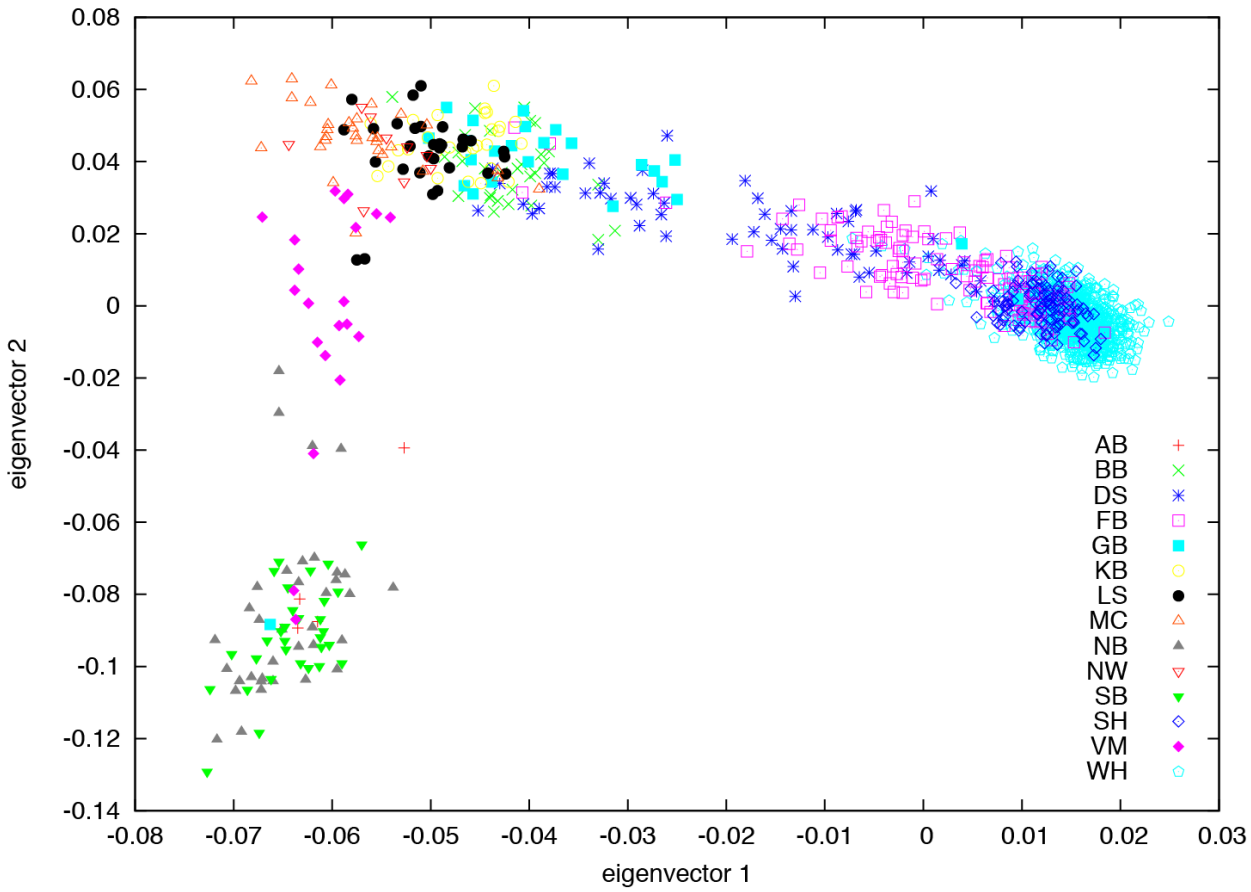

Figure A6.2. Principal component analysis (PCA) of 1416 polar bears sampled from across the Canadian North. AB = Arctic Basin, BB = Baffin Bay, DS = Davis Strait, FB = Foxe Basin, GB = Gulf of Boothia, KB = Kane Basin, LS = Lancaster Sound, MC = M'Clintock Channel, NB = Northern Beaufort Sea, SB = Southern Beaufort Sea, SH = Southern Hudson Bay, VM = Viscount Melville, WH = Western Hudson Bay. Note that because PCA is sensitive to unequal sample size and 857 samples are drawn from WH, this plot of the first two principal components does not accurately represent Canada-wide population structure.